The influence of receptor-ligand interactions on gene expression and phagosome functions in mouse macrophages

Dissertation

zur Erlangung des akademischen Grades
doctor rerum naturalium (Dr. rer. nat.)
der Mathematisch-Naturwissenschaftlichen Fakultät
der Universität Rostock

urn:nbn:de:gbv:28-diss2008-0050-9

vorgelegt von
Eik Hoffmann
aus Siggelkow

Rostock, Dezember 2007

Gutachter: PD Dr. Sergei A. Kuznetsov, Universität Rostock
Prof. Albert Haas, Universität Bonn

Datum des Wissenschaftlichen Kolloquiums: 10.03.2008

Für meinen Opa

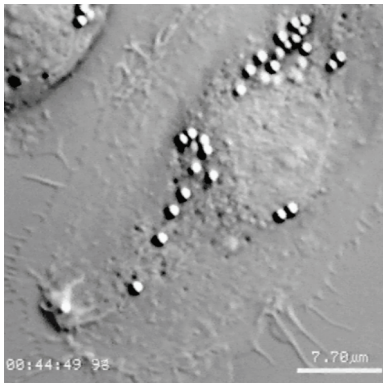

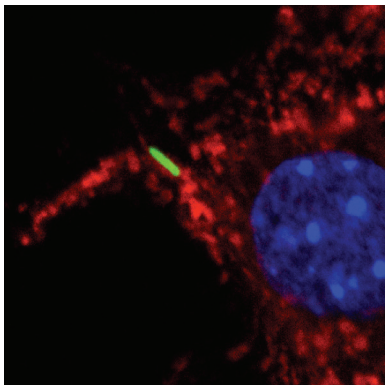

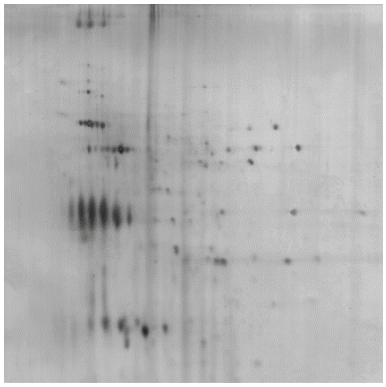

“Das entspricht vollkommen meinen an Daphnien gewonnenen Angaben und lässt sich einfach dahin formuliren, dass Riesenzellen Bacillen auffressen und sie dann ertödten. Dass daraus noch nicht der definitive Sieg der Phagocyten unbedingt folgt, leuchtet von selbst ein.”

Elias Metschnikoff, 1883,
Archiv für pathologische Anatomie und Physiologie und für klinische Medicin

Supplement

Table S1. Comprehensive list of identified phagosomal proteins by LC MS/MS

A	common to avidin , IgG and mannan LBP
B1	unique to avidin LBP
B2	unique to IgG LBP
B3	unique to mannan LBP

Summary

Phagocytosis, the cellular uptake of large particles, such as pathogens or apoptotic cells, usually starts with the recognition of specific ligands on the particle surface. The receptors engaged during phagocytic particle uptake determine the signalling events that occur during phagosome formation and maturation. However, pathogens generally have multiple ligands, making it difficult to dissect the roles of individual receptors in these processes.

In this study, I used latex beads coupled to single ligands, focusing on IgG, mannan, LPS, avidin and gelatin, as a model system of receptor mediated phagocytosis in mouse macrophages. The major aim of this thesis was to analyse whether initial receptor ligand interactions are able to influence not only the phagocytic uptake but also later events in phagocytosis, such as phagosome maturation. After the addition of coated latex beads to J774 macrophages, different phagocytic functions, such as phagocytic uptake rates and fusion of phagosomes with lysosomes, as well as macrophage gene expression were investigated. Additionally, phagosomes containing coated latex beads were isolated and their proteomic composition as well as their capability to bind to actin filaments *in vitro* were analysed. The following results could be obtained:

1. The model system of latex beads coupled to single or multiple ligands allows the investigation of several aspects of receptor mediated phagocytosis in more detail.
2. Particles coupled to mannan were internalised at higher rates and their phagosomes fused with lysosomes earlier after uptake than the ones formed by the other ligands.
3. The pattern of gene expression showed that each bead ligand upregulated a distinct pattern of genes, arguing against a common set of genes influenced during phagocytosis in general.
4. The analysis of phagosomal proteomes exhibited similar results, because the protein composition of isolated phagosomes was predominantly unique to the bead ligand.
5. Furthermore, isolated phagosomes also displayed differences in their capability to bind to actin filaments *in vitro* influenced by their ligand recognition during receptor specific phagocytosis.

These results demonstrate that interactions between receptor and ligand specifically modulate gene expression and protein composition of forming phagosomes that, collectively, contribute to cellular signalling and inflammatory processes as well as later stages of phagosome maturation and the association of phagosomes with actin filaments. The conclusion can be drawn that the activation of each receptor initiates a specific ‘signature’ that lasts many hours and influences several phagosome functions.

Introduction

1.1 Phagocytosis

Phagocytosis is one type of endocytosis, which generally describes the uptake of extracellular material. Phagocytosis is a process by which cells engulf large particles of a diameter >0.5 μm. Other endocytic routes exist, such as pinocytosis, which involves the ingestion of fluids and solutes and receptor mediated endocytosis, which can be subdivided into those dependent on clathrin and other, less well understood mechanisms, like pathways initiated by caveolae and lipid rafts (reviewed in Mousavi et al. 2004, Mayor & Pagano 2007).

The Ukrainian zoologist and microbiologist Ilya Mechnikov, also known as Elias Metschnikoff, first described phagocytosis nearly 125 years ago in the small fresh water crustacean Daphnia (Metschnikoff 1883). In protozoans, phagocytosis is mainly dedicated to nutrition, whereas in metazoans this activity is predominantly restricted to specialized cells, called professional phagocytes. Phagocytosis is essential for host defense against invading pathogens and the clearance of apoptotic cells, thereby playing a central role in tissue homeostasis. In addition, internalization and degradation of pathogenic microbes by professional phagocytes trigger activation of the innate and adaptative immune response after antigen presentation at the surface of the phagocytic cell. The phagocytic process is initiated by the recognition of specific ligands present on the surface of the phagocytosed particle. These interactions between receptor and ligand trigger a specific signalling pathway that activates actin cytoskeleton and membrane remodeling, leading to particle uptake. The organelle with the enclosed particle, termed phagosome, then fuses transiently and sequentially with the endosomal and lysosomal machinery to eventually degrade the phagosome content (Aderem & Underhill 1999).

Professional phagocytes are equipped for rapid and efficient uptake of invading microorganisms at sites of inflammation. In addition, these cells are crucial for antigen presentation and release of cytokines and chemokines to induce inflammation and the recruitment of components of the adaptive immune system (Aderem 2003). In mammals this task is mainly accomplished by two types of cells, members of the mononuclear phagocytic system like monocytes, macrophages and dendritic cells or by polymorphonuclear neutrophils. Members of the last group are short living cells (1 2 days) that are abundantly found in the blood of infected individuals but rarely in tissues. In contrast, macrophages are long living cells (several months) that can be located in different tissues, such as the connective tissue, the submucosa of the gastro intestinal tract, the lungs, the liver (Kupffer cells), the central nervous system (microglia), the bones (osteoclasts) and throughout the spleen, where they remove senescent blood cells (Janeway et al. 2004). All those cell types

originate from pluripotent stem cells present in the bone marrow that differentiate in response to hematopoietic factors. After differentiation, mononuclear phagocytes are released in the blood and remain circulating as monocytes, unless they are recruited to sites of inflammation by chemotactic signals and become macrophages which enter tissues (Janeway et al. 2004).

Macrophages have three major functions: phagocytosis, antigen presentation and the modulation of immune responses through production of various cytokines and growth factors. Macrophages thus represent a major defense against invasion of the host by a wide variety of microorganisms, including bacteria, viruses, fungi and protozoa. They play a critical role in the initiation, maintenance, and resolution of inflammation and are activated and deactivated during the inflammatory process. In response to cytokines and microbial products, macrophages become activated and express specialized and polarized functional properties. Macrophage activation is divided in the classical and the alternative pathway dependent on the involved cytokines released from T helper cells (Gordon 2003; Ma et al. 2003). Activation signals include cytokines like interferon gamma (IFN γ), granulocyte monocyte colony stimulating factor (GM CSF), and tumor necrosis factor alpha (TNF α), but also bacterial lipopolysaccharides, extracellular matrix proteins and other chemical mediators. Inhibition of inflammation by removal or deactivation of mediators and inflammatory effector cells is crucial to repair damaged tissues. Activated macrophages can be deactivated by anti inflammatory cytokines like interleukin 10 (IL 10) or transforming growth factor beta as well as by antagonist cytokines that are mainly produced by the macrophage itself.

In addition to professional phagocytes several other cell types, like epithelial cells and fibroblasts have been shown to be capable of phagocytosis and are referred as non professional phagocytes. These cells differ by their low efficiency of uptake and the limited range of particles that they internalise (Rabinovitch 1995). Often, such phagocytes can be induced by pathogens, e.g. by the interaction of *Shigella* species with epithelial cells (Clerc & Sansonetti 1987).

The phagocytic process is very complex, and one single model cannot be applied to describe the diverse cellular structures and signalling pathways associated with particle internalisation. However, this process can be divided into four major steps: 1.) binding of the particle to specific receptors present on the surface of the phagocytic cell triggering signalling events beneath the plasma membrane; 2.) internalisation through actin myosin cytoskeleton activation and plasma membrane deformation leading to an intracellular vesicle, termed the phagosome, enclosing the phagocytosed partice; 3.) a change of the intraphagosomal environment to antimicrobial conditions by fusion events with endosomal/lysosomal compartments and the acquisition of various hydrolases, the production of large quantities of

superoxide radicals from molecular oxygen and nitric oxide radicals from arginine as well as the acidification of the phagosome lumen by a membrane embedded proton pumping ATPase complex, all together termed as phagosome maturation; and 4.) degradation of the phagolysosomal content which can be accompanied by antigen cross presentation (Houde et al. 2003). Degradable substances may be used by the cell, are secreted from the cell via exocytic routes or in the case of non degradable material stay in phagolysosomes or lysosomes as residual bodies. Subsequently, these different steps of phagocytosis are described in more detail.

1.1.1 Phagocytic receptors

The phagocytic uptake is initiated by the recognition of ligands present on the surface of particles, especially microbes, by one or multiple selective receptor types that trigger specific signalling pathways activating particle internalisation. The ability of phagocytes to discriminate between different particles, cell debris and potential pathogens depends on those cell surface receptors. Two general mechanisms of receptor particle interaction have been identified in macrophages and neutrophils. Receptors can either interact directly with structural determinants on the particle surface (non opsonic phagocytosis) or bind indirectly to the particle via host supplied opsonins located on the surface of potential pathogens (opsonin dependent phagocytosis). Opsonins are mainly complement compounds and immunoglobulins delivered by the adaptive immunity response.

Professional phagocytes have evolved to express a broad array of membrane receptors that allow them to recognize a wide range of specific molecular determinants on phagocytic targets, which makes them a powerful tool of the immune system (Taylor et al. 2005). The signalling pathways triggered by the different phagocytic receptors are diverse and complex (Figure 1). This complexity can be also increased by the capacity of a variety of microbes to influence their fate as they are internalized. The fact that most particles are recognized by more than one receptor, and that these receptors are capable of signalling crosstalk and synergy, further complicates our understanding. In addition, many phagocytic receptors have a dual function, often mediating both adhesion and particle internalisation, and a complex relationship exists between these two related processes (Aderem & Underhill 1999). A primary challenge to the innate immune system is the discrimination of a large number of potential pathogens from self, utilizing a restricted number of phagocytic receptors. This challenge has been solved by the evolution of a variety of receptors that recognize conserved motifs on pathogens that are not found in higher eukaryotes (Kabelitz &

Medzhitov 2007). These motifs have essential roles in the biology of the invading agents, and they are therefore not subjected to high mutation rates. Janeway has proposed to call the phagocytic receptors, “pattern recognition receptors” and the targets of those receptors “pathogen associated molecular patterns” (Janeway 1992). Pathogen associated motifs include mannans in the yeast cell wall, formylated peptides, lipopolysaccharides and lipoteichoic acids on the surface of Gram negative and Gram positive bacteria. While direct pathogen recognition is a fundamental aspect of innate immunity, opsonisation allows diversification of the phagocyte recognition repertoire (Stuart & Ezekowitz 2005).

In macrophages, their involved receptors (Figure 1) can be classified in non opsonic phagocytic receptors, such as lectins (mannose receptor, DC SIGN, β glucan receptor), integrins and scavenger receptors (SR) or opsonic phagocytic receptors, like members of the Fc receptor (FcR) family, complement receptors (CR) and collectin receptors. A third group contains toll like receptors (TLR) which often function as co receptors in phagocytosis by their detection of a broad range of microbial products including lipopolysaccharide, peptidoglycan and bacterial lipopeptides (Underhill & Ozinsky 2002). Some of macrophage receptors that are essential for this study are characterized in more detail below.

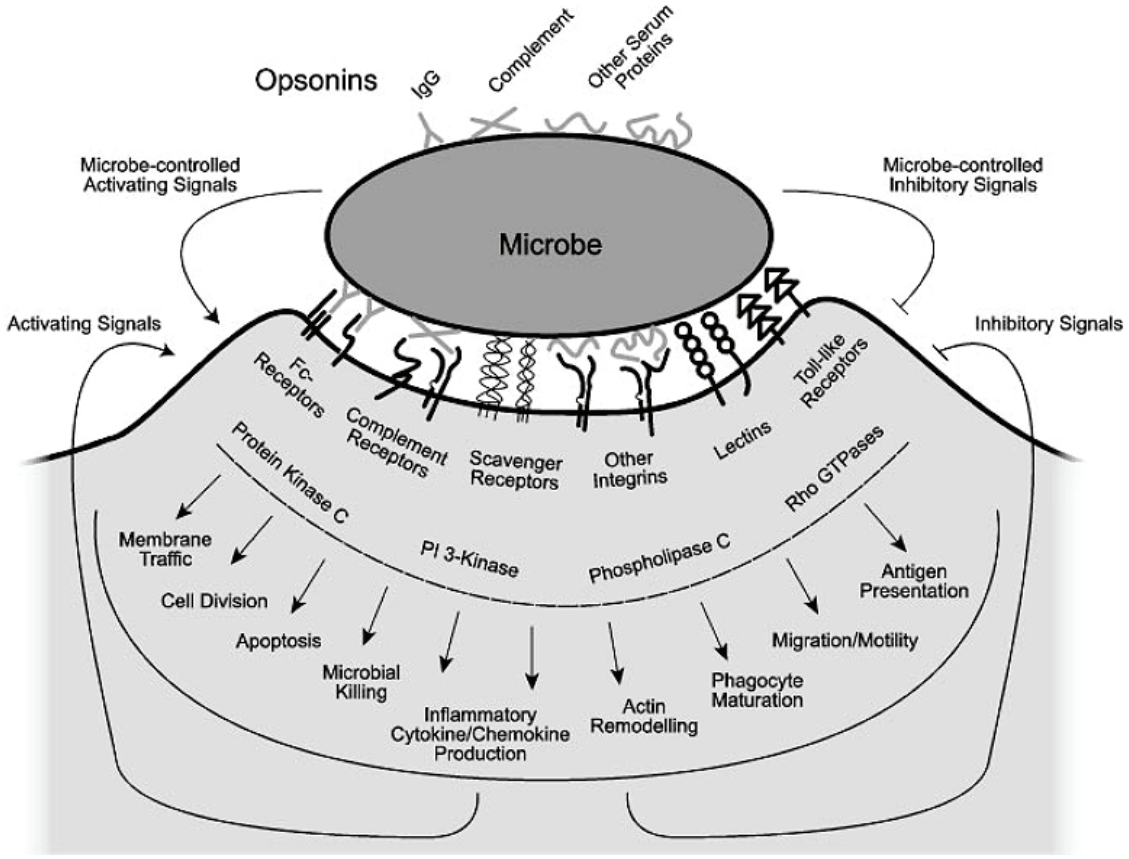

Figure 1. Receptor and signalling interactions during phagocytosis of microbes. Multiple receptors simultaneously recognise microbes both through direct binding and by binding to opsonins on their surface. Receptor engagement induces many intracellular signals by different enzymes that activate or inhibit further phagocytosis and microbe-induced responses (adapted from Underhill & Ozinsky 2002).

Mannose receptor (MR)

The mannose receptor (CD206) on macrophages has been identified as a 175 kDa membrane glycoprotein (Wileman et al. 1986) that recognizes mannose and fucose on the surfaces of pathogens and requires calcium and neutral pH for optimal ligand binding (reviewed in Stahl & Ezekowitz 1998). The MR is a single chain receptor with a short cytoplasmic tail and an extracellular domain including eight lectin like carbohydrate binding domains that share homology with other C type lectins including the mannose binding protein and the phospholipase A2 receptor (Ezekowitz et al. 1990). The cytoplasmic tail is crucial to both the endocytic and phagocytic functions of the receptor, but little is known about the signals that lead to phagocytosis.

Several studies suggested that exclusive activation of the mannose receptor cannot induce phagocytosis and other co receptors are usually needed (Kang et al. 2005; Taylor et al. 2005). The high affinity of this receptor for branched mannose and fucose oligosaccharides makes the MR a phagocytic receptor with broad pathogen specificity. Importantly, the mannose receptor is able to recognize a prominent lipoglycan of the cell wall of *Mycobacterium tuberculosis*, the terminal mannose capped lipoarabinomannan (ManLAM) which contributes together with complement receptors to the internalisation of these pathogens (Fenton et al. 2005). In contrast, phosphatidylmyoinositol capped lipoarabinomannan (PILAM) from avirulent *Mycobacterium smegmatis* does not engage the MR (Schlesinger et al. 1994), but rather toll like receptor 2 (TLR2), and thereby activating a proinflammatory response (Means et al. 1999). Thus, the terminal components of ManLAM are very important in host cell recognition and response and induce an anti inflammatory program (Nigou et al. 2001). However, in addition to this and dependent on the recognized ligands, also proinflammatory signals can be also generated upon MR ligation, like production of TNF α and IL 12 (Garner et al. 1994; Shibata et al. 1997).

The signalling events during mannose receptor mediated phagocytosis modulate cytoskeletal rearrangements as well as changes in phagosomal trafficking. As an example, MR dependent phagocytosis of zymosan mobilizes the actin cytoskeleton around nascent phagosomes, and proteins such as F actin, talin, PKC and myosin I are recruited (Allen & Aderem 1996). However, in contrast to FcR and CR mediated phagocytosis, vinculin and paxillin are not recruited to MR phagosomes, reinforcing the notion that different phagocytic receptors send different signals to the actin cytoskeleton and initiate different mechanisms of internalisation (Allen & Aderem 1996). The MR has also been implicated in antigen uptake and processing (Prigozy et al. 1997).

Scavenger receptors (SR)

Scavenger receptors are a family of structurally diverse receptors having broad ligand specificity that includes low density lipoproteins, phosphatidylserine and polyanionic compounds (Krieger & Herz 1994). Based on primary sequence information, SRs have been divided into at least six groups, and receptors from several of these groups are expressed on macrophages. One member, SR A, is a homotrimeric glycoprotein with an extracellular ligand binding domain and represents an important nonopsonic receptor involved in foam cell formation as well as host defense (Krieger 1997). Direct evidence for involvement of SR A in macrophage phagoctosis of apoptotic cells comes from studies on the phagocytosis of apoptotic thymocytes by thymus derived macrophages *in vitro* (Platt et al. 1996). Several studies with wild type and knockout mice have implicated SR A in microbial susceptibility to bacterial infection *in vivo* including *Listeria monocytogenes* and *Staphylococcus aureus* (Platt et al. 2002). However, scavenger receptors are also believed to recognise but not significantly cause internalisation of different particles and could participate in the more non specific uptake of ligands like avidin and gelatin.

Fc family of receptors (FcR)

Most of our understanding of the signalling pathways leading to phagocytosis in macrophages comes from studies of receptors binding to the Fc region of immunoglobulin (Ig), the so called Fc receptors (FcR). Receptors for IgG (FcγR), IgE (FcεR) and IgA (FcαR) have been described (Janeway et al. 2004). Interaction of FcRs with their immunoglobulin ligands triggers a wide series of leukocyte responses including phagocytosis, respiratory burst, antibody dependent cell mediated cytotoxity, release of pro inflammatory mediators and production of cytokines (Sanchez Mejorada & Rosales 1998). Among FcRs, only FcαR und FcγR are capable of mediating phagocytosis. FcαR is expressed in neutrophils, monocytes and macrophages. The three classes of FcγRs (FcRI, FcRII, FcRIII) are expressed differentially in many cell types of the immune system.

In all mammalian species studied to date, four different classes of Fcγ receptors have been defined: FcγRI (CD64), FcγRII (CD32), FcγRIII (CD16), and FcγRIV (Nimmerjahn & Ravetch 2006). Whereas FcγRI displays high affinity for the antibody constant region and restricted isotype specificity, FcγRII and FcγRIII have low affinity for the Fc region of IgG but a broader isotype binding pattern (Hulett & Hogarth, 1994). FcγRIV is a recently identified receptor, conserved in all mammalian species with intermediate affinity and restricted subclass specificity (Nimmerjahn et al., 2005). Functionally, there are two different classes of Fc receptors: the activation and the inhibitory receptors, which transmit their signals via

immunoreceptor tyrosine based activation (ITAM) or inhibitory motifs (ITIM), respectively (Ravetch & Lanier, 2000). The paired expression of activating and inhibitory molecules on the same cell is the key for the generation of a balanced immune response. When an opsonized particle binds to Fcγ receptors, the receptors cluster, a process initiating the assembly of a signalling complex on the cytoplasmatic side of the membrane. After its phosphorylation, the ITAM motif acts as a docking site for members of the Syk family of tyrosine kinases which cause their phosphorylation and subsequent activation. Syk has been reported to be involved in activating F actin rearrangement that sustains phagocytic cup formation (Greenberg 1999).

Toll-like receptors (TLR)

Toll like receptors recognize specific patterns of microbial components, especially those from pathogens, and regulate the activation of both innate and adaptive immunity. First characterised in *Drosophila*, the TLR family in mammals consists of more than 10 members and is characterized structurally by the presence of a leucine rich repeat (LRR) domain (Takeda et al. 2003). While TLR2 recognizes a variety of microbial components from Gram negative and Gram positive bacteria, including mycobacteria, *Staphylococcus* sp. (Underhill et al. 1999) as well as some atypical LPS (Werts et al. 2001), TLR4 is the central receptor for the recognition of lipopolysaccharide (LPS), a major cell wall component of Gram negative bacteria (Poltorak et al. 1998). Recognition of LPS requires other molecules in addition to TLR4, like CD14 and LPS binding protein, which interact to initiate signalling pathways (Jiang et al. 2000). In addition to LPS, TLR4 recognizes several other ligands present on murine retroviruses (Rassa et al. 2002) and some heat shock proteins (Asea et al. 2002), being likely the receptor responsible for the inflammatory responses elicited by those proteins. Thus, TLR4 is presumably involved in several aspects of the inflammatory response by recognizing endogenous ligands produced during inflammation, even in the absence of infection. However, it should be noted that all endogenous TLR4 ligands activate immune cells only at very high concentration, which is in sharp contrast to the much lower concentrations required for LPS.

CD14

In addition to membrane spanning hydrophobic residues for the association with plasma membrane, cell surface receptors can also use a phosphatidylinositol based glycolipid (GPI) to anchor in cell membranes. One example that is highly expressed in macrophages is CD14 which was identified as a receptor for LPS (Wright et al. 1990). Because CD14 does not contain a transmembrane domain, accessory molecules are needed for signal transduction.

The N terminal portion of CD14 is important for LPS binding and the interaction with accessory receptors (Juan et al. 1995). In recent years, TLR4 and TLR2 were identified as co receptors with CD14 for specific microbial ligands (Triantafilou & Triantafilou 2002). In addition to this, CD14 has also been implicated in recognition and internalisation of apoptotic cells. Interestingly, although apoptotic cells bind to CD14 at a site close to the LPS binding site, they do not elicit inflammatory responses, such as TNF α production, that are induced in macrophages by LPS (Devitt et al. 1998).

It is important to mention that during phagocytosis, ligands on the surface of a particle orchestrate a set of signalling events that are necessary to engulf the particle and enclose it in the phagosome. Although a single ligand on the particle can efficiently induce phagocytic uptake, most pathogens have many different ligands on their surface. The more complex process of phagocytic uptake of pathogens occurs via multi ligand interactions, which also offer the opportunity of more specific immune responses. In this case many receptors are engaged, as it occurs during uptake via the zipper mechanism (see below). The different ligand receptor interactions undoubtedly contribute into the overall process of phagocytosis, even in the later stage of phagosome maturation. How these interactions influence the final steady state identity of the phagosome is less well understood. At present, it is unclear for example whether multiple receptors signal in synergy and in the same extent in response to ligand binding or whether a single receptor will dominate the different induced signalling pathways.

1.1.2 Phagocytic internalisation and signalling

After the recognition of ligands on the surface of a particle by phagocytic receptors, signalling events occur leading to phagocytic cup formation and uptake of the particle (Garcia Garcia & Rosales 2002). Phagosome formation is a complex sequence of events requiring not only signalling, but also transduction of information and engagement of the cytoskeleton and of membrane fusion and fission machinery. Two models have been proposed to describe the uptake process. First, the “zipper” mechanism that was mentioned before, proposed that the particle internalisation occurs by sequential recruitment of cell surface receptors to ligands on the particle surface, closing tightly and progressively the plasma membrane around it (Griffin & Silverstein 1974; Griffin et al. 1975). Studies on FcγR mediated phagocytosis support this hypothesis (Show & Griffin 1981; Montesano et al. 1983). The “zipper” mechanism is characterized by the extension of long and thin membrane pseudopods around the particle.

In contrast, pathogens bound to CR3 do not cause major membrane deformation, but rather seem to sink into the cell (Underhill & Ozinsky 2002). The second model is called the “trigger” mechanism, where upon particle binding an all or none phagocytic response is initiated. In this case, large membrane protrusions will extend and enclose rapidly the particle in one step. This type of uptake has been described for bacterial entry into epithelial cells and macrophages (Swanson & Baer 1995).

The remodeling of the plasma membrane during phagocytic cup formation, in particular the initial extension of pseudopodia that grow and enclose the particle, requires the localized and rapid assembly of actin filaments (F actin) at the site of ingestion (Allison et al. 1971). Studies on the regulation of F actin reorganization have identified several proteins and lipids playing a direct role in this process. Key regulators of cytoskeleton dynamics during phagocytosis include guanine nucleotide exchange factors (GEFs), adaptor molecules with associated GEF activity, Rho family GTPases, actin nucleation promoting factors, such as the Arp2/3 complex and contractile activity provided by several myosin isoforms (Castellano et al. 2001; Brandt et al. 2007). In dependence of the involved receptors different enzymes can be involved in the early signalling pathways (Garcia Garcia & Rosales 2002). Phagocytosis by FcR is initiated by the clustering of these receptors followed by phosphorylation of specific tyrosine residues within special amino acid motifs (Isakov 1997). It is caused by enzymes of the Src tyrosine kinase family. At least six members of the Src family have been identified in phagocytes: Fgr, Fyn, Hck, Lyn, Yes, and Src, which have been found associated to specific receptors (Korade Mirnics & Corey 2000). After phosphorylation, the tyrosine kinase Syk is recruited and activated to phagocytic sites (Darby et al. 1994), which is essential for actin remodeling by forming a molecular complex containing several proteins that contribute to the regulation of actin reorganization (Coppolino et al. 2001). The downstream pathways stimulated by active Syk are not completely understood, but include many signalling molecules, such as calcium, protein kinase C, phospholipase A2, C and D as well as phosphatidylinositol 3 kinase and the extracellular signal regulated kinase ERK (Garcia Garcia & Rosales 2002).

These enzymes modulate several classes of lipids, which are involved in phagosome formation including 1) glycerophospholipids, 2) cholesterol, 3) sphingolipids and 4) phosphoinositides (Yeung & Grinstein 2007). 1) The group of glycerophospholipids contains phosphatidylcholine (PC), which is hydrolyzed by phospholipase D to generate the metabolically active phosphatidic acid (PA), as well as phosphatidylserine (PS), lysophosphatidic acid (LPA) and arachidonic acid (AA). After exposure to immunoglobulin G opsonized targets, macrophages produce PA, which is involved in particle engulfment and

promotes membrane fission (Kusner et al. 1999). External PS serves as a major recognition signal for phagocytosis of apoptotic cells (Marguet et al. 1999). LPA activates G protein coupled receptors and binds to cognate cell surface receptors that are coupled to heterotrimeric G proteins that signal through the MAPK pathway (Fueller et al. 2003). Arachidonic acid is a key lipid in cellular signalling with multiple functions and is generated on engagement of phagocytic receptors by phospholipase A2 (Fernandez et al. 2003). It activates subunits of the NADPH oxidase (Li & Catheart 1997) and is important in various physiological and pathological processes, including inflammation, because it is metabolized to leukotrienes and prostaglandins, which are potent proinflammatory mediators (Diaz & Arm 2003). 2) Cholesterol is taken up by cells through the receptor mediated internalization of lipoprotein complexes and is delivered to the endocytic pathway (Ikonen 2006). It is present in phagosomes and modulates targeting and retention of Rab family GTPases (Holtta Vuori & Ikonen 2006). 3) The third group of signalling lipids contains sphingolipids like ceramides, sphingomyelin (SM) and sphingosine, which form cellular lipid rafts including Src family kinases (Kwiatkowska et al. 2003), as well as sphingosine 1 phosphate (S1P), which is involved in phagosome formation (Treede et al. 2007) and maturation (Spiegel & Milstien 2007). 4) Phosphoinositides, which exist as mono , bi or triphosphoinositides in the cell, possess multiple functions in phagocytosis (Yeung & Grinstein 2007). Phosphatidylinositol 4,5 bisphosphate [PI(4,5)P2], which is important for this study, is well known for its role in actin remodeling and was identified at the forming phagosome (Botelho et al. 2000). PI(4,5)P2 can be hydrolyzed to generate the second messengers inositol 1,4,5 triphosphate (IP3) and diacylglycerol (DAG), which mobilize calcium stores and activate protein kinase C.

Several studies have shown that different enzymes and lipids are involved in signalling cascades, which induce the initial steps of phagocytosis, like the extension of pseudopods. Essentially, *de novo* polymerized actin filaments provide the structural network that supports myosin driven contractile activity to tightly enclose the particle (Swanson et al. 1999). Several myosin isoforms from myosin classes I, II, V, VII, IX and X have been found located around nascent phagosomes, suggesting that they are required transiently for phagosome internalization and closure (Figure 2). Myosin IC, IXb and X seem to be key players in the extension of phagocytic cup pseudopods (Swanson et al. 1999; Diakonova et al. 2002; Cox et al. 2002), whereas myosin II promotes closure of the cup (Olazabal et al. 2002). Myosin VII has been implicated in phagocytic uptake both in *D. discoideum* and mammalian cells (Titus 1999). Following internalization, myosin V regulates the early stage of phagosome maturation. This motor protein rapidly associates with the phagosome after phagocytic cup closure and modulates the transitional step of phagosomal binding to cortical

actin filaments followed by switching to the microtubule network (Al Haddad et al. 2001). Microtubule association of phagosomes is crucial for their centripetal movement towards the center of the cell and their fusion with endo lysosomal compartments (Blocker et al. 1998; Araki 2006), which is essential for the degradation of the phagosomal content (described below).

After phagocytic cup closure, F actin is rapidly depolymerised and the newly formed phagosome becomes accessible for fusion events with compartments of the endocytic pathway (Swanson & Baer 1995). The following steps, referred to as phagosome maturation, are defined as the process by which phagosomes change their functional capacity as they age within cells. The main inducer of these alterations in phagosome behaviour is thought to be the sequential process of fusion, which takes place first with early endosomes and then with the late endosomes and lysosomes (Pitt et al. 1992a; Griffiths 2004).

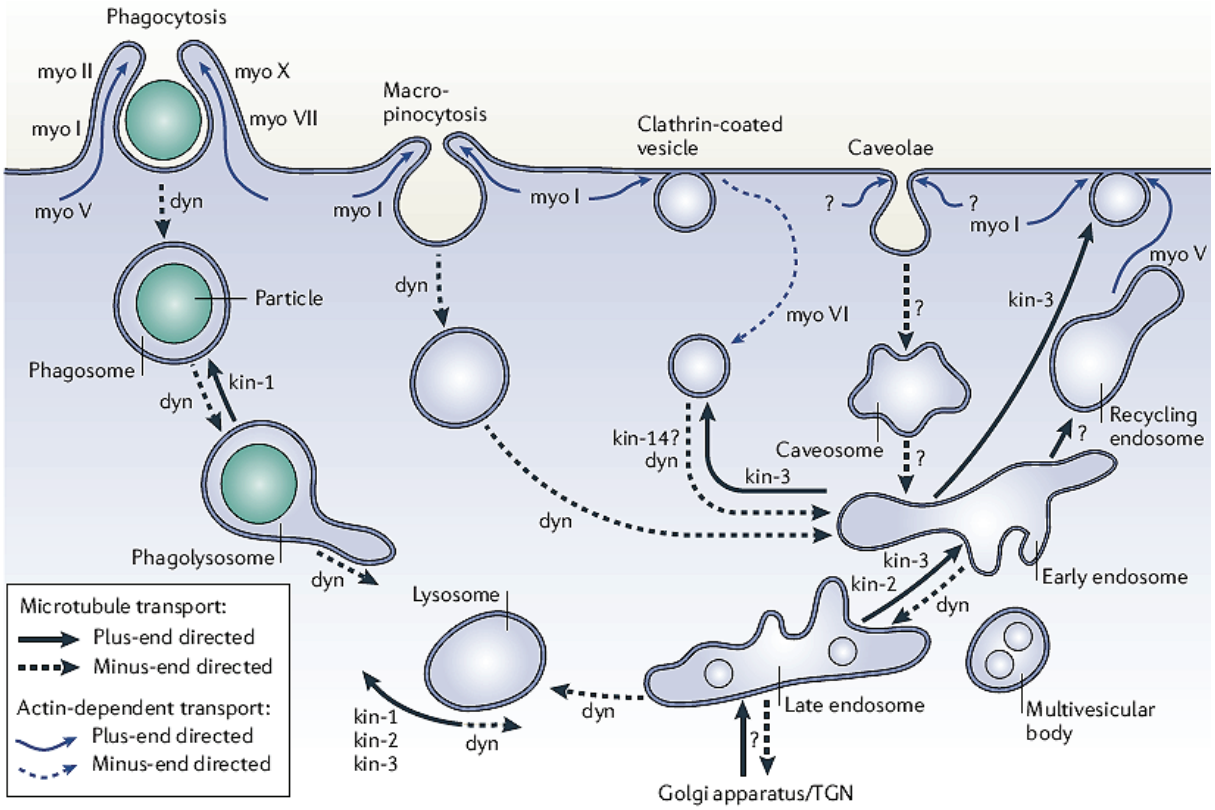

Figure 2. Overview of the motors that are involved in endocytic and recycling traffic (adapted from Soldati & Schliwa 2006). Cargoes are transported within cells along actin filaments or microtubules by the help of different classes of myosin (myo), kinesin (kin) or dynein (dyn). Shown are different pathways that are implicated in endocytic traffic, like phagocytosis, macropinocytosis, the clathrin-dependent pathway and the caveolae pathway. The different cargoes are destined for degradation or are recycled either to the plasma membrane (directly or through recycling endosomes) or to the Golgi apparatus.

1.1.3 Phagosome maturation

After the enclosure of particles at the cell surface the newly formed phagosomes are interacting with compartment of the endocytic pathway. The membrane that is needed to form nascent phagocytic vacuoles is composed largely of the plasmalemma, as it derives from its extension or inward deformation. However, it was shown that supplementary membrane from intracellular pools is delivered to forming phagosomes (Aderem 2002). For example, recycling endosomes fuse with phagosomes during their formation, a process known as focal exocytosis (Bajno et al. 2000). Many proteins, mostly identified for their role in membrane traffic, are required for the fusion of vesicles with the forming phagosome. These include SNAREs, proteins known to promote vectorial docking and fusion of membranes; Rab 11, a GTPase that promotes the trafficking of recycling endosomes to the plasma membrane and amphiphysin and dynamin 2, two interacting proteins involved in regulating endocytosis (Aderem & Underhill 1999; Greenberg & Grinstein 2002). More recently, studies presented a significant body of evidence indicating that the endoplasmic reticulum is also directly involved in the formation of nascent phagosomes (Müller Taubenberger et al. 2001; Gagnon et al. 2002). ER mediated phagocytosis is believed enabling phagosomes to play a direct role in the processing and presentation of exogenous peptides on major histocompatibility complex class I molecules, a process referred to as cross presentation (Houde et al. 2003; Desjardins 2003). Although the extent of contribution of the ER to forming phagosomes is still a matter of debate, there are compelling recent results that support this hypothesis (Hatsuzawa et al. 2006; Stuart et al. 2007).

Phagosomes undergo changes in their composition due to a progressive maturation process that ultimately leads to a hybrid organelle, the phagolysosome (Mayorga et al. 1991; Desjardins et al. 1994). The primary function of the phagolysosome is to degrade the phagocytosed particle. To fulfil this function, phagolysosomes possess a variety of complementary degradative properties, including a very low pH, hydrolytic enzymes for particle digestion, defensins and other bactericidal peptides and the ability to generate toxic oxidative compounds (Tapper 1996; Tjelle et al. 2000). The maturation process that equipped the phagosome with lytic activity depends critically on the interaction of the nascent vacuole with the endocytic pathway, which is organized as a continuum of organelles ranging from early endosomes to lysosomes.

During endocytosis, solutes, membrane bound ligands and transmembrane proteins are trapped in small vesicles derived from the plasma membrane. Following formation, endocytic vesicles are first targeted to early (or sorting) endosomes. These organelles are

often tubulovesicular and can be typically recognized by the presence of the small GTPase Rab5 or early endosome antigen 1 (EEA1). The lumen of early endosomes is relatively poor in proteases and is mildly acidic with a pH of ~6.0 (Barbieri et al. 1996). From these organelles cargo can be directed towards recycling endosomes, which are morphologically and biochemically distinct and less acidic (pH ~6.5) or to late endosomes which are comparatively enriched in hydrolytic enzymes with a pH ~5.5 (Vieira et al. 2002). Recycling endosomes can be identifed by the presence of Rab11 (Ullrich et al. 1996), whereas the multivesicular late endosomes are characterized by the presence of Rab7, Rab9, mannose 6 phosphate receptor and lysosomal associated membrane proteins (LAMP; Somsel Rodman & Wandinger Ness 2000). It is agreed that lysosomes are the final step during endosomal trafficking, that they contain the bulk of active proteases and lipases and are extremely acidic (pH ~4.5 5.5). They characteristically contain LAMPs and hydrolytic enzymes such as cathepsin D, but, while these proteins were thought to be unique to lysosomes, it is now apparent that they are also found in late endosomes. Therefore the best method for lysosome identification is their labelling by pulse/chase loading with fluid phase markers, such as fluorochrome conjugated dextran (Kielian et al. 1982), or labelled nanometer sized gold particles that accumulate in these organelles (Deng et al. 1991).

Interactions between phagosomes and endosomes occur soon after phagosome sealing, in a fashion that recapitulates the endocytic sequence (Figure 3): nascent phagosomes fuse initially with early endosomes, followed by late endosomes and ultimately lysosomes (Desjardins et al. 1994; 1997). There are several lines of evidence that early phagosomes interact preferentially with early endocytic vesicles and display markers such as transferrin receptor (TfR), EEA1 and Rab5 but are devoid of late endosomal/lysosomal markers (Pitt et al. 1992a; Scianimanico et al. 1999; Duclos et al. 2000). Afterwards integral and peripheral proteins such as TfR and EEA1 are eliminated from phagosomes during maturation and some phagosomal proteins, including Fc and mannose receptors, were shown to traffic retrogradely to the plasma membrane, suggesting that recycling from phagosomes occurs (Muller et al. 1983; Pitt et al. 1992b). Phagosomes rapidly lose the characteristics of early endosomes while recruiting those of late endosomes, best exemplified by the presence of Rab7, the mannose 6 phosphate receptor and lysobisphosphatidic acid (Via et al. 1997). The existence of late endosome components on phagosomes is followed by a transition into phagolysosomes by association with lysosomal compartments identified by the presence of hydrolytic proteases, such as different cathepsins, and by the acquisition of an extremely acidic pH, reported to be as low as 4.5 (Clemens & Horwitz 1995).

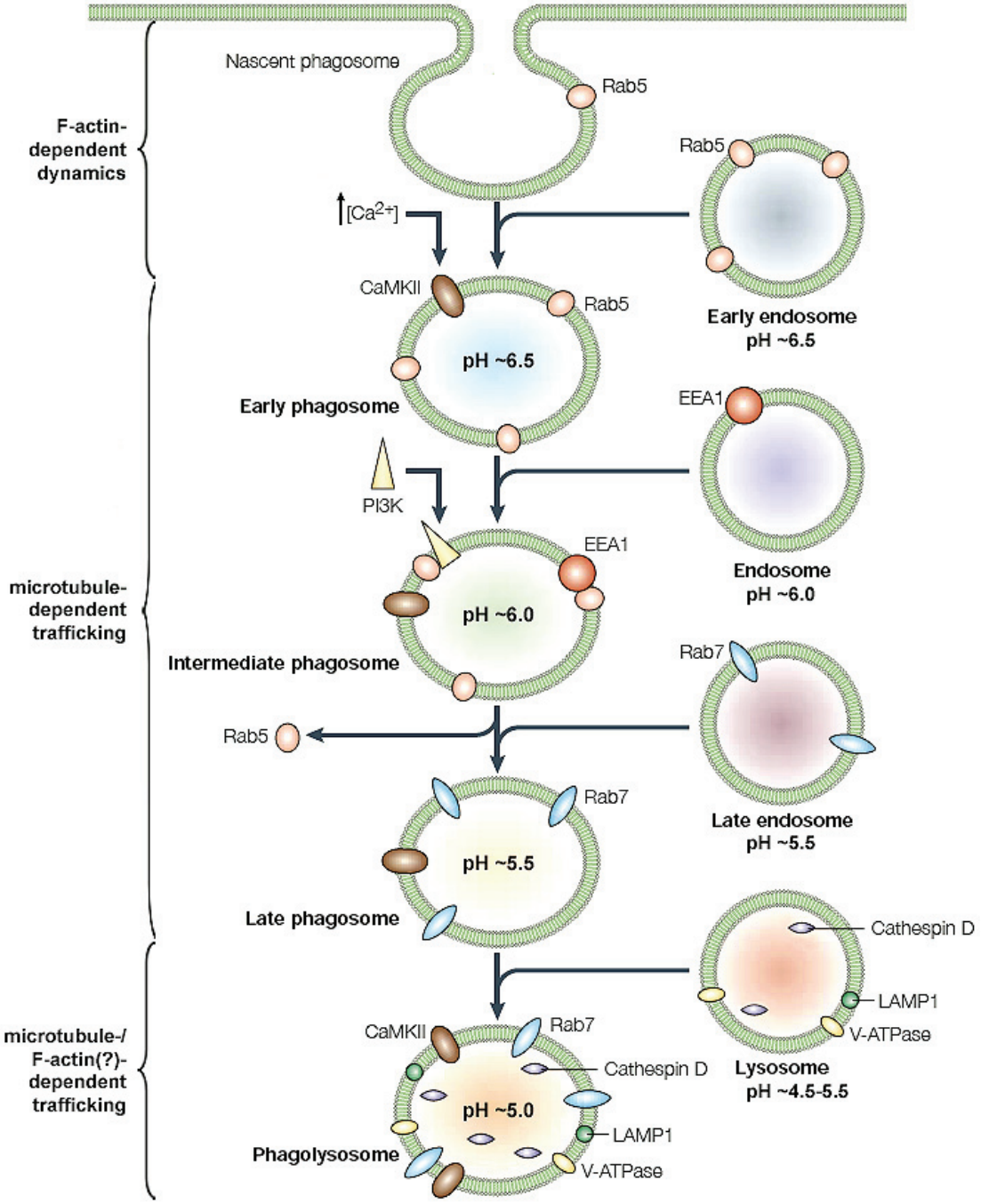

Figure 3. Phagosomal maturation pathway in macrophages (adapted from Koul et al. 2004). Nascent phagosomes acquire the GTPase Rab5 either from the plasma membrane or by fusion with early endosomes. Ca^{2+} activates the calmodulin-dependent protein kinase (CaMKII), which, together with Rab5, is necessary for recruitment of phosphatidylinositol-3-kinase (PI3K). PI3K generates phosphatidylinositol-3-phosphate (PI3P) followed by subsequent recruitment of early endosomal antigen (EEA1) from endosomes. EEA1 is a Rab5 effector that triggers fusion of phagosomes with late endosomes. During the course of phagosomal maturation, the early endosomal markers Rab5 and EEA1 are lost from the intermediate phagosome, which then fuses with late endosomes and thereby acquires Rab7. Late phagosomes fuse with lysosomes to form phagolysosomes, which are characterized by the presence of hydrolytic proteases, such as cathepsin D, the proton-ATPase pump (V-ATPase) and lysosome-associated membrane glycoprotein 1 (LAMP1). During maturation, fusion events change the pH of phagosomes from neutral to acidic conditions. F-actin dynamics are important for engulfment and formation of phagosomes, whereas subsequent phagosomal/endosomal trafficking rely predominantly on microtubules. Although there are hints for the involvement of F-actin and associated proteins at later stages of phagosome maturation, their contribution is not clear.

Subsequent to phagocytosis in macrophage, there is an abrupt increase of superoxide formation known as the oxidative burst, which is catalyzed by an NADPH oxidase enzyme complex. The NADPH oxidase is a membrane associated enzyme complex that generates superoxide (O_2^-) by the one electron reduction of oxygen, using NADPH as the electron donor (Babior, 1999). The NADPH oxidase is activated on phagosomes and generates superoxide to aid in the killing of phagocytosed microorganisms. It is important that superoxide is primarily released into phagosomes to prevent damage to surrounding cells (Ridley, 2001). The subsequent superoxide formation mainly occurs through FcR activation. However, the stimulation of CR3 by anti CR3 antibody coated particles (Serrander et al., 1999), by Staphylococcus particles coated with anti CD18 antibodies (Lofgren et al., 1999) induces superoxide production. The pathway linking generation of ROS to downregulation of Rho involves inhibition of the low molecular weight protein tyrosine phosphatase and then an increase in the tyrosine phosphorylation and activation of its target, p190Rho GAP (Nimnual et al., 2003). Despite the multiple events associated with superoxide formation, it remains to be studied in detail how NADPH oxidase complex is activated. As for the cell death and apoptosis of phagocytes including macrophages and neutrophils, studies have mainly been focused on conditions that lead to endogenous production of ROS or nitric oxide (NO). Earlier studies showed that phagocytotic apoptosis was induced through CR and FcR ligation (Coxon et al., 1996; Gamberale et al., 1998) and Rho GTPases regulates the phagocytosis mediated through FcR and CR3 (Caron and Hall, 1998; Massol et al., 1998), which may be implicated to the superoxide formation. On the other hand, overexpression of src homology 2 domain containing inositol 5' phosphatase (SHIP) in macrophages leads to an inhibition of phagocytosis mediated by FcγR and CR3 (Cox et al., 2001).

The active role of phagosomes in directing their own maturation is supported by *in vitro* experiments showing that phagosomes isolated 1 h after formation fuse preferentially with lysosomes, but not with earlier endocytic organelles (Desjardins et al. 1997; Jahraus et al. 1998; Kjeken et al. 2004). The fusion processes that occur between phagosomes and endocytic organelles can be completely or only partially. The latter case is known as “kiss and run” hypothesis (Desjardins 1995) that describes transient fusion events between these organelles, which allows the transfer of selected membrane and luminal contents between phagosomes and endosomes. This is promptly followed by a fission event preventing the complete intermixing of the two compartments.

The dynamic role of the cytoskeleton in phagosome maturation

The intracellular localization as well as the trafficking of many organelles of the endocytic pathway is strongly dependent on their association with cytoskeleton components (Figure 2). There are several lines of evidence that endocytic organelles including phagosomes interact with microtubules and actin filaments as well as their associated motor proteins during different maturation stages (Araki 2006; Soldati & Schliwa 2006). Newly formed phagosomes that have lost their F actin coat after internalisation, rapidly engage in centripetal motion that is arrested by microtubule disruption (Blocker et al. 1998). Interestingly, phagosomes were shown to possess bidirectional movement along microtubules both *in vitro* and *in vivo*, although displacement towards the minus ends predominated (Blocker et al. 1997). It is widely accepted that microtubule based motility is essential for correct phagosomal maturation (Blocker et al. 1996; Funato et al. 1997) which is supported by the observations of Desjardins and co workers, who found that phagosomes acquired 5 fold less LAMP 2, when microtubules were disrupted by nocodazole (Desjardins et al. 1994).

As mentioned before, actin filaments together with different classes of associated motor proteins are responsible for particle engulfment and phagosome formation. Actin filaments do not only play an essential role during phagocytic particle ingestion. There are many hints suggesting that organelle motility and distribution not only depend on microtubules, but also involve the actin cytoskeleton (Kelleher & Titus 1998; DePina & Langford 1999). A role for actin in phagosome maturation appears to be contrary to the notion that, once severed from the plasma membrane, phagosomes are devoid of actin. This simplistic view has been changed by several observations. First, in cells mature phagosomes were reported to be often surrounded by an actin rich coat (Toyohara & Inaba 1989). Secondly, actin was identified by western blotting and proteomic analysis on isolated late phagosomes from macrophages (Desjardins et al. 1994; Garin et al. 2001). Lastly, it was shown that actin filaments can assemble *de novo* on the surface of isolated late phagosomes without any additional cytoplasmic components (Defacque et al. 2000; Kjeken et al. 2004). These observations correlate with the fact that numerous actin binding proteins, including myosins, annexins, α actinin and coronin are found associated with phagosomes (Al Haddad et al. 2001; Morrissette et al. 1999) and can be found in proteomic analyses of phagosomes (Garin et al. 2001; Gotthardt et al. 2002; Stuart et al. 2007). Like microtubules, actin filaments are highly dynamic and polarized polymers and can associate with endosomes and lysosomes (vanDeurs et al. 1995; Taunton 2001). It has been observed that endosomes and lysosomes can be propelled in the cell by the formation of actin comet tails in a manner dependent on N WASP, Cdc42 and protein kinase C (Taunton et al. 2000).

What is the relationship between actin and the phagosome after its detachment from the surface membrane? One explanation proposed by Griffiths and co workers is summarized in the so called actin track model (Kjeken et al. 2004). This group has shown that the actin filaments assembled at the phagosomal membrane display their fast growing barbed end at the membrane and the minus end growing away from it, meaning that the monomers are inserted at the membrane. In addition, they demonstrated that this process is modulated by ezrin and moesin (Defacque et al. 2000). Because the majority of myosins move unidirectionally along actin filaments toward the barbed end (Hasson & Cheney 2001), the actin filaments could provide tracks that guide vectorially the myosin bound cargo, e.g. lysosomes, toward the actin nucleating phagosome. Therefore, an actin assembly of maturing phagosomes could help to facilitate lysosomes clustering around phagosomes and subsequent fusion events between the two organelles.

1.1.4 Degradation and antigen presentation

The last step of the phagocytic process is marked by the degradation of the phagosomal content, which can be accompanied by antigen presentation on the surface of the macrophage (Niedergang & Chavrier 2004). Hydrolases delivered to the phagosomal lumen contribute to the degradation of the ingested material. Interestingly, evidence indicates that hydrolases are not acquired by phagosomes through a simple one step fusion event with lysosomes all at once, as implied in the term ‘phagolysosomes’. Instead, as indicated by the protein profile of phagosomes obtained by two dimensional gel electrophoresis, the subsets of hydrolases acquired by phagosomes vary throughout the maturation process whereby newly formed phagosomes become phagolysosomes (Garin et al. 2001). The kinetics of protease acquisition may also vary between phagocytes, for instance, it is faster in macrophages than in dendritic cells (Lennon Duménil et al. 2002). The proteins present on engulfed particles encounter an array of degrading proteases in phagosomes. Peptides derived from processing are then loaded onto major histocompatibility complex (MHC) class II molecules, originating mostly from newly synthetized pools stored in endocytic compartments, such as late endosomes or multivesicular bodies, as well as lysosomes and lamellar bodies (Hiltbold & Roche 2002). Phagosomes containing latex beads have been shown to acquire MHC class II molecules both from a recycling pool on the plasma membrane and from a newly synthesized pool (Ramachandra & Harding 2000). Although several cysteine proteases can be involved, the step of processing is mainly dependent on cathepsin S (Watts 2004). MHC class II molecules are then expressed on the surface of the

phagocytic cell to activate CD4+ T lymphocytes (reviewed in Ramachandra et al. 1999; Jutras & Desjardins 2005).

The common view has long been that exogenous proteins, internalized by endocytosis or phagocytosis, are presented by the MHC class II pathway. A large body of evidence indicates that antigens from pathogens, including mycobacteria, *Salmonella* and *Leishmania*, can elicit an MHC class I dependent response (Kaufmann & Schaible 2005). These peptides presented by MHC class I molecules can activate cytotoxic CD8+ T lymphocytes in a process called 'cross presentation' (reviewed in Lehner & Cresswell 2004; Jutras & Desjardins 2005). Peptide loading on MHC class I molecules normally occurs in the endoplasmic reticulum (ER) after translocation of the peptides processed via the cytosolic degradative proteasome complex. Further insights into the molecular mechanisms linked to cross presentation came from proteomics analysis of latex bead containing phagosomes indicating that several ER proteins known to play a role in MHC class I mediated antigen presentation, but no Golgi resident protein, were present on phagosomes (Garin et al. 2001). On the basis of these observations, it was shown that the ER is recruited to phagocytic cups to provide some of the membrane required for the formation of phagosomes (Gagnon et al. 2002). Fusion of phagosomes with the ER provides this organelle with components of the class I presentation machinery: Sec61 transporters, chaperones, the ubiquitination machinery, proteasome subunits and TAP (transporter associated with antigen presentation) proteins have been found associated with the phagosome (Houde et al. 2003; Guermonprez et al. 2003; Ackerman et al. 2003).

The described mechanisms link both, innate and adaptive immunity. Additional to immune responses, phagocytes are also able to ultimately recycle the phagosomal content out of the cell. This property, long considered a peculiarity of *Dictyostelium discoideum*, has also been observed in macrophages (Di et al. 2002). The fact that several proteins involved in membrane trafficking, including annexins, synaptobrevin and syntaxins, are found on phagosomal membranes suggested that mature phagosomes potentially fuse with membraneous structures including the plasma membrane. Furthermore, it was demonstrated that microtubules participate in the egestion process, whereas cortical actin prevents it (Damiani & Colombo 2003).

1.1.5 Alteration of phagosome functions by pathogens

The above described events of phagocytic uptake and phagosome maturation are part of innate immunity and serve predominantly to destroy invading pathogens. However,

numerous microorganisms have evolved strategies to prevent killing by phagocytes and moreover, have developed mechanisms to live intracellularly into phagocytic vacuoles and replicate within their host (reviewed in Knodler et al. 2001; Rosenberger & Finlay 2003; Haas 2007). Intracellular pathogens can be classified into the following groups concerning their survival strategies in phagocytes: (1) Those, such as *Listeria monocytogenes* and *Francisella tularensis* that disrupt the membrane of the maturing phagosome to escape into the cytoplasm which protects them from encounter with lysosome agents (Goetz et al. 2001). (2) Pathogens (e.g. *Mycobacterium tuberculosis* and *Rhodococcus equi*) that are able to arrest phagosome maturation at an early stage before reaching phagolysosomal characteristics and therefore avoid contact with lysosomal contents (Russell 2001; Fernandez Mora et al. 2005). (3) Microbes that redirect phagosome maturation during or soon after uptake and remain in a vacuole without endocytic characteristics, as it is the case for *Legionella pneumophila* (Kagan & Roy 2002) and *Afipia felis* (Lührmann et al. 2001). (4) A last group represents pathogens, such as *Leishmania donovani* and *Coxiella burnettii*, which force the maturation machinery to slow down but not permanently inhibit phagolysosome formation and survive within these vacuoles (Scianimanico et al. 1999; Maurin et al. 1992). All these strategies demonstrate how pathogens are able to interfere with phagosome maturation processes and adapt the host as an environment to their own benefits. Pathogens that block phagolysosomal maturation, are often responsible for diseases which have a strong impact on humans. Around one third of mankind is infected with *Mycobacterium tuberculosis*, the agent that causes tuberculosis, and more than 1.6 million humans die because of it annually (http://www.who.int/tb/en/; Berrington & Hawn 2007). The capacity of this pathogen does not only prevent phagosome maturation, it also affects antigen processing and presentation. For instance, in phagosomes containing *M. tuberculosis*, the formation of bacterial antigen MHC class II complexes is decreased when live bacteria, rather than heat killed bacteria, are phagocytosed (Ramachandra et al. 2001).

The complex process of phagocytic uptake of pathogens occurs via multi ligand interactions and engages many receptors. Although a single ligand on the particle can efficiently induce phagocytic uptake, most pathogens have many different ligands on their surface. This makes it very difficult to dissect the contribution of different ligand receptor interactions into the overall process of phagocytosis, and, in the case of a pathogen that lives intracellularly in phagosomes, in influencing the final steady state identity of the phagosome. At present, it is unclear for example whether multiple receptors can signal in parallel in response to phagocytosis or whether a single receptor will dominate the signalling pathways. In this study, a system will be introduced that can eventually be adapted to answer such

questions. By the help of a well characterized phagocyte model system, the latex bead system, it is possible to investigate down stream cellular events induced by contact of phagocytic particles with J774 macrophages in more detail. Moreover, the coupling of specific ligands to latex beads allows analysis of receptor dependent mechanisms that influence not only the phagocytic uptake but also the maturation of phagosomes containing these particles.

1.2 Latex beads as a phagosome model

The method using inert latex beads as a model system to study phagocytosis was introduced by Wetzel and Korn more than 35 years ago (Wetzel & Korn 1969) and was re discovered and expanded by Griffiths and co workers in the early 1990's (Desjardins et al. 1994a). The ability of latex bead phagosomes (LBP) to display most of the functions of phagosomes containing other particles, such as apoptotic cells or non pathogenic bacteria, qualified it as a system suitable to analyse the phagocytic process. LBP display fission and fusion events with endosomes and lysosomes over long time periods (Desjardins et al. 1994a; Jahraus et al. 1998; Kjeken et al. 2004), bind and move along microtubules (Blocker et al. 1997), promote the assembly of actin filaments (Jahraus et al. 2001) and bind to them (Al Haddad et al. 2001) and become acidified (Defacque et al. 2002). Phagosomes containing non pathogenic *Mycobacterium smegmatis*, but not those containing the pathogens *M. tuberculosis* and *M. avium*, have also been shown to assemble actin (Anes et al. 2003), confirming that LBPs are a good model for providing insights into the behavior of phagosomes containing non pathogenic bacteria. Moreover, the use of LBP provides other unique advantages for the study of receptor dependent phagocytosis, which are of high importance for this study. In contrast to pathogens, which are internalised after multiple ligand interactions, latex beads can be coupled to single ligands and offers the opportunity for the analysis of single receptor recognition pathways that influence not only uptake and signalling but also phagosomal maturation events (Desjardins & Griffiths 2003). In previous studies the use of latex beads coated with proteins from *Shigella flexneri* or *Listeria monocytogenes* provided important insights into the functions of pathogens interacting with host cells (Menard et al. 1996; Lecuit et al. 1997). Additionally, LBP are easily detectable by electron microscopy and can readily be labelled with fluorochromes, allowing studies by fluorescence microscopy.

However, one of their biggest advantages is the fact that latex bead phagosomes can be isolated simply and cleanly in a one step procedure by flotation in a discontinous sucrose

gradient (Korn 1974; Gotthardt et al. 2006b), whereas other membrane bound organelles require multiple steps of purification. Isolated LBP are organelles with the highest degree of purity (>95 %), and only very few contaminant proteins are present in enriched phagosome fractions (Stuart et al. 2007). Therefore, beside the option of studies on phagosomal behaviour *in vitro*, they provide an opportunity for the analysis and identification of phagosomal lipids and proteins. One of the first proteomic studies using LBP determined a partial proteome of these organelles in the mouse J774 macrophage cell line and identified 171 phagosomal proteins (Garin et al. 2001). A continuation of this analysis has since identified more than 800 of the estimated 1000 proteins in mouse macrophage phagosomes (M. Desjardins, personal communication). Burlak and co workers identified about 200 proteins in a proteomic analysis of LBP from human neutrophils (Burlak et al. 2005). In addition to mammalian studies, LBP have also been applied to analyse phagocytosis in other organisms. A proteomic analysis on magnetic bead phagosomes isolated from the human protozoan pathogen *Entamoeba histolytica* identified around 150 proteins including myosins and other actin binding proteins (Marion et al. 2005). LBP have also been used in extensive proteomics analyses of phagosomes from *Drosophila* identifying more than 600 proteins (Stuart et al. 2007) and *Dictyostelium discoideum*, which revealed around 1380 proteins, 179 being identified (Gotthardt et al. 2002; Gotthardt et al. 2006a). Many orthologs to mammalian proteins could be found in these organisms, indicating a high degree of conservation. Proteins of similar function are consistently detected in all the phagosomes studied. In mature phagosomes, major classes of luminal proteins include hydrolases and other bacteriocidal proteins. In the phagosome membrane are found the various subunits of the proton transporter H+ ATPase, other transporters and ion channels, heterotrimeric G proteins, monomeric GTPases of the Rab and Rho families, SNARE fusion machinery, actin binding and microtubule binding proteins, clathrin and COP proteins of vesicle coats, and a spectrum of signalling proteins such as protein kinase C and phospholipase D. Collectively, these analyses leave no doubt that the phagosome, even when it contains only an inert bead, is a complex signalling machine.

1.3 Aims of the study

The latex bead system provides many advantages to analyse phagocytosis in more detail. A former study of our lab investigated the capability of latex bead phagosomes to bind to actin filaments and established a light microscopy based assay that reconstitutes phagosomal binding to pre assembled F actin *in vitro* (Al Haddad et al. 2001).

In this study, we wanted to extend the analysis to phagosomes containing particles that were internalised via specific, receptor dependent pathways to analyse the influence of early events at the cell surface on subsequent phagosome functions. Additional to the investigation of phagosomes containing pathogenic and non pathogenic mycobacteria, which are recognised by more than one phagocytic receptor type, the latex bead system offers the possibility to conjugate beads to single ligands in order to trigger defined receptor mediated uptake. In this study, I focused on IgG, mannan, LPS, avidin and gelatin as coupling ligand to investigate non opsonic and opsonic internalisation routes.

In addition to the characterization of the capability of these phagosomes to bind to F actin, other phagocytic functions and macrophage gene expression should be analysed to gain more insight in how receptor ligand interactions influence the phagocytic process.
Therefore, the specific aims of this study were:

1. To reconstitute the binding of maturing mycobacterial and coupled latex bead phagosomes to F actin *in vitro* and to characterize the influence of cytosolic factors as well as of signalling molecules, such as different phospholipids.

2. To analyse early phagocytic events of ligand coupled latex beads, like their uptake and protein tyrosine phosphorylation, as well as later phagocytic processes, such as phagosome maturation.

3. To investigate macrophage gene expression in response to the receptor mediated uptake of latex beads coupled to IgG, mannan, LPS and avidin.

4. To identify and compare phagosomal proteins after the internalisation of coated latex beads to analyse whether receptor ligand interactions also modulate the proteome of maturing phagosomes.

Material & Methods

2.1 Cells and bacteria

2.1.1 Used material, reagents and instruments

- Phosphate-buffered saline (PBS): 80 g/l NaCl + 2 g/l KCl + 11.5 g/l Na_2HPO_4 * $2H_2O$ + 2 g/l KH_2PO_4 (Merck, Germany)
- Fetal bovine serum (FBS), Lot. #55H (Biochrom KG, Germany)
- Culture medium of J774 macrophages: DMEM (4500 mg/l glucose) + 1 % 10 000 U/10 000 µg/ml Penicillin/Streptomycin + 1% 200 mM L-Glutamine + 1 % non-essential amino acids (Invitrogen, Germany)
- Culture medium of primary mouse bone-marrow macrophages (MBMM) and L929 fibroblasts: RPMI 1640 + 1 % 100 U/10 000 µg/ml Penicillin/Streptomycin + 1% 200 mM L-Glutamine + 1 % non-essential amino acids (Invitrogen, Germany)
- Luria Broth (LB) medium, D-Glucose, Tween-80, Dimethylsulfoxide (DMSO), 2-Mercaptoethanol (Sigma-Aldrich, USA)
- Middlebrook 7H9 medium, ADC and OADC nutrient broth (Difco, BD Diagnostic Systems, Germany)
- Trypsin-EDTA, Hygromycin B, Ampicillin (Invitrogen, Germany)
- sterile cell culture material, like pipettes, dishes and flasks, cell scraper, centrifuge tubes etc. (TPP, Switzerland)
- Cryotubes, LabTek cell culture chambers (Nalge, USA); sterile filters (Sarstedt, Germany); syringes, cannula (Braun, Germany)
- Flow Hood (BDK, Germany); Centrifuge ZK 380 (Hermle, Germany); Incubator BB 16 (Heraeus, Germany) adjusted to 37 °C, 5 % CO_2

2.1.2 Cultivation of cells

Unless otherwise stated, all experiments were carried out using the mouse macrophage-like cell line J774A.1 (ACC170) obtained from the German Resource Center of Biological Material (DSMZ, Germany). J774 cells express a variety of phagocytic receptors and are frequently used for studies on phagocytosis. To avoid the influence of changes in the internalisation characteristics of this cell line, J774 macrophages were only used up to passage 25. New passages were obtained from stocks that were frozen in FBS supplemented with 10 % DMSO kept in liquid nitrogen. Confluent cell layers were split using Trypsin-EDTA. For some experiments, primary mouse macrophages were isolated from bone marrow (MBMM) as described in Al-Haddad et al. (2001). Bone marrow cells were obtained by rinsing tibia and femur of mice legs. MBMM from 3 weeks old Bmp5se wild type mice and myosin Va-deficient mice (homozygous strain DLS/Le a/a Myo5ad-l; Jackson Laboratories, Bar Harbor, USA) were grown in MBMM medium (see 2.1.1) supplemented with supernatant obtained from confluent mouse L929 fibroblasts (CCL1; American Type Culture Collection, USA) at a ratio of 1:5. Addition of L929 supernatant to macrophage medium is essential because of the macrophage colony-stimulating factor (M-CSF) produced by L929 cells (Nolte et al. 1997). MBMM cells were viable for around three weeks, could be passaged two to three times by scraping and were used for experiments two weeks after initial plating usually in passage 2 or 3.

2.1.3 Cultivation of bacteria

Non-pathogenic *Mycobacterium smegmatis* mc2 155 harbouring a p19-(long-lived) EGFP plasmid (Anes et al. 2003) was grown in medium containing Middlebrook's 7H9 broth and 10 % ADC nutrient broth, supplemented with 0.5 % D-glucose and 0.05 % Tween-80 at 37 °C on a shaker at 220 rpm until exponential phase. In order to stabilize GFP expression, medium was supplemented with 50 µg/ml Hygromycin B and bacteria were subcultured every day in fresh medium for 7-10 days before used for experiments. Fresh cultures were made out of glycerol stocks (50 % glycerol, 50 % bacteria in 7H9 medium) kept at -80 °C. The slow-growing, pathogenic strains *M. bovis* BCG Pasteur (ATCC 35734) and *M. avium* (ATCC 25291) were grown in the same medium, but were supplemented with 10 % OADC instead of ADC. Non-pathogenic *Escherichia coli* strain TG1 stably expressing GFP (Kunert et al. 2003) was kindly provided by PD Dr. M. Hagemann (University of Rostock). Bacteria were grown in LB medium supplemented with 70 µg/ml ampicillin at 37 °C on a shaker at 220 rpm until exponential phase.

2.2 Preparation and coupling of latex beads to ligands

2.2.1 Used material and reagents

Latex beads

- Blue-fluorescent carboxylate-modified microspheres containing 2 % solids of diameter 1 µm (Cat. F8815; Invitrogen, Germany)
- Non-fluorescent Polybead® carboxylate-modified microspheres containing 2.68 % solids of diameter 1 µm (Cat. #08226; Polysciences, Inc., USA)

Ligands

- Fish skin gelatin (FSG; Cat. G7765; Sigma-Aldrich, USA)
- Avidin (Cat. A2666; Invitrogen, Germany)
- mouse IgG, whole molecule (Cat. I5381; Sigma-Aldrich, Germany) and Fc fragment of mouse IgG (Cat. 31205; Pierce Biotechnology, USA)
- Complement purified from murine serum was kindly provided by the group of Dr. Gareth Griffiths, EMBL Heidelberg, Germany
- Lipopolysaccharides from *Klebsiella pneumoniae* (LPS; Cat. L4268; Sigma-Aldrich, USA)
- Mannan from *Saccharomyces cerevisae* (Man; Cat. M7504; Sigma-Aldrich, USA)

Reagents

- MES buffer (Cat. M8250; Sigma-Aldrich): 500 mM stock solution in Aqua dest.; diluted 100 mM and 50 mM solutions were adjusted to pH 6.7
- Stop buffer: 1 % Triton X-100 in 10 mM Trizma base (Sigma-Aldrich, USA); adjusted to pH 9.4

- Bicarbonate buffer: 50 mM Na_2CO_3 + 50 mM $NaHCO_3$ (both from Sigma-Aldrich, USA); adjusted to pH 9.6
- modified Phosphate buffer (PBS): 50 mM Na_3PO_4 * 12 H_2O + 0.9 % NaCl (both from Sigma-Aldrich, USA); adjusted to pH 7.4
- Activator of surface carboxyl groups: N-(3-Dimethylaminopropyl)-N′-ethylcarbodiimide hydrochloride (EDAC; Cat. E1769; Sigma-Aldrich, USA); 10 mg/ml stock solution in Aqua dest., prepared freshly
- Cross-linker: Concanavalin A from *Canavalia ensiformis* (ConA; Cat. C2010; Sigma-Aldrich, USA)
- Bovine serum albumin (BSA), IgM (M5909) and sodium azide (all from Sigma-Aldrich, USA)

2.2.2 Coupling of latex beads to fish skin gelatin (FSG)

Blue-fluorescent latex beads were vortexed and sonicated in an ultrasonic waterbath for 2 min. 5 ml of bead suspension were mixed with 10 mg FSG diluted in 50 mM MES and filled to a final volume of 10 ml with 50 mM MES. The suspension was mixed on a vertical tube rotator for 15 min. at RT. Subsequently, 0.4 ml EDAC stock solution was added to bead suspension, mixed by vortexing and adjusted to pH 6.5 using about 10-15 μl 0.8 N NaOH (checked with pH indicator sticks). The suspension was mixed on a vertical tube rotator for 2 hrs. at RT. To quench the reaction, glycine powder was added to give a final concentration of 100 mM. The suspension was incubated for another 30 min. on the vertical tube rotator at RT. Coupled latex beads were transferred to conical Eppis and centrifuged with 6.000 g for 5 min. at 4 °C to separate particles from unreacted protein. Pellets were resuspended in PBS and wash was repeated twice. Pellets were resuspended and combined in PBS and suspension was adjusted to 1 % solids by measuring OD_{600nm} using a photospectrometer.

2.2.3 Coupling of latex beads to avidin

Non-fluorescent latex beads were vortexed and sonicated in an ultrasonic waterbath for 2 min. 4 ml of bead suspension were mixed with 5 mg avidin diluted in 2 ml 50 mM MES. Suspension was filled to a final volume of 10 ml with 100 mM MES and mixed on a vertical tube rotator for 15 min. at RT. Subsequently, 0.14 ml EDAC stock solution was added to bead suspension and mixed on a vertical tube rotator for 1 hr. at RT. Another 0.14 ml EDAC were added and mixed for 1 hr. Afterwards, 2 ml stop buffer were added to the suspension, which was centrifuged in conical Eppis with 6.000 g for 5 min. at 4 °C. Pellets were resuspended in stop buffer and centrifuged again followed by three washes in PBS. Coupled latex beads were resuspended and combined in PBS containing 0.03 % FSG and suspension was adjusted to 1 % solids by measuring OD_{600nm} using a photospectrometer.

2.2.4 Coupling of latex beads to IgG (whole molecule or Fc fragment)

Blue-fluorescent latex beads were vortexed and sonicated in an ultrasonic waterbath for 2 min. 5 ml of bead suspension were mixed with 0.5 mg mouse IgG (whole molecule or only the Fc fragment). The following steps were carried out identical to the protocol of coupling beads to avidin. Latex bead

suspensions coupled to the whole IgG molecule tend to aggregate easily and therefore caused problems during uptake of single beads. Alternatively, coupling to the Fc fragment was carried out, which did not cause much aggregation.

2.2.5 Coupling of latex beads to mouse complement

Non-fluorescent latex beads were vortexed and sonicated in an ultrasonic waterbath for 2 min. 4 ml of bead suspension were mixed with 1 mg IgM and filled to a final volume of 10 ml with 100 mM MES. Suspension was mixed on a vertical tube rotator for 15 min. at RT. Subsequently, 0.14 ml EDAC stock solution was added to bead suspension and mixed on a vertical tube rotator for 1 hr. at RT. Another 0.14 ml EDAC were added and mixed for 1 hr. Afterwards, 2 ml stop buffer were added to the suspension, which was centrifuged in conical Eppis with 6.000 g for 5 min. at 4 °C. Pellets were resuspended in PBS and centrifuged again followed by another two washes in PBS. Pellets were resuspended in 9.5 ml PBS and 0.5 ml mouse serum. Suspension was mixed on a vertical tube rotator for 30 min. at RT. Afterwards, 2 ml stop buffer were added to the suspension, which was centrifuged in conical Eppis with 6.000 g for 5 min. at 4 °C. Pellets were resuspended in stop buffer and centrifuged again followed by three washes in PBS. Coupled latex beads were resuspended and combined in PBS containing 0.03 % FSG and suspension was adjusted to 1 % solids by measuring OD_{600nm} using a photospectrometer.

2.2.6 Coupling of latex beads to lipopolysaccharides (LPS)

Blue-fluorescent latex beads were vortexed and sonicated in an ultrasonic waterbath for 2 min. 5 ml of bead suspension were washed in bicarbonate buffer twice. Latex beads were resuspended in 10 ml bicarbonate buffer containing 0.05 mg/ml LPS and mixed on a vertical tube rotator for 2 hrs. at RT. Suspension was transferred to conical Eppis and centrifuged with 6.000 g for 5 min. at 4 °C. Pellets were resuspended in bicarbonate buffer and centrifuged again followed by two washes in bicarbonate buffer. Latex beads were resuspended in 10 ml PBS containing 5 % BSA and mixed on a vertical tube rotator for 1 hr. at RT. Suspension was transferred again to conical Eppis, centrifuged and washed twice in PBS containing 5 % BSA. Coupled latex beads were resuspended in the same buffer and adjusted to 1 % solids by measuring OD_{600nm} using a photospectrometer.

2.2.7 Coupling of latex beads to mannan

Blue-fluorescent latex beads were vortexed and sonicated in an ultrasonic waterbath for 2 min. 5 ml of bead suspension were mixed with 0.5 mg ConA and filled to a final volume of 10 ml with 100 mM MES. Suspension was mixed on a vertical tube rotator for 15 min. at RT. Subsequently, 0.14 ml EDAC stock solution was added to bead suspension and mixed on a vertical tube rotator for 1 hr. at RT. Another 0.14 ml EDAC were added and mixed for 1 hr. Afterwards, suspension was centrifuged in conical Eppis with 6.000 g for 5 min. at 4 °C, pellets were resuspended in PBS and centrifuged again followed by another two washes in PBS. Pellets were resuspended in 7.5 ml PBS and 2 mg mannan

were added. Suspension was mixed on a vertical tube rotator for 15 min. at RT. Afterwards, 2 ml stop buffer were added to the suspension, which was centrifuged in conical Eppis again. Pellets were resuspended in stop buffer and centrifuged again followed by another spin down in stop buffer. Coupled latex beads were washed three times in PBS, resuspended in PBS containing 0.03 % FSG and suspension was adjusted to 1 % solids by measuring OD_{600nm} using a photospectrometer.

All coupled 1 % latex bead suspensions were stored at 4 °C after adding 3 mM sodium azide.

2.3 Isolation of phagosomes and cytosol

2.3.1 Used material, reagents and instruments

- Internalisation medium: DMEM (Invitrogen, Germany) + 1 % HEPES (Sigma-Aldrich, USA)
- Protease inhibitor (PI) Cocktail Set III containing 100 mM AEBSF, 0.08 mM Aprotinin, 5 mM Bestatin, 1.5 mM E-64 protease inhibitor, 2 mM Leupeptin and 1 mM Pepstatin A (Calbiochem, Merck, Germany)
- Homogenisation buffer (HB), adjusted to pH 7.4: Aqua dest. containing 250 mM (= 8.6 %) sucrose, 3 mM imidazole, 1 mM DTT, 1 mM PMSF (all from Sigma-Alrich, USA), 1:1000 PI
- Solutions for discontinous sucrose gradient centrifugation: HB containing 62 %, 55 %, 37 % and 25 % sucrose, respectively
- Salt-stripping buffer: Aqua dest. containing 2.6 M NaCl, 48 % sucrose, 3 mM imidazole, pH 7.4, 1 mM DTT, 1 mM PMSF (all from Sigma-Alrich, USA), 1:1000 PI
- HBKS buffer, adjusted to pH 7.4: Aqua dest. containing 0.1 mM EDTA, 2 mM EGTA, 2 mM $MgCl_2$, 50 mM KCl, 25 mM HEPES, 10 % sucrose, 2 mM DTT, 1 mM PMSF (all from Sigma-Aldrich, USA), 1:1000 PI
- Syringes, needles (Braun, Germany)
- Trypan blue, FITC-labelled biotin (Sigma-Aldrich, USA)
- Cell culture centrifuge ZK 380 (Hermle, Germany)
- Ultracentrifuge, UltraClear centrifuge tubes of different sizes, SW60Ti rotor, TLA 120.1 rotor (Beckman Coulter, USA)
- Centrifuge tubes, Sorvall TH-641 rotor (Thermo Fisher Scientific, USA)

2.3.2 Isolation of latex bead-containing phagosomes (LBP)

Isolation of LBP was carried out as described previously (Kühnel et al. 2006) with slight modifications. J774 macrophages were grown in cell culture dishes until they reached around 80 % confluency. Latex bead suspensions adjusted to 1 % solids were vortexed, sonicated and washed three times in PBS to remove sodium azide. Stock solution of latex beads was added to prewarmed internalisation medium at a ratio of 1:25. Cells were washed with PBS and internalisation medium was added. Uptake of latex beads (‘pulse’ time) was allowed for 1 hr. at 37 °C under continuous wiping to increase internalisation efficiency. Non-internalised beads were removed by intensive washing of the cells with PBS followed by another hour of incubation in cell culture medium at 37 °C and 5 % CO_2 (‘chase’ time).

Subsequently, the medium was removed, cells were washed with PBS and harvested by detaching them from the dish with a cell scraper in ice-cold PBS. Cells were collected in 50 ml tubes and centrifuged with 800 rpm for 7 min. at 4 °C. Pellets were resuspended in ice-cold PBS and centrifuged with 1500 rpm for 5 min. at 4 °C. Cell pellets were resuspended in ice-cold HB and centrifuged with 2500 rpm for 5 min. at 4 °C. The final volume of the cell pellet was mixed with the same amount of ice-cold HB and lysed with a 1 ml syringe fitted to a 22-gauge needle on ice using 15-20 strokes. Homogenisation success and cell breakage was monitored by phase contrast microscopy after adding trypan blue. After centrifugation at 800 g for 15 min. at 4 °C to remove nuclei and intact cells (Fig. 5A"), the post-nuclear supernatant (PNS, Fig. 5A') containing phagosomes was collected and gently mixed with the same amount of HB containing 62 % sucrose. Isolation of LBP was accomplished in a sucrose gradient, which was prepared by overlaying 3-4 ml of the PNS / 62 % sucrose mix with 5 ml HB containing 25 % sucrose and 2 ml HB containing 8.6 % sucrose on top in ultracentrifugation tubes. Centrifugation was carried out in a Beckman ultracentrifuge and a Sorvall TH-641 rotor at 100.000 g for 60 min. at 4 °C. Afterwards enriched and purified LBP (Fig. 5B) formed a visible band between the 8.6 % and the 25 % sucrose interphase, which was collected by penetrating the tube wall with a 22-gauge needle. After determination of the concentration by measuring OD at 600 nm, isolated LBP were aliquoted, frozen in liquid nitrogen and stored at -80 °C. Integrity of the prepared phagosomes was checked by incubation with 5 nM FITC-biotin for 10 min. Broken phagosomes containing avidin-coupled beads were detectable by fluorescence microscopy, while intact Avidin-LBP could not be stained by the label. Routinely around 80 % of the isolated phagosomes were found to be intact.

For some preparations, additional salt-stripping was applied to isolated LBP to remove membrane-bound proteins. Isolated LBP were mixed with the same amount of salt-stripping buffer and incubated on a vertical tube rotator for 40 min. at 4 °C. Salt-stripped LBP were adjusted to 40 % sucrose including 1.3 M NaCl and purified by discontinuous sucrose gradient centrifugation. 1 ml of the 40 % sucrose suspension was overlaid with 1.5 ml HB containing 25 % sucrose and 0.5 ml HB containing 8.6 % sucrose. Centrifugation was carried out in a Beckman ultracentrifuge and SW60Ti rotor at 45.000 g for 60 min. at 4 °C. Afterwards, concentration of purified LBP was determined and suspension was aliquoted, snap-frozen in liquid nitrogen and stored at -80 °C.

2.3.3 Isolation of bacteria-containing phagosomes

Isolations of phagosomes containing mycobacteria or *E. coli* were carried out as described previously (Chakraborty et al. 1994; Kühnel et al. 2006) with slight modifications. Cultures were grown until exponential growth phase was reached (OD_{600nm}= 0.2; corresponds to ~10^8 cells/ml). Bacteria were washed twice in PBS and resuspended in PBS to a final concentration of 5 x 10^9 cells/ml. The suspension was treated for 2 min. in a waterbath sonicator at RT using four times 30 sec. pulses to disperse clumps. Subsequently, bacteria were passed through a 23-gauge needle to disrupt remaining bacterial clumps. Before infection, residual bacterial aggregates were removed by low speed centrifugation at 120 g for 2 min. The absence of bacterial clumps was finally verified by phase contrast microscopy. For some experiments, bacteria were heat-inactivated for 15 min. at 80 °C.

J774 macrophages were grown in cell culture dishes until they reached around 80 % confluency and washed with PBS before infection. Mycobacteria suspensions were resuspended in prewarmed internalisation medium and macrophages were infected at an OD_{600nm}= 0.2. Uptake of bacteria ('pulse' time) was allowed for 1 hr. at 37 °C under continuous wiping to increase internalisation efficiency. Non-internalised bacteria were removed by intensive washing of the cells with PBS followed by another hour of incubation (or different 'chase' times) in cell culture medium at 37 °C and 5 % CO_2. Subsequently, the medium was removed, cells were washed with PBS and harvested by detaching them from the dish with a cell scraper in ice-cold PBS. Cells were collected in 50 ml tubes and centrifuged with 800 rpm for 7 min. at 4 °C. Pellets were resuspended in ice-cold PBS and centrifuged with 1500 rpm for 5 min. at 4 °C. Cell pellets were resuspended in ice-cold HB and centrifuged with 2500 rpm for 5 min. at 4 °C. The final volume of the cell pellet was mixed with ice-cold HB at a 2:1 ratio and lysed with a 5 ml syringe fitted to a 25-gauge needle on ice using 5-10 strokes. Homogenisation success and cell breakage was monitored by phase contrast microscopy after adding trypan blue. After another centrifugation step at 900 g for 15 min. at 4 °C to remove nuclei and intact cells, the post-nuclear supernatant (PNS) containing phagosomes was collected. Isolation of phagosomes was accomplished in a sucrose gradient, which was prepared by 2 ml HB containing 62 % sucrose overlaid by 3 ml HB containing 55 % sucrose, 5 ml HB containing 37 % sucrose and 2 ml PNS on top. Centrifugation was carried out in a Beckman ultracentrifuge and a Sorvall TH-641 rotor at 100.000 g for 30 min. at 4°C. After centrifugation, three different bands were visible. One laid on top of the 37 % gradient along with the majority of endocytic organelles, another in the interface between 55 % and 37 % sucrose with the bacterial phagosomes and, in the case of more mature phagosomes, a third one was seen between the 55 % and the 62 % sucrose interphase. Material of the 37 % / 55 % sucrose interphase was collected by penetrating the tube wall with a 22-gauge needle. The isolated phagosomes were aliquoted, snap-frozen in liquid nitrogen and stored at -80 °C.

2.3.4 Isolation of macrophage cytosol

J774 and MBMM macrophages were grown in cell culture dishes until they reached around 80 % confluency. Culture medium was removed, cells were washed with PBS and harvested by detaching them from the dish with a cell scraper in ice-cold PBS. Cells were collected in 50 ml tubes and centrifuged with 800 rpm for 7 min. at 4 °C. Pellets were resuspended in ice-cold PBS and centrifuged with 1500 rpm for 5 min. at 4 °C. Cell pellets were resuspended in ice-cold HBKS and centrifuged with 2500 rpm for 5 min. at 4 °C. The final volume of the cell pellet was mixed with ice-cold HBKS at a ratio of 3:1 and lysed on ice with a 5 ml syringe fitted to a 24-gauge needle using 15 strokes followed by a 25-gauge needle using around 10 strokes. Homogenisation success and cell breakage was monitored by phase contrast microscopy after adding trypan blue. After a centrifugation step at 9.100 g for 15 min. at 4 °C using a Beckman TLA 120.1 rotor, supernatant was collected, transferred to a new tube and centrifuged at 145.000 g for 60 min. at 4 °C. Protein concentration was determined according to Bradford (1976). Cytosol aliquots were snap-frozen in liquid nitrogen and stored at -80 °C.

2.4 Isolation of G-actin from rabbit muscle

2.4.1 Used material, reagents and instruments

- Rabbit muscle acetone powder (M0637; Sigma-Aldrich, USA)
- Cheesecloth; Teflon-coated homogeniser; semi-permeable dialysis tubing, pore-size diameter: 5 nm, MW cut-off: 14 kDa (all from Roth, Germany)
- G-buffer, adjusted to pH 8.0: Aqua dest. containing 5 mM Trizma base, 0.2 mM $CaCl_2$, 0.2 mM Na-ATP and 0.1 % 2-mercaptoethanol (all from Sigma-Aldrich, USA)
- Ultracentrifuge, Ti50 rotor (Beckman Coulter, USA)
- Sorvall T 647.5 rotor (Thermo Fisher Scientific, USA)

2.4.2 Isolation of G-actin

G-actin was isolated by the method of Spudich & Watt (1971) with slight modifications. 5 g of rabbit muscle acetone powder were washed in Aqua dest. twice for 5 min. at 4 °C to remove remaining an- and cations. Solutions were passed through several layers of sterile cheesecloth. Washed powder was incubated in 100 ml ice-cold G-buffer under continuous stirring (500 rpm) for 40 min. at 4 °C. Solution was again passed through several layers of sterile cheesecloth. Filtrate was centrifuged in a T 647.5 rotor with 30.000 rpm for 15 min. at 4 °C and supernatant (S1 in Fig. 4) was transferred to a beaker. While stirring slowly at 4 °C, solution was brought to 50 mM KCl, 2 mM $MgCl_2$ and 1 mM Na-ATP. The beaker was sealed with parafilm and incubated without stirring for 2 hrs. at 4 °C. The viscosity of the solution increased significantly during incubation. While gentle stirring, KCl concentration was increased to 0.6 M by adding crystalline KCl to remove tropomyosin complexes. Solution was gently stirred for 60 min. at 4 °C followed by centrifugation using the T 647.5 rotor with 40.000 rpm for 2 hrs. at 4 °C. The supernatant (S2 in Fig. 4) was discarded and pellet was resuspended in 7.5 ml G-buffer. The solution was homogenised using a Teflon-coated rod homogeniser and transferred to dialysis tubing. While gentle stirring, the actin solution was dialysed against 1 l G-buffer for 36 hrs. at 4 °C. During dialysis, G-buffer was replaced completely every 8 hrs. After first dialysis cycle, solution was centrifuged again using the Ti50 rotor with 40.000 rpm for 2 hrs. at 4 °C. Supernatant (S3 in Fig. 4) containing G-actin was partly aliquoted and frozen in liquid N_2 while pellet (P2 in Fig. 4) was discarded.

6 ml of supernatant were transferred to a new tube and salt concentrations were increased again (50 mM KCl, 2 mM $MgCl_2$, 1 mM Na-ATP). The tube was sealed and incubated without stirring for 48 hrs. at 4 °C. The solution was centrifuged again using the Ti50 rotor with 40.000 rpm for 2 hrs. at 4 °C. The supernatant (S2b in Fig. 4) was discarded and pellet was resuspended in 4 ml G-buffer. The solution was homogenised again and transferred to dialysis tubing. While gentle stirring, the actin solution was dialysed against 1 l G-buffer for 36 hrs. at 4 °C. During dialysis, G-buffer was replaced completely every 8 hrs. After second dialysis cycle, solution was centrifuged again using the Ti50 rotor with 40.000 rpm for 2 hrs. at 4 °C. Pellet and supernatant (P3 and S4 in Fig. 4) containing purified G-actin were aliquoted, frozen in liquid nitrogen and stored at -80 °C.

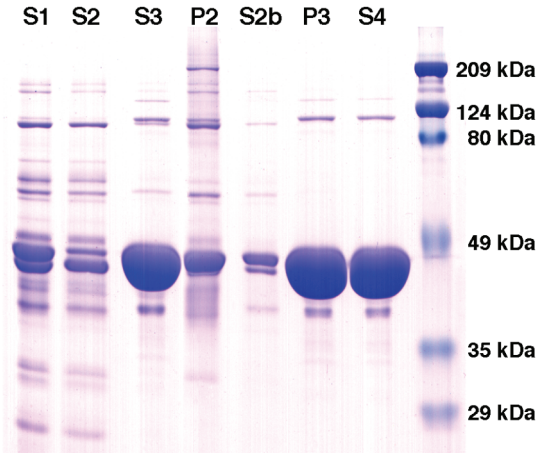

Figure 4. SDS-PAGE (10 % gel) of supernatant (S) and pellet (P) fractions during isolation of G-actin from rabbit muscle. Proteins were stained with Coomassie Blue. Lane designations are described in the text. Final fractions after dialysis (S3, P3, S4) contained purified G-actin (42 kDa).

2.5 *In vitro* actin-binding assay

Isolated G-actin from rabbit muscle (0.05 mM) was polymerised on ice in the presence of 2 mM $MgCl_2$ overnight. After overnight polymerisation, F-actin was stabilised and labelled on ice with the same concentration (ratio: 1:1) of rhodamine-conjugated phalloidin (Sigma-Aldrich, USA) for 2 hrs. Prepared and stabilised F-actin fractions were kept on ice and were used for experiments within two weeks.

Microscopy chambers were built from glass microscopy slides and 11 mm glass coverslips (Menzel GmbH, Germany) sealed onto two pieces of double-sided tape (3M Scotch, USA) forming a reaction chamber of around 3 µl volume. Before sealing, coverslips were coated with 0.1 mg/ml poly-L-lysine (PLL; P1274; Sigma-Aldrich, Germany) diluted in Aqua dest. for 15 min. at RT to maintain homogenous F-actin network formation on the glass surface. Unbound PLL was removed by intensive rinsing with Aqua dest. All experiment incubations were carried out in a moist chamber at RT.

Stabilised and labelled filamentous actin was diluted in G-buffer (5 mM Trizma base, pH 8.0, 0.2 mM $CaCl_2$, 0.2 mM Na-ATP, 2 mM DTT) at a ratio of 1:200. Diluted F-actin was perfused into the chamber and incubated for 3 min. followed by a wash-out with 10 µl G-buffer. Nonspecific binding was blocked by perfusion of the chamber with 10 µl 3 mg/ml casein (Sigma-Aldrich; USA) diluted in HB buffer (25 mM HEPES, pH 7.4, 2 mM, $MgCl_2$, 2 mM EGTA, 0.1 mM EDTA) for 5 min. Subsequently, excess F-actin and casein were washed out by 10 µl HBS (HB containing 10 % sucrose and 0.3 mg/ml casein). Binding reaction mixtures were prepared in HBS on ice with a final volume of 8-10 µl. Reaction mixtures were freshly prepared in the following order: 1.) HBS, 2.) phagosomes, 3.) cytosol and 4.) additional factors, such as lipids, inhibitors etc. Isolated latex bead phagosomes were usually diluted to a working concentration of 0.006 % [wt/vol]. Binding reaction mixtures were perfused into the chamber and incubated for 20 min. Afterwards, unbound phagosomes were washed out by perfusion of 10 µl HBS. Chambers were sealed using VaLaP (vaseline, lanolin and paraffin at the same ratio).

Phagosomal binding was analysed by fluorescence microscopy (Fig. 5C) or video-enhanced contrast differential interference contrast (VEC-DIC) microscopy using a Nikon Diaphot 300 inverted microscope equipped with an oil immersion condenser (numerical aperture 1.4) and a 60x DIC PlanApo oil objective (numerical aperture 1.4; Nikon, Japan). Bound phagosomes were counted by eye per view field, and in each experiment, values from at least 20 fields were averaged. The error bars reported are standard deviations of at least three independent experiments.

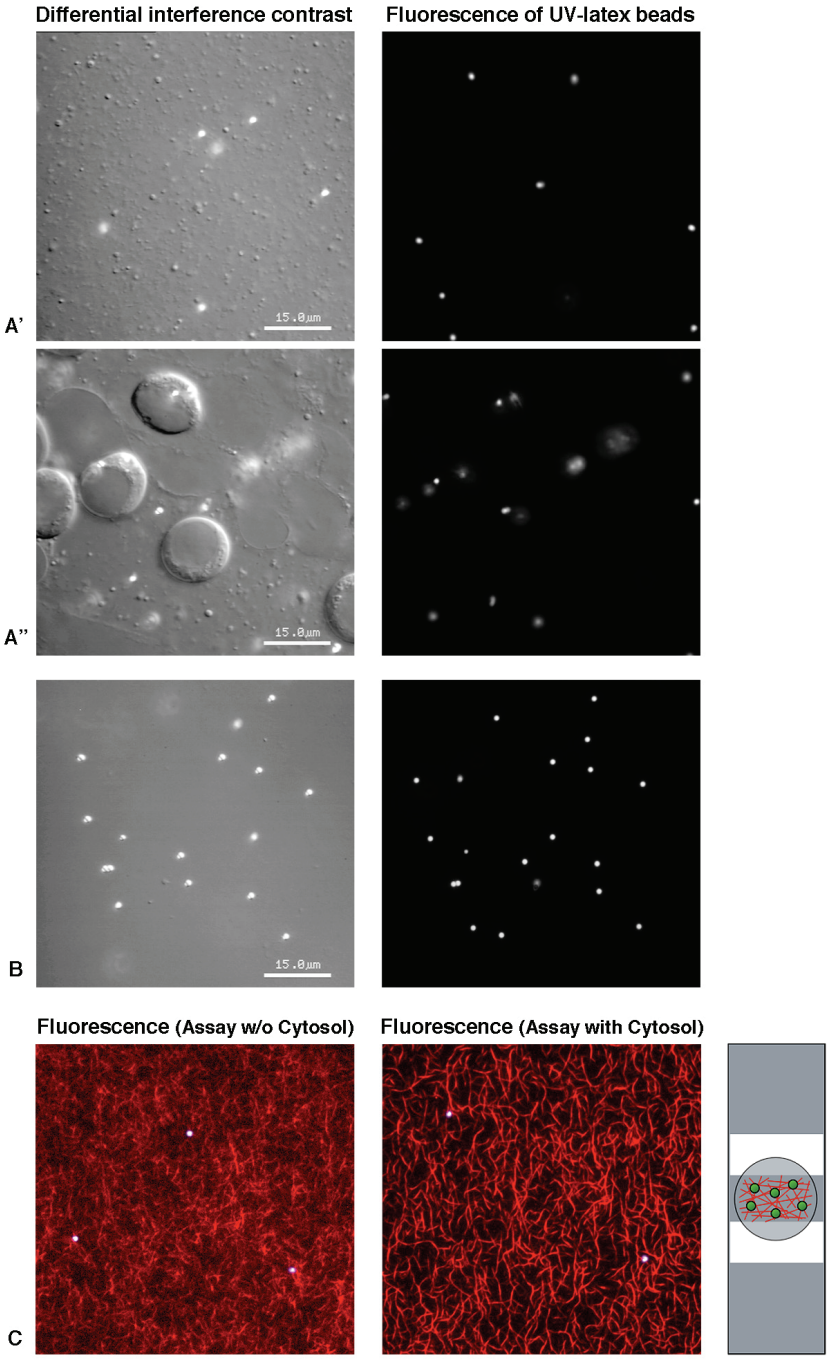

Figure 5. Light microscopy images illustrating purity of isolated latex bead phagosomes (LBP). During isolation, post-nuclear supernatant containing several cell organelles (**A'**) was separated from pelleted cell nuclei and whole intact cells (**A"**). Purified, enriched LBP were obtained after discontinuous sucrose gradient centrifugation (**B**). Subsequently, binding of LBP to F-actin networks (red) *in vitro* was analysed by binding assays in the absence (**C, left**) and presence of isolated cytosol (**C, right**).

Table 1. List of used lipids and inhibitors in binding assay studies:

Component	Assay conc.	Solvent	Supplier
Arachidonic Acid (AA)	125 μM	EtOH	Sigma-Aldrich, USA
Ceramide (Cer)	5 μg/ml	EtOH	Sigma-Aldrich, USA
C_{16}Ceramide (C_{16}Cer)	5 μg/ml	EtOH	Sigma-Aldrich, USA
Diacylglycerol (DAG)	50 μM	EtOH	Avanti Polar Lipids, USA
Eicosapentaenoic acid (EPA)	10 μM	EtOH	Sigma-Aldrich, USA
Leukotriene B4	0.1-1 μM	EtOH	Sigma-Aldrich, USA
Prostaglandin A1	0.1-1 μM	EtOH	Sigma-Aldrich, USA
Prostaglandin F2 alpha	0.1-1 μM	EtOH	Sigma-Aldrich, USA
PtdIns (4,5)-bisphosph. (PIP_2)	50 μM	EtOH	Sigma-Aldrich, USA
Sphingomyelin (SM)	10 μM	EtOH	Sigma-Aldrich, USA
Sphingosine (Sph)	10 μM	EtOH	Sigma-Aldrich, USA
Sphingosine-1-phosphate (S1P)	10 μM	MeOH	Merck, Calbiochem, Germany
Na-ATP	1 mM	A. dest.	Sigma-Aldrich, USA
Genistein	10 μM	DMSO	Merck, Calbiochem, Germany
LY294002	50 μM	DMSO	Merck, Calbiochem, Germany
Ocadaic acid	0.02 μM	DMSO	Merck, Calbiochem, Germany
PLA2 inhibitor	1 μM	DMSO	Merck, Calbiochem, Germany
Sodium vanadate	1 mM	DMSO	Merck, Calbiochem, Germany
Staurosporine	2 μM	DMSO	Merck, Calbiochem, Germany
Wortmannin	1 μM	DMSO	Merck, Calbiochem, Germany

2.6 Light microscopy studies

2.6.1 Fusion assay and analysis of phagocytic uptake rates

Analysis of phagosome-lysosome fusion events was carried out by detection of lysosomal markers, such as LAMP-2, on phagosomes by immunofluorescence labelling or by another, more elegant approach applicable in live cells that was recently described (Anes et al. 2006). For this, 10 nm gold particles prepared according to Slot and Geuze (Malik et al., 2003) were saturated with 20 % of BSA and centrifuged for 45 min. at 10.000 g at 4 °C. The pellet was resuspended in PBS containing 1 mg/ml rhodamine-NHS (N-hydroxysuccinimide) esters (Invitrogen, Germany) and rotated on a wheel for 1 hr. The suspension was washed three times with PBS containing 50 mM glycine and was resuspended in PBS containg 50 mM glycine and 0.02 % sodium azide for storage. The OD was estimated at 520 nm and rhodamine-conjugated gold particles were used with an $OD_{520\ nm}$ =1 in culture medium in all fusion experiments. Macrophages were pulsed for 1 hr. with labelled gold particles, washed three times with PBS and chased for another hour in culture medium leaving particles time to accumulate within lysosomes. Uptake of latex beads coupled to different ligands diluted at a ratio of 1:100 in internalisation medium (corresponding to 0.01 % solids) was then allowed for different times. After incubation, cells were fixed and, in the case of avidin, outside beads were stained by anti-avidin antibody before cell permeabilisation. Similarly, in IgG samples outside beads were labelled by

Alexa488 goat anti-mouse antibody for 20 min. After permeabilisation, in avidin samples all beads were stained for 20 min. with FITC-conjugated biotin. In the remaining samples (gelatin, LPS, mannan), F-actin was labelled by FITC-phalloidin for 30 min. In all samples, 50 cells were analysed by confocal microscopy to determine total number of beads, the amount of internalised beads and the percentage of LBP positive for the lysosomal markers LAMP-2 and rhodamine-gold, respectively. Avidin and IgG samples could be analysed by the described inside-outside stain. In the other samples containing fluorescent latex beads, 30 z-stacks of each field were recorded and internalised beads could be distinguished by the help of F-actin staining using the cross-section view of the confocal software. For uptake experiments, at least two independent experiments were analysed and averaged.

Table 2. List of markers and antibodies used for immunofluorescence labelling (IF), western blotting (WB) and antibody inhibitor experiments in actin-binding assays:

Label	Host	Used dilution	Supplied by
PRIMARY ANTIBODIES			
anti-mouse CD14	rat	1:500	BD Pharmingen, Germany
anti-mouse Fcγ receptor I	rat	1:500	R&D Systems, USA
anti-mouse Mannose receptor	rat	1:1000	P. Stahl (Fiani et al. 1998)
anti-Actin	mouse	1:2000	Abcam, UK
anti-α-Tubulin, clone B-5-1-2	mouse	1:5000	Sigma-Aldrich, USA
anti-Dynamin-A	rabbit	1:1000	D. Manstein (Wienke et al. 1999)
anti-Ezrin	rabbit	1:500	Cell Signaling, USA
anti-phospho ERM	rabbit	1:1000	Cell Signaling, USA
anti-Filamin-A	rabbit	1:1000	Cell Signaling, USA
anti-IQGAP1	rabbit	1:500	R. Grosse (Fukata et al. 2002)
anti-mDia1	rabbit	1:500	R. Grosse (Brandt et al. 2007)
anti-Moesin, clone 38	mouse	1:500	BD Pharmingen, Germany
anti-Myosin Va (DIL-2)	rabbit	1 μg/ml	J.A. Hammer (Wu et al. 1997)
anti-N-WASP	rabbit	1:500	S. Marion (Egile et al. 1999)
anti-Cathepsin-D	goat	1:200	Santa Cruz Biotechnology, USA
anti-LAMP-2	rat	1:200 (IF) / 1:1000 (WB)	Iowa Hybridoma bank, USA
anti-Phosphotyrosine	mouse	1:1000	Sigma-Aldrich, USA
anti-Tumor necrosis factor alpha	mouse	0.5 μg/ml	BD Pharmingen, Germany
SECONDARY ANTIBODIES			
anti-goat HRP	donkey	1:10000	Dianova, Germany
anti-mouse HRP	sheep	1:5000	GE Healthcare, UK
anti-rabbit HRP	donkey	1:5000	GE Healthcare, UK
anti-rat HRP	goat	1:5000	Pierce Biotechnology, USA
anti-mouse Alexa-488 and -594	goat	1:300	Invitrogen, Germany
anti-rabbit Alexa-488 and -594	goat	1:300	Invitrogen, Germany
anti-rat Cy3	goat	1:300	Invitrogen, Germany
MARKERS			
Hoechst bisbenzimide (DNA)	-	1:1000	Sigma-Aldrich, USA
FITC-phalloidin (F-actin label)	-	1:500	Sigma-Aldrich, USA
TRITC-phalloidin (F-actin label)	-	1:500	Sigma-Aldrich, USA

2.6.2 Fixation and labelling of cells

Cells were fixed in PBS containing 4 % paraformaldehyde and 4 % sucrose (pH 7.4; Sigma-Aldrich, USA) for 20 min. at RT followed by quenching in PBS containing 50 mM NH_4Cl (Merck, Germany) for 10 min. at RT. Permeabilisation, when required, was achieved by treatment with 0.2 % Triton X-100 (Roth, Germany) in PBS for 5 min. at RT. After blocking of unspecific binding sites with PBS containing 1 % white gelatin 'gold' (Sigma-Aldrich, USA) for 60 min., samples were incubated with primary antibody (see table 2) diluted in blocking solution for 60 min. at RT, followed by three washes with PBS containing 0.2 % gelatin. Secondary antibodies (see table 2) were applied for 45 min. at RT, again followed by three washes. If necessary, samples were stained with markers for actin or cell nuclei for 20 min. at RT. Coverslips were washed in PBS containing 0.2 % gelatin, PBS alone, in Aqua dest. and were mounted on glass slides (Menzel GmbH, Germany) using ProLong gold mounting medium (Invitrogen, Germany). Fluorescence labelling and viability test of mycobacteria were performed as described (Anes et al. 2003; Kühnel et al. 2006).

2.6.3 Conventional and confocal microscopy

Actin-binding assays were analysed by conventional epifluorescence microscopy as described previously (Al-Haddad et al. 2001) or, in the case of non-fluorescent LBP, by video-enhanced differential interference contrast (VEC-DIC) microscopy according to Allen (Weiss et al. 1999). A Diaphot 300 inverted microscope (Nikon, Japan) equipped with an oil immersion condenser (NA 1.4) and a 60x DIC PlanApo oil immersion objective (NA 1.4) and a mercury arc lamp HBO 103W (Osram, Germany) were used for microscopic observations. A C2400-07 Newvicon camera was used for acquiring DIC images (Hamamatsu Photonics, Germany). First, all video signals were subjected to analogue contrast enhancement followed by a real-time digital image processing with the following steps: 1. subtraction of an out-of-focus background, 2. averaging of images to increase signals-to-noise ratio and 3. digital contrast enhancement by selection of desired range of gray levels. Analogue and digital image processing of VEC-DIC signals was performed using an Argus 20 real-time image processor (Hamamatsu Photonics, Germany). Images were transferred to a MacIntosh 9600 computer (Apple, USA) equipped with a LG-3 frame-grabber (Scion, USA) using IPLab Spectrum software (Scanalytics, USA). Fluorescence images were recorded by a chilled SenSys CCD camera system (Photometrics Inc., USA) and an Uniblitz D122 shutter (Vincent Associates, USA). For selective excitation and specific detection of emitted radiation of used fluorescent dyes, different filter sets were available (Nikon, Japan). Images were again transferred to a MacIntosh computer and analysed by IPLab Spectrum software.

Live cell imaging at 37 °C and analysis of fusion assays as well as uptake rates of fixed macrophages were performed by confocal fluorescence microscopy using a TCS SP2 laser-scanning microscope (Leica, Germany) equipped with a 405 nm diode laser, an argon-krypton laser with lines at 458, 476, 488, 514 nm and helium-neon lasers with 543, 594 and 633 nm lines. The system also contained acousto-optical tuneable filters (AOTF), an acousto-optical beam splitter (AOBS) and four

prism spectrophotometer detectors that permitted simultaneous excitation and detection of multiple fluorochromes. Three-dimensional scans of usually 30 z-stacks were recorded and analysed by the help of the cross-sectioning option of Leica confocal software. Staining of cellular F-actin allowed to distinguish between outside or only attached latex beads and fully internalised beads forming latex bead phagosomes. Additionally, LBP were analysed for the presence of lysosomal markers (LAMP-2, rhodamine-gold particles). Only phagosomes completely surrounded by lysosomal markers were counted as positive for phagosome-lysosome fusion events.

2.7 Investigation of macrophage gene expression by microarray analysis

2.7.1 Used material, reagents and instruments

- RNAeasy Mini kit and DNase I (Qiagen, Germany)
- NanoDrop 1000 spectrophotometer (Thermo Fisher Scientific, USA)
- CodeLink™ iExpress expression assay reagent kit containing a bacterial mRNA control set (Applied Microarrays, Inc., USA)
- CodeLink™ Mouse Whole Genome Bioarray, spotted oligonucleotide (Applied Microarrays, Inc., USA); platform ID used in NCBI GEO database GPL5825, EMBL30807
- Bioanalyzer and GeneSpring GX software (Agilent Technologies, Inc., USA)
- Excel Compare software (Formula Software, Inc., USA)
- Two Tone Table Lens (TTTL) programmed by Mathias John, Christian Tominski and Heidrun Schumann (Institute for Computer Science, University of Rostock, Germany)

2.7.2 RNA isolation, preparation of cRNA and hybridization

J774 macrophages were seeded into 6-well plates two days prior the experiment and were grown as monolayer. After reaching around 75 % confluency, cells in passage 19 were used for feeding experiments with latex beads conjugated to avidin, the Fc fragment of mouse IgG, LPS from *Klebsiella pneumoniae* and mannan from S*accharomyces cerevisiae* as described before. Macrophages were washed with PBS and incubated in serum-free DMEM containing 0.02 % coupled latex beads (1 % stock solution at a ratio of 1:50, corresponding to final OD=3.6) for 30 and 60 minutes at 37 °C and 5 % CO_2. Controls were incubated with serum-free DMEM without latex beads. All samples including controls (one well per sample) were processed in duplicates. Cells were washed three times with PBS and lysed using the lysis buffer supplied by the RNAeasy Mini kit. Isolation of total RNA was carried out using this kit following the manufacturers' instructions. After the addition of DNase to all samples, the concentration and purity of isolated RNA was determined by the NanoDrop photospectrometer. Isolated RNA was stored in RNase-free tubes at -70 °C.

The preparation of cRNA and hybridization was carried out using the CodeLink™ iExpress expression assay reagent kit following the manufacturers' instructions by the help of the Genomics Core facility (EMBL Heidelberg). Briefly, the biotin-labelled cRNA target was prepared by a linear amplification method. The poly(A)+ RNA (mRNA) subpopulation within the total RNA population was primed for reverse transcription by a DNA oligonucleotide. After second-strand cDNA synthesis, the cDNA served as the template for an *in vitro* transcription (IVT) reaction to produce the target cRNA. The IVT was performed in the presence of biotinylated nucleotides to label the target cRNA. This method produced approximately 1,000- to 5,000-fold linear amplification of the input RNA. Hybridization was performed overnight in a shaking incubator at 37 °C and 300 rpm. Post-hybridization processing included a stringent wash to remove unbound and non-specifically hybridized target molecules, a secondary labelling step using a Cy5-Streptavidin conjugate and several washing steps to remove unbound conjugate. Following a final rinse, the Mouse Whole Genome bioarrays were dried by centrifugation and scanned. The intensity values were normalised against median of spot-based raw intensity.

2.7.3 Data processing and comparison

Bioarray data was processed using the GeneSpring GX software by the help of Bibhuti Mishra (Molecular Pathogenesis Centre, University of Lisbon, Portugal). First, all array data were normalised and clustered using the 'condition tree' method. Similar branches were merged and computed locally to analyse whether duplicates of controls and different bead types cluster together. The controls as well as the samples of the same bead type were found in clusters, therefore gene expression of the J774 mouse macrophage-like cell line could be analysed after importing mouse whole genome data into the software. Due to the high amount of sample data, in this study only the significant upregulation of genes was analysed. Data were filtered on fold change and all bead coating conditions were compared to untreated control conditions or versus each other. Because of the existence of all conditions in duplicates, each comparison resulted in four test possibilities (upregulation of coating X1 vs. control 1 and control 2 as well as coating X2 vs. control 1 and control 2). Data arrays of gene upregulation were exported as Excel files. For further comparison, only upregulated genes were analysed, which appeared minimum two times in all four test possibilities. By the help of Excel Compare software, upregulated genes, which appeared common to all coatings, as well as genes, which were upregulated uniquely for a particular coating ligand, were determined. All microarray data were submitted to the NCBI Gene Expression Omnibus (GEO) public database and can be found as accession GSE9859 (http://www.ncbi.nlm.nih.gov/projects/geo/query/acc.cgi?acc=GSE9859). To confirm the observed changes in gene expression, a limited number of expressed proteins were analysed in these samples by western blotting.

2.8 One-dimensional SDS-PAGE and Immunoblotting

2.8.1 Used reagents and instruments

SDS PAGE (according to Laemmli 1970)

- 4x Protein sample buffer, pH 6.8: 250 mM Trizma base, 30 mM EDTA, 40 % glycerol, 4 % 2-mercaptoethanol, 4 % sodium dodecyl sulfate (SDS), 0.01 % bromphenolblue (all from Sigma-Aldrich, USA)
- 10 % separation gels: 13.33 ml 30 % acrylamide/bisacrylamide (Roth, Germany), 10 ml 4x LGS (1.5 M Trizma base, pH 8.8, 0.4 % SDS), 16.66 ml Aqua bidest., 45 µl TEMED and 20 µl 40 % ammonium peroxide sulfate (all from Sigma-Aldrich, USA); 12 % separation gels were adjusted to necessary acrylamide concentration.
- Stacking gels: 0.575 ml 30 % acrylamide/bisacrylamide (Roth, Germany), 1.25 ml 4x UGS (0.5 M Trizma base, pH 6.8, 0,4 % SDS), 3.175 ml Aqua bidest. + 15 µl TEMED + 6.3 µl 40 % ammonium peroxide sulfate (all from Sigma-Aldrich, USA)
- Running buffer: 25 mM Trizma base, 192 mM glycine, 0.1 % SDS (all from Sigma-Aldrich, USA)
- Coomassie staining solution: 0.125 % Coomassie R250 (Serva, Germany), 50 % methanol and 10 % acetic acid (both from Roth, Germany); Destain solution I: 50 % methanol and 10 % acetic acid; Destain solution II: 5 % methanol + 7 % acetic acid
- Molecular weight marker (BioRad, USA)
- Thermostat 5320 (Eppendorf, Germany), Mighty Small II electrophoresis device (Hoefer, Inc., USA), PowerPac 200 (BioRad, USA)

Immunoblotting (according to Towbin et al. 1979)

- Used antibodies: see list in chapter 2.6
- Blot buffer: 25 mM Trizma base, 200 mM glycine, 20 % methanol
- TBS, adjusted to pH 7.4: 10 mM Trizma base, 149 mM NaCl (Merck, Germany)
- TTBS: TBS containing 0.1 % Tween-20 (Merck, Germany)
- Blocking buffer: TTBS containing 5 % non-fat dry milk (Nestlé Food Co., USA)
- Ponceau S staining solution: 0.2 % Ponceau S, 3 % TCA (Serva, Germany)
- Hybond nitrocellulose membranes, Hyperfilm and ECL western blot detection reagent (Amersham, GE Healthcare, UK)
- MiniProtean tank blotting device (BioRad, USA)

2.8.2 1D SDS-PAGE

Cells were washed with PBS twice and 1x SDS sample buffer was added to lyse cells. Isolated phagosomes, cytosol and actin fractions were incubated with 1x SDS sample buffer directly. Subsequently, all SDS samples were boiled at 90 °C for 5 min. to denaturate proteins. Remaining DNA was destroyed by a short ultrasonic treatment on ice. The proteins were separated by vertical gel electrophoresis using 10 % or 12 % polyacrylamide gels. The samples were migrated in 1x running buffer in an electrophoresis device per gel set to constant 10 mA for around 15 min. followed by a run

at constant 20-30 mA for 70-100 min. After separation, proteins were stained using Coomassie or silver staining or were transferred onto nitrocellulose membranes for further immunoblotting (2.8.3).

For Coomassie staining, gels were incubated with Coomassie R250 staining solution for 45 min. under vigorous shaking. Afterwards the stained gels were washed and fixed with destain solution I for 45 min. and destain solution II for minimum 60 min. Silver staining was carried out following the manufacturer's instructions. Images of stained gels were taken with a conventional flat-bed scanner.

2.8.3 Immunoblotting

Following separation in acrylamide gels, protein mixtures were transferred to nitrocellulose (NC) membranes to analyse them for the presence of specific proteins applying antibodies, a method known as immuno- or western blotting. NC membranes, filter papers, sandwich pads and migrated acrylamide gels containing proteins were equilibrated in blot buffer for 20 min. and assembled in cassettes following the manufacturer's instructions. The samples were transferred onto nitrocellulose membranes using a tank blotting device in blot buffer at constant 30 V overnight. Success of transfer was checked by protein staining using Ponceau S solution for 3 min. Afterwards the membranes were rinsed with Aqua dest. and images were taken using a conventional flat-bed scanner.

Before labeling, the membranes were incubated in blocking buffer containing 5 % dry milk or, dependent on the antibody, BSA to block unspecific binding sites. Afterwards dilutions of primary antibodies were prepared in blocking buffer and were applied for 1 hr. at RT or overnight at 4 °C. Membranes were washed with TTBS three times for 10 min. followed by incubation with horseradish peroxidase (HRP)-conjugated secondary antibodies for 45-60 min. After another three washes in TTBS for 10 min. and a final rinse in TBS, the NC membranes were exposed to ECL solution for 5 min. at room temperature. Subsequently, chemiluminescent signals were visualised onto films and scanned for quantification.

2.8.4 Quantification of stained gels, NC membranes and films

Protein signals were quantified using Image Gauge software (Fujifilm, Japan) to determine quantity differences between samples. After scanning, images were converted to PICT format and analysed without further image enhancement. Whole lanes or single spots were selected manually followed by automatic measurement of grey levels. Relative signal intensities were compared using MS Excel.

2.9 Two-dimensional SDS-PAGE

2.9.1 Used material, reagents and instruments

- Acetone, methanol, urea, CHAPS, 2-iodoacetamide, tris-(hydroxymethyl)-amino-methane, ammonium peroxodisulfate, glycine, SDS, TEMED, sodium thiosulfate, silver nitrate, sodium carbonate, formaldehyde, formic acid (Merck, Germany)

- Biolyte® pH 3-10, Ready Strip™ IPG strips, tributyl phosphine (TBP) and acrylamide/bisacrylamide solution (BioRad, USA)
- DTT, Triton X-100, protease inhibitor cocktail P2714 (Sigma-Aldrich, USA)
- Protean™ IEF Cell and II xi 2-DE Cell (BioRad, USA)

2.9.2 2D SDS-PAGE

Two-dimensional gel electrophoresis was performed by the help of Sabrina Rüggeberg (Proteomics core facility, EMBL Heidelberg) according to the procedures reviewed by Görg et al. (2000). The same amount (100 µl; OD=0.18) of isolated phagosomes (1 hr./1 hr.) containing latex beads coupled to the Fc fragment of mouse IgG and mannan, respectively, were used. After lysis in 2 % Triton-X100, 10 mM DTT, 50 mM Tris pH 8.0 and protease inhibitors for 15 min. at 4 °C, latex beads were removed by centrifugation and phagosomal proteins were precipitated in acetone for two hours at -20 °C. The solutions were centrifuged with 14.000 rpm for 60 min. at 4 °C and precipitates were solubilised in sample solution (9 mol/L urea, 16 mmol/L CHAPS, 2 mmol/L TBP, 0.25 % Biolyte, protease inhibitor cocktail). Both samples were applied to 11 cm IPG strips at pH 3 to 10 with rehydration loading overnight as described elsewhere (Bjellqvist et al. 1982). The samples were mixed with rehydration solution (8 mol/L urea, 16 mmol/L CHAPS, 2 mmol/L TBP, 0.25 % Biolyte) giving a final volume of 200 µL. For isoelectric focusing (first dimension), the Protean™ IEF Cell was loaded with re-hydrated IPG strips and focused for about 80 kV/h at a maximum voltage of 6.000 V at 20 °C. After focusing, each IPG strip was emerged first for 10 min. into reduction solution (6 mol/L urea, 30 % glycerol, 0.05 mol/L Tris pH 8.8, 173 mmol/L SDS, bromophenolblue) containing 5 mmol/L TBP and then into alkylation solution containing 270 mmol/L 2-iodoacetamide. Subsequently, the IPG strips were loaded on top of the gel for the second dimension for separation by size. The Protean™ II xi 2-DE was used to run 12 % SDS polyacrylamide gels according to the method described in Laemmli (1970). The gels were run for 45 min. at 20 mA per gel and then for 600 V/h at 15 mA/gel in a second step. Visualisation was achieved by using the silver staining method according to Shevchenko et al. (1996).

2.10 Liquid chromatography and tandem mass spectroscopy (LC-MS/MS)

The same samples were also used for mass spectroscopy to identify phagosomal proteins. The same amount of phagosomes isolated after 1 hr./1 hr. containing latex beads coupled to the Fc fragment of mouse IgG and mannan were used (500 µl; OD=0.18). Additionally, LBP coated with avidin isolated following the same method after same pulse and chase times were used for analysis (kindly provided by Sabrina Marion, EMBL Heidelberg). Purified phagosomes were lysed in 2 % Triton X-100, 10 mM DTT, 50 mM Tris, pH 8.0 and protease inhibitors by vortexing and incubation at 4 °C for 15 min. Latex beads were removed by centrifugation and phagosomal proteins were precipitated in acetone for two hours at -20 °C. The solutions were centrifuged with 14.000 rpm for 60 min. at 4 °C. The pellet was

dissolved, reduced with DTT and alkylated with iodoacetamide before being digested with 1 µg of Promega-modified trypsin for 24 hrs. at room temperature. A second 1 µg of trypsin was added and digestion was allowed to proceed for 24 more hours. The sample was acidified to 5 % acetic acid and then desalted on a C18 column. Approximately 25 % of the digest was introduced into the mass spectrometer for analysis using two run conditions. The complete procedure for LC-MS/MS was performed by the Biomolecular Research Facility at the Virginia University in Charlottesville, USA by the group of Dr. Nicholas Sherman. The LC-MS system consisted of a Finnigan LCQ ion trap mass spectrometer system (Thermo Fisher Scientific, Inc., USA) with a Protana nanospray ion source interfaced to a self-packed 8 cm × 75 µm id Phenomenex Jupiter 10 µm C18 reversed-phase capillary column. The extracts (0.5-10 µl volumes) were injected and the peptides were eluted from the column by an acetonitrile/0.1 M acetic acid gradient at a flow rate of 0.25 µl/min. The nanospray ion source was operated at 2.8 kV. The digest was analysed using the double play capability of the instrument acquiring full scan mass spectra to determine peptide molecular weights and product ion spectra to determine amino acid sequence in sequential scans. This mode of analysis produces approximately 3000 CAD spectra of ions ranging in abundance over several orders of magnitude.

The data were analysed by database searching using the Sequest algorithm (developed by J. Eng and J. Yates, The Scripps Research Institute, La Jolla, USA) against mouse IPI accessions. This program converted the character-based representation of amino acid sequences in a protein database to fragmentation patterns, which were compared against the MS/MS spectrum generated on the target peptide. The algorithm initially identified amino acid sequences in the database that match the measured mass of the peptide, compared fragment ions against the MS/MS spectrum and generated a preliminary score for each amino acid sequence. Then, a cross-correlation analysis was performed by correlating theoretical, reconstructed spectra against the experimental spectrum. Identified proteins were analysed using Scaffold software (Proteome Software, Inc., USA) applying different protein identification probability filter settings. The correlation score (X_{corr}), which was included by the mass spectrometry lab in Virginia, was corrected for length of the peptide that gives a very high probability of being correct, but excluded proteins with lower probability, peptide length etc., which were expected on LBP known from comparable previous studies (Garin et al. 2001, Rogers & Foster 2007). Therefore, in this study I used a different scoring system for the proteomic analysis based on the peptide/protein prophet included in the software. By this analysis, less protein sequences were covered by unique peptide spectra, slightly increasing the chance of false positives and negatives appearing in the list, but still gave identification results of high confidence. Used filter settings were:

- minimum protein identification probability[1]: 80 %
- minimum number of peptides[2]: 1
- minimum peptide identification probability[3]: 95 %

[1] minimum requirement for Scaffold's calculated probability of correct protein identification (ID)
[2] number of unique peptides that must be found for one protein in order to consider to be identified
[3] how certain a peptide ID must be before it can be counted toward the minimum number of peptides

Results

3.1 Characterization of the binding of phagosomes to F-actin using an *in vitro* binding assay

Phagosomes are membrane bound organelles, which associate with many cytoskeleton components. Actin filaments and their associated proteins play an important role during particle uptake and formation of phagosomal membranes from the plasma membrane, but it is also well accepted that phagosomes rapidly lose their abundant actin coats within minutes of finishing the internalisation process. The participation of actin and its associated proteins in later events of phagocytosis like the maturation of phagosomes, which includes acidification by fission and fusion events with compartments of the endo /lysosomal system, is less clear. There are several hints which support an involvement in these processes, like the capability of maturing phagosomes to nucleate actin (Defacque *et al.* 2000, Jahraus *et al.* 2001), to interact with and recruit actin associated proteins (Stockinger *et al.* 2006) as well as the presence of actin and many of its proteins in mature phagosomes determined by proteomic analysis (Desjardins *et al.* 1994, Garin *et al.* 2001, Gotthardt *et al.* 2006). Besides the ability of phagosomes to nucleate actin *de novo*, it is still an open question what an impact the binding of phagosomes to F actin possesses during their maturation. However, given the plethora of actin binding proteins (17 identified ones in the study of Garin *et al.* 2001) it seems inescapable that they must bind F actin in cells.

To investigate the binding of phagosomes to actin filaments and the contribution of their associated proteins, an *in vitro* assay was developed in our lab, which allows analysis of these events step by step. By the help of this assay, it already could be demonstrated that binding between actin filaments and phagosomes containing latex beads (LBPs), a well characterized model system, occurs *in vitro*. Furthermore, the interactions between LBPs and F actin were dependent on actin binding proteins (ABPs), which contribute to this binding differently. So far, three different factors were found to be involved, two stimulatory ones and one inhibitory factor of low molecular mass. Of the stimulatory factors, one high molecular weight protein functions independent of ATP, whereas the other one could be identified as the ATP dependent motor protein Myosin Va (Al Haddad *et al.* 2001).

The actin binding assay relies on the step wise perfusion of components in small chambers on a glass slide. After the formation of stabilised actin networks on coverslips coated with poly L lysine and blocking of unspecific binding sites, phagosomes and additional factors are perfused into the chamber to allow binding to these pre formed actin networks. After incubation unbound components are washed out and samples are analysed by conventional fluorescence microscopy by determining numbers of bound phagosomes to

actin filaments per microscopic field (see chapter 2.5). This simple assay is not only highly reproducable, but also gives highly quantitative results.

In this study, I wanted to extend the investigation of phagosomes and their capability to bind to actin filaments, not only those enclosing latex beads but also pathogenic and non pathogenic bacteria. They represent important targets of professional phagocytes like macrophages, which help to destroy invading microorganisms and are essential part of the innate immune system.

3.1.1 Binding of isolated phagosomes containing latex beads

Phagosomes containing inert latex particles of same size provide an elegant model system to study different aspects of phagocytosis and can be isolated in high purities. The analysis of these phagosomes and their binding to actin filaments *in vitro* is important to understand the underlying molecular mechanisms, if they are compared to phagosomes containing microbes. It was therefore important to investigate these organelles in more detail. The experiments of the Al Haddad *et al.* study (2001) were carried out using phagosomes containing 1 μm latex beads coated non specifically with fish skin gelatin (FSG), which were isolated from macrophages by sucrose gradient centrifugation after one hour pulse followed by an additional chase time of one hour. In this study, I started with the same phagosomes to analyse and confirm the basic conditions of LBP binding to F actin *in vitro*.

First, the system was validated and basic conditions were controlled. The formation of homogenous actin networks on coverslips need a pre coating of glass surfaces with 0.1 mg/ml poly L lysine (Fig. 5). Blocking of non specific binding sites of F actin is sufficient to maintain stable phagosomal binding to filaments and reduces background interactions of components. Non coated latex beads do not bind to these networks in the absence and presence of cytosol. Coated latex beads without surrounding phagosome membrane only bind weakly to actin networks (Fig. 6A). After checking the basic conditions phagosomal binding could be investigated in the assay.

Phagosomes containing FSG coupled latex beads were analysed without any further treatment after isolation or the addition of cytosolic factors to the assay. Interestingly, these phagosomes were able to bind to actin filaments *in vitro* in the absence of cytosolic components (Fig. 6A). This demonstrates that LBPs carry the factors, which are involved in mediating binding to F actin, also after their isolation. The addition of different concentrations of cytosol isolated from non activated J774 macrophages induced no stimulation of phagosomal binding (Fig. 6A). As expected, a salt stripping of these phagosomes strongly

reduced the binding capability in the assay by removing membrane bound proteins, like motor enzymes, whereas the addition of J774 cytosol again restored the binding of stripped phagosomes (Fig. 6A). The range of the stimulatory potential was dependent on individual cytosols used in combination with individual phagosomes, but the addition of low concentrations of cytosolic factors was already sufficient to mediate binding of salt stripped LBPs to actin networks. During this study, 16 different J774 cytosol isolations were carried out, which possessed their most stimulatory capability at protein concentrations between 0.05 and 2 mg/ml (see example in Fig. 6B, black line). Higher protein concentrations always caused reduced binding capabilities of phagosomes, most probably because of the increased presence of a low molecular mass inhibitor (Al Haddad *et al.* 2001), which still remains to be characterized. I was also able to confirm that the stimulatory activity of cytosolic factors is partly ATP dependent, because the addition of 1 mM Na ATP to the assay caused a reduction in binding activity of more than 50 %, demonstrating that ATP dependent actin binding proteins (ABPs) are involved, namely motor proteins of the myosin superfamily. The participation of Myosin Va in mediating binding of LBPs to actin filaments has been already shown in our lab as well as the fact, that Myosin II is not involved in this process (Al Haddad *et al.* 2001).

Immunoblotting analysis of phagosomes is supporting these findings, because actin binding proteins (like Moesin, mDia1 and Myosin Va) can be removed by salt stripping or restored by re incubation with cytosol. As an example, immunoblotting with an antibody against Myosin Va is shown in Fig. 6A'. The protein is present on non stripped phagosomes, salt stripping removes it from phagosomal membranes. After an incubation of salt stripped LBP with 1 mg/ml cytosol on ice for 20 min. followed by re flotation over a sucrose gradient, Myosin Va is again detectable on the organelle membrane. Immunoblotting using an antibody against actin revealed that it also rebinds to phagosomes, if they are incubated with cytosol (Fig. 6A'), arguing that the observed association of phagosomes to actin networks could be due to actin actin interactions by actin crosslinkers. However, previous experiments with the actin depolymerising drugs cytochalasin D and latrunculin already have shown that actin actin interactions are not responsible and that binding proteins contribute to this association (Al Haddad *et al.* 2001). Besides Myosin Va, it is known that many different motor proteins are involved in the interaction of phagosomes with actin filaments. However, actin binding proteins without motor activity can also have an impact on these processes and different classes of these proteins were identified in different phagosome proteomes (see references in Griffiths & Mayorga 2007). Many of them belong to the groups of cross linkers, bundling proteins and actin nucleators.

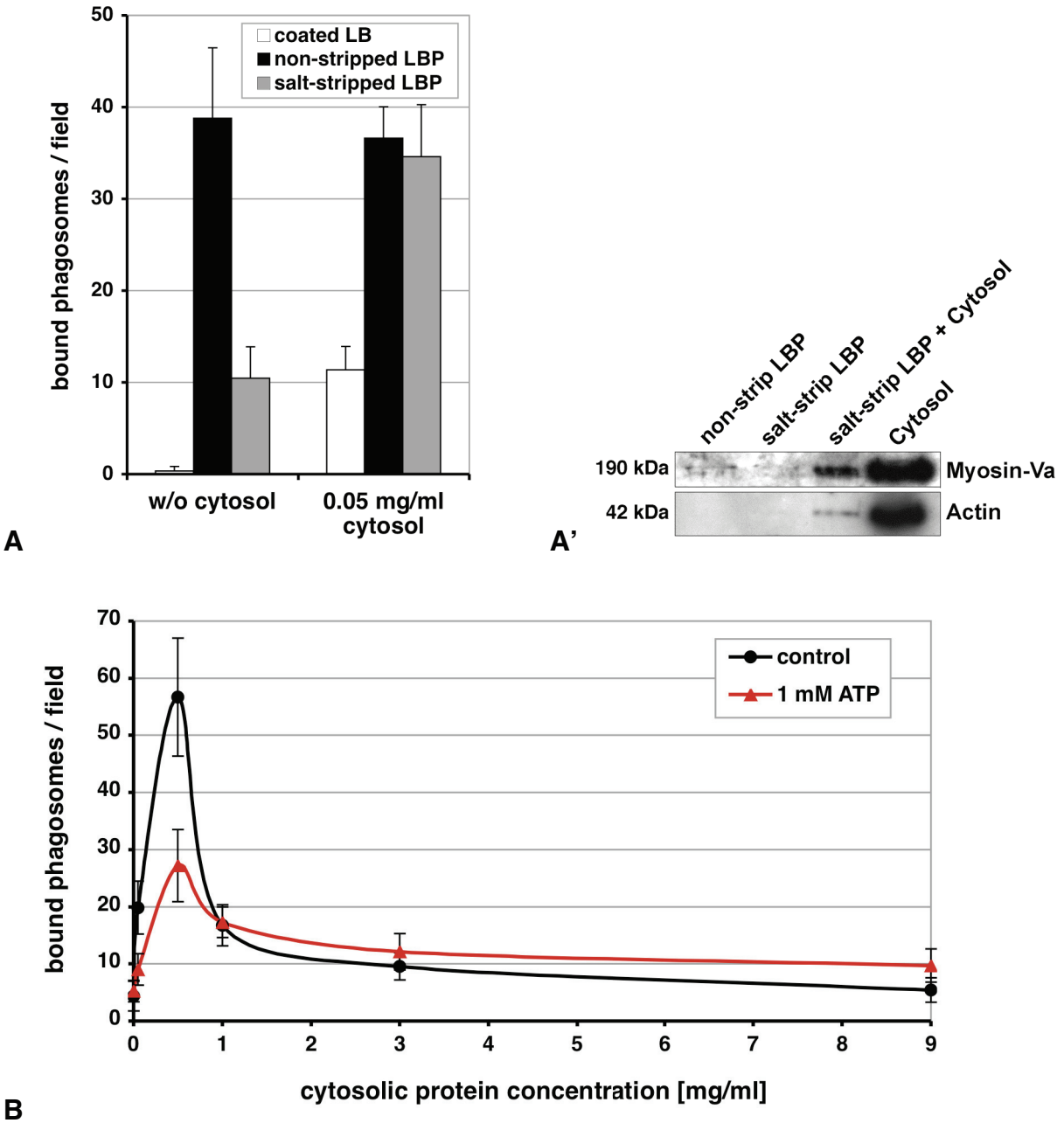

Figure 6. Binding behaviour of isolated J774 latex bead phagosomes *in vitro*. **(A)** Shown are averages of bound LBPs of 20 analysed microscopic fields in the actin-binding assay. Pure coated latex beads (LB) without a phagosomal membrane bind weakly to F-actin. Non-stripped LBPs (black bars) are able to bind in the absence of cytosolic factors, whereas salt-stripping (grey bars) causes a reduction of binding capability. The addition of cytosol isolated from J774 macrophages to the assay restores binding of salt-stripped but exhibits no effect on non-stripped phagosomes. **(A')** Analysis of components applied in the binding assay by immunoblotting using an antibody against actin and the actin-binding protein Myosin-Va. Actin is present in cytosol (lane 4) and rebinds to phagosomes (lane 3). Myosin-Va is detectable in cytosol (lane 4) and on non-stripped LBPs (lane 1), but can be removed from phagosomes by salt-stripping (lane 2). Myosin-Va rebinds to salt-stripped LBPs, if they are incubated with cytosol (lane 3; shown are only pre-incubated phagosomes after re-flotation in a sucrose gradient). The same amount of phagosomes was loaded in lanes 1-3 as well as the same concentration of cytosol in lanes 3 and 4. **(B)** The stimulatory capability of cytosol is located between protein concentrations of 0.05 and 2 mg/ml determined in the actin-binding assay (black line). An addition of 1 mM Na-ATP to the assay (red line) reduced binding by 55 % at 0.05 mg/ml cytosol and by 52 % at 0.5 mg/ml cytosol. Furthermore, the stimulatory potential is also dependent on individual cytosol preparations, e.g. comparison of cytosol XIV in (A) and cytosol VIII in (B).

In this study, I concentrated on the influence of some likely candidates of the last group to investigate how they alter the observed association of phagosomes with F actin in the *in vitro* binding assay. Antibodies (see Table 2 in chapter 2.6) were used at 0.5 mg/ml to block the function of Ezrin, Moesin, N WASP, mDia1 and IQGAP1, respectively. Ezrin, Moesin and N WASP are nucleating actin on membranes, whereas mDia1 and IQGAP1 are activators of the actin nucleating machinery. Previous studies demonstrated that they are associated with phagosomes or they could be identified on phagosomal membranes by mass spectrometry. In addition to the proteins mentioned above, an antibody against Myosin Va was also used in the assay to validate the results of this experiment with previous findings (Al Haddad et al. 2001). To exclude an influence of the order of application of phagosomes, cytosol and antibody in assay samples, a pre incubation of cytosol and antibody was tested on ice for 20 min. as well as the direct application of all three components in the assay. No differences could be detected between these two experimental conditions.

The antibody against Myosin Va reduced binding of salt stripped phagosomes to F actin *in vitro* in the presence of cytosol by nearly 40 % (Fig. 7, upper chart), confirming it's role in maintaining interaction between phagosome and actin filaments. The same experiment in the absence of cytosol caused no effect (data not shown), which again indicates that Myosin Va is recruited from the cytosol. Significant influences on binding of salt stripped LBPs to F actin *in vitro* also appeared, when antibodies against Ezrin and N WASP were applied (Fig. 7, upper chart). Here, an increased binding activity could be observed, both of around 40 %, arguing for inhibitory functions of these proteins in the assay. Blocking of Moesin, IQGAP1 and mDia1 caused no significant differences (Fig. 7, upper chart), although it cannot be excluded that the antibodies used in the assay were not blocking their functions properly. The inhibitory function of Ezrin and N WASP, proteins expected to be part of the actin nucleation machinery, on binding observed in the assay was surprising. These data gave the first hint that the nucleation of actin on phagosomal membranes could play the opposite role than the binding of phagosomes to actin filaments.

I further investigated whether the antibodies, which exhibited significant effect in the binding assay, are able to detect the particular protein in J774 macrophages and analysed their sub cellular localisation. The cells were allowed to internalise FSG coated latex beads for 1 hour followed by a chase time of 1 hour to maintain the same phagosomes that were used in the *in vitro* assay. The samples were fixed with paraformaldehyde, permeabilised and afterwards labelled with the respective antibody. Both antibodies were able to confirm the presence of Myosin Va and Ezrin on phagosomes in macrophages (Fig. 7,middle) and support the effects observed *in vitro*.

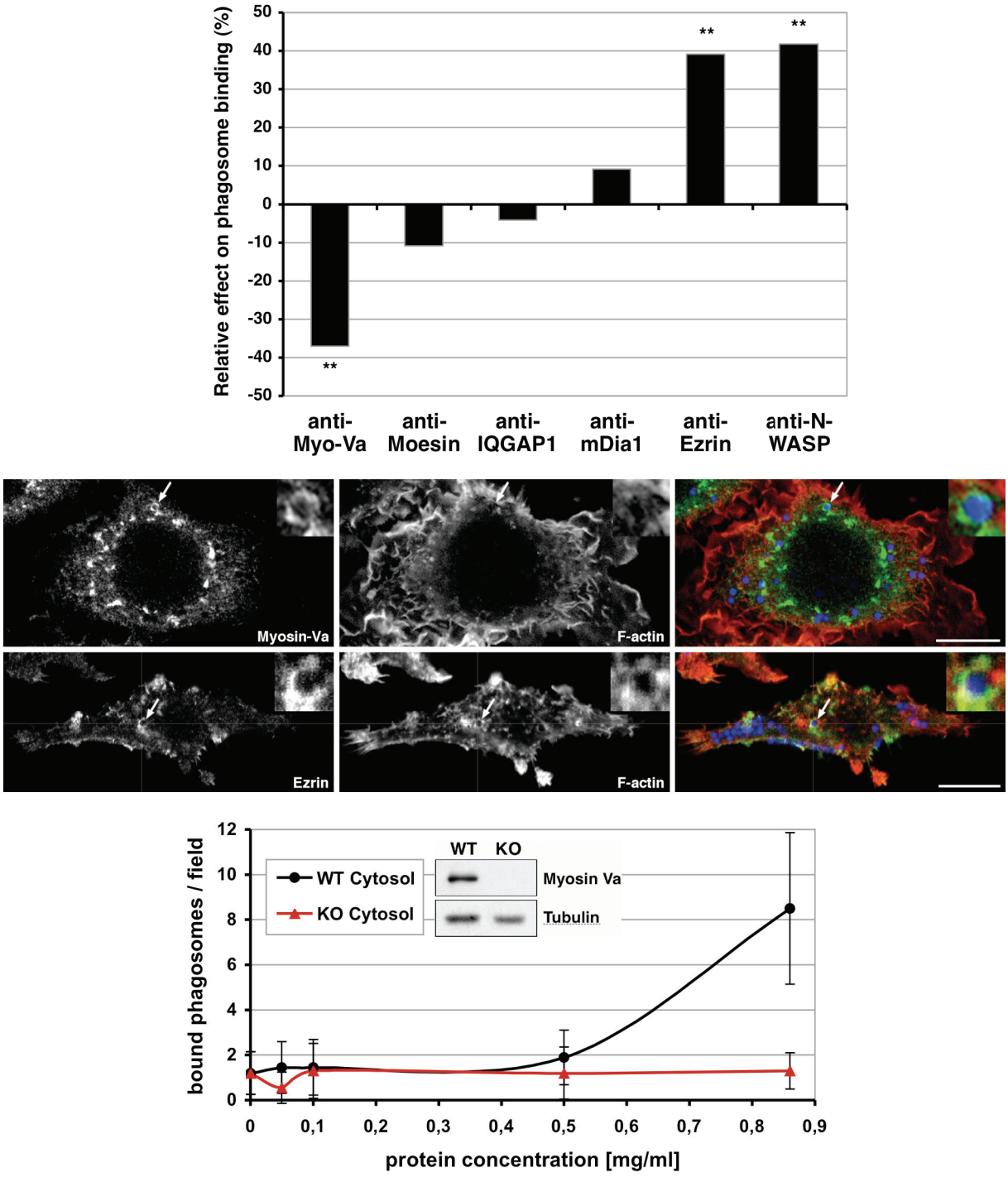

Figure 7. Upper chart: Binding of salt-stripped LBP to F-actin *in vitro* in presence of 0.5 mg/ml J774 cytosol. Shown are relative effects in phagosomal binding compared to mock controls, when antibodies against actin-binding proteins were applied to the assay at 0.5 mg/ml. Significant inhibitory and stimulatory influence on binding could be demonstrated for antibodies against Myosin-Va, Ezrin and N-WASP, whereas blocking of Moesin, IQGAP1 and mDia1 exhibited no or only weak differences. Significance of results was tested using Student's t-test (** $P<0.01$). **images, middle:** Two of these antibodies were probed to detect Myosin-Va and Ezrin (both in green) in fixed J774 cells by confocal microscopy. Shown are single z-stacks of whole cells and phagosomes after 1 hr. pulse and 1 hr. chase that displayed detectable protein signals (arrow), also shown as insets. Bars represent 10 μm. **Lower chart:** A similar result could be obtained, when cytosol isolated from wild type (WT) and Myosin-Va knock-out (KO) primary macrophages was added to LBP in the *in vitro* actin-binding assay. Binding was inhibited in the absence of Myosin-Va (inset: western blot image of total cell lysates).

Additionally, it was interesting to analyse whether kinases or phosphatases are able to alter the stimulatory activity of cytosolic components, because many membrane proteins including several actin binding proteins are regulated by phosphorylation and dephosphorylation events. The addition of kinase and phosphatase inhibitors to the assay (see table 1 in chapter 2.5) allowed the investigation of these enzymes under *in vitro* conditions. Staurosporine was used to block kinases in general (especially protein kinases like PKC and calmodulin dependent kinases), sodium vanadate to inhibit phosphatases non specifically. PI3 kinase was affected by using two inhibitors, wortmannin and LY294002, and tyrosine kinase by the addition of genistein to the assay. The phosphatases 1A and 2A were specifically blocked by ocadaic acid. All inhibitors were used at concentrations, which affects these enzymes under *in vitro* conditions as shown in a comparable *in vitro* assay developed in our lab (Wöllert et al. 2002) and tested for significance versus DMSO mock controls.

The inhibition of all tested kinases and phosphatases did not affect significantly, or only slightly, the binding behaviour of salt stripped phagosomes in the absence and presence of cytosolic factors (Fig. 8). These results suggest that phosphorylation and dephosphorylation events are not involved in the binding of phagosomes to actin filaments at later phagocytic stages. Of course, the phosphorylation of ABPs, e.g. Myosin Va, is likely to be essential for the regulation of these proteins in living cells, but an inhibition seems to not disturb the binding of phagosomes to actin networks *in vitro*.

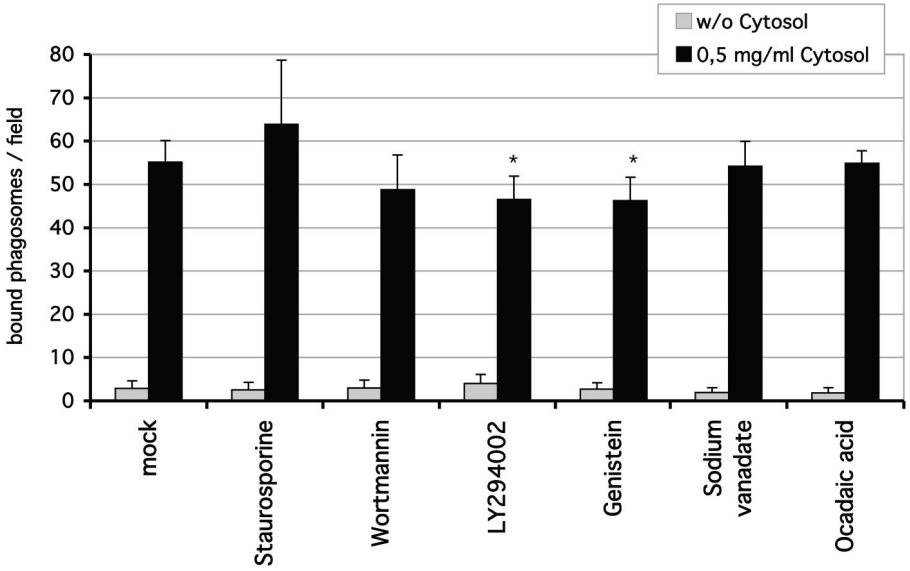

Figure 8. Binding behaviour of salt-stripped latex bead phagosomes in the *in vitro* binding assay in the absence and presence of 0.5 mg/ml J774 cytosol after the addition of kinase and phosphatase inhibitors. Shown are averages of LBP's bound to F-actin of 20 analysed microscopic fields. No effect had the inhibition of kinases in general (staurosporine), of PI3-kinase using wortmannin, of phosphatases in general (sodium vanadate) and of phosphatase-1A and -2A (ocadaic acid). Only the addition of the inhibitor LY294002 to block PI3-kinase and genistein to affect tyrosine kinases had slight effects. Significance of results was tested using Student's t-test (* $P<0.05$).

In summary, the analysis of the binding behaviour of phagosomes containing latex beads *in vitro* showed that these phagosomes need cytosolic factors to interact with F actin, one factor was previously identified as the motor protein Myosin Va. The majority of these factors is still present on phagosomal membranes after isolation, because non stripped phagosomes also bound in the absence of cytosol. Salt stripping of phagosomes removed membrane proteins and reduced phagosomal binding to actin networks, which could be restored by the addition of isolated cytosols at concentrations between 0.05 and 2 mg/ml dependent on individual cytosols. The addition of salt stripped phagosomes, cytosol and additional factors allowed a step wise investigation of these events. Experiments with kinase and phosphatase inhibitors showed no differences relative to control conditions, demonstrating that phosphorylation and dephosphorylation events are not important for regulating *in vitro* binding. Studies with antibodies against some actin binding proteins interfered with phagosomal binding to actin filaments, pointed to contradictory roles of binding and actin nucleation events.

3.1.2 Binding of isolated phagosomes containing pathogenic and non-pathogenic bacteria

After investigating the binding of LBPs to F actin in more detail, the next aim of this study was the analyis of the binding behaviour of phagosomes containing non pathogenic and pathogenic species of mycobacteria. Members of this family, *Mycobacterium tuberculosis* and *M. leprae*, are causative agents of the infectious diseases tuberculosis and lepra and, in the case of tuberculosis, are responsible for the death of more than 1.6 million humans annually (http://www.who.int/tb/en/). Phagocytes are internalising mycobacteria by selective, receptor mediated uptake. Depending on bacterial species and pathogenicity, different receptor types can be involved in this process. In the case of *M. tuberculosis* it is well accepted that the mannose receptor (MR), the complement receptor 3 (CR3), scavenger receptors and, after opsonisation, Fcγ receptors contribute to its internalisation (Ernst 1998). After uptake, mycobacteria are localised in vacuoles that display characteristics of phagosomes of early endosomal origin, like the presence of their markers Rab5 and early endosomal antigen 1 (EEA1), but pathogenic species are able to interfere with subsequent steps of phagosome maturation. They modulate several host cell mechanisms, like phagosomal acidification, to prevent their killing and moreover, are able to replicate within these cells to spread infection in the host (Russell *et al.* 2001, Vergne *et al.* 2004, Kusner *et al.* 2005). In addition to alterations in phagosome maturation, it was found that pathogenic

mycobacteria also prevent actin nucleation on their phagosome membranes, whereas phagosomes containing non pathogenic species polymerise actin *de novo* (Anes *et al.* 2003). It was therefore of interest to examine, whether binding of phagosomes to actin filaments *in vitro* is also influenced by mycobacteria and is of importance during phagosome maturation.

After their isolation, phagosomes containing the non pathogenic strain *Mycobacterium smegmatis* as well as the pathogenic species *M. avium* and *M. bovis* BCG were compared in the actin binding assay. As controls latex bead phagosomes were also analysed in the same assays. All phagosomes containing mycobacteria failed to bind to actin networks *in vitro* in the absence (data not shown) as well as in the presence of cytosol (Fig. 9A), whereas LBPs bound to F actin as decribed in chapter 3.1.1. To exclude the influence of endogenous or exogenous factors on this result, several possibilities were tested in the *in vitro* assay. All phagosomal samples where titrated and analysed in assays to avoid that concentration dependent effects influence the association with actin filaments. However, independent on the used concentrations mycobacterial phagosomes exhibited no comparable binding to actin networks. In opposite to LBPs, which contain undegradable content, mycobacterial phagosomes mature differently compared to LBP. Previous studies showed that phagosomes containing *M. smegmatis* are dynamic compartments and do not degrade their content linearly. Moreover, initial killing phases are followed by bacterial multiplication and additional killing phases afterwards (Anes *et al.* 2006; Jordao et al. 2007).

In order to avoid the possibility that different maturation stages of mycobacterial phagosomes are responsible for the lack of actin interaction, isolations of different ages were also tested in actin binding assays. The following phagosomes were checked for binding to F actin *in vitro*: *M. smegmatis* 1 hr./1 hr., 1 hr./2 hrs., 1 hr./7 hrs., 1 hr./11 hrs. and 1 hr./23 hrs.; *M. avium* 1 hr./1 hr. and 1 hr./11 hrs. and *M. bovis* BCG 1 hr./3 hrs. and 1 hr./23 hrs. None of these isolations contained phagosomes that were able to bind to actin networks in the presence of 1 mg/ml J774 cytosol (Fig. 9A). I also analysed whether the physiological state of the phagosome content possessed an influence and studied phagosomes containing not only live mycobacteria but also heat killed *M. smegmatis* (1 hr./11 hrs. and 1 hr./23 hrs.) and *M. bovis* BCG (1 hr./3 hrs. and 1 hr./23 hrs.), but no different results could be obtained (Fig. 9B). Additionally to mycobacterial species, I also checked phagosomes containing another Gram positive, rod shaped bacterium of relatively the same size (non pathogenic *E. coli* GFP strain TG1 used in Kunert et al. 2003) in binding to actin networks *in vitro* to exclude that mycobacteria family specific factors, signalling pathways or signatures are involved in preventing binding. As shown in Fig. 9A, *E. coli* phagosomes did also not bind to F actin *in vitro* significantly.

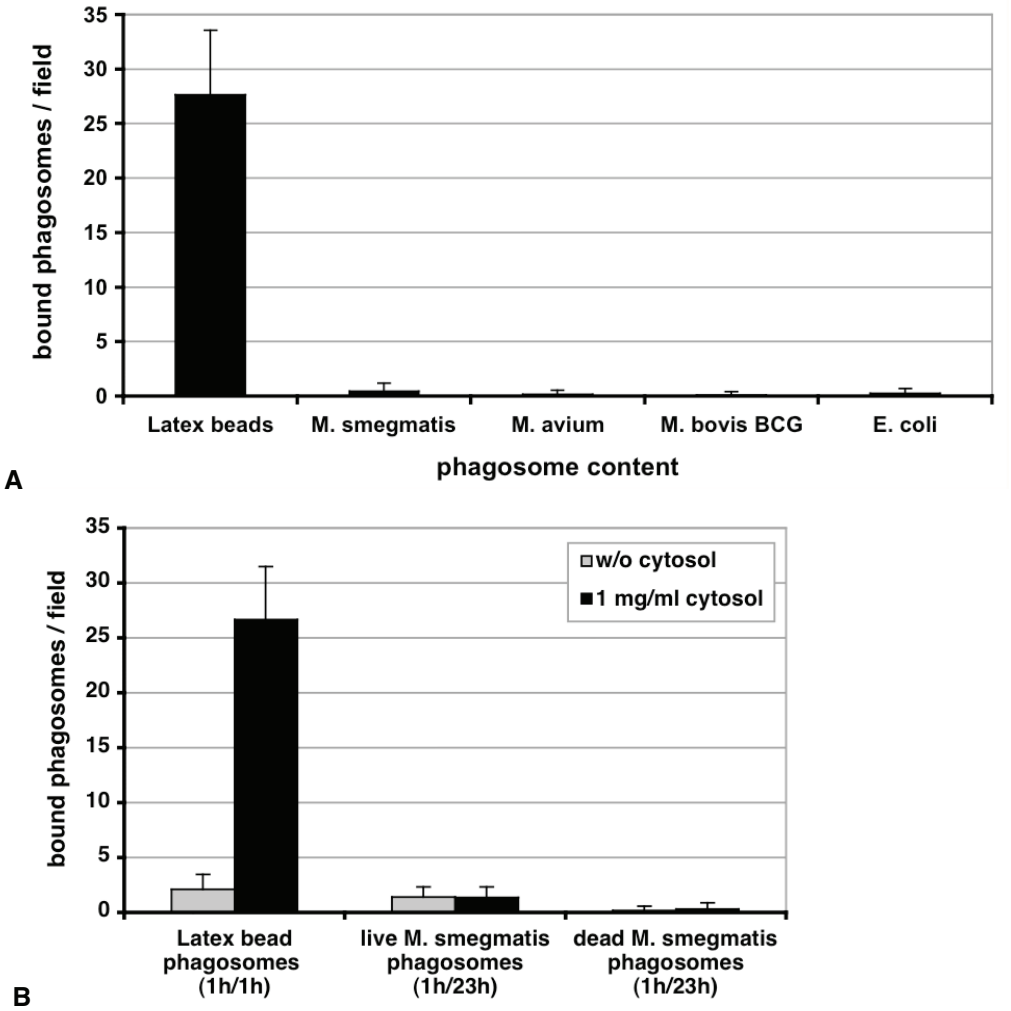

Figure 9. (A) Binding behaviour of phagosomes to actin networks *in vitro* isolated from J774 macrophages containing latex beads and bacteria in the presence of 1 mg/ml J774 cytosol. Shown are results of 1 hr./1 hr. phagosomes (FSG-coated latex beads, *Mycobacterium smegmatis*, *M. avium* and *E. coli*) and 1 hr./3 hrs. phagosomes (*M. bovis* BCG). **(B)** Phagosomal binding to F-actin *in vitro* of LBP and phagosomes containing live or heat-killed *M. smegmatis* isolated after 1 hr. pulse and 23 hrs. maturation. No binding above background conditions occured in bacteria-containing phagosomes at all tested conditions (different bacteria species, maturation ages, live or dead individuals etc.).

Phagosomes containing latex beads with membranes tightly located around the bead differ ultrastructurally and physiologically from phagosomes containing mycobacteria species with membranes losely around the bacterium because of sugar residues in bacterial cell walls. Isolated phagosomes were checked for membrane integrity by staining them for LAMP 1, a lysosomal membrane protein, which also appears on mature phagosome membranes as well as labeling of bacterial DNA using propidiumiodide and ethiumbromide (see material and methods for more details). In both tests more than 70 % of isolated mycobacterial phagosomes possessed closed membranes, showing that the investigated phagosomes were mostly intact. Moreover, also pure *M. smegmatis* individuals were not able to bind to actin networks *in vitro*. The mycobacterial cell wall, comprised predominantly of

lipids and carbohydrates, is the first to contact host cellular constituents, and therefore play a major role in facilitating host cell entry and response. To check whether mycobacterial cell wall components interfere with the phagosome membrane and therefore modulate or prevent binding to actin filaments, the phagosomal membrane was pre treated and then studied in the binding assay. Phagosomes containing *M. smegmatis* were salt stripped with 1.3 M NaCl, permeabilised with Triton X 100 or dialysed against buffer containing no sucrose to analyse whether factors around the membrane, like proteins and lipids or sugars from the isolation buffer, prevent phagosomal binding to actin filaments. However, also after these treatments no difference in binding behaviour of phagosomes could be observed.

Besides the phagosomes, another factor important in the assay is the addition of cytosol to mediate binding between F actin and phagosomes. So far only cytosol preparations isolated from non stimulated macrophages were analysed, but macrophages are often getting activated, if they meet microorganisms, especially pathogens, to induce increased signalling and defense strategies. Therefore, also cytosols isolated from J774 macrophages activated by incubation with live *M. smegmatis* for 2 hrs. or LPS from *E. coli* (6 hrs. at 1 μg/ml) were added to mycobacterial phagosomes in the assay, but did not have an influence on binding. Finally, it was investigated whether the addition of isolated actin binding protein or Myosin V fractions from J774 cytosols do mediate binding of phagosomes containing *M. smegmatis*, but did not alter the results shown before.

So far, it is not clear whether the lack of binding of mycobacterial compared to latex bead phagosomes to actin filaments *in vitro* is a physiological phenomenon or is due to technical problems linked to the assay conditions. However, I decided to apply another approach to study the binding of bacteria containing phagosomes to F actin by combining the latex model system with some characteristics of pathogenic bacteria. The latex bead surface was coated with ligands present on the surface of microorganisms or with host components involved in opsonin mediated uptake. Feeding of these particles partly mimicked bactera entry, triggered receptor specific uptake and caused ligand specific phagocytosis functions.

3.1.3 Binding of isolated phagosomes containing latex beads coupled to different ligands

Ligand receptor interactions are an essential part of phagocytosis not only during internalisation but also for the intracellular fate of phagosomes. The uptake of pathogens but also of other particles like cell debris in macrophages is associated with many early intracellular signalling events and the contribution and number of involved receptors are tremendous. Dependent on the characteristics of the ligand on the surface, target specific

receptors are triggered and mediate receptor dependent phagocytosis. Pathogenic mycobacteria, like *M. tuberculosis*, are believed to be recognised and internalised in non opsonic pathways predominantly by mannose receptors, whereas opsonised particles, like erythrocytes, are taken up by immunoglobulin dependent Fc receptors.

The surface of latex beads can be coupled to a variety of ligands to get internalised by phagocytes in receptor specific pathways. So far the results in this study were obtained by the use of latex beads coupled to fish skin gelatin, a protein coating which causes non specific uptake via a mixture of different receptors. Carboxylated microspheres offer the possibility to interact with different proteins and carbohydrates, which form covalent bounds with the surface of the bead. To enter cells in different receptor dependent pathways, latex beads were coupled to murine immunoglobulin G (whole molecule or only partly in form of the Fc fragment), complement isolated from mouse serum, lipopolysaccharides (LPS) obtained from *Klebsiella pneumoniae* and mannan from *Saccharomyces cerevisiae*. These coupling agents triggered specific uptake via receptor classes which are mainly involved in the recognition of these ligands: IgG via Fcγ and complement via complement receptors, both opsonic receptor classes, whereas the recognition of LPS via CD14 and toll like receptors and of mannan predominantly via the mannose receptor belong to non opsonic receptor classes.

As it was already mentioned in the introduction in more detail, particle recognition and uptake are not results of single receptor molecules, but are based on the cooperation of specific receptor classes, which interact and identify pattern on the particle surface. In comparison to these receptor specific internalisation processes beads coupled to gelatin and avidin were used for comparison. Both are ligands which are believed to be taken up in non specific receptor pathways by the help of different receptor classes, e.g. by the involvement of scavenger receptors.

The J774 macrophage cell line, originally isolated in 1968 and deposited by P. Ralph (Ralph *et al.* 1976), possesses different receptor expression patterns dependent on the used clone. In this study, we were using the A.1 clone, which displays expression of FcγRI (Sears *et al.* 1990), of CR3 (Ralph *et al.* 1977), of MR (Fiani *et al.* 1998) as well as of CD14 (Hara Kuge *et al.* 1990), TLR2/4 (Yang *et al.* 2001, Jouault *et al.* 2003) and others, like scavenger receptors (Nishikawa *et al.* 1990). These findings make this cell line suitable for a detailed analysis of phagocytic processes using ligands named above.

The coupling of latex bead surfaces was carried out following protocols described in chapter 2.2 and J774 macrophages were fed with the same amount of the different coated beads. All phagosome types were isolated after one hour pulse and one hour chase by the

same method using flotation over a sucrose gradient. The optical density of all isolated phagosomes was determined to maintain that the same number of phagosomes was used in experiments. Afterwards, LBP were analysed for their ability to bind to actin networks *in vitro*. First, titration experiments were carried out to exclude that phagosomes display differences in binding due to over saturating concentrations. Reproducible results, which are comparable to former studies could be achieved when phagosomes were used at 0.006 % solids in solution. All phagosome types were used at this concentration and analysed for their binding behaviour in the absence and presence of cytosolic components.

Surprisingly, the tested phagosome types exhibited different capabilities to bind to F actin *in vitro* in the binding assay in the presence of cytosol (Fig. 10). Phagosomes containing beads coupled to mannan showed higher binding compared to control levels (binding capability of FSG and avidin LBP), whereas phagosomes containing IgG , complement and LPS beads possessed a decreased ability to bind to actin filaments.

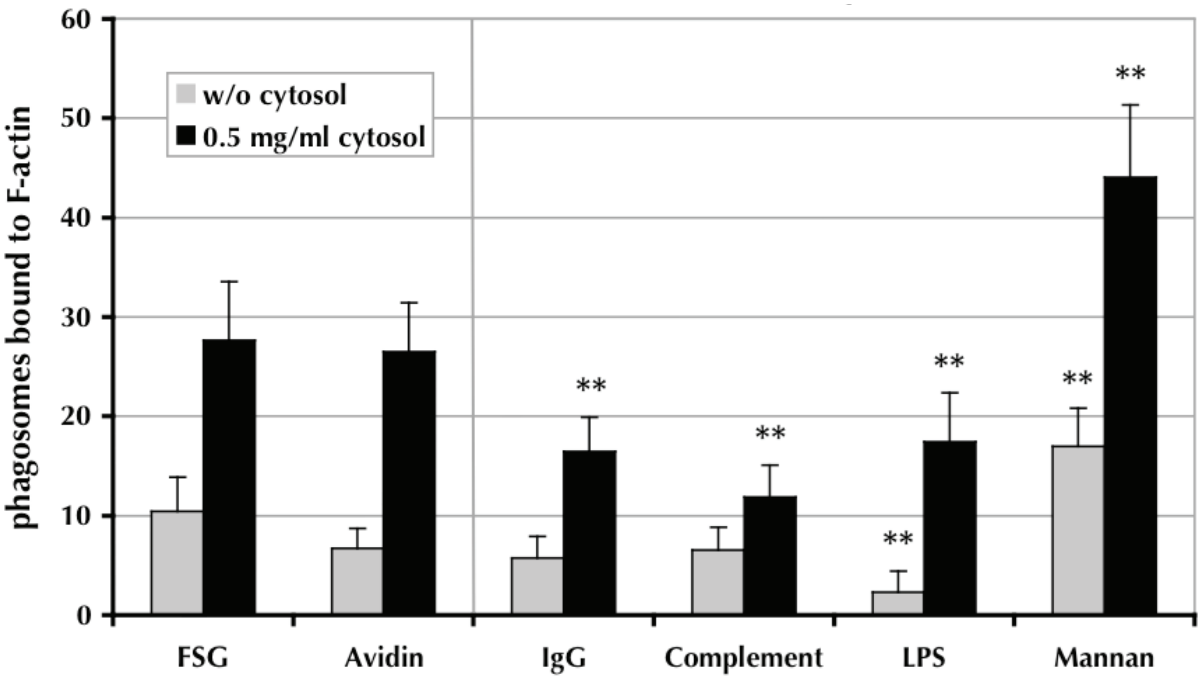

Figure 10. Binding behaviour of phagosomes containing latex beads coupled to different ligands in the *in vitro* binding assay in the absence and presence of 0.5 mg/ml J774 cytosol. Particles coated with FSG and avidin were internalised non-specifically via mixed receptors and their formed phagosomes were used as controls, whereas particles coupled to IgG, complement, LPS and mannan entered cells in receptor-dependent pathways predominantly via their specific receptor families. All phagosomes were isolated after 1 hr. pulse followed by 1 hr. chase and the same concentration was used in all assays for all samples as determined by their optical density. Shown are averages of at least two independent experiments. Significance of results was tested using Student's t-test (** $P<0.01$).

An increased binding capability to F actin could suggest that in cells organelles display an increase in attachment and anchoring to cortical, actin rich regions. Receptor dependent uptake of particles triggers different signalling pathways that influence the later stage of phagosome maturation. Since the analysed LBP were isolated after two hours, they already undergo maturation events. Binding to actin filaments seems to be not only important at early times of the phagocytic process. It also contributes differently dependent on the type of internalised particles and the involved receptors. This was one of the first hints in this study, pointing out that receptor specific interactions at the cell surface can influence phagosome functions not only during internalisation but also at later events of phagocytosis.

Phagosomal maturation and actin dependent processes are influenced significantly by various signalling molecules, such as certain lipids. Detailed analysis of actin nucleation on phagosomal membranes containing latex beads and non pathogenic as well as pathogenic mycobacteria species revealed several lipids having an impact on phagosome maturation (Anes et al. 2003). Therefore, it was of special interest whether these signalling mediators also alter the binding capability of LBP coupling to ligands to F actin *in vitro*. Since the mannose receptor is significantly involved in the uptake of mycobacteria species and mannan coated LBP exhibited more efficient binding to F actin, I compared these phagosomes together with FSG coupled LBP in this analysis. Different glycerophospholipids, sphingosines and phosphoinositides were tested in binding assays mainly at concentrations shown to have an influence on actin nucleation (see table 1 in chapter 2.5) and results were compared to mock controls.

Several lipids had both, inhibitory and stimulatory, effect on phagosomal binding dependent on the presence or absence of cytosolic factors, but also in dependence on the type of phagosome (table 3). For example, the key regulator of various membrane associated signalling events, arachidonic acid (AA), had less stimulatory impact on mannan LBP than on FSG LBP in the presence of cytosol, whereas the addition of its synthesised cellular products, prostaglandins and leukotrienes, did not alter the binding of phagosomes to F actin. Interestingly, some lipids exhibited specific effects only on one type of phagosome, e.g. diacylglycerol only inhibited binding of FSG LBP. Furthermore, it is notable that, in the absence of cytosol, many tested lipids exhibited the opposite effect on phagosomal binding to actin compared to the actin nucleation activity, which was analysed without additional cytosolic components. For example, AA, PIP_2, SM and S1P stimulated actin nucleation but inhibited binding to F actin *in vitro*, in general more strongly in FSG LBP samples.

Table 3. Results of actin-binding assay studies using LBP containing gelatin- (FSG) and mannan-coupled beads in the presence of signalling lipids (see chapter 2.5 for applied lipid concentrations). Shown are relative effects compared to solvent controls (mock) in the presence or absence of 0.5 mg/ml J774 cytosol averaged of at least two independent experiments. Stimulatory (green) and inhibitory (red) influences on the binding capability of LBP to F-actin *in vitro* are highly significant (P>0.01) as determined by Student's t-test.

	w/o Cytosol		with Cytosol	
	FSG-LBP	**Man-LBP**	**FSG-LBP**	**Man-LBP**
Arachidonic Acid (AA)	-80 %	-90 %	+250 %	+90 %
Eicosapentaenoic acid (EPA)	-100 %	-80 %	+110 %	+200 %
Diacylglycerol (DAG)	-40 %	0	-50 %	0
PtdIns 4,5-bisphosphate (PIP_2)	-70 %	-90 %	0	-60 %
Sphingomyelin (SM)	-60 %	0	+60 %	+60 %
Sphingosine (Sph)	+80 %	+130 %	0	0
Sph-1-phosphate (S1P)	-60 %	0	0	0
Ceramide (Cer)	0	0	0	0
C_{16}Ceramide (C_{16}Cer)	0	0	0	0
Prostaglandin A_1 and $F_{2\alpha}$	0	0	0	0
Leukotriene B_4	0	0	0	0

After the detailed analysis of phagosomal interaction to actin *in vitro*, which suggested that phagosomes are equipped with an early 'signature' influencing their intracellular fate, I decided to better characterise the impact of such an early event as receptor ligand, interaction, on both the cell level and the phagosome itself. First, I applied light microscopy based methods to investigate the rate of phagocytic uptake and fusion of LBP coupled to different ligands (chapter 3.2). Second, I wanted to find out how the ligand recognition at the cell surface influenced macrophage signalling and immune responses by determining gene expression changes early after the exposure of coated latex beads using a microarray approach (chapter 3.3). And third, what conclusions can be drawn from the dissection of the proteome of maturing phagosomes containing different ligand coated beads (chapter 3.4), possibly helping to explain observed differences of phagosomal properties in dependence on their receptor specific uptake.

3.2 Investigation of phagocytosis of latex beads coupled to different ligands in mouse macrophages

3.2.1 Phagocytic uptake and fusion with lysosomal compartments

Involvement of different receptors at the macrophage surface during particle recognition implies different phagocytic efficiency in dependence on the triggered signalling events, which are essential for particle engulfment and subsequent phagosome maturation. J774

mouse macrophages were pulsed with similar concentrations of fluorescent 1 μm latex beads coated with avidin, FSG, IgG, LPS or mannan and fixed at different time points. Internalisation was studied on cross sections of images taken by confocal microscopy using either inside/outside labelling of beads (avidin and IgG beads) or by staining cell cortical F actin using FITC phalloidin to analyse full particle enclosure. Only particles that were fully internalised into the cell were included into quantification. Latex beads that were bound to the cellular surface of macrophages or particles that were only engulfed by plasma membrane extensions were not included into analysis of phagosomes.

All ligands coupled to latex beads induced a linear uptake of beads over a time course of 60 min. However, many significant differences were seen between the different receptor dependent internalisation pathways. Mannan coated beads were internalised at the highest rate, followed by LPS beads and the ones coupled to the Fc fragment of IgG (Fig. 11A). The uptake of gelatin and avidin coated latex beads displayed the lowest uptake rate, which could be increased to rates comparable to mannan beads by exposing cells to four times higher numbers of beads.

Next, I asked whether subsequent stages of phagocytosis, such as fusion of phagosomes with late endosomal and lysosomal compartments, are also influenced by receptor mediated uptake. These fusion events are linked to phagosomal acidification and the release of hydrolases, all processes known as phagosome maturation that usually lead to the digestion of enzymatically susceptible phagosome content. As a fluid phase endocytic marker, which accumulates in late endosomes and lysosomes (Anes et al. 2006), J774 macrophages were allowed to internalise 10 nm rhodamine conjugated gold particles before beads were added. Macrophages that had internalised latex beads coupled to different ligands for different times were fixed and secondary accumulation of rhodamine conjugated gold in phagosomes was analysed by confocal microscopy. Surprisingly, phagosomes containing mannan coated latex beads acquired the marker more rapidly, because more than 90 % of them were already positive for rhodamine gold after 5 min. (Fig. 11B, C). In contrast, the frequency of fusion events for phagosomes containing LPS and IgG coupled beads appeared significantly slower. After 5 min., around 60 % of IgG and 70 % of LPS bead containing phagosomes were positive rhodamine gold. Rates of 90 % could only be observed after incubation times of 30 min. or longer. Fusion of phagosomes containing gelatin coupled beads started to occur later, after around 15 min. Labelling using an antibody against the lysosome associated membrane protein 2 (LAMP 2), a specific marker of late endosomes and lysosomes, confirmed these results (Fig. 11D, E). Again, LBP containing mannan beads acquired the lysosomal marker rapidly after internalisation.

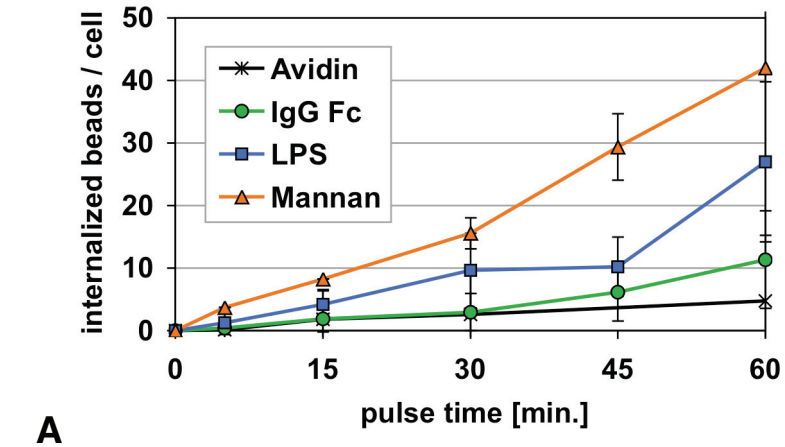

A

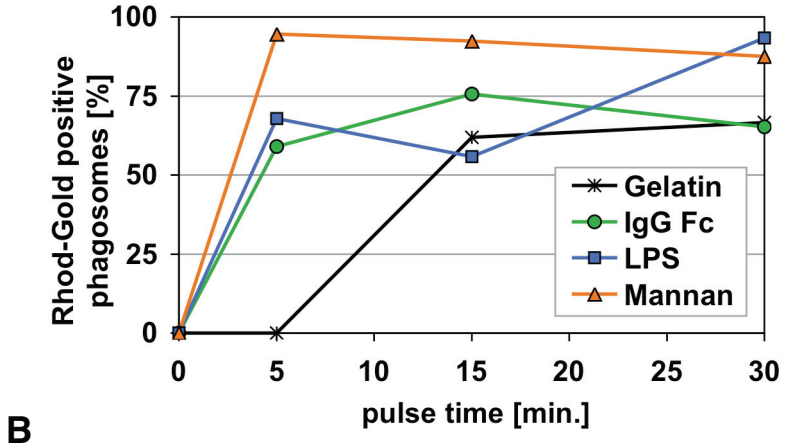

B

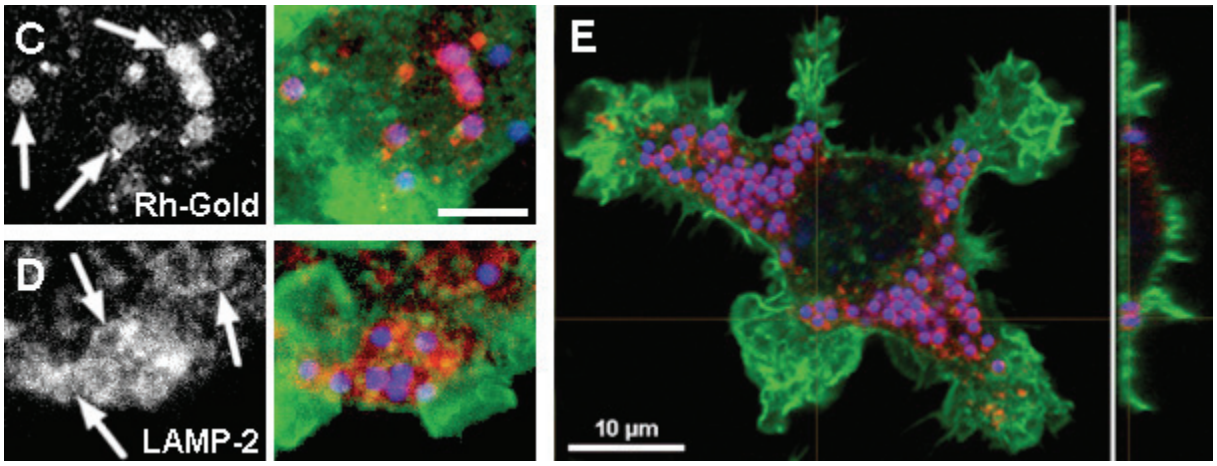

Figure 11. (**A**) Internalisation rates of 1 μm latex beads coupled to avidin, the Fc fragment of IgG, LPS and mannan in J774 macrophages over a time course of 60 min. The same concentration of beads (OD=1.6) was applied to all samples and 50 cells were analysed. Shown are averages of two independent experiments. Uptake of gelatin-coupled beads (not shown) was comparable to avidin. (**B**) Fusion of phagosomes with lysosomal compartments over a time course of 30 min. determined by their colocalisation with rhodamine-gold particles. Shown are relative numbers of phagosomes that were positive for rhodamine-gold analysed in 50 cells per latex bead ligand and time point. (**C-E**) Confocal images of fixed J774 cells pulsed with mannan-coated latex beads (blue) for 5 min. (**C, D**) and 2 hrs. (**E**). Late endosomal/lysosomal compartments (red) were labelled with rhodamine-gold (**C**) or an antibody against LAMP-2 (**D, E**). F-actin (green) was stained with FITC-phalloidin. Arrows indicate phagosomes that were positive for lysosomal markers already after 5 min. Bar (in C): 5 μm

3.2.2 Analysis of receptor expression and tyrosine phosphorylation events during phagocytosis

The observed differences of phagocytic uptake in response to the type of phagocytic particle raised the question of how the expression of involved receptors is modulated during phagocytosis. As mentioned above, the murine J774A.1 clone is equipped with a variety of different receptors. Protein expression levels of the receptors thought to be involved in the uptake IgG , mannan and LPS beads, the Fcγ receptor I (FcγRI), the mannose receptor (MR) and CD14, respectively, were analysed by western blotting using specific antibodies. J774 cells were incubated with beads coupled to these ligands at the same concentration of previous experiments over a time course of four hours and total cell lysates were prepared after 10, 30, 60, 120, 180 and 240 min. Same protein amounts were used for western blotting, demonstrated by ponceau S staining (Fig. 12A) and detection of other cellular proteins that should remain constant (Fig. 15). All three probed receptors displayed bead and time dependent differences in their expression (Fig. 12A), which were quantified by Image Gauge software (Fig. 12B D). Although, quantification was associated with a high error due to the quality of protein signals (which could not be improved by several tries) and measurements avoiding noisy quantification areas, tendencies in response to coupled beads were visible (Fig. 12B D). The mature form of the MR (172 kDa) was expressed at higher rates in response to mannan especially after three to four hours (Fig. 12B'), whereas expression of the precursor (157 kDa) also increased upon addition of IgG and LPS beads (Fig. 12B"). CD14 expression was increased at earlier times in mannan samples, but was finally expressed nearly three times more in both, LPS and mannan samples, after four hours compared before the addition of beads. The expression of FcγRI was higher during the first two hours of phagocytosis of latex beads coupled to the Fc fragment of IgG and mannan.

Receptor engagement during phagocytosis can be associated with tyrosine phosphorylation events, which influence signalling and induce engulfment. Therefore, it also was of interest to analyse modulation of these processes during phagocytosis of beads coupled to different ligands. A monoclonal anti phosphotyrosine antibody was used for western blotting of cell lysates to detect changes in tyrosine phosphorylation in general and revealed differences between the bead ligands (Fig. 13). The total level of tyrosine phosphorylation was slightly increased, but remained relatively constant during phagocytosis of avidin and IgG coupled beads over a period of four hours. However, uptake of mannan and LPS coupled caused a significant decrease of the total level of tyrosine phosphorylation over time. Additionally, selected spots of high signal intensity of around 90, 50, 30 and 17 kDa size were analysed, which exhibited similar patterns: IgG beads (and for some extent

avidin ones) caused an increase in phosphorylation, whereas mannan and LPS beads caused an increase only at very early time points of phagocytosis but predominantly reduced tyrosine phosphorylation over time.

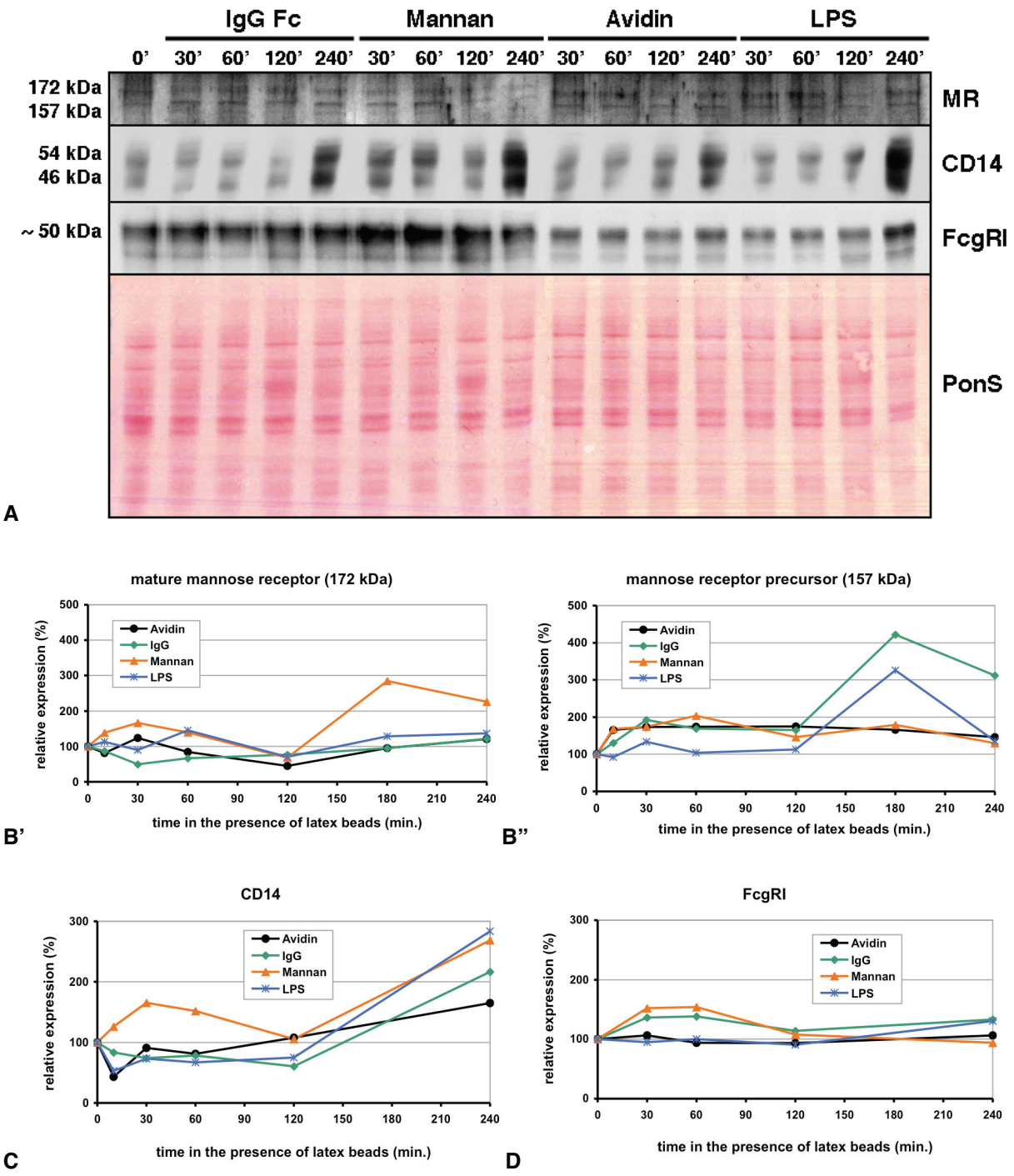

Figure 12. (**A**) Western blotting of J774 lysates probed for mannose receptor (MR), CD14 and Fcγ receptor I (FcγRI). Before lysis, J774 cells were incubated with latex beads coupled to different ligands for designated times. Protein staining using Ponceau S (PonS) demonstrates equal loading. Quantification of expression levels of MR, both the mature (**B'**) and the precursor form (**B''**) as well as of CD14 (**C**) exhibited clear differences dependent on the bead ligand, whereas expression of FcγRI remained more constant over time and was only increased slightly soon after the addition of IgG and mannan beads.

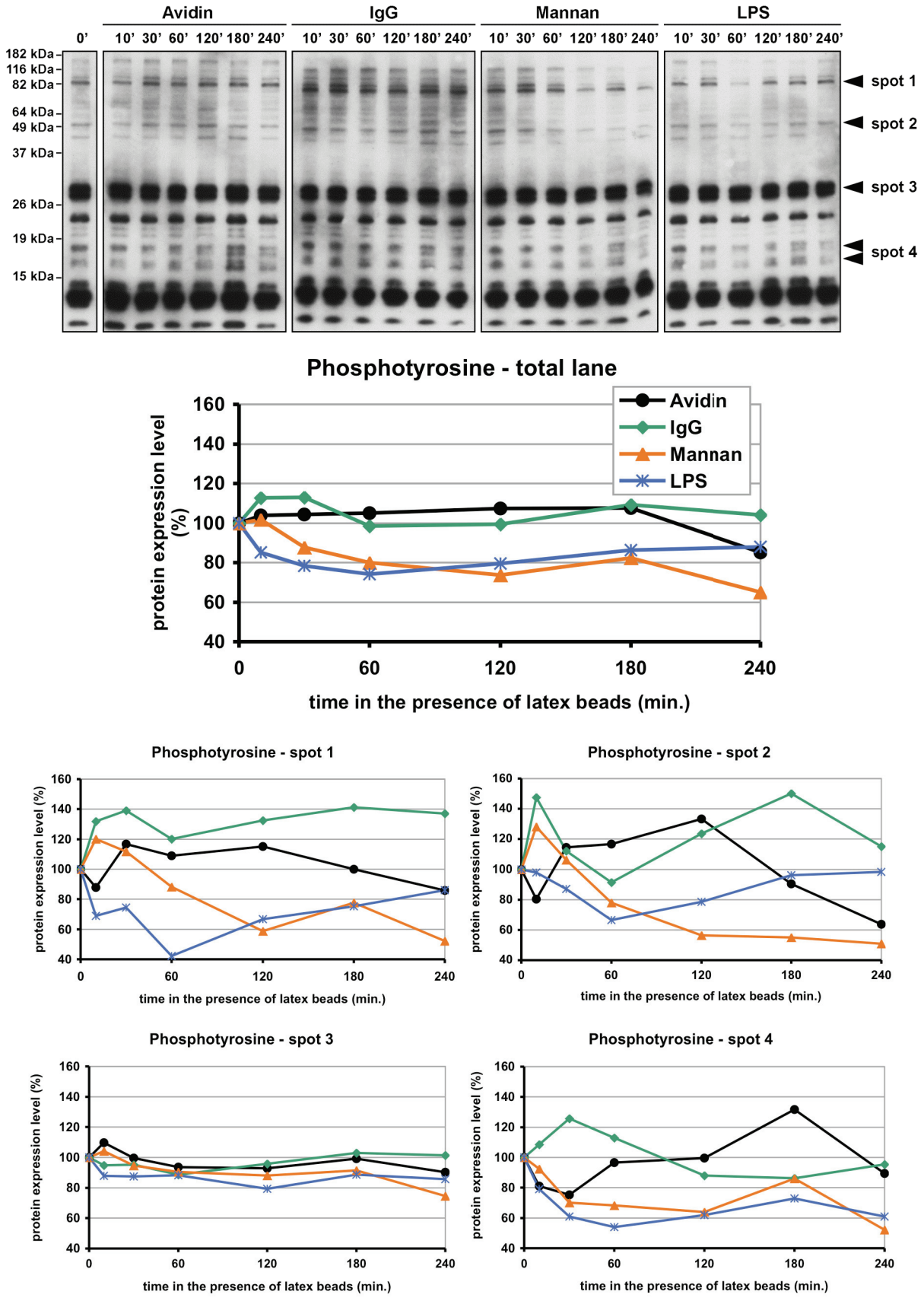

Figure 13. Western blotting of J774 lysates probed for tyrosine phosphorylation of cellular proteins. Before lysis, J774 cells were incubated with latex beads coupled to different ligands for designated time points. Relative tyrosine phosphorylation of proteins was quantified in total (analysis of the whole lane) as well as of four selected spots of different molecular weights (shown in the image above).

3.3 Influence of phagocytosis of ligand-coupled latex beads on macrophage gene expression

So far, this study provided a number of hints that receptor ligand interactions are able to modulate phagosome characteristics and functions. Previous work of numerous labs presented evidences that ligand recognition at the cell surface triggers many signalling cascades, which lead to changes in the expression of several genes involved in phagocytosis and inflammation. In addition, the changes that I observed in the expression of receptors and tyrosine phosphorylation events suggest that different bead ligands could differently influence signalling and gene expression. To test this hypothesis, a microarray approach was applied using the whole mouse genome library to validate the influence of receptor ligand interactions on macrophage gene expression.

J774.A1 cells were incubated with internalisation medium containing 0.01 % latex beads coupled to avidin, the Fc fragment of mouse IgG, LPS and mannan for 30 and 60 minutes to concentrate on early events during phagocytosis. Controls were incubated with internalisation medium in the absence of beads. All samples were carried out in duplicates. After incubation, total RNA of macrophages was extracted and each sample was hybridised to CodeLink™ mouse whole genome bioarray slides. Due to the high amount of obtained data, only the upregulation of genes versus control conditions was analysed in this study. Comprehensive data sets of this analysis can be found at the NCBI Gene Expression Omnibus (GEO) website as accession GSE9859 (http://www.ncbi.nlm.nih.gov/projects/geo/query/acc.cgi?acc=GSE9859).

3.3.1 Global study of changes in gene expression determined by microarray analysis

As a first step of analysis, upregulation of genes was investigated on a global scale to identify the contribution of specific ligands on the whole level of gene expression. In table 4 total numbers of upregulated genes are shown for both time points of phagocytic uptake as well as the numbers of genes that were common to all or unique to either one of the ligands. Additionally, pie charts are illustrating the relative distribution of genes (Fig. 14). Surprisingly, the percentage of upregulated genes that were common to cells incubated with avidin, IgG, LPS or mannan was not more than 10 %. Furthermore, genes that shared appearance in only two or three of the samples contributed with less than 15 %. The majority of identified genes switched on after 30 min. and 60 min. of phagocytic uptake was unique to each ligand.

Table 4. Summary of gene upregulation in J774 cells 30 and 60 min. after the addition of coated latex beads in comparison to control conditions determined by microarray analysis.

	30 min.	60 min.
Total number of identified genes	4904	6157
Common to all samples	846	938
Unique to avidin	388	1731
Unique to IgG	502	365
Unique to LPS	563	292
Unique to mannan	744	497

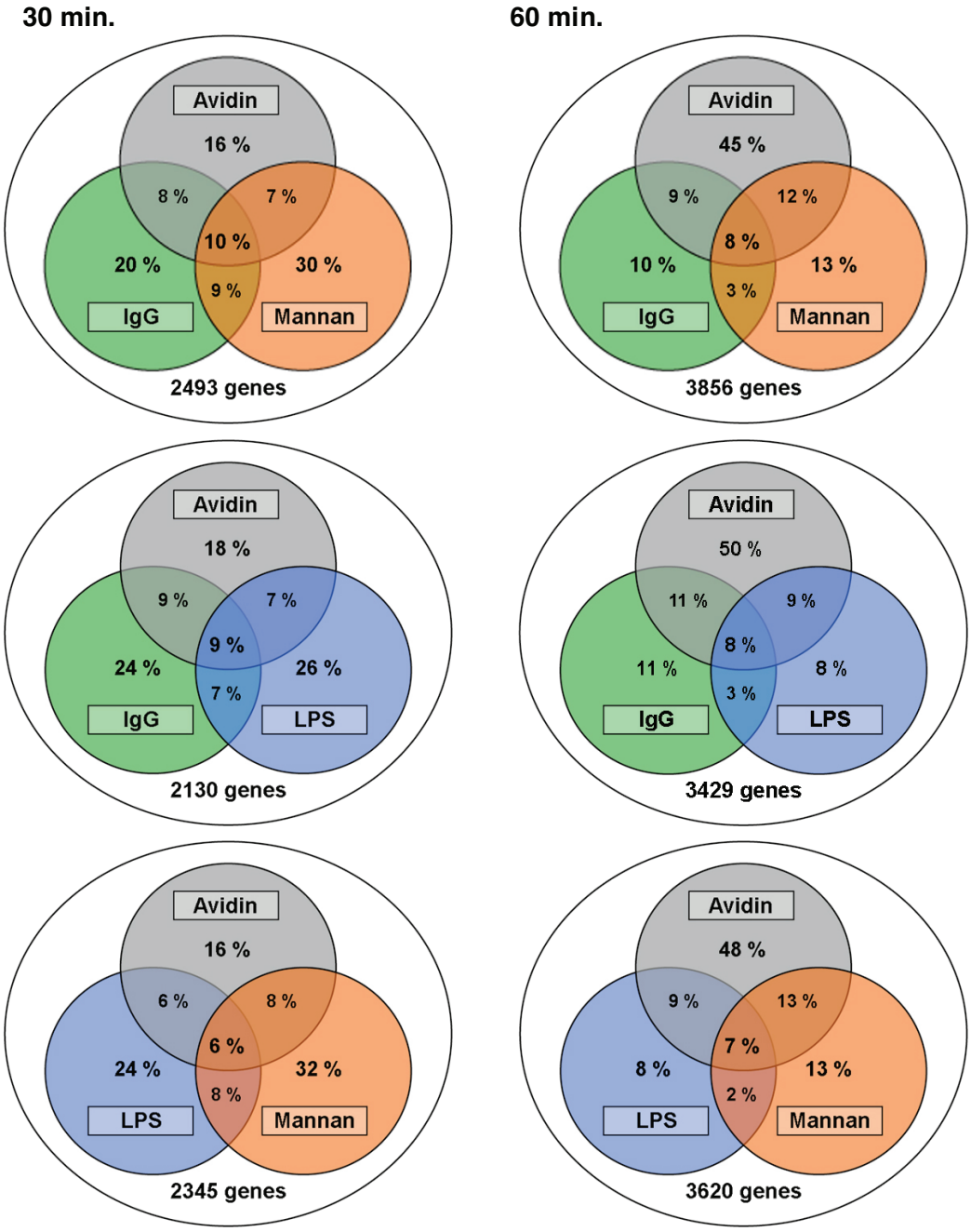

Figure 14. Pie charts representing the relative distribution of upregulated genes in J774 macrophages incubated with latex beads coupled to different ligands for 30 min. (left) and 60 min. (right) compared to untreated controls determined by microarray analysis. Percentage values display the distribution of common, overlapping and unique genes in these samples.

3.3.2 Upregulated genes common to all latex bead ligands

The data of the global analysis argue that only a small subset of common genes are activated by all the ligands analysed. These genes can be predicted to play general roles in the process of phagocytosis independent on the signalling induced by specific receptors. Some common upregulated genes encode proteins with 'house keeping' functions, such as metabolic enzymes, several protein phosphatases and ion channel subunits. However, the majority were molecules, which are involved in different stages of phagosome maturation and signal transduction and were upregulated at both tested time points. For example, genes of proteins could be identified that modulate phagosomal acidification like proton ATPase subunits and lysosomal proteases as well as signalling molecules, like CD47, various chemokines and interleukin 17, which participate in immune responses of macrophages. Additionally, several actin associated proteins could be found, supporting the importance of the actin cytoskeleton during phagocytosis; as well as Rab37, a GTPase believed to play a role in secretory vesicular trafficking. A selection of identified upregulated genes that are common to all samples is shown in table 5 categorised into functional groups of metabolism, receptors, signalling molecules, cytoskeletal proteins and trafficking regulators.

Table 5. Functionally classified list of selected genes commonly upregulated in J774 macrophages when latex beads coupled to avidin, IgG, LPS and mannan were added for 30 and 60 min. Fold changes of gene expression are colour-coded by their values (see legend).

Fold change: not upregulated; < 2.0; 2.1-3.0; 3.1-4.0; 4.1-5.0; > 5.0

Gene name	Description	Avidin 30'	Avidin 60'	IgG 30'	IgG 60'	LPS 30'	LPS 60'	Man 30'	Man 60'
METABOLISM									
GE1536298	**ATPase, aminophospholipid transporter, class I**								
GE36869	**ATPase, aminophospholipid transporter-like, class I**								
GE1547926	**ATPase, H+ transporting, V1 subunit B**								
GE41425	**ATPase, H+ transporting, V1 subunit E-like 2**								
GE1438002	**ATPase, Na+/K+ transporting, alpha 1 polypeptide**								
GE1388523	Similar to **ATP synthase, H+ transporting, mitoch. F1**								
GE38157	**Cathepsin M**								
GE1568879	**Cathepsin Q**								
GE37739	**Cathepsin R**								
GE1532833	**Inositol polyphosphate-4-phosphatase, type I**								
GE1558757	**Inositol polyphosphate-4-phosphatase, type II**								
GE1493428	**Peroxisomal biogenesis factor 6**								
GE1464801	Similar to **Phosphoinositide-3-kinase, subunit 4**								
GE1434800	**Phospholipase C, epsilon 1**								
GE129835	**Proteasome 26S subunit, non-ATPase, 14**								

GE1537300	**Protein kinase C, epsilon**	
GE34217	**Protein kinase C, theta**	
GE1557430	**Protein kinase C, zeta**	

RECEPTORS

GE36960	**Complement component 6**	
GE1436911	**Complement component factor h**	
GE42474	**Complement component factor i**	
GE1394498	**G protein-coupled bile acid receptor 1**	
GE138620	**G protein-coupled receptor 26**	
GE112563	**G protein-coupled receptor 30**	
GE1499256	**G protein-coupled receptor 61**	
GE1518573	**G protein-coupled receptor 150**	
GE1396962	Similar to **Ig heavy-chain (V-J-region) precursor**	
GE1456115	Similar to **Immunoglobulin light chain variable region**	
GE1573808	**Interleukin 7 receptor**	
GE1462835	**Mannose receptor-like precursor**	
GE1536109	**Peroxisome proliferative activated receptor, gamma**	
GE126397	**Prostaglandin E receptor 1 (subtype EP1)**	
GE35960	**Prostaglandin E receptor 3 (subtype EP3)**	
GE1488284	**Purinergic receptor P2Y, G-protein coupled 10**	
GE137828	**Scavenger receptor class A, member 3**	

SIGNALLING

GE32954	**CD8 antigen, alpha chain**	
GE1482495	**CD47 antigen (integrin-associated signal transducer)**	
GE33486	**CD59a antigen**	
GE1468507	**CD72 antigen**	
GE118349	**Chemokine (C-X-C motif) ligand 2**	
GE39024	**Chemokine-like factor super family 2A**	
GE1554492	Similar to **Defensin beta 123 precursor**	
GE35301	**Defensin beta 2**	
GE1536704	**Defensin beta 35**	
GE130058	**Ephrin A3**	
GE1462654	Similar to **Interferon-inducible GTPase**	
GE118971	**Interleukin 17**	
GE1424617	**Phosphodiesterase 4D, cAMP specific**	
GE1458683	**Phosphodiesterase 8B**	
GE128101	**Phosphodiesterase 10A**	

CYTOSKELETON

GE41402	**Actin related protein M2**	
GE32927	**Actin, alpha 1, skeletal muscle**	
GE121211	**Actin-like 7b**	
GE37971	**CDC42 effector protein (Rho GTPase binding) 5**	
GE1501704	Similar to **Elongation factor 2 (EF-2)**	
GE110761	**Formin-like 1**	
GE36667	**Integrin alpha 3**	
GE1440188	**Kinesin family member 13A**	
GE1463528	**Kinesin family member 14**	
GE34068	**Myosin Vb**	
GE1502859	**Myosin XVIIIb**	
GE119117	**Myosin, light polypeptide 2, regulatory, cardiac, slow**	
GE42771	**Profilin 2**	
GE124879	**Profilin 3**	
GE1423786	**Wiskott-Aldrich syndrome protein interacting protein**	

TRAFFICKING

GE112275	**ADP-ribosylation factor-like 4**	
GE1393824	**ADP-ribosylation factor-like 6 interacting protein 1**	
GE37628	**Coatomer protein complex, subunit zeta 2**	
GE37942	**Rab37**	

3.3.3 Upregulated genes unique to each latex bead ligand

The global analysis of gene expression demonstrated that the majority of upregulated genes during phagocytosis were unique to each bead ligand suggesting a receptor dependent 'signature' of gene regulation. Interestingly, the higher percentage of unique upregulated genes (50 %) were found in macrophages internalising avidin coupled latex beads for 60 min. (Fig. 14). This finding argues that time dependent signalling and trafficking events take place at a later time point in cells that internalised "non specificic" ligand coated beads. The involvement of specialised receptors like FcγR, CD14, TLR4 and MR during phagocytosis stimulated an upregulation of different genes. A selection of identified upregulated genes that are unique to either one of the ligands at a given time point is shown in table 6, again categorised into the same functional groups as shown in table 5.

Phagocytic uptake of latex beads coupled to avidin caused an upregulation of interleukins 9 and 20, several phosphodiesterases and phospholipases, but also of actin dependent motor proteins like myosin IB and IIIA. The uptake of IgG coated latex beads caused stimulated gene expression of protein tyrosine phosphatases, CD63 and CD83, the interleukins 1 and 10, chemokines and tumor necrosis factor (TNF) as well as numerous of TNF related proteins, suggesting a pro inflammatory immune response. Striking is the fact that less cytoskeletal proteins and trafficking regulators were stimulated upon addition of IgG beads. Only IQGAP1 was found to be upregulated uniquely to the IgG beads. Macrophages internalising latex beads coupled to LPS exhibited an upregulation of specific phosphodiesterases, interferon induced proteins and defensin beta, but of less receptors and cytoskeletal proteins. Mannan coupled beads stimulated the expression of other chemokines than the ones found in IgG samples and of pro inflammatory cytokines, such as interleukins 12b and 1a, suggesting a different immune response. Major histocompatibility complex (MHC) molecules and many cytoskeleton proteins were found to be upregulated during uptake of mannan beads, e.g. dynamin, filamin, myosin Vc and Rab8b, demonstrating the important contribution of trafficking events during maturation of these phagosomes. This data could be related to the highest and fastest rate of maturation of these phagosomes compared to all other ligand coated beads tested in this study. Surprisingly, several enzymes, such as matrix metalloproteinases, tyrosine phosphatases and phosphodiesterases, exhibited isotype or class dependent changes implicating fine tuned responses to ligand specific uptake. However, not only the unique appearance of gene upregulation was striking between the bead ligands, also fold change differences found for some genes suggest receptor specific 'signatures' during phagocytosis. For example, the prostaglandin E receptor 3 was upregulated three times more in mannan samples than in avidin, IgG and LPS (table 5).

Table 6. Functionally classified list of selected genes upregulated in J774 macrophages unique to either one of the bead ligands at 30 min. or 60 min. of incubation. Fold changes of gene expression are colour-coded by their values (see legend).

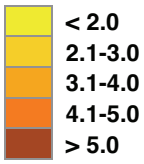

Gene name	Description	Avidin 30'	Avidin 60'	IgG 30'	IgG 60'	LPS 30'	LPS 60'	Man 30'	Man 60'
METABOLISM									
GE1494005	**ATPase, H+ transporting, lysosomal V0 subunit a1**								
GE34881	**Carboxypeptidase D**								
GE37629	**Cathepsin F**								
GE1499721	**Cathepsin O**								
GE36392	**Cathepsin W**								
GE1403879	**Diacylglycerol kinase, beta**								
GE119542	**G protein-coupled receptor kinase 1**								
GE34507	**Glycosylphosphatidylinositol phospholipase D1**								
GE126950	**Inositol 1,4,5-trisphosphate 3-kinase C**								
GE1389505	**Inositol polyphosphate-5-phosphatase D**								
GE37558	**Matrix metalloproteinase 16**								
GE37943	**Matrix metalloproteinase 19**								
GE121873	**Matrix metalloproteinase 28 (epilysin)**								
GE128735	**Peroxisomal acyl-CoA thioesterase 2A**								
GE1444288	**Phosphatidylinositol 4-kinase, catalytic, beta**								
GE33242	**Phospholipase A1 member A**								
GE1522516	**Phospholipase A2, group IIC**								
GE121922	**Phospholipase A2, group III**								
GE42118	**Phospholipase C, zeta 1**								
GE114922	**Proteasome 26S subunit, non-ATPase, 1**								
GE42712	**Protein tyrosine phosphatase, non-receptor type 5**								
GE35969	**Protein tyrosine phosphatase, non-receptor type 21**								
GE33006	**Protein tyrosine phosphatase, receptor type, B**								
GE1472788	**Protein tyrosine phosphatase, receptor type, D**								
GE33007	**Protein tyrosine phosphatase, receptor type, F**								
RECEPTORS									
GE1415468	**Cd200 receptor 2**								
GE35170	**Chemokine (C-C motif) receptor 6**								
GE33509	**Chemokine (C-C motif) receptor 7**								
GE33510	**Chemokine (C-C motif) receptor 8**								
GE37196	**Chemokine (C-C motif) receptor-like 2**								
GE42896	**Chemokine-like receptor 1**								
GE123906	**G protein-coupled receptor 23**								
GE38153	**G protein-coupled receptor 35**								
GE1510061	**G protein-coupled receptor 64**								
GE1521225	**G protein-coupled receptor 68**								
GE1542692	**G protein-coupled receptor 113**								
GE1388074	**G protein-coupled receptor 114**								
GE1507650	**G protein-coupled receptor 133**								
GE1477361	**G protein-coupled receptor 155**								
GE113679	**G protein-coupled receptor 171**								
GE1392764	**Inositol 1,4,5-triphosphate receptor 3**								
GE35229	**Interleukin 8 receptor, beta**								
GE118001	**Interleukin 18 receptor 1**								

GE137047	**Killer cell lectin-like receptor family E member 1**
GE35658	**Killer cell lectin-like receptor subfamily C, member 2**
GE35926	**Peroxisome proliferator activated receptor gamma**
GE34289	**Prostaglandin E receptor 4 (subtype EP4)**
GE37767	**Purinergic receptor P2Y, G-protein coupled, 14**
SIGNALLING	
GE1526117	**Annexin A5**
GE33483	**CD1d2 antigen**
GE33027	**CD34 antigen**
GE34829	**CD63 antigen**
GE35188	**CD83 antigen**
GE120028	**CD160 antigen**
GE33950	**Chemokine (C motif) ligand 1**
GE36049	**Chemokine (C-C motif) ligand 2**
GE36050	**Chemokine (C-C motif) ligand 3**
GE36045	**Chemokine (C-C motif) ligand 12**
GE37868	**Chemokine (C-X-C motif) ligand 10**
GE37421	**Chemokine (C-X-C motif) ligand 11**
GE37451	**Chemokine (C-X-C motif) ligand 14**
GE129362	**Defensin beta 7**
GE1548281	**Defensin related cryptdin 5**
GE1544467	**Histocompatibility 60**
GE1571183	**Interferon induced with helicase C domain 1**
GE119745	**Interferon response element binding factor 1**
GE36900	**Interferon, alpha-inducible protein**
GE35586	**Interferon-induced protein with TPR 3**
GE35598	**Interleukin 1 alpha**
GE34640	**Interleukin 1 beta**
GE118015	**Interleukin 9**
GE35595	**Interleukin 10**
GE34632	**Interleukin 12b**
GE130876	**Interleukin 17D**
GE120607	**Interleukin 20**
GE37054	**Phosphodiesterase 1A, calmodulin-dependent**
GE34174	**Phosphodiesterase 1B, Ca2+-calmodulin dependent**
GE33089	**Phosphodiesterase 3B, cGMP-inhibited**
GE1574898	**Phosphodiesterase 6B, cGMP, beta polypeptide**
GE1410436	**Phosphodiesterase 7B**
GE34291	**Prostaglandin I2 (prostacyclin) synthase**
GE35961	**Prostaglandin-endoperoxide synthase 2**
GE107990	**Regulator of G-protein signalling like 2**
GE36806	**Tumor necrosis factor**
GE35385	**Tumor necrosis factor (ligand) superfamily, 6**
GE36222	**Tumor necrosis factor (ligand) superfamily, 7**
GE33829	**Tumor necrosis factor (ligand) superfamily, 9**
GE1421441	**Tumor necrosis factor (ligand) superfamily, 11**
GE33827	**Tumor necrosis factor receptor superfamily, 18**
GE1517077	**Tumor necrosis factor receptor superfamily, 1a**
GE42133	**Tumor necrosis factor, alpha-induced protein 9**
GE118972	**Type 1 tumor necrosis factor receptor regulator**
CYTOSKELETON	
GE38166	**Actin-binding LIM protein 1**
GE126449	**Dynamin 2**
GE137904	**Dynamin 3**
GE34375	**Fascin homolog 1, actin bundling protein**

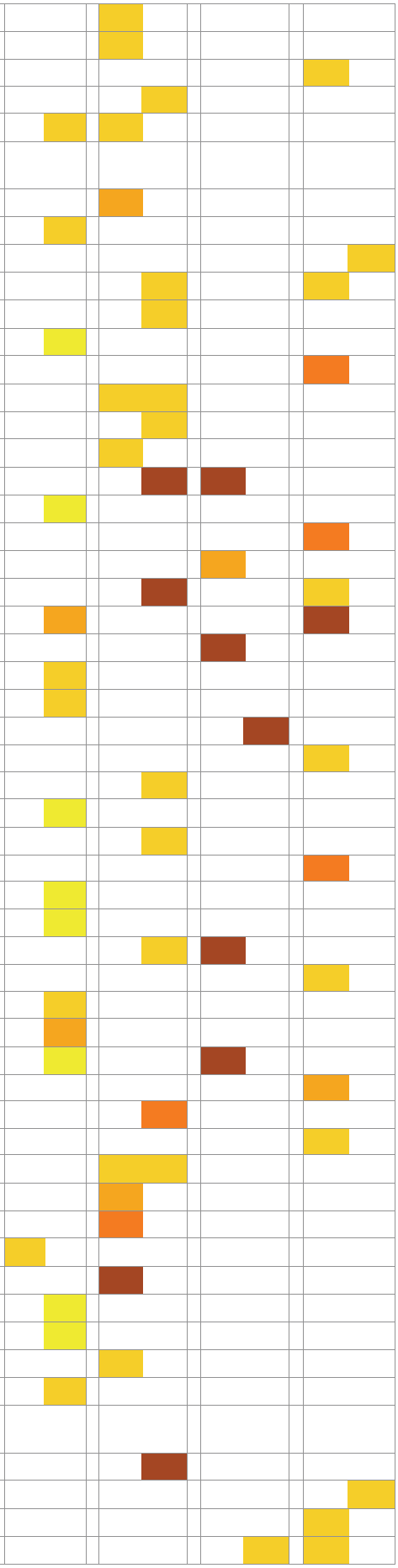

GE1390121	**Fascin homolog 2, actin-bundling protein**	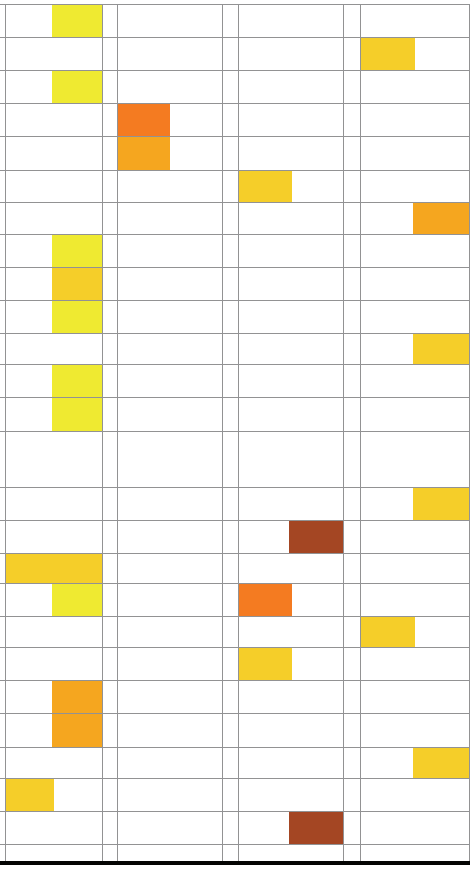
GE1419956	**Filamin, beta**	
GE36669	**Integrin beta 7**	
GE1491767	**IQ motif containing GTPase activating protein 1**	
GE1395625	**Kinesin family member 2B**	
GE34693	**Kinesin family member 5A**	
GE115401	**Kinesin family member 7**	
GE1424158	**Myosin binding protein C, fast-type**	
GE131310	**Myosin IB**	
GE136335	**Myosin IIIA**	
GE130925	**Myosin VC**	
GE1440347	**Myosin, heavy polypeptide 4, skeletal muscle**	
GE1498071	**Myosin, heavy polypeptide 8, skeletal muscle**	
TRAFFICKING		
GE41582	**ADP-ribosylation factor 4-like**	
GE102188	**ADP-ribosylation factor related protein 1**	
GE33341	**ADP-ribosylation factor-like 6 interacting protein 4**	
GE34812	**Caveolin 3**	
GE41484	**Rab3C**	
GE123053	**Rab6**	
GE38685	**Rab6 interacting protein 1**	
GE1568848	**Rab6 interacting protein 2**	
GE1405969	**Rab8B**	
GE40540	**Rab27A**	
GE39534	**Rab-like 4**	

3.3.4 Analysis of altered gene expression on the protein level

The microarray approach detected several changes in macrophage gene expression during the phagocytic uptake of latex beads coupled to different ligands. To determine whether these changes are also visible on the protein level and could be associated to obtained microarray results, J774 lysates were probed for selected proteins (Fig. 15). Interestingly, expression of LAMP 2, of actin and some of the analysed actin associated proteins (filamin, myosin Va and dynamin) exhibited ligand specific regulation during uptake of coupled latex beads, although these changes could not be directly linked to the microarray results. However, the changes in protein expression observed for tumor necrosis factor alpha (TNFα) by western blotting confirmed findings of the microarray analysis. Both experimental approaches demonstrated that phagocytic uptake of IgG coupled beads increased TNFα gene and protein expression early after internalisation (30 to 60 min.), whereas uptake of LPS beads increased its expression at a later time point (4 hrs.). Mannan and avidin coated beads only resulted a decrease or no changes in TNFα expression over the whole analysed period. Although the presence of TNFα in the culture medium of these cell samples was not investigated and secretion of this cytokine could not be analysed, its higher subcellular abundance in response to two of the ligands demonstrates a modulated immune response.

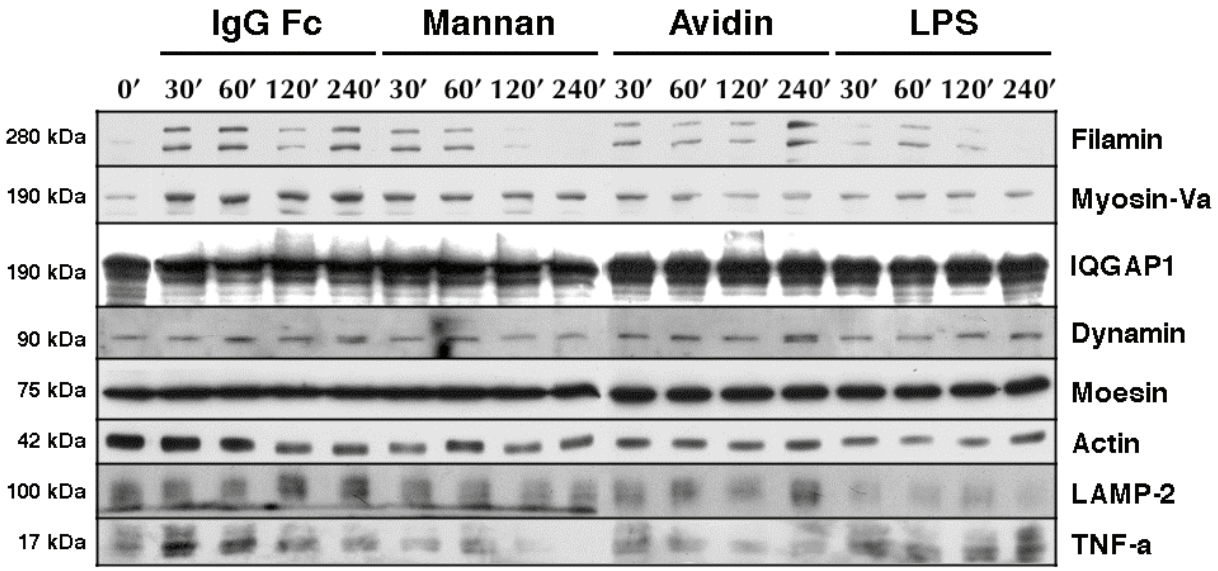

Figure 15. Western blotting of J774 cell lysates after incubation with latex beads coupled to different ligands for designated time points using 10 % (proteins of more than 50 kDa) and 12 % polyacrylamide gels (proteins less than 50 kDa). Equal protein concentrations were loaded in all lanes. Lysates were probed for different actin-binding proteins, the lysosomal marker LAMP-2 and tumor necrosis factor alpha (TNF-a) using specific antibodies (see table 2).

3.4 Proteomic analysis of phagosomes containing latex beads coupled to different ligands

The results obtained in this study so far, demonstrated that phagocytosis of coupled latex beads stimulated many cellular functions including particle uptake, phagosome maturation, their interaction with actin filaments as well as gene expression in response to the ligand. These findings raised the hypothesis that the protein composition of phagosomes containing different ligand coated beads exhibits many differences as well, possibly helping to explain the observed differences of phagosomal properties in dependence on their receptor specific uptake. Therefore, maturing phagosomes were isolated after one hour pulse and one hour chase and were analysed by two dimensional SDS PAGE and mass spectroscopy to dissect their proteomes. This time point has been most commonly used for many assays, including other proteomic studies (Garin et al. 2001; M. Desjardins, personal communication).

3.4.1 Two-dimensional SDS-PAGE of phagosomal proteins

First, isolated phagosomes containing latex beads coupled to the Fc fragment of IgG (representing an opsonic phagocytosis pathway) and to mannan (representing a non opsonic pathway) were migrated in 2D gels, which were processed for silver staining. The results after two dimensional migration of phagosomal proteins are shown in figure 16.

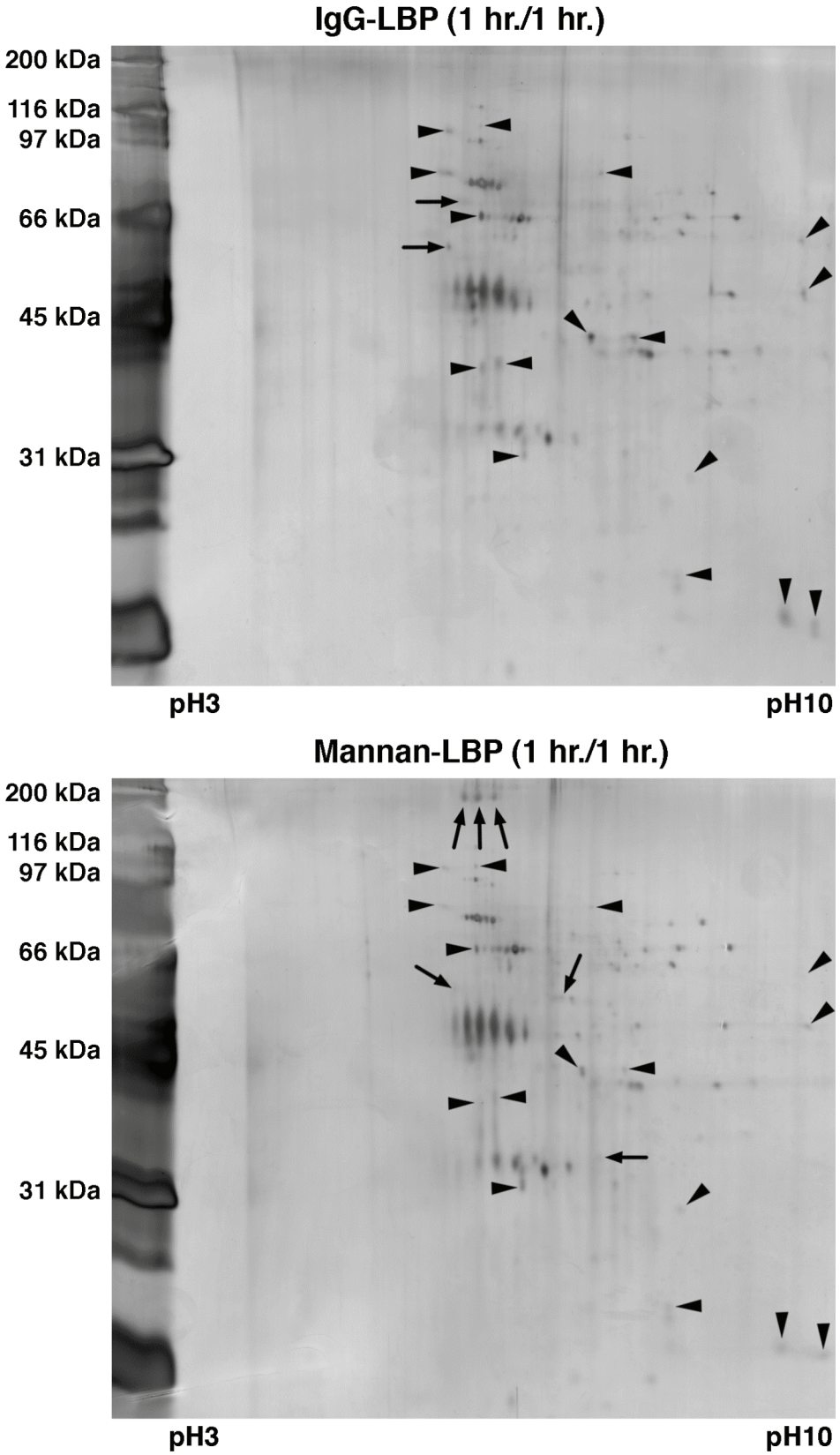

Figure 16. Silver-stained gels after two-dimensional gel electrophoresis of phagosomes containing latex beads coupled to the Fc fragment of IgG and mannan isolated from J774 macrophages after one hour pulse followed by one hour chase. The same amount of protein was used for gel migration allowing qualitative and quantitative assessment of phagosome samples. In both, proteins can be found that are unique, either to IgG- or mannan-LBP (arrows), as well as proteins that appear at different abundances in the stained gels (arrowheads).

Although the same sample concentration of both phagosome types was used, qualitative as well as quantitative differences between them could be detected in the stained gels. The finding that some proteins appeared at different abundances in the two samples (arrowheads in Fig. 16) demonstrates how, on one hand, these phagosomes are equipped with the same protein, but on the other hand, are also specifically modulated in its appearance. Other proteins could only be found unique to one of the samples (arrows in Fig. 16) arguing that different proteins are also influencing the intracellular fate of these phagosomes at a particular time point. Due to the low protein amount in the gels, it was not possible to pick and identify certain protein spots, but the same LBP samples were prepared for direct application in a mass spectroscopy approach to dissect proteomic similarities and differences between these phagosomes.

3.4.2 Phagosomal protein composition determined by mass spectroscopy (LC-MS/MS)

The phagosomes made in response to beads coupled to the Fc fragment of IgG, mannan and, additionally, to avidin were isolated after 2 hours internalisation and phagosomal proteins were precipitated. Liquid chromatography and tandem mass spectroscopy (LC MS/MS) of these samples were carried out by Dr. Nicholas Sherman in the Biomedical Mass Spectrometry Laboratory of the University of Virginia, USA as described in chapter 2.10. The analysis of identified proteins revealed several interesting findings, supporting the hypothesis that receptor specific uptake is influencing subsequent phagosome functions to a high extent. Surprisingly, less than 20 % of all identified proteins were common to all three LBP types. Similar to results obtained by the microarray approach, the majority of proteins was unique to avidin, IgG or mannan phagosomes (table 7, figure 17). Interestingly, like in the micorarray, avidin samples possessed most of the unique ones again (30 % of all identified proteins).

Table 7. Summary of identified proteins from isolated phagosomes (1 hr./1 hr.) containing latex beads coupled to avidin, IgG and mannan as determined by mass spectroscopy. **Figure 17.** Pie chart shows distribution of common, overlapping and unique proteins in these samples.

	N
Total number of identified proteins	1194
Common to all samples	224
Unique to avidin	359
Unique to IgG	193
Unique to mannan	189

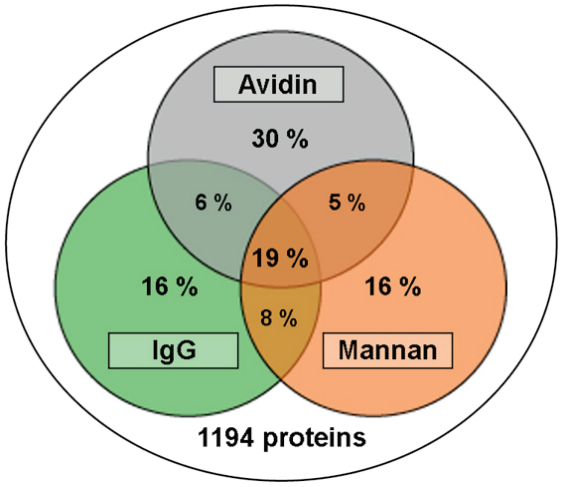

A more detailed look at the identified proteins demonstrated that differences between the three LBP types can be found in several functional classes. In table 8 a selection of them is shown subdivided in receptors, antigen interaction molecules, phagosomal and lysosomal markers, Rab GTPases and actin associated proteins. A comprehensive list of all 1194 proteins identified by mass spectroscopy including numbers of their unique spectra during identification is shown in the supplement at the end of this thesis.

Many known phagosomal proteins were found in all LBP types, such as several ATPase subunits, LAMP 1 and 2, cathepsins B and D as well as Rab5 and 7. The presence of various receptors in phagosome samples demonstrated that numerous of them could be involved in internalisation and could be detected even after two hours. Many actin associated proteins were also found in maturing phagosomes supporting the findings that actin and its associated proteins are not only important during early stages of phagocytosis, but also could contribute to functions during phagosome maturation. Interestingly, isoform dependent differences were found for some of these proteins, e.g. filamin A, coronin1, Rab5 and Rab8, arguing for fine tuned control and modulation of phagosome functions.

Although the presence or absence of proteins in LBP samples determined by mass spectroscopy cannot be linked directly to differences in gene expression detected by microarray analysis, a few results associated both techniques. For example, in the microarray, many genes encoding MHC molecules were upregulated upon response to mannan coated beads. Mass spectroscopy also detected several MHC molecules exclusively in phagosomes containing these beads confirming microarray findings.

In order to validate findings of the LC MS/MS approach, phagosomes containing latex beads coupled to avidin, IgG and mannan were also analysed by western blotting using specific antibodies to confirm the absence or presence of some proteins (Fig. 18). Unfortunately, I was unable to validate mass spectroscopy results by this method, e.g. IQGAP1 was found in all three LBP types by western blotting, but quantitative differences could be detected. For example, moesin was found at higher quantities on IgG phagosomes, whereas more cathepsin D could be detected in mannan phagosomes.

In summary, results of several experimental approaches in this study demonstrated and supported the hypothesis that uptake of ligand coated beads triggered specific events on the gene, on the protein as well as on the functional level that lead to different phagocytic functions of formed phagosomes. This raised the idea of ligand specific ‘signatures’ that influence several aspects during receptor mediated phagocytosis.

Table 8. Selection of identified proteins in isolated 1 hr./1 hr. LBP samples determined by LC-MS/MS sorted in functional groups. **Figure 18.** Selected proteins were also identified by western blotting.

	Av	IgG	Man
Receptors			
CD14	x	x	x
Ig gamma-1, membrane-bound form		x	
IgG, Fc receptor, isoform 1		x	x
LDL receptor-related protein 1		x	x
MCSF-1 receptor		x	x
Mannose-6-phosphate receptor	x		x
Peroxisome prolif.-activated receptor		x	
Scavenger receptor, types I and II		x	x
Toll-like receptor 7 precursor	x	x	x
Toll-like receptor 12 precursor		x	
Transferrin receptor protein 1	x	x	x
Antigen interaction			
Histocompatibility, class I, H2-D1	x	x	x
Histocompatibility, class II, Cd74			x
Histocompatibility 2, H2-K1			x
Minor histocompatibility, H13			x
Phagosomal/lysosomal markers			
ATPase, H+ transporting, various	x	x	x
ATP synthase, vacuolar, various	x	x	x
Cathepsins-B, -D, -Z	x	x	x
Cathepsin-L		x	x
Cathepsin-S			x
EEA1		x	x
Flotillin-1	x		
Flotillin-2			x
LAMP-1, -2	x	x	x
Lysosome membrane protein 2	x	x	x
Rab proteins			
Rab-5A		x	
Rab-5B, -5C, -7	x	x	x
Rab-8A		x	
Rab-8B	x		x
Rab-11B		x	x
Actin & associated proteins			
Actin, cytoplasmic	x	x	x
alpha-Actinin	x	x	x
Arp2/3 complex	x	x	x
CapZ (F-actin capping protein)	x	x	x
Cofilin-1, -2	x	x	x
Coronin-1A	x	x	x
Coronin-1C		x	
Elongation factor 1 and 2	x	x	x
Filamin-A, isoform 1	x	x	x
Filamin-A, isoform 2			x
Formin-like protein 1		x	
IQGAP1	x	x	
Moesin	x	x	x
Myosin-IB, -IC			x
Myosin-II, heavy polypeptide 9	x	x	x

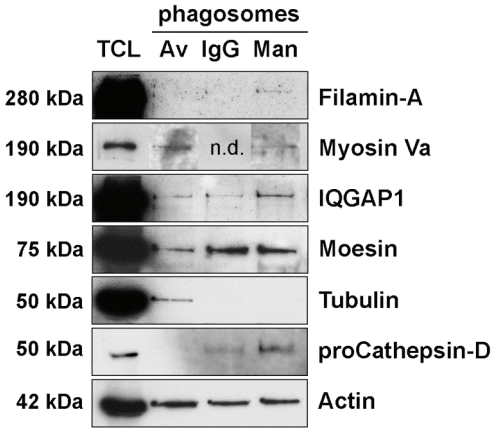

Discussion

4.1 The latex bead phagosome system and receptor-ligand interactions

Phagocytosis, which is initiated by particle recognition at the plasma membrane, and its sub stages of internalisation, phagosomal trafficking and maturation are highly complex processes. It is well established that the initial contact of any ligand coated bead (or pathogen) with cell surface receptors triggers an immediate signalling response. It is also clear that different receptors on cells, such as macrophages, induce different patterns of signalling. When several ligands are present on the surface of the phagocytosed particle, as it is the case for microbes, there is an extensive overlap and crosstalk between different pathways. It is then difficult to specify the detailed signalling response of one defined receptor (Lee & Kim 2007). Several studies on pathogens, such as *Mycobacterium tuberculosis* (Clemens & Horwitz 1995) and *Toxoplasma gondii* (Mordue & Sibley 1997), gave evidence that recognition events at the phagocyte surface modulate phagosomal fate. Although the influence of receptors and associated signalling pathways were analysed in previous studies (Stahl & Ezekowitz 1998; Blander & Medzhitov 2004), their contribution to later stages of phagocytosis are still poorly understood.

The major questions of this study were: “How do macrophages respond to the binding and phagocytic uptake of beads covered with different ligands?” and “How does this receptor ligand interaction influence the intracellular fate of phagosomes?”. The applied latex bead system was well suited to find answers to these questions since 1.) it allows to isolate phagosomes with a high degree of purity, 2.) the isolated organelle is functionally active for a wide spectrum of functions (Desjardins & Griffiths 2003) and 3.) a number of proteomic analyses have been published in different eukaryotic systems unravelling around 1000 different proteins and several hundreds of lipids (Griffiths & Mayorga 2007). In addition, another major advantage was the possibility to couple latex beads to single ligands and study their selective receptor mediated uptake and following maturation processes in more detail. In this study, interactions of macrophages with beads conjugated to IgG, mannan, LPS, avidin and gelatin were analysed. Irrespective of the ligand, the macrophage was able to bind and internalise the beads in a morphologically similar manner. The investigations included functional assays in macrophages, such as measuring the rate of phagocytic uptake and phagosomal fusion with lysosomal compartments, as well as performing an *in vitro* assay to examine the capability of phagosomes to associate with actin filaments. Furthermore, these functional analyses were extended by investigating cellular gene expression changes upon internalisation of a specific ligand coated bead and the proteomic composition of the

subsequent isolated phagosomes. This study allowed to gain more insight in defining how early phagocytic events modulate different phagosomal functions.

4.2 The binding to F-actin is important for latex bead phagosomes during their maturation.

Interaction between phagosomes and cytoskeleton components play an essential role for the maturation of these organelles. Actin with its associated proteins is a major component in phagocytosis not only for the actin driven engulfment of particles but also at later stages during phagosomal maturation (Guerin & de Chastellier 2000; Anes et al. 2003; Kjeken et al. 2004). Previous work using an *in vitro* assay, which was developed in our lab, could demonstrate that phagosomal binding to actin filaments is essential to modulate the switching of phagosomes from cortical F actin to microtubules (Al Haddad et al. 2001). This marks one of the first steps of phagosome maturation, because microtubules and their motor proteins are believed to be important for the long range centripetal movement of phagosomes towards the cell center during their maturation (Blocker et al. 1996; Blocker et al. 1997; Harrison et al. 2003). In addition, maturing phagosomes were shown to nucleate actin filaments (Defacque et al. 2000; Jahraus et al. 2001, Anes et al. 2003) and recruit actin associated proteins (Stockinger et al. 2006). It was suggested that the *de novo* actin filament assembly regulates phagosome fusion with lysosomes. During the first part of my work, I examined in more detail the F actin binding activity of isolated latex bead phagosomes. In particular, I analysed how different ligands on the surface of the bead and therefore different phagosome contents influence the phagosome binding capability. I also analysed the role of some proteins and signalling molecules in this activity. LBP were isolated after 1 hr. pulse and 1 hr. chase, which represents a model system of maturing phagosomes. The capability of non stripped LBP to bind to F actin in the absence of cytosol to the same extent as salt stripped LBP in the presence of cytosolic components clearly demonstrates that phagosomes carry the binding machinery at their membranes. I could also show by western blotting that cytosolic proteins were recruited to salt stripped phagosomes to mediate their binding to cytoskeleton components. From the Al Haddad et al. study it is known that the motor protein myosin Va as well as an unknown protein of high molecular weight stimulate the binding of LBP to F actin. Whereas the unknown protein is going to be characterized by an accompanying study in our lab, I could confirm the function of myosin Va as one responsible membrane protein that mediates binding of LBP to F actin in a concentration and ATP dependent manner.

Interestingly, binding assays in the presence of functional antibodies against different actin associated proteins revealed that proteins previously known to activate actin nucleation on LBP phagosomal membranes in macrophages (ezrin, moesin, N WASP) downregulate the F actin binding capability. Both activities play a role in phagosome maturation. It was shown that conditions activating the actin nucleation process lead to an increase of phagosome fusion with lysosomes and subsequent killing of mycobacteria, whereas negative regulation of phagosomal actin assembly facilitate growth of these pathogens (Anes et al. 2003). In opposite, studies on phagosomes containing other pathogens, such as *Leishmania donovani*, have shown that F actin accumulation around these phagosomes is able to delay or prevent their maturation (Lerm et al. 2006).

Similar conclusions can be drawn from results of binding assays using signalling molecules like certain lipids. Whereas previous studies have provided evidence that lipids like arachidonic acid (AA) and phosphatidylinositol (4,5) bisphosphate (PIP_2) stimulate polymerisation of actin on phagosomal membranes (Anes et al. 2003), they exhibited inhibiting effects on binding of LBP to F actin in the absence of cytosol during my experiments. Although the addition of metabolic products of AA (prostaglandins and leukotrienes) and the involved enzymes (cyclooxygenase and lipoxygenase) had no direct influence in the assay, the lipid itself clearly exhibited a concentration dependent effect on phagosomal binding. In previous studies it was shown that arachidonic acid indeed alters the actin cytoskeleton (Anes et al. 2003; Fischer et al. 2005). Numerous findings support the fact that also PIP_2 has a broad range of potential to alter actin not only during phagocytosis (Hilpelä et al. 2004; Scott et al. 2005).

My results on LBP suggested that the *de novo* actin assembly and F actin binding activities could influence these organelles in a 'tug of war' mechanism. In a state where nucleation is 'switched on', the binding capability is 'switched off' and vice versa. We can propose that LBP at early stages of their maturation process may need to be anchored to the actin cytoskeleton and thereby be transiently "immobilised". This phenomenon could facilitate their fusion with early endosomal compartments and/or delay their displacement towards the lysosomal system. The *de novo* actin assembly at the phagosome membrane has been shown to promote the phagosome fusion with late endosomal compartments and lysosomes, but the mechanism underlying this function is still unknown (Kjeken et al. 2004). However, recent studies from Gareth Griffiths' lab showed that phagosomes nucleating *de novo* actin at their membrane can be propulsed throughout the cell by the formation of an actin comet. Experiments need to be done in order to clarify this hypothesis, in particular, it is important to confirm that phagosomes that have nucleated actin at their membrane are indeed blocked in

binding a pre formed actin network. Another important aspect is to find conditions where the actin binding capability of phagosomes is inhibited in cells and examine the consequences on their maturation process and particular the rate of fusion with late endosomal compartments.

Surprisingly, in this study it was impossible to reconstitute any significant binding of bacterial phagosomes to F actin *in vitro*. Numerous strategies to induce binding of phagosomes containing live and heat killed non pathogenic (*Mycobacterium smegmatis*) as well as pathogenic mycobacteria (*M. avium*; *M. bovis* BCG) to F actin *in vitro* failed. Any change of assay conditions, like addition of cytosol isolated from activated and non activated macrophages or even purified actin binding protein fractions, had no influence on the obtained results. Moreover, various treatments of the phagosomal membranes, such as permeabilisation or salt stripping before the addition of cytosolic binding factors, caused no binding of mycobacterial phagosomes to F actin.

The capacity of mycobacteria to interfere with host phagosome lysosome fusion pathways relies on the expression of several virulence factors and the influence of host cell and mycobacterial lipids that ensure their retention within mycobacterial phagosomes (Vergne et al. 2005; Nguyen & Pieters 2005). Previous studies have shown that mycobacteria are able to rearrange the membrane cytoskeleton network during phagocytosis (Peyron et al. 2000; Gatfield et al. 2005). For example, coronin 1 transiently accumulates on phagosomal membranes and is actively retained by mycobacteria to block phagosome lysosome fusion (Jayachandran et al. 2007). Notably, the lipid rich cell wall of mycobacteria containing glycosylated lipoarabinomannans and phosphatidylinositol mannosides has also been recognised to have an effective influence on the innate immune defense (Briken et al. 2004). Therefore, the observed incapability of mycobacterial phagosomes to bind to F actin *in vitro* could be a physiological phenomenon, although some of the results (*E. coli* or heat killed mycobacterial phagosomes do not bind) argue against being a phenomenon specifically associated with the bacteria. Further evidences are necessary to finally conclude that mycobacterial phagosomes that can nucleate actin (Anes et al. 2003) are indeed incapable to bind to F actin *in vitro* and *in vivo*. One hypothesis would be that the specific rod like shape of phagosomes containing mycobacteria, in opposite to the round shape of LBP, decreases the actin binding capability in a two dimensional network, which might not be the case in the three dimensional actin network existing in cells. Investigations with latex beads coated with purified mycobacterial cell wall components and binding assays applying phagosomes with coccal instead of rod shaped pathogenic and non pathogenic bacteria, or alternatively latex beads of various shapes, could provide further insight into the physiological

relevance of the observed phenomenon. It can also be mentioned that preliminary experiments, in which isolated mycobacterial phagosomes were 'forced' onto actin filaments using an optical tweezer system, also failed to induce significant binding (Holger Kress & Eik Hoffmann, unpublished results).

4.3 Receptor-mediated uptake regulates the actin-binding activity of late phagosomes.

In this study, another alternative was used to investigate the binding behaviour of bacteria like phagosomes. By coupling latex beads to single ligands, surface characteristics of bacteria were partly mimicked and receptor dependent uptake in macrophages was stimulated. Beads coated with mouse IgG or complement imitated opsonised targets and were internalised by Fcγ receptors and complement receptors, respectively (Le Cabec et al. 2002), whereas particles coupled to mannan and LPS engaged predominantly the mannose receptor or toll like receptor 4 and CD14 (Shibata et al. 1997; Berntzen et al. 1998), respectively. Latex beads coated with fish skin gelatin or avidin were used for, what is generally considered as, non specific phagocytic uptake (Muller et al. 1989), and were compared to the ones triggering more specific receptor mediated phagocytosis. All these LBP were isolated after one hour pulse followed by one hour chase to analyse maturing phagosomes and tested in actin binding assays. Interestingly, many differences could be found in their binding capability, implicating that phagosomes possess specific membrane characteristics depending on receptor ligand interactions during their recognition and formation at the plasma membrane, which could also influence their subsequent trafficking during maturation. Phagosomes containing IgG , complement and LPS coated beads bound less to F actin *in vitro* compared to gelatin and avidin beads, whereas latex beads coupled to mannan displayed higher binding capabilities.

Few is known about how the first step of ligand receptor interaction influences phagosomal functions at later stages of phagocytosis, such as the binding of phagosomes to the actin cytoskeleton. It was shown that Rho GTPases play an important role in initiating a specific signalling pathway upon receptor binding. They are considered as main molecular switches that could differentiate the fate of opsonin dependent receptor mediated phagocytosis (Fc and complement; Caron & Hall 1998) from the opsonin independent phagocytosis reported for the mannose receptor (Zhang et al. 2005). One interesting candidate that could be involved in the observed differences in the phagosome binding activity is moesin. In cells, moesin mediates the direct link between the plasma membrane and the underneath actin cytoskeleton. This protein is present on late phagosomes (1 hr./1

hr.) and could play a role in anchoring directly the phagosome to actin filaments. In addition, it was shown that moesin interacts with CD93, which is implicated in FcR and CR mediated uptake (Zhang et al. 2005). My data also support this observation, because I could detect by western blotting that moesin is more abundant on isolated IgG LBP compared to mannan and avidin LBP (Fig. 18), supporting a putative role of this cross linker in the actin binding activity of phagosomes. Further studies on this protein are now currently performed in the lab to confirm this hypothesis.

The receptor dependent uptake of particles, followed by phagosome formation and subsequent interactions of phagosomes with actin based motor enzymes are not well understood. Several myosins are modulated and linked to organelle membranes by Rab GTPases (Seabra & Coudrier 2004). Although several myosin classes are implicated in endosomal trafficking, only myosins of class V seem to interact with fully internalised and maturing phagosomes in macrophages. Myosin Va, the motor shown to be involved in binding phagosomes to F actin *in vitro* (Al Haddad et al. 2001), interacts with Rab27a (Wu et al. 2002). Myosin Vb has been shown to associate with Rab11a (Lapierre et al. 2001) and Rab8a (Roland et al. 2007), whereas myosin Vc could be involved in cellular distribution of distinct endocytic compartments labelled for Rab8 and the transferrin receptor (Rodriguez & Cheney 2002). Giving the complexity of Rab GTPase association with organelles and receptors (Schwartz et al. 2007), it is possible that these interactions are influencing dynamics of maturing phagosomes in a receptor dependent manner, which could be one explanation for the observed differences in the binding assay.

In conclusion for this part of my work, I could emphasise that an activity such as the capability of phagosome to bind to actin filaments, which plays a crucial role in regulating the maturation process of the phagosome, seems to be already regulated at the first step of receptor ligand interaction. Some interesting questions rise from this observation: Are phagosomes carrying the complete programme that decides their fate as soon as they are internalised? How much is the maturation process of phagosomes regulated by the surrounding environment in the cell, participating in the intracellular fate of maturing phagosomes?

4.4 In macrophages, latex beads coupled to mannan are taken up at higher rates and fuse faster with lysosomes than beads coupled to other ligands.

After the first hints obtained by the *in vitro* assay that receptor ligand interactions can influence particular phagosome functions, such as binding to actin filaments, it was of impact

to investigate phagocytosis in the context of a whole cell. For this purpose, same numbers of latex beads coupled to IgG, mannan, LPS, gelatin and avidin were applied to J774 macrophages and receptor expression, phagocytic uptake rates and lysosomal fusion of phagosomes were analysed.

The expression of all three tested receptors FcγRI (CD64), CD14 and MR was analysed by western blotting of total cell lysates over a time course of four hours and was found to be influenced in response to ligand coupled beads. The expression of FcγRI was higher during the first two hours of phagocytosis of beads coupled to IgG and mannan, implicating that this receptor is predominantly responsible for the uptake of IgG beads but may also be affected by mannan coupled beads. CD14 expression was increased at earlier times in mannan samples, but was finally expressed nearly three times more in both, LPS and mannan samples, after four hours compared before the addition of beads. CD14, an abundant protein in macrophages, is a co receptor for the recognition of bacterial lipopolysaccharides present on the surface of bacteria, but seems to participate also in the interaction with mannose groups. Moreover, CD14 was also present on isolated phagosomes containing different ligand coupled beads determined by proteomic analysis.

The mannose receptor showed differences in the expression level of its precursor form and the mature receptor upon response to different ligands. The addition of mannan coupled latex beads increased the expression of the mature MR as well as slightly the addition of LPS beads, whereas the two other bead types had no effect or a reduced MR expression (Fig. 12). Recognition of LPS by the MR was previously described (Zamze et al. 2002). The addition of all coated latex beads increased the expression levels of the inactive MR precursor compared to the rate before phagocytosis. From these results it remains to be determined, how much of the mature MR is expressed at the cell surface, because macrophages contain a large intracellular pool of MR (Stahl et al. 1984). Additionally, the MR undergoes continual rapid recycling (5 to 10 minutes) to the cell surface (Stahl et al. 1980). The expression of the MR in J774.A1 cells, which were used in this study, only appears at moderate levels in comparison to the J774.E clone (Fiani et al. 1998), but seems to be very important for the uptake of mannan coated beads like results from microarray and mass spectrometry approaches implicated.

The analysis of phagocytic uptake rates and lysosomal fusion of phagosomes exhibited clear differences between the different phagosome types and again, mannose receptor mediated phagocytosis exhibited the strongest effect. Latex beads coupled to mannan were internalised at clearly higher rates (at 30 min.: 6 fold more compared to avidin, 5 fold to IgG and 1.6 fold to LPS) and fused very rapidly with late endosomal/lysosomal

compartments. More than 90 % of the phagosomes containing mannan beads acquired pre loaded gold nanoparticles from lysosomes already after five minutes uptake time. In contrast, less than 60 % of the phagosomes containing beads coated with IgG, and less than 70 % of the LPS LBP acquired the lysosomal marker at this time. Phagosomes containing latex beads coupled to gelatin and avidin started to fuse efficiently with these compartments not before 15 minutes after internalisation. Labelling for the lysosome associated membrane protein 2 (LAMP 2) confirmed these results, because mannan LBP recruited this late endosome/lysosome marker more rapidly than phagosomes containing other bead types.

Previous observations provided evidence that receptor engagement at the cell surface and different subsequent signalling pathways could trigger different uptake rates during receptor mediated phagocytosis (Ward & Kaplan 1990). It has been already shown that dependent on the type of particle or bacterium, phagocytosis occurs with different efficiency (O'Brien & Melville 2003). The mannose receptor, which is predominantly engaged for the non opsonic internalisation of several pathogens, including *Candida albicans* and mycobacteria, was shown to play an important role in the uptake process (Kaposzta et al. 1999). Previous work using beads coated with terminal mannosyl units of the *M. tuberculosis* surface lipoglycan demonstrated that uptake via MR mediated phagocytosis occurs very rapidly within minutes (Kang & Schlesinger 1998). On the other hand, a contrary study using IgG opsonised (FcR engagement) and non opsonised zymosan particles (MR and beta glucan R engagement) showed that opsonised particles were taken up at slightly higher rates than non opsonised ones (Allen et al. 2002).

The finding of this study that MR mediated internalisation stimulated lysosome fusion very rapidly is in good agreement with a previous study analysing uptake of *Candida* yeast cells (Kaposzta et al. 1999). There, the majority of phagosomes containing *Candida albicans* also started to fuse with late endosomes and lysosomes already after 5 minutes. Other findings in alveolar macrophages demonstrated that the MR stimulates the secretion of lysosomal enzymes (Ohsumi & Lee 1987), which facilitates extracellular degradation. Moreover, a recent study showed that innate immune recognition triggers the secretion of lysosomal enzymes, such as GILT, cathepsin D and S and prosaposin in a TLR mediated inflammatory response (Lackman et al. 2007). Although it remains to be proven, it is conceivable that, in addition to having a secretory function, these vesicles can also deliver their contents to phagosomes and contribute to the observed rapid acidification of phagosomes containing beads conjugated to mannan and LPS.

Interactions between mannan as bead ligand and mannose receptors seems to trigger fast uptake into macrophages and signalling pathways, which mediate fast acquisition

of lysosomal enzymes and therefore rapid phagosome maturation. Phagosome maturation is a complex process, and different results suggest that not only the ligand receptor interactions but also the nature of the internalised particle itself plays an important role in modulating the rate and perhaps the quality of the process. A previous study demonstrated that the fusion capacity of phagosomes containing *Staphylococcus* A particles internalised via the Fc receptor were restricted to early endosomes and did not fuse with lysosomes (Mayorga et al. 1991). Thus, it is likely that both the receptor that mediates particle internalisation and the nature of the internalised particle (e.g. live versus dead pathogen) play important roles in phagosome maturation and phagosome lysosome fusion.

Additional to the quantification of phagocytic uptake rates and phagosome lysosome fusion events, tyrosine phosphorylation in macrophages was analysed. FcγR mediated phagocytosis stimulated several tyrosine protein kinases and induced tyrosine phosphorylation of many proteins (Majeed et al. 2001). In this study, I was able to show that IgG coupled beads triggered tyrosine phosphorylation at a greater extent than the other coated beads. This is supported by the finding of the tyrosine protein kinase Yes uniquely on IgG LBP, which was confirmed by a recent study (Rogers & Foster 2007). Previous work has shown that Yes is rapidly activated on interaction with IgG coated particles, localises to both, forming and closed phagosomes, in close contact with F actin and could help to regulate phagosome lysosome fusion (Majeed et al. 2001).

4.5 Macrophage gene expression is strongly influenced by the type of analysed receptor-ligand interaction compared to changes of genes with common function.

To gain more insight of the impact of receptor mediated phagocytosis on cellular signalling, gene expression of macrophages was analysed using a microarray approach. In this study, up regulation of genes was analysed 30 and 60 minutes after the addition of IgG , mannan , LPS and avidin coupled latex beads. The used CodeLink™ microarray chip contained the whole mouse genome and analysis of gene upregulation in macrophages during phagocytosis compared to control conditions (resting macrophages) revealed many astonishing results.

The pie charts of Fig. 14 show the comparison of the list of genes that were upregulated in response to the different bead ligands. What is particularly striking is the fact that only about 10 % of these genes were common to all ligands. These genes included metabolic enzymes, such as ATPases and phosphatases, receptors that were triggered by all ligands, signalling molecules, membrane trafficking regulators and some cytoskeleton

proteins. Surprisingly, the majority of upregulated genes that were common to samples of all four different coatings were not directly linked to general phagocytic functions. For example, in all cases the beads are internalised in a phagocytic cup that shared similar morphologic criteria. One could expect that known genes involved in actin dynamics during phagocytic cup formation, such as N WASP, Arp2/3, PI3 kinase, will be upregulated. We found only few common upregulated genes linked to these dynamics. This suggests that those proteins are not *de novo* synthesised upon bead internalisation, but rather that the existing cellular pool is enough to sustain the entry of the beads and the subsequent trafficking of phagosomes. A higher upregulation could only be found for the Wiskott Aldrich syndrome protein interacting protein (Wip), forming like 1 and profilin. Wip participates in the reorganisation of the actin based cytoskeleton and stabilises actin filaments (Antón et al. 2007). Recently, formin like 1 was also implicated in actin reorganisation (Gomez et al. 2007), whereas profilin was associated directly with phagocytic events (Pearson et al. 2003).

However, a larger fraction of upregulated genes were unique to each ligand receptor interaction. This argues that each receptor stimulates its own specific 'signature' of gene expression. Quite prominent was the upregulation of pro inflammatory and anti inflammatory cytokines in response to the bead ligands. Macrophages play a critical role in the initiation, maintenance and resolution of inflammation and are getting activated and deactivated in the inflammatory process. Pro inflammatory cytokines, such as gamma interferon, tumor necrosis factor alpha (TNFα) and bacterial lipopolysaccharides stimulate macrophage activation, whereas anti inflammatory cytokines, like interleukin 10 and transforming growth factor beta, cause a deactivation (Martinez et al. 2008). 30 min. after the addition of IgG coated latex beads, TNFα and related proteins were strongly upregulated, which could be shown by microarray analysis as well as on the protein level by western blotting of cell lysates treated with these beads. Interestingly, IgG beads also caused on upregulation of the anti inflammatory cytokine interleukin 10 after 60 min. incubation, arguing for a deactivation of macrophages at later time points of IgG bead phagocytosis. In contrast, Mannan coated beads stimulated an upregulation of other interleukins, such as interleukin 12b and 1a, suggesting a different inflammatory response (Shibata et al. 1997). Several other chemokines and interleukins were triggered by specific receptor ligand interactions suggesting signalling processes closely linked to the type of coated bead. Furthermore, the isotype specific and time dependent regulation of phosphodiesterase classes, enzymes that are essential for signal transduction (Jin et al. 2005), also supports the hypothesis of a specific signalling 'signature' upon the contact between ligand and receptor.

Striking was the fact that opsonin dependent phagocytosis (IgG beads) stimulated nearly no upregulation of cytoskeletal proteins and trafficking regulators, whereas non opsonic uptake of mannan coated latex beads caused an upregulation of major histocompatibility complex (MHC) molecules, Rab proteins as well as dynamin, filamin and myosin Vc. Previous studies have shown that the MR represents an important pathway for antigen recognition, uptake and delivery to MHC class I and II molecules (Apostolopoulos & McKenzie 2001). The proteomic identification of several MHC molecules, CD74 and cathepsin S on phagosomes containing mannan beads confirmed this importance. CD74 is the cell surface form of the MHC class II invariant chain (Leng et al. 2003), which is processed by the protease cathepsin S (Maubach et al. 2007). The finding of an upregulation of myosin Vc upon addition of mannan coupled latex beads is supported by the proteomic result of the presence of myosin Vc on mannan LBP (although myosin Vc could only be detected when protein identification filter settings were decreased to 40 %, see chapter 2.10). Myosin Vc is implicated to be associated with transferrin receptor trafficking (Rodriguez & Cheney 2002), but may also be involved in phagosome dynamics. In contrast, myosin Vb, which participates in non clathrin dependent endocytosis and recycling (Roland et al. 2007), was found to be upregulated in response to all coated beads, but at a different extent. Additionally, Rab8a, Eps 15 and Arf6 interacting proteins were upregulated in cells pulsed with different latex beads, all three molecules, which help to facilitate association between phagosomes and myosin Vb (Roland et al. 2007).

4.6 Phagosomal protein composition displays similar unique changes after receptor-dependent internalisation.

A significant number of the proteins that are synthesised in response to a phagocytic signal can be expected to play a general role in phagosome maturation and functions. The most obvious class of proteins that can influence these processes are those that are inserted into the membrane or delivered within the lumen of the phagosome. Given that each receptor induced a significant fraction of its own specific set of genes, it was interesting to compare the protein composition of the different phagosomes. For this purpose, latex bead phagosomes are well equipped since they can be easily purified from cells after sucrose gradient purification (Griffiths 2003). At this stage, it was of great interest to analyse the protein content of the different bead containing phagosomes. Main questions arise: Which proteins are synthesised *de novo* upon incubation with coated beads or can be found localised later to the phagosome itself? Can we find the same degree of differences for the phagosome protein content that we have observed for gene expression profiles?

The comparison of phagosomal proteomes after mass spectrometry analysis displayed many differences after ligand specific phagosome formation between the samples analysed. First of all, the percentages of common, unique and overlapping proteins are remarkably similar to the pattern observed for upregulated genes after microarray analysis. All three analysed phagosomal proteomes (avidin, IgG and mannan) revealed 1194 proteins in total, and only less than 20 % of them shared common appearance. Around 30 % are unique for avidin phagosomes and 16 % for each of the other phagosome types (IgG and mannan). This pattern supports the hypothesis that receptor ligand interactions during particle recognition at the cell surface are essential determinants of phagosomal fate including maturation and trafficking events.

Several phagosomal and lysosomal markers, such as LAMP 1 and 2, cathepsin B, D and Z, Rab7 and various proton ATPase subunits, could be detected in all three phagosome types and were already found in LBP proteomic approaches before (Garin et al. 2001, Stuart et al. 2007). However, two cathepsins, namely L and S, were only found in IgG and mannan or in mannan LBP alone, respectively. It is known that cathepsins are regulated differently in a cell (Brix et al. 2007) and previous results have demonstrated that hydrolases of the cathepsin family are not delivered simultaneously to phagosomes during their maturation (Munier Lehmann et al. 1996). A proteomic study of LBP in mouse macrophages has presented evidence that cathepsin A is the earliest one followed later by B, Z, and D, whereas the acquisition of cathepsin L and especially cathepsin S take place after several hours (Garin et al. 2001). So, the appearance of cathepsin S exclusively in 1 hr./1 hr. mannan LBP but not in IgG or avidin LBP could be a hint of more rapid maturation events of these phagosomes as detected by their faster acquisition of lysosomal markers, such as pre loaded rhodamine gold particles.

The appearance of the membrane bound Ig gamma 1 chain on IgG LBP is consistent with these phagosomes being formed as a consequence of FcγR mediated phagocytosis, although also a precursor of FcεR was found, implicating that other Fc receptors could be additionally involved. The specific presence of the Rab5A isoform on these phagosomes points to macrophage activation events, because previous work has shown that this GTPase isoform is involved in trafficking in activated macrophages, whereas Rab5B, 5C, 7 and 11 remained unaffected in the same study (Alvarez Dominguez & Stahl 1998). Rab5A appears to play two roles: (1) by mediating fusion events within the phagosomal endosomal compartment and (2) by facilitating or initiating phagosome maturation culminating in phagosome lysosome fusion (Alvarez Dominguez & Stahl 1998).

Recently, a sophisticated, quantitative proteomic analysis of phagosomes containing IgG coupled latex beads in RAW 264.7 macrophages was published following different time points over a maturation period of two hours (Rogers & Foster 2007). Nearly two third (60 %) of the 317 identified proteins from the Rogers & Foster study could be found in the list of the 588 identified proteins of the IgG Fc coupled phagosomes of this study (see table S1 in the supplement). Their findings also confirmed the presence of some proteins, which seems to be unique to IgG phagosomes, such as Rab5A and the membrane bound Ig gamma 1 chain.

At the first glance, high throughput analyses, such as cellular gene expression profiling and mass spectrometry of phagosomes, show the complexity of phagocytic processes. In this study, the results obtained from these approaches were mostly used for meta analyses to define functional groups of genes or proteins to compare them between the different receptor ligand responses. However, these data can be used in several ways: (1) they can be scanned, and individual genes or proteins can be picked for more detailed studies; (2) more focused experiments, for example using defined cellular mutants, can be performed; (3) detailed regulator gene analyses can be carried out; and (4) the data from all types of experiment can be collated and more sophisticated meta analyses can be performed.

4.7 Advantages of the latex bead model system for the study of receptor-mediated phagocytosis – future prospects.

Latex bead phagosomes are a versatile model system, which allows the detailed analysis of a variety of functions during phagocytosis *in vitro* and in cells. Work on LBP over the last 15 years led to the development of several *in vitro* assays using isolated phagosomes for detailed proteomics and lipidomics analyses and the characterization of various phagosome functions in living macrophages (Desjardins & Griffiths 2003; Griffiths & Mayorga 2007). *In vitro* assays were applied to monitor microtubule binding and motility, actin assembly and binding as well as fusion events with different endocytic compartments (Desjardins & Griffiths 2003). Furthermore, the *in vitro* actin assembly assay has opened up a system to analyse pathogen induced signalling networks regulating defined and complex membrane functions (Anes et al. 2003; Kalamidas et al. 2006).

In the case of membranous organelles, an obvious requirement for *in vitro* assays and biochemical analyses is that these organelles be as pure as possible. For most intracellular organelles, including phagosomes containing microorganisms, it is very difficult to achieve this goal and a variable, and often significant, extent of contamination can hardly

be avoided. Therefore it seems an inescapable conclusion that many groups will continue to use the powerful latex bead phagosome system towards improving our understanding the molecular mechanisms that are responsible for all the complex functions that are undertaken by phagosomes.

However, a limiting factor in our understanding until now is that crucial receptors that internalise beads or pathogens are either unknown or too many to be analysed in detail. There is also a kind of broad consensus about the fact that phagosome maturation indeed exists and vectorially follows a kind of 'clock' as the cellular set of phagosomes lose and gain proteins, lipids and functions. One might expect that phagosomes containing a given microbe or type of particle that entered cells via the same receptors would behave the same, at least in a single cell. Surprisingly, different findings show that phagosomes formed via the same receptors can find themselves in different chemical states even within the same macrophage supporting the idea of the 'individuality' of phagosomes (Griffiths 2004).

By using coated latex beads, this study and the approaches it introduces provide a platform for understanding interactions between phagocytic particles having defined ligands with specific receptors on macrophages and open ways to determine how many different phagosomal states are possible in a single cell. Although it is important to address phagocytic processes and signalling events at cellular and tissue levels, it seems likely that detailed mechanisms will ultimately emerge from the use of *in vitro* systems where all components are under the control of the investigator.

Bibliography

Ackerman AL, Kyritsis C, Tampe R, Cresswell P. 2003. Early phagosomes in dendritic cells form a cellular compartment sufficient for cross presentation of exogenous antigens. *PNAS.* 100:12889-12894.

Aderem A. 2002. How to Eat Something Bigger than Your Head. *Cell.* 110:5-8.

Al-Haddad A, Shonn MA, Redlich B, Blocker A, Burkhardt JK, Yu H, Hammer JA 3rd, Weiss DG, Steffen W, Griffiths G, Kuznetsov SA. Myosin Va bound to phagosomes binds to F-actin and delays microtubule-dependent motility. *Mol Biol Cell.* 12:2742-2755.

Allen LA & Aderem A. 1996. Molecular definition of distinct cytoskeletal structures involved in complement- and Fc receptor-mediated phagocytosis in macrophages. *J Exp Med.* 184:627-637.

Allen LA, Yang C, Pessin JE. 2002. Rate and extent of phagocytosis in macrophages lacking vamp3. *J Leukoc Biol.* 72:217-221.

Allison AC, Davies P, De Petris S. 1971. Role of contractile microfilaments in macrophage movement and endocytosis. *Nat New Biol.* 232:153-155.

Alvarez-Dominguez C & Stahl PD. 1999. Increased expression of Rab5a correlates directly with accelerated maturation of *Listeria monocytogenes* phagosomes. *J Biol Chem.* 274:11459-11462.

Anes E, Kühnel MP, Bos E, Moniz-Pereira J, Habermann A, Griffiths G. 2003. Selected lipids activate phagosome actin assembly and maturation resulting in killing of pathogenic mycobacteria. *Nat Cell Biol.* 5:793-802.

Anes E, Peyron P, Staali L, Jordao L, Gutierrez MG, Kress H, Hagedorn M, Maridonneau-Parini I, Skinner MA, Wildeman AG, Kalamidas SA, Kuehnel M, Griffiths G. 2006. Dynamic life and death interactions between *Mycobacterium smegmatis* and J774 macrophages. *Cell Microbiol.* 8:939-960.

Antón IM, Jones GE, Wandosell F, Geha R, Ramesh N. 2007. WASP-interacting protein (WIP): working in polymerisation and much more. *Trends Cell Biol.* 17:555-562.

Apostolopoulos V & McKenzie IF. 2001. Role of the mannose receptor in the immune response. *Curr Mol Med.* 1:469-474.

Asea A, Rehli M, Kabingu E, Boch JA, Bare O, Auron PE, Stevenson MA, Calderwood SK. 2002. Novel signal transduction pathway utilized by extracellular HSP70: role of toll-like receptor (TLR) 2 and TLR4. *J Biol Chem.* 277:15028-15034.

Bajno L, Peng XR, Schreiber AD, Moore HP, Trimble WS, Grinstein S. 2000. Focal exocytosis of VAMP3-containing vesicles at sites of phagosome formation. *J Cell Biol.* 149:697-706.

Barbieri MA, Roberts RL, Mukhopadhyay A, Stahl PD. 1996. Rab5 regulates the dynamics of early endosome fusion. *Biocell.* 20:331-338.

Berntzen G, Flo TH, Medvedev A, Kilaas L, Skjåk-Braek G, Sundan A, Espevik T. 1998. The tumor necrosis factor-inducing potency of lipopolysaccharide and uronic acid polymers is increased when they are covalently linked to particles. *Clin Diagn Lab Immunol.* 5:355-361.

Berrington WR & Hawn TR. 2007. *Mycobacterium tuberculosis*, macrophages, and the innate immune response: does common variation matter? *Immunol Rev.* 219:167-186.

Bjellqvist B, Ek K, Righetti PG, Gianazza E, Görg A, Westermeier R, Postel W. 1982. Isoelectric focusing in immobilized pH gradients: principle, methodology and some applications. *J Biochem Biophys Methods.* 6:317-339.

Blander JM & Medzhitov R. 2004. Regulation of phagosome maturation by signals from toll-like receptors. *Science.* 304:1014-1018.

Blocker A, Severin FF, Habermann A, Hyman AA, Griffiths G, Burkhardt JK. 1996. Microtubule-associated protein-dependent binding of phagosomes to microtubules. *J Biol Chem.* 271:3803-3811.

Blocker A, Severin FF, Burkhardt JK, Bingham JB, Yu H, Olivo JC, Schroer TA, Hyman AA, Griffiths G. 1997. Molecular requirements for bi-directional movement of phagosomes along microtubules. *J Cell Biol.* 137:113-129.

Blocker A, Griffiths G, Olivo JC, Hyman AA, Severin FF. 1998. A role for microtubule dynamics in phagosome movement. *J Cell Sci.* 111:303-312.

Botelho RJ, Teruel M, Dierckman R, Anderson R, Wells A, York JD, Meyer T, Grinstein S. 2000. Localized biphasic changes in phosphatidylinositol-4,5-bisphosphate at sites of phagocytosis. *J Cell Biol.* 151:1353-1368.

Bradford MM. 1976. A rapid and sensitive method for the quantitation of microgram quantities of protein utilizing the principle of protein-dye binding. *Anal Biochem.* 72:248-254.

Briken V, Porcelli SA, Besra GS, Kremer L. 2004. Mycobacterial lipoarabinomannan and related lipoglycans: from biogenesis to modulation of the immune response. *Mol Microbiol.* 53:391-403.

Brix K, Dunkhorst A, Mayer K, Jordans S. 2007. Cysteine cathepsins: Cellular roadmap to different functions. *Biochimie*. Aug 6 [Epub ahead of print]

Burlak C, Whitney AR, Mead DJ, Hackstadt T, Deleo FR. 2005. Maturation of human neutrophil phagosomes includes incorporation of molecular chaperones and endoplasmic reticulum quality control machinery. *Mol Cell Proteomics.* 5:620-634.

Carroll MC. 1998. The role of complement and complement receptors in induction and regulation of immunity. *Annu Rev Immunol.* 16:545-568.

Castellano F, Chavrier P, Caron E. 2001. Actin dynamics during phagocytosis. *Semin Immunol.* 13:347-355.

Chakraborty P, Sturgill-Koszycki S, Russell DG. 1994. Isolation and characterization of pathogen-containing phagosomes. *Methods Cell Biol.* 45:261-276.

Clemens DL & Horwitz MA. 1995. Characterization of the *Mycobacterium tuberculosis* phagosome and evidence that phagosomal maturation is inhibited. *J Exp Med.* 181:257-270.

Clerc P & Sansonetti PJ. 1987. Entry of *Shigella flexneri* into HeLa cells: evidence for directed phagocytosis involving actin polymerization and myosin accumulation. *Infect Immun.* 55:2681-2688.

Cooper AM, Solache A, Khader, SA. 2007. Interleukin-12 and tuberculosis: an old story revisited. *Curr Opin Immunol.* 19:441-447.

Coppolino MG, Krause M, Hagendorff P, Monner DA, Trimble W, Grinstein S, Wehland J, Sechi AS. 2001. Evidence for a molecular complex consisting of Fyb/SLAP, SLP-76, Nck, VASP and WASP that links the actin cytoskeleton to Fcgamma receptor signalling during phagocytosis. *J Cell Sci.* 114:4307-4318.

Cox D, Tseng CC, Bjekic G, Greenberg S. 1999. A requirement for phosphatidylinositol 3-kinase in pseudopod extension. *J Biol Chem.* 274:1240-1247.

Cox D, Berg JS, Cammer M, Chinegwundoh JO, Dale BM, Cheney RE, Greenberg S. 2002. Myosin X is a downstream effector of PI(3)K during phagocytosis. *Nat Cell Biol.* 4:469-477.

Damiani MT & Colombo MI. 2003. Microfilaments and microtubules regulate recycling from phagosomes. *Exp Cell Res*. 289:152-161.

Darby C, Geahlen RL, Schreiber AD. 1994. Stimulation of macrophage Fc RIIIA activates the receptor-associated protein tyrosine kinase Syk and induces phosphorylation of multiple proteins including p95Vav and p62/GAP-associated protein. *J Immunol.* 152:5429-5437.

Defacque H, Egeberg M, Habermann A, Diakonova M, Roy C, Mangeat P, Voelter W, Marriott G, Pfannstiel J, Faulstich H, Griffiths G. 2000. Involvement of ezrin/moesin in *de novo* actin assembly on phagosomal membranes. *EMBO J.* 19:199-212.

Deng YP, Griffiths G, Storrie B. 1991. Comparative behavior of lysosomes and the pre-lysosome compartment (PLC) in in vivo cell fusion experiments. *J Cell Sci.* 99:571-582.

DePina AS & Langford GM. 1999. Vesicle transport: the role of actin filaments and myosin motors. *Microsc Res Tech.* 47:93-106.

Desjardins M, Huber LA, Parton RG, Griffiths G. 1994. Biogenesis of phagolysosomes proceeds through a sequential series of interactions with the endocytic apparatus. *J Cell Biol.* 124:677-688.

Desjardins M. 1995. Biogenesis of phagolysosomes: the 'kiss-and-run' hypothesis. *Trends Cell Biol.* 5:183-186.

Desjardins M, Nzala NN, Corsini R, Rondeau C. 1997. Maturation of phagosomes is accompanied by changes in their fusion properties and size-selective acquisition of solute materials from endosomes. *J Cell Sci.* 110:2303-2314.

Desjardins M. 2003. ER-mediated phagocytosis: a new membrane for new functions. *Nat Rev Immunol.* 3:280-291.

Devitt A, Moffatt OD, Raykundalia C, Capra JD, Simmons DL, Gregory CD. 1998. Human CD14 mediates recognition and phagocytosis of apoptotic cells. *Nature.* 392:505-509.

Di A, Krupa B, Bindokas VP, Chen Y, Brown ME, Palfrey HC, Naren AP, Kirk KL, Nelson DJ. 2002. Quantal release of free radicals during exocytosis of phagosomes. *Nat Cell Biol.* 4:279-285.

Diaz BL & Arm JP. 2003. Phospholipase A2. *Prostaglandins Leukot Essent Fatty Acids*. 69:87-97.

Duclos S, Diez R, Garin J, Papadopoulou B, Descoteaux A, Stenmark H, Desjardins M. 2000. Rab5 regulates the kiss and run fusion between phagosomes and endosomes and the acquisition of phagosome leishmanicidal properties in RAW 264.7 macrophages. *J Cell Sci.* 113:3531-3541.

Egile C, Loisel TP, Laurent V, Li R, Pantaloni D, Sansonetti PJ, Carlier MF. 1999. Activation of the CDC42 effector N-WASP by the *Shigella flexneri* IcsA protein promotes actin nucleation by Arp2/3 complex and bacterial actin-based motility. *J Cell Biol.* 146:1319-1332.

Ernst JD. 1998. Macrophage receptors for *Mycobacterium tuberculosis*. *Infect Immun.* 66:1277-1281.

Ezekowitz RA, Sastry K, Bailly P, Warner A. 1990. Molecular characterization of the human macrophage mannose receptor: demonstration of multiple carbohydrate recognition-like domains and phagocytosis of yeasts in Cos-1 cells. *J Exp Med.* 172:1785-1794.

Fenton MJ, Riley LW, Schlesinger LS. 2005. Receptor-mediated recognition of *Mycobacterium tuberculosis* by host cells. In *Tuberculosis and the Tubercle Bacillus*. ASM Press, New York. 405-426.

Fernandez N, Renedo M, Alonso S, Crespo MS. 2003. Release of arachidonic acid by stimulation of opsonic receptors in human monocytes: the FcgammaR and the complement receptor 3 pathways. *J Biol Chem.* 278:52179-52187.

Fernandez-Mora E, Polidori M, Lührmann A, Schaible UE, Haas A. 2005. Maturation of *Rhodococcus equi*-containing vacuoles is arrested after completion of the early endosome stage. *Traffic.* 6:635-653.

Fischer L, Poeckel D, Buerkert E, Steinhilber D, Werz O. 2005. Inhibitors of actin polymerisation stimulate arachidonic acid release and 5-lipoxygenase activation by upregulation of Ca2+ mobilisation in polymorphonuclear leukocytes involving Src family kinases. *Biochim Biophys Acta.* 1736:109-119.

Fueller M, Wang DA, Tigyi G, Siess W. 2003. Activation of human monocytic cells by lysophosphatidic acid and sphingosine-1-phosphate. *Cell Signal*. 15:367-375.

Fukata M, Watanabe T, Noritake J, Nakagawa M, Yamaga M, Kuroda S, Matsuura Y, Iwamatsu A, Perez F, Kaibuchi K. 2002. Rac1 and Cdc42 capture microtubules through IQGAP1 and CLIP-170. *Cell.* 109:873-885.

Funato K, Beron W, Yang CZ, Mukhopadhyay A, Stahl PD. 1997. Reconstitution of phagosome-lysosome fusion in streptolysin O-permeabilized cells. *J Biol Chem.* 272:16147-16151.

Gagnon E, Duclos S, Rondeau C, Chevet E, Cameron PH, Steele-Mortimer O, Paiement J, Bergeron JJ, Desjardins M. 2002. Endoplasmic reticulum-mediated phagocytosis is a mechanism of entry into macrophages *Cell.* 110:119-131.

Garin J, Diez R, Kieffer S, Dermine JF, Duclos S, Gagnon E, Sadoul R, Rondeau C, Desjardins M. 2001. The phagosome proteome: Insight into phagosome functions. *J Cell Biol.* 152:165-180.

Garner RE, Rubanowice K, Sawyer RT, Hudson JA. 1994. Secretion of TNF-alpha by alveolar macrophages in response to *Candida albicans* mannan. *J Leuk Biol.* 55:161-168.

Gatfield J & Pieters J. 2000. Essential role for cholesterol in entry of mycobacteria into macrophages. *Science.* 288:1647-1650.

Gatfield J, Albrecht I, Zanolari B, Steinmetz MO, Pieters J. 2005. Association of the leukocyte plasma membrane with the actin cytoskeleton through coiled coil-mediated trimeric coronin 1 molecules. *Mol Biol Cell.* 16:2786-2798.

Görg A, Obermaier C, Boguth G, Harder A, Scheibe B, Wildgruber R, Weiss W. 2000. The current state of two-dimensional electrophoresis with immobilized pH gradients. *Electrophoresis.* 21:1037-1053.

Goetz M, Bubert A, Wang G, Chico-Calero I, Vazquez-Boland JA, Beck M, Slaghuis J, Szalay AA, Goebel W. 2001. Microinjection and growth of bacteria in the cytosol of mammalian host cells. *PNAS.* 98:12221-12226.

Gomez TS, Kumar K, Medeiros RB, Shimizu Y, Leibson PJ, Billadeau DD. 2007. Formins regulate the actin-related protein 2/3 complex-independent polarization of the centrosome to the immunological synapse. *Immunity.* 26:177-190.

Gordon S. 2003. Alternative activation of macrophages. *Nat Rev Immunol.* 3:23-35.

Gotthardt D, Warnatz HJ, Henschel O, Brückert F, Schleicher M, Soldati T. 2002. High-resolution dissection of phagosome maturation reveals distinct membrane trafficking phases. *Mol Biol Cell.* 13:3508-3520.

Gotthardt D, Blancheteau V, Bosserhoff A, Ruppert T, Delorenzi M, Soldati T. 2006a. Proteomics fingerprinting of phagosome maturation and evidence for the role of a Galpha during uptake. *Mol Cell Proteomics.* 5:2228-2243.

Gotthardt D, Dieckmann R, Blancheteau V, Kistler C, Reichardt F, Soldati T. 2006b. Preparation of intact, highly purified phagosomes from Dictyostelium. Methods Mol Biol. 346:439-448.

Greenberg S & Grinstein S. 2002. Phagocytosis and innate immunity. *Curr Opin Immunol.* 14:136-145.

Greenberg S. 1999. Modular components of phagocytosis. *J Leukoc Biol.* 66:712-717.

Griffin FM Jr, Griffin JA, Leider JE, Silverstein SC. 1975. Studies on the mechanism of phagocytosis. I. Requirements for circumferential attachment of particle-bound ligands to specific receptors on the macrophage plasma membrane. J Exp Med. 142:1263-1282.

Griffin, FM Jr & Silverstein SC. 1974. Segmental response of the macrophage plasma membrane to a phagocytic stimulus. *J Exp Med.* 139:323-336.

Guerin I & de Chastellier C. 2000. Disruption of the actin filament network affects delivery of endocytic contents marker to phagosomes with early endosome characteristics: the case of phagosomes with pathogenic mycobacteria. *Eur J Cell Biol.* 79:735-749.

Guermonprez P, Saveanu L, Kleijmeer M, Davoust J, van Endert P & Amigorena S. 2003. ER-phagosome fusion defines an MHC class I cross-presentation compartment in dendritic cells. *Nature.* 425:397-402.

Haas A. 2007. The phagosome: compartment with a license to kill. *Traffic.* 8:311-330.

Harrison RE, Bucci C, Vieira OV, Schroer TA, Grinstein S. 2003. Phagosomes fuse with late endosomes and/or lysosomes by extension of membrane protrusions along microtubules: role of Rab7 and RILP. *Mol Cell Biol.* 23:6494-6506.

Hasson T & Cheney RE. 2001. Mechanisms of motor protein reversal. *Curr Opin Cell Biol.* 13:29-35.

Hatsuzawa K, Tamura T, Hashimoto H, Hashimoto H, Yokoya S, Miura M, Nagaya H, Wada I. 2006. Involvement of syntaxin 18, an endoplasmic reticulum (ER)-localized SNARE protein, in ER-mediated phagocytosis. *Mol Biol Cell.* 17:3964-3977.

Hilpelä P, Vartiainen MK, Lappalainen P. 2004. Regulation of the actin cytoskeleton by PI(4,5)P2 and PI(3,4,5)P3. *Curr Top Microbiol Immunol.* 282:117-163.

Hiltbold EM & Roche PA. 2002. Trafficking of MH class II molecules in the late secretory pathway. *Curr Opin Immunol.* 14:30-35.

Holtta-Vuori M & Ikonen E. 2006. Endosomal cholesterol traffic: vesicular and non-vesicular mechanisms meet. *Biochem Soc Trans.* 34:392-394.

Houde M, Bertholet S, Gagnon E, Brunet S, Goyette G, Laplante A, Princiotta MF, Thibault P, Sacks D, Desjardins M. 2003. Phagosomes are competent organelles for antigen cross-presentation. *Nature.* 425:402-406.

Hulett MD & Hogarth PM. 1994. Molecular basis of Fc receptor function. *Adv Immunol.* 57:1-127.

Huynh KK, Eskelinen EL, Scott CC, Malevanets A, Saftig P, Grinstein S. 2007. LAMP proteins are required for fusion of lysosomes with phagosomes. *EMBO J.* 26:313-324.

Ikonen E. 2006. Mechanisms for cellular cholesterol transport: defects and human disease. *Physiol Rev.* 86:1237-1261.

Isakov N. 1997. Immunoreceptor tyrosine-based activation motif (ITAM), a unique module linking antigen and Fc receptors to their signal cascades. *J Leukoc Biol.* 61:6-16.

Jahraus A, Tjelle TE, Berg T, Habermann A, Storrie B, Ullrich O, Griffiths G. 1998. *In vitro* fusion of phagosomes with different endocytic organelles from J774 macrophages. *J Biol Chem.* 273:30379-30390.

Janeway CA Jr. 1992. The immune system evolved to discriminate infectious nonself from noninfectious self. *Immunol Today.* 13:11-16.

Jayachandran R, Sundaramurthy V, Combaluzier B, Mueller P, Korf H, Huygen K, Miyazaki T, Albrecht I, Massner J, Pieters J. 2007. Survival of mycobacteria in macrophages is mediated by coronin 1-dependent activation of calcineurin. *Cell.* 130:37-50.

Jiang Q, Akashi S, Miyake K, Petty HR. 2000. Cutting Edge: Lipopolysaccharide induces physical proximity between CD14 and Toll-like receptor 4 (TLR4) prior to nuclear translocation of NF-kB. *J Immunol.* 165:3541-3544.

Jin SL, Lan L, Zoudilova M, Conti M. 2005. Specific role of phosphodiesterase 4B in lipopolysaccharide-induced signaling in mouse macrophages. *J Immunol.* 175:1523-1531.

Jordao L, Bleck CK, Mayorga L, Griffiths G, Anes E. 2007. On the killing of mycobacteria by macrophages. *Cell Microbiol.* Nov 6 [Epub ahead of print]

Juan TS, Hailman E, Kelley MJ, Busse LA, Davy E, Empig CJ, Narhi LO, Wright SD, Lichenstein HS. 1995. Identification of a lipopolysaccharide binding domain in CD14 between amino acids 57 and 64. *J Biol Chem.* 270:5219-5224.

Jutras I & Desjardins M. 2005. Phagocytosis: at the crossroads of innate and adaptive immunity. *Annu Rev Cell Dev Biol.* 21:511-527.

Kabelitz D & Medzhitov R. 2007. Innate immunity - cross-talk with adaptive immunity through pattern recognition receptors and cytokines. *Curr Opin Immunol.* 19:1-3.

Kagan JC & Roy CR. 2002. *Legionella* phagosomes intercept vesicular traffic from endoplasmic reticulum exit sites. *Nat Cell Biol.* 4:945-954.

Kang PB, Azad AK, Torrelles JB, Kaufman TM, Beharka A, Tibesar E, DesJardin LE, Schlesinger LS. 2005. The human macrophage mannose receptor directs Mycobacterium tuberculosis lipoarabinomannan-mediated phagosome biogenesis. *J Exp Med.* 202:987-999.

Kaposzta R, Maródi L, Hollinshead M, Gordon S, da Silva RP. 1999. Rapid recruitment of late endosomes and lysosomes in mouse macrophages ingesting *Candida albicans*. *J Cell Sci.* 112:3237-3248.

Kaufmann SH & Schaible UE. 2005. Antigen presentation and recognition in bacterial infections. *Curr Opin Immunol.* 17:79-87.

Kelleher JF & Titus MA. 1998. Intracellular motility: how can we all work together? *Curr Biol.* 8:R394-R397.

Kielian MC, Steinman RM, Cohn ZA. 1982. Intralysosomal accumulation of polyanions. I. Fusion of pinocytic and phagocytic vacuoles with secondary lysosomes. *J Cell Biol.* 93:866-874.

Kjeken R, Egeberg M, Habermann A, Kuehnel M, Peyron P, Floetenmeyer M, Walther P, Jahraus A, Defacque H, Kuznetsov SA, Griffiths G. 2004. Fusion between phagosomes, early and late endosomes: a role for actin in fusion between late, but not early endocytic organelles. *Mol Biol Cell.* 15:345-358.

Knodler LA, Celli J, Finlay BB. 2001. Pathogenic trickery: deception of host cell processes. *Nat Rev Mol Cell Biol.* 2:578-588.

Korade-Mirnics Z & Corey SJ. 2000. Src kinase-mediated signaling in leukocytes. *J Leukoc Biol.* 68:603-613.

Korn ED. 1974. The isolation of the amoeba plasma membrane and the use of latex beads for the isolation of phagocytic vacuole (phagosome) membranes from amoebae including the culture techniques for amoebae. *Methods Enzymol.* 31:686-698.

Krieger M & Herz J. 1994. Structures and functions of multiligand lipoprotein receptors: macrophage scavenger receptors and LDL receptor-related protein (LRP). *Annu Rev Biochem.* 63:601-637.

Krieger M. 1997. The other side of scavenger receptors: pattern recognition for host defense. *Curr Opin Lipidol.* 8:275-280.

Kühnel M, Anes E, Griffiths G. 2006. Isolation of latex bead- and mycobacteria-containing phagosomes. In *J. Celis (Ed.): Cell Biology - A Laboratory Handbook*, chapter VIII, 3rd edition, Academic Press, San Diego. 57-62.

Kunert A, Vinnemeier J, Erdmann N, Hagemann M. 2003. Repression by Fur is not the main mechanism controlling the iron-inducible isiAB operon in the cyanobacterium *Synechocystis* sp. PCC 6803. *FEMS Microbiol Lett.* 227:255-262.

Kusner DJ, Hall CF, Jackson S. 1999. Fc gamma receptor-mediated activation of phospholipase D regulates macrophage phagocytosis of IgG-opsonized particles. *J Immunol.* 162:2266-2274.

Kwiatkowska K, Frey J, Sobota A. 2003. Phosphorylation of FcgammaRIIA is required for the receptor-induced actin rearrangement and capping: the role of membrane rafts. *J Cell Sci*. 116:537-550.

Lackman RL, Jamieson AM, Griffith JM, Geuze H, Cresswell P. 2007. Innate immune recognition triggers secretion of lysosomal enzymes by macrophages. *Traffic.* 8:1179-1189.

Laemmli UK. 1970. Cleavage of structural proteins during the assembly of the head of bacteriophage T4. *Nature.* 227:680-685.

Lapierre LA, Kumar R, Hales CM, Navarre J, Bhartur SG, Burnette JO, Provance DW Jr, Mercer JA, Bahler M, Goldenring JR. 2001. Myosin vb is associated with plasma membrane recycling systems. *Mol Biol Cell.* 12:1843-1857.

Le Cabec V, Carréno S, Moisand A, Bordier C, Maridonneau-Parini I. 2002. Complement receptor 3 (CD11b/CD18) mediates type I and type II phagocytosis during nonopsonic and opsonic phagocytosis, respectively. *J Immunol.* 169:2003-2009.

Lecuit M, Ohayon H, Braun L, Mengaud J, Cossart P. 1997. Internalin of *Listeria monocytogenes* with an intact leucine-rich repeat region is sufficient to promote internalization. *Infect Immun.* 65:5309-5319.

Lee MS & Kim YJ. 2007. Pattern-recognition receptor signaling initiated from extracellular, membrane, and cytoplasmic space. *Mol Cells.* 23:1-10.

Lehner PJ & Cresswell P. 2004. Recent developments in MHC-class-I-mediated antigen presentation. *Curr Opin Immunol.* 16:82-89.

Leng L, Metz CN, Fang Y, Xu J, Donnelly S, Baugh J, Delohery T, Chen Y, Mitchell RA, Bucala R. 2003. MIF signal transduction initiated by binding to CD74. *J Exp Med.* 197:1467-1476.

Lennon-Duménil AM, Bakker AH, Maehr R, Fiebiger E, Overkleeft HS, Rosemblatt M, Ploegh HL, Lagaudrière-Gesbert C. 2002. Analysis of protease activity in live antigen-presenting cells shows regulation of the phagosomal proteolytic contents during dendritic cell activation. *J Exp Med.* 196:529-540.

Lerm M, Holm A, Seiron A, Sarndahl E, Magnusson KE, Rasmusson B. 2006. *Leishmania donovani* requires functional Cdc42 and Rac1 to prevent phagosomal maturation. *Infect Immun.* 74:2613-2618.

Li Q & Cathcart MK. 1997. Selective inhibition of cytosolic phospholipase A2 in activated human monocytes. Regulation of superoxide anion production and low density lipoprotein oxidation. *J Biol Chem*. 272:2404-2411.

Lofgren R, Serrander L, Forsberg M, Wilsson A, Wasteson A, Stendahl O. 1999. CR3, FcgammaRIIA and FcgammaRIIIB induce activation of the respiratory burst in human neutrophils: the role of intracellular Ca(2+), phospholipase D and tyrosine phosphorylation. Biochim Biophys Acta. 1452:46-59.

Lührmann A, Streker K, Schüttfort A, Daniels JJ, Haas A. 2001. *Afipia felis* induces uptake by macrophages directly into a non-endocytic compartment. *PNAS.* 98:7271-7276.

Luzio JP, Rous BA, Bright NA, Pryor PR, Mullock BM, Piper RC. 2000. Lysosome-endosome fusion and lysosome biogenesis. *J Cell Sci.* 113:1515-1524.

Ma J, Chen T, Mandelin J, Ceponis A, Miller NE, Hukkanen M, Ma GF, Konttinen YT. 2003. Regulation of macrophage activation. *Cell Mol Life Sci.* 60:2334-2346.

Majeed M, Caveggion E, Lowell CA, Berton G. 2001. Role of Src kinases and Syk in Fcgamma receptor-mediated phagocytosis and phagosome-lysosome fusion. *J Leukoc Biol.* 70:801-811.

Malik ZA, Thompson CR, Hashimi S, Porter B, Iyer SS, Kusner DJ. 2003. Cutting edge: *Mycobacterium tuberculosis* blocks Ca2+ signaling and phagosome maturation in human macrophages via specific inhibition of sphingosine kinase. *J Immunol.* 170:2811-2815.

Marguet D, Luciani MF, Moynault A, Williamson P, Chimini G. 1999. Engulfment of apoptotic cells involves the redistribution of membrane phosphatidylserine on phagocyte and prey. *Nat Cell Biol*. 1:454-456.

Marion S, Laurent C, Guillen N. 2005. Signalization and cytoskeleton activity through myosin IB during the early steps of phagocytosis in *Entamoeba histolytica*: a proteomic approach. *Cell Microbiol.* 7:1504-1518.

Martinez FO, Sica A, Mantovani A, Locati M. 2008. Macrophage activation and polarization. *Front Biosci.* 13:453-461.

Maubach G, Lim MC, Kumar S, Zhuo L. 2007. Expression and upregulation of cathepsin S and other early molecules required for antigen presentation in activated hepatic stellate cells upon IFN-gamma treatment. *Biochim Biophys Acta.* 1773:219-231.

Maurin M, Benoliel AM, Bongrand P, Raoult D. 1992. Phagolysosomes of *Coxiella burnettii*-infected cell lines maintain an acidic pH during persistent infection. *Infect. Immun.* 60:5013-5016.

Mayor S & Pagano RE. 2007. Pathways of clathrin-independent endocytosis. Nat Rev Mol Cell Biol. 8:603-612.

Mayorga LS, Bertini F, Stahl PD. 1991. Fusion of newly formed phagosomes with endosomes in intact cells and in a cell-free system. *J Biol Chem.* 266:6511-6517.

Means TK, Lien E, Yoshimura A, Wang S, Golenbock DT, Fenton MJ. 1999. The CD14 ligands lipoarabinomannan and lipopolysaccharide differ in their requirement for toll-like receptors. *J Immunol.* 163:6748-6755.

Menard R, Prevost MC, Gounon P, Sansonetti P, Dehio C. 1996. The secreted Ipa complex of *Shigella flexneri* promotes entry into mammalian cells. *PNAS.* 93:1254-1258.

Metschnikoff E. 1883. Ueber eine Sprosspilzkrankheit der Daphnien. Beitrag zur Lehre ueber den Kampf der Phagocyten gegen Krankheitserreger. *Arch Pathol Anat.* 96:177-195.

Montesano R, Mossaz A, Vassalli P, Orci L. 1983. Specialization of the macrophage plasma membrane at sites of interaction with opsonized erythrocytes. *J Cell Biol*. 96:1227-1233.

Mordue DG & Sibley LD. 1997. Intracellular fate of vacuoles containing *Toxoplasma gondii* is determined at the time of formation and depends on the mechanism of entry. *J Immunol.* 159:4452-4459.

Morrissette NS, Gold ES, Guo J, Hamerman JA, Ozinsky A, Bedian V, Aderem AA. 1999. Isolation and characterization of monoclonal antibodies directed against novel components of macrophage phagosomes. *J Cell Sci.* 112:4705-4713.

Mousavi SA, Malerod L, Berg T, Kjeken R. 2004. Clathrin-dependent endocytosis. Biochem J. 377:1-16.

Muller S, Masson V, Droesch S, Donner M, Stoltz JF. 1989. Phagocytosis and membrane fluidity: application to the evaluation of opsonizing properties of fibronectin. *Biorheology.* 26:323-330.

Muller WA, Steinmann RM, Cohn ZA. 1983. Membrane proteins of the vacuolar system: III: Further studies on the composition and recycling of endocytic vacuole membrane in cultured macrophages. *J Cell Biol*. 96:29-36

Müller-Taubenberger A, Lupas AN, Li H, Ecke M, Simmeth E, Gerisch G. 2001. Calreticulin and calnexin in the endoplasmic reticulum are important for phagocytosis. *EMBO J.* 20:6772-6782.

Munier-Lehmann H, Mauxion F, Bauer U, Lobel P, Hoflack B. 1996. Re-expression of the mannose 6-phosphate receptors in receptor-deficient fibroblasts. Complementary function of the two mannose 6-phosphate receptors in lysosomal enzyme targeting. *J Biol Chem.* 271:15166-15174.

Nguyen L & Pieters J. 2005. The Trojan horse: survival tactics of pathogenic mycobacteria in macrophages. *Trends Cell Biol.* 15:269-276.

Niedergang F & Chavrier P. 2004. Signaling and membrane dynamics during phagocytosis: many roads lead to the phagos(R)ome. *Curr Opin Cell Biol.* 16:422-428.

Nigou J, Zelle-Rieser C, Gilleron M, Thurnher M, Puzo G. 2001. Mannosylated liparabinomannans inhibit IL-12 production by human dendritic cells: evidence for a negative signal delivered through the mannose receptor. *J Immunol.* 166:7477-7485.

Nimmerjahn F & Ravetch JV. 2006. Fcgamma receptors: old friends and new family members. *Immunity.* 24:19-28.

Nimmerjahn F, Bruhns P, Horiuchi K, Ravetch JV. 2005. FcgammaRIV: a novel FcR with distinct IgG subclass specificity. *Immunity.* 23:41-51.

Nolte C, Kirchhoff F, Kettenmann H. 1997. Epidermal growth factor is a motility factor for microglial cells in vitro: evidence for EGF receptor expression. *Eur J Neurosci.* 9:1690-1698.

O'Brien DK & Melville SB. 2003. Multiple effects on *Clostridium perfringens* binding, uptake and trafficking to lysosomes by inhibitors of macrophage phagocytosis receptors. *Microbiology.* 149:1377-1386.

Ohsumi Y & Lee YC. 1987. Mannose-receptor ligands stimulate secretion of lysosomal enzymes from rabbit alveolar macrophages. *J Biol Chem.* 262:7955-7962.

Olazabal IM, Caron E, May RC, Schilling K, Knecht DA, Machesky LM. 2002. Rho-kinase and myosin-II control phagocytic cup formation during CR, but not FcgammaR, phagocytosis. *Curr Biol.* 12:1413-1418.

Park JB. 2003. Phagocytosis induces superoxide formation and apoptosis in macrophages. *Exp Mol Med.* 35:325-335.

Peachman KK, Rao M, Palmer DR, Zidanic M, Sun W, Alving CR, Rothwell SW. 2004. Functional microtubules are required for antigen processing by macrophages and dendritic cells. *Immunol Lett.* 95:13-24.

Pearson AM, Baksa K, Rämet M, Protas M, McKee M, Brown D, Ezekowitz RA. 2003. Identification of cytoskeletal regulatory proteins required for efficient phagocytosis in Drosophila. *Microbes Infect.* 5:815-824.

Peyron P, Bordier C, N'Diaye EN, Maridonneau-Parini I. 2000. Nonopsonic phagocytosis of *Mycobacterium kansasii* by human neutrophils depends on cholesterol and is mediated by CR3 associated with glycosylphosphatidylinositol-anchored proteins. *J Immunol.* 165:5186-5191.

Pitt A, Mayorga LS, Stahl PD, Schwartz AL. 1992a. Alterations in the protein composition of maturing phagosomes. *J Clin Invest.* 90:1978-1983.

Pitt A, Mayorga LS, Schwartz AL, Stahl PD. 1992b. Transport of phagosomal components to an endosomal compartment. *J Biol Chem.* 267:126-132.

Platt N, Suzuki H, Kurihara Y, Kodama T, Gordon S. 1996. Role for the class A macrophage scavenger receptor in the phagocytosis of apoptotic thymocytes *in vitro*. *PNAS.* 93:12456-12460.

Platt N, Haworth R, Darley L, Gordon S. 2002. The many roles of the class A macrophage scavenger receptor. *Int Rev Cytol.* 212:1-40.

Poltorak A, He X, Smirnova I, Liu MY, Van Huffel C, Du X, Birdwell D, Alejos E, Silva M, Galanos C, Freudenberg M, Ricciardi-Castagnoli P, Layton B, Beutler B. 1998. Defective LPS signaling in C3H/HeJ and C57BL/10ScCr mice: mutations in *Tlr4* gene. *Science.* 282:2085-2088.

Prigozy TI, Sieling PA, Clemens D, Stewart PL, Behar SM, Porcelli SA, Brenner MB, Modlin RL, Kronenberg M. 1997. The mannose receptor delivers lipoglycan antigens to endosomes for presentation to T cells by CD1b molecules. *Immunity.* 6:187-197.

Ramachandra L & Harding CV. 2000. Phagosomes acquire nascent and recycling class II MHC molecules but primarily use nascent molecules in phagocytic antigen processing. *J Immunol.* 164:5103-5112.

Ramachandra L, Noss E, Boom WH, Harding CV. 1999. Phagocytic processing of antigens for presentation by class II major histocompatibility complex molecules. *Cell Microbiol.* 1:205-214.

Rassa JC, Meyers JL, Zhang Y, Kudaravalli R, Ross SR. 2002. Murine retroviruses activate B cells via interaction with Toll-like receptor 4. *PNAS.* 99:2281-2286.

Ravetch JV & Lanier LL. 2000. Immune inhibitory receptors. *Science.* 290:84-89.

Ravetch JV. 1994. Fc receptors: rubor redux. *Cell.* 78:553–560.

Ridley AJ. 2001. Rho family proteins: coordinating cell responses. *Trends Cell Biol.* 11:471-477.

Roland JT, Kenworthy AK, Peranen J, Caplan S, Goldenring JR. 2007. Myosin Vb interacts with Rab8a on a tubular network containing EHD1 and EHD3. *Mol Biol Cell.* 18:2828-2837.

Rosenberger CM & Finlay BB. 2003. Phagocyte sabotage: disruption of macrophage signalling by bacterial pathogens. *Nat Rev Mol Cell Biol.* 4:385-396.

Russell DG. 2001. *Mycobacterium tuberculosis*: here today, and here tomorrow. *Nat Rev Mol Cell Biol.* 2:569-577.

Sanchez-Mejorada G & Rosales C. 1998. Signal transduction by immunoglobulin Fc receptors. *J Leukoc Biol.* 63: 521-533.

Schlesinger LS, Hull SR, Kaufman TM. 1994. Binding of the terminal mannosyl units of lipoarabinomannan from a virulent strain of *Mycobacterium tuberculosis* to human macrophages. *J Immunol.* 152:4070-4079.

Schwartz SL, Cao C, Pylypenko O, Rak A, Wandinger-Ness A. 2007. Rab GTPases at a glance. *J Cell Sci.* 120:3905-3910.

Scianimanico S, Desrosiers M, Dermine JF, Meresse S, Descoteaux A, Desjardins M. 1999. Impaired recruitment of the small GTPase rab7 correlates with the inhibition of phagosome maturation by *Leishmania donovani* promastigotes. *Cell Microbiol.* 1:19-32.

Scott CC, Dobson W, Botelho RJ, Coady-Osberg N, Chavrier P, Knecht DA, Heath C, Stahl P, Grinstein S. 2005. Phosphatidylinositol-4,5-bisphosphate hydrolysis directs actin remodeling during phagocytosis. *J Cell Biol.* 169:139-149.

Seabra MC & Coudrier E. 2004. Rab GTPases and myosin motors in organelle motility. *Traffic.* 5:393-399.

Serrander L, Larsson J, Lundqvist H, Lindmark M, Fallman M, Dahlgren C, Stendahl O. 1999. Particles binding beta(2)-integrins mediate intracellular production of oxidative metabolites in human neutrophils independently of phagocytosis. *Biochim Biophys Acta.* 1452:133-144.

Shevchenko A, Wilm M, Vorm O, Mann M. 1996. Mass spectrometric sequencing of proteins silver-stained polyacrylamide gels. *Anal Chem.* 68:850-858.

Shibata Y, Metzger WJ, Myrvik QN. 1997. Chitin particle-induced cell-mediated immunity is inhibited by soluble mannan: Mannose receptor-mediated phagocytosis initiates IL-12 production. *J Immunol.* 159:2462-2467.

Show DR, & Griffin FM Jr. 1981. Phagocytosis requires repeated triggering of macrophage phagocytic receptors during particle ingestion. *Nature.* 289:409-411.

Somsel Rodman J & Wandinger-Ness A. 2000. Rab GTPases coordinate endocytosis. J Cell Sci. 113:183-192.

Spiegel S & Milstien S. 2007. Functions of the multifaceted family of sphingosine kinases and some close relatives. *J Biol Chem.* 282:2125-2129.

Spudich JA & Watt S. 1971. The regulation of rabbit skeletal muscle contraction. I. Biochemical studies of the interaction of the tropomyosin-troponin complex with actin and the proteolytic fragments of myosin. *J Biol Chem.* 246:4866-4871.

Stahl P, Schlesinger PH, Sigardson E, Rodman JS, Lee YC. 1980. Receptor-mediated pinocytosis of mannose glycoconjugates by macrophages: characterization and evidence for receptor recycling. *Cell.* 19:207-215.

Stahl PD, Wileman TE, Diment S, Shepherd VL. 1984. Mannose-specific oligosaccharide recognition by mononuclear phagocytes. *Biol Cell.* 51:215-218.

Stahl PD & Ezekowitz RA. 1998. The mannose receptor is a pattern recognition receptor involved in host defense. *Curr Opin Immunol.* 10:50-55.

Stockinger W, Zhang SC, Trivedi V, Jarzylo LA, Shieh EC, Lane WS, Castoreno AB, Nohturfft A. 2006. Differential requirements for actin polymerization, calmodulin, and Ca2+ define distinct stages of lysosome/phagosome targeting. *Mol Biol Cell.* 17:1697-1710.

Stuart LM, Boulais J, Charriere GM, Hennessy EJ, Brunet S, Jutras I, Goyette G, Rondeau C, Letarte S, Huang H, Ye P, Morales F, Kocks C, Bader JS, Desjardins M, Ezekowitz RA. 2007. A systems biology analysis of the Drosophila phagosome. *Nature.* 445:95-101.

Swanson J, Bushnell A, Silverstein SC. 1987. Tubular lysosome morphology and distribution within macrophages depend on the integrity of cytoplasmic microtubules. *PNAS.* 84:1921-1925.

Swanson JA & Baer SC. 1995. Phagocytosis by zippers and triggers. *Trends Cell Biol.* 5:89-93.

Takeda K, Kaisho T, Akira S. 2003. Toll-like receptors. *Annu Rev Immunol.* 21:335-376.

Tapper H. 1996. The secretion of preformed granules by macrophages and neutrophils. *J Leukoc Biol.* 59:613-622.

Taunton J, Rowning BA, Coughlin ML, Wu M, Moon RT, Mitchison TJ, Larabell CA. 2000. Actin-dependent propulsion of endosomes and lysosomes by recruitment of N-WASP. *J Cell Biol.* 148:519-530.

Taunton J. 2001. Actin filament nucleation by endosomes, lysosomes and secretory vesicles. *Curr Opin Cell Biol.* 13:85-91.

Taylor PR, Gordon S, Martinez-Pomares L. 2005. The mannose receptor: linking homeostasis and immunity through sugar recognition. *Trends Immunol.* 26:104-110.

Taylor PR, Martinez-Pomares L, Stacey M, Lin HH, Brown GD, Gordon S. 2005. Macrophage receptors and immune recognition. *Annu Rev Immunol.* 23:901-944.

Tenner AJ, Robinson SL, Ezekowitz RA. 1995. Mannose binding protein (MBP) enhances mononuclear phagocyte function via a receptor that contains the 126,000 M(r) component of the C1q receptor. *Immunity.* 3:485-493.

Tjelle TE, Lovdal T, Berg T. 2000. Phagosome dynamics and function. *BioEssays.* 22:255-263.

Toyohara A & Inaba K. 1989. Transport of phagosomes in mouse peritoneal macrophages. *J Cell Sci.* 94:143-153.

Treede I, Braun A, Sparla R, Kühnel M, Giese T, Turner JR, Anes E, Kulaksiz H, Füllekrug J, Stremmel W, Griffiths G, Ehehalt R. 2007. Anti-inflammatory effects of phosphatidylcholine. *J Biol Chem.* 282:27155-27164.

Triantafilou M & Triantafilou K. 2002. Lipopolysaccharide recognition: CD14, TLRs and the LPS-activation cluster. *Trends Immunol.* 23:301-304.

Towbin H, Staehelin T, Gordon J. 1979. Electrophoretic transfer of proteins from polyacrylamide gels to nitrocellulose sheets: procedure and some applications. *PNAS.* 76:4350-4354.

Ullrich O, Reinsch S, Urbe S, Zerial M, Parton RG. 1996. Rab11 regulates recycling through the pericentriolar recycling endosome. *J Cell Biol.* 135:913-924.

Underhill DM & Ozinsky A. 2002. Phagocytosis of microbes: complexity in action. *Annu Rev Immunol.* 20:825-52.

Underhill DM, Ozinsky A, Hajjar AM, Stevens A, Wilson CB, Bassetti M, Aderem A. 1999. The Toll-like receptor 2 is recruited to macrophage phagosomes and discriminates between pathogens. *Nature.* 401:811-815.

van Deurs B, Holm PK, Kayser L, Sandvig K. 1995. Delivery to lysosomes in the human carcinoma cell line HEp-2 involves an actin filament-facilitated fusion between mature endosomes and preexisting lysosomes. *Eur J Cell Biol.* 66:309-323.

Ward DM & Kaplan J. 1990. The rate of internalization of different receptor-ligand complexes in alveolar macrophages is receptor-specific. *Biochem J.* 270:369-374.

Watts C. 2004. The exogenous pathway for antigen presentation on major histocompatibility complex class II and CD1 molecules. *Nat Immunol.* 5:685-692.

Weiss DG, Maile W, Wick RA, Steffen W. 1999. Video microscopy. In *Electronic light microscopy in biology – a practical approach.* IRL Press, Oxford. 221-278.

Werts C, Tapping RI, Mathison JC, Chuang TH, Kravchenko V, Saint Girons I, Haake DA, Godowski PJ, Hayashi F, Ozinsky A, Underhill DM, Kirschning CJ, Wagner H, Aderem A, Tobias PS, Ulevitch RJ. Leptospiral lipopolysaccharide activates cells through a TLR2-dependent mechanism. *Nat Immunol.* 2:346-352.

Wetzel MG & Korn ED. 1969. Phagocytosis of latex beads by *Acanthamoeba castellanii* (Neff). 3. Isolation of the phagocytic vesicles and their membranes. *J Cell Biol*. 43:90-104.

Wienke DC, Knetsch ML, Neuhaus EM, Reedy MC, Manstein DJ. 1999. Disruption of a dynamin homologue affects endocytosis, organelle morphology, and cytokinesis in *Dictyostelium discoideum*. *Mol Biol Cell.* 10:225-243.

Wileman TE, Lennartz MR, Stahl PD. 1986. Identification of the macrophage mannose receptor as a 175-kDa membrane protein. *PNAS.* 83:2501-2505.

Wright SD, Ramos RA, Tobias PS, Ulevitch RJ, Mathison JC. 1990. CD14, a receptor for complexes of lipopolysaccharide (LPS) and LPS binding protein. *Science.* 249:1431-1433.

Wu X, Bowers B, Wei Q, Kocher B, Hammer JA 3rd. 1997. Myosin V associates with melanosomes in mouse melanocytes: evidence that myosin V is an organelle motor. *J Cell Sci.* 110:847-859.

Wu XS, Rao K, Zhang H, Wang F, Sellers JR, Matesic LE, Copeland NG, Jenkins NA, Hammer JA 3rd. 2002. Identification of an organelle receptor for myosin-Va. *Nat Cell Biol.* 4:271-278.

Yeung T & Grinstein S. 2007. Lipid signaling and the modulation of surface charge during phagocytosis. *Immunol Rev.* 219:17-36.

Zamze S, Martinez-Pomares L, Jones H, Taylor PR, Stillion RJ, Gordon S, Wong SY. 2002. Recognition of bacterial capsular polysaccharides and lipopolysaccharides by the macrophage mannose receptor. *J Biol Chem.* 277:41613-41623.

Zhang J, Zhu J, Bu X, Cushion M, Kinane TB, Avraham H, Koziel H. 2005. Cdc42 and RhoB activation are required for mannose receptor-mediated phagocytosis by human alveolar macrophages. *Mol Biol Cell.* 16:824-834.

Most of this work has been done in the Light Microscopy Centre of the University of Rostock over the past four years. Parts of the study were carried out in collaboration with the European Molecular Biology Laboratory (EMBL) in Heidelberg. The project was financially supported by the DFG (DA 208/7-1; KU 1528/2-1). Numerous people helped me during the whole duration of this study, whom I want to thank for their continuous support.

First, I would like to thank PD Dr. Sergei Kuznetsov for being my supervisor and teacher at the University of Rostock over the past six years. He has introduced me to the fascinating science of the cytoskeleton and phagocytosis and kindly offered me to work on these topics in his lab. I am very grateful to all his suggestions and help over the years as well as critical reading of the manuscript. I thank Prof. Dieter Weiss for his patience and guidance during my whole study, the stimulating discussions we had and the opportunity to work in his department. I am also really thankful to Dr. Gareth Griffiths from the EMBL Heidelberg, who provided expertise on many aspects of this study, the possibility to work in his lab, his help and advices as well as the financial support and his comments on the manuscript. Many thanks to Prof. Albert Haas to have agreed to be a referee of my PhD thesis.

Furthermore, I would like to thank all previous and recent members of the Kuznetsov and the Griffiths lab for all their practical help, the nice atmosphere and numerous fruitful talks about life and science. Some of them I want to mention here, so thank you Katja, Ramona, Devang, Sabrina, Daniela and Mark for all your help. Bibhuti and Paras helped me tremendously with the analysis and confirmation of the microarray part of this study. I am grateful to all people in the Department of Cell Biology in Rostock, especially Jana Frahm, Bärbel Redlich, Maren Bagrowski and Anne Mahrwald. I thank Christian Klasen and the EMBL Transgenic Service for taking care of the mice used in this study, Sabrina Rüggeberg and the EMBL Proteomics Core Facility as well as Tomi Bähr-Ivacevic and the EMBL Genomics Core Facility for their superb expertise. I am grateful to Dr. Nicholas Sherman and the W.M. Keck Biomedical Mass Spectrometry Laboratory, funded by the Pratt Committee of the University of Virginia, USA, for the proteomic analysis of my samples and their constructive help.

Finally, I want to acknowledge the support I got from all my friends and their open ears and minds over the last years. Torsten, thank you not only for critical reading of my thesis and scientific advice, but mostly for your friendship and everything far away from science. I thank Peter for being my friend and anchor, for his optimism and patience and especially for the times we shared above and under water. I also thank Fatima, Mohamed and their precious little ones, Hana and Haia, for enlightening many of my days in Rostock, but also for showing me new horizons.

Sabrina, la danseuse, qui a touché mon coeur et partagé le sien avec moi, je la remercie pour son amour et le soutien qu'elle m'a apporté même dans les moments difficiles, mais surtout pour tout ce qui, loin de la science, la rend si exceptionnelle à mes yeux.

Meiner Familie sage ich aus tiefstem Herzen Dank für den Rückhalt und die Unterstützung, die sie mir fortwährend in all den Jahren gegeben haben, aber auch dafür, wie wir in Zeiten eines Verlustes gemeinsam füreinander da waren. Tim danke ich besonders dafür, dass er mir nicht nur Bruder sondern auch ein guter Freund in jeder Hinsicht war.

Curriculum vitae

Personal Information

Name:	Eik Hoffmann
Date & Place of Birth:	27 August 1976 in Forst / Lausitz, Germany

Education

since Jun 2003:	PhD thesis in the lab of PD Dr. S.A. Kuznetsov, University of Rostock
Oct 1996 – Feb 2003:	Studies of Biology and Diploma at the University of Rostock
Aug 1991 – Jul 1995:	High School “Friedrich Franz” in Parchim, Abitur
Sep 1983 – Jul 1991:	Comprehensive School “Fritz Reuter” in Parchim

Practical Experience

since Aug 2007:	Member of the group of Dr. G. Griffiths, CBB unit, EMBL Heidelberg
Jul 2003 – Jun 2007:	Scientific assistant, University of Rostock, DFG project “Signalling networks and actin membrane assembly in latex bead & mycobacterial phagosomes”
Jan 2002 – Feb 2003:	Diploma thesis: “The involvement of the motor protein myosin-Va in cytoskeleton organization and cellular morphogenesis”, PD Dr. S.A. Kuznetsov
Mar – Nov 2000:	Practical periods at Wageningen University, Netherlands, Supervisor: Dr. G. Alink and at the University of Essen, Germany, Supervisor: PD Dr. E. Dopp

Publications

Hoffmann, E., Marion, S., Mishra, B.B., Kratzke, R., Ahmad, F., John, M., Holzer, D., Anand, P.K., Weiss, D.G., Griffiths, G. and Kuznetsov, S.A. The phagocytic receptor programs gene expression and phagosome functions in macrophages. *Molecular Systems Biology.* [submitted]

Kühnel, M.P., Reiss, M., Anand, P.K., Treede, I., Holzer, D., Hoffmann, E., Klapperstück, M., Markwardt, F. and Griffiths, G. S1P receptors stimulate macrophage plasma membrane actin assembly via ADP release, ATP synthesis and $P2X_7$ receptor activation. *Nature Cell Biology.* [submitted]

Schwarz, R., Liang, C., Kaleta, C., Kühnel, M., Hoffmann, E., Kuznetsov, S., Hecker, M., Griffiths, G., Schuster, S. and Dandekar, T. 2007. Integrated network reconstruction, visualization and analysis using YANAsquare. *BMC Bioinformatics*. 8:313.

Bhattacharya, K., Hoffmann, E., Hartmann, L.M., Albrecht, C., Rettenmeier, A.W. and Dopp, E. 2007. Cellular uptake and toxicity of inhalable arsenopyrite particles and of its natural analogue hematite. *Naunyn-Schmiedebergs Archives of Pharmacology.* 375:78-79. 382:Suppl.1.

Geh, S., Yücel, R., Duffin, R., Albrecht, C., Borm, P.J.A., Armbruster, L., Raulf-Heimsoth, M., Brüning, T., Hoffmann, E., Rettenmeier, A.W. and Dopp, E. 2006. Cellular uptake and cytotoxic potential of respirable bentonite particles with different quartz contents and chemical modifications in human lung fibroblasts. *Archives of Toxicology* 80:98-106.

Roder, A., Hoffmann, E., Hagemann, M. and Berg, G. 2005. Synthesis of the compatible solutes glucosylglycerol and trehalose by salt-stressed cells of *Stenotrophomonas* strains. *FEMS Microbiology Letters* 243:219-226.

Kröger, W., Hoffmann, E. und Weiss, D.G. 2005. Hochaufgelöst, schnell, schonend und spektral: 3D-Lichtmikroskopie. *BioSpektrum* 11:450-453. [in German]

Burmeister, B., Schwerdtle, T., Poser, I., Hoffmann, E., Hartwig, A., Müller, W.-U., Rettenmeier, A.W., Seemayer, N.H. and Dopp, E. 2004. Effects of asbestos on initiation of DNA damage, induction of DNA-strand breaks, p53-expression and apoptosis in primary, SV40-transformed and malignant human mesothelial cells. *Mutation Research* 558:81-92.

Hoffmann, E., Weiss, D.G., Kuznetsov, S.A. und Wöllert, T. 2003. Lichtmikroskopische Analyse der ER-Dynamik im Zellzyklus. *BioSpektrum* 9:414-417. [in German]

Selbstständigkeitserklärung

Ich versichere hiermit an Eides statt, dass ich die vorliegende Arbeit selbstständig angefertigt und ohne fremde Hilfe verfasst habe, keine außer den von mir angegebenen Hilfsmitteln und Quellen dazu verwendet habe und die den benutzten Werken inhaltlich und wörtlich entnommenen Stellen als solche kenntlich gemacht habe.

Rostock, 28.12.2007 .....
Eik Hoffmann

Supplement

Table S1. List of all identified proteins in isolated 1 hr./1 hr. phagosomes containing latex beads coupled to avidin (Av), the Fc fragment of IgG (IgG) and mannan (Man) determined by LC-MS/MS. *Legend: MW (protein molecular weight in kDa), PIDP (protein identification probability), UP (number of unique peptides), US (number of unique spectra), TS (number of total spectra), SCov (Sequence coverage)

Av	IgG	Man	Protein name	Accession #	MW*	PIDP*	UP*	US*	TS*	SCov*
x	x	x	- 11 kDa protein	IPI00458748	11	88,0%	1	1	2	13,7%
x	x	x	- 17 kDa protein	IPI00275455	17	88,0%	1	1	1	6,3%
x	x	x	- 18 kDa protein	IPI00458341	18	99,8%	2	2	2	14,6%
x	x	x	- 39 kDa protein	IPI00133580	39	100,0%	2	2	4	6,3%
x	x	x	2210013K02Rik Blastocyst blastocyst cDNA, RIKEN full-length enriched library, clone:I1C0023I18 product:Spinster-like protein	IPI00111254	57	88,0%	1	1	1	2,7%
x	x	x	2400001E08Rik UPF0404 protein C11orf59 homolog	IPI00315187	18	100,0%	2	3	5	16,1%
x	x	x	Abcb6 Mitochondrial ATP-binding cassette sub-family B member 6	IPI00120094	94	99,8%	2	2	2	3,8%
x	x	x	Acta1 Actin, alpha skeletal muscle	IPI00110827	42	100,0%	8	11	18	26,8%
x	x	x	Actb Actin, cytoplasmic 1	IPI00110850	42	100,0%	7	8	13	30,9%
x	x	x	Actn4 Alpha-actinin-4	IPI00118899	105	88,0%	1	1	1	1,2%
x	x	x	Actr2 Actin-like protein 2	IPI00177038	45	88,0%	1	1	1	3,1%
x	x	x	Actr3 Actin-like protein 3	IPI00115627	47	88,0%	1	1	1	2,4%
x	x	x	Ahnak AHNAK nucleoprotein isoform 1	IPI00553798	604	98,9%	1	1	1	0,3%
x	x	x	Alb1 Serum albumin precursor	IPI00131695	69	88,0%	1	2	3	2,1%
x	x	x	Aldoa Fructose-bisphosphate aldolase A	IPI00221402	39	100,0%	6	6	7	22,3%
x	x	x	Anxa2 Annexin A2	IPI00468203	39	100,0%	13	16	36	47,2%
x	x	x	Anxa4 29 kDa protein	IPI00830586	29	88,0%	1	1	2	3,9%
x	x	x	Anxa4 Annexin A4	IPI00353727	36	100,0%	8	11	24	33,2%
x	x	x	Anxa5 Annexin A5	IPI00317309	36	100,0%	6	7	12	19,1%
x	x	x	Anxa6 13 days embryo forelimb cDNA, RIKEN full-length enriched library, clone:5930413M14 product:annexin A6, full insert sequence	IPI00310240	75	99,9%	2	2	2	4,8%
x	x	x	Arbp 60S acidic ribosomal protein P0	IPI00314950	34	99,8%	2	2	3	7,9%
x	x	x	Arhgdia Rho GDP-dissociation inhibitor 1	IPI00322312	23	100,0%	3	4	5	22,1%
x	x	x	Arl8b ADP-ribosylation factor-like protein 8B	IPI00133218	22	98,3%	1	1	1	4,8%
x	x	x	Arpc4;Ttll3 Actin-related protein 2/3 complex subunit 4	IPI00138691	20	88,0%	1	1	2	6,6%
x	x	x	Arsb Isoform 2 of Arylsulfatase B precursor	IPI00406459	48	88,0%	1	1	1	4,6%
x	x	x	Asah1 Acid ceramidase precursor	IPI00125266	45	99,8%	2	3	3	7,4%
x	x	x	Atp1a1 Sodium/potassium-transporting ATPase alpha-1 chain precursor	IPI00311682	113	100,0%	4	4	5	4,5%
x	x	x	Atp1a3 Sodium/potassium-transporting ATPase alpha-3 chain	IPI00122048	112	88,0%	1	1	1	1,1%
x	x	x	Atp5a1 ATP synthase subunit alpha, mitochondrial precursor	IPI00130280	60	100,0%	6	6	7	13,6%
x	x	x	Atp6v0c Vacuolar ATP synthase 16 kDa proteolipid subunit	IPI00138378	16	88,0%	1	1	1	11,6%
x	x	x	Atp6v0d1 Vacuolar ATP synthase subunit d	IPI00313841	40	100,0%	4	5	8	12,5%
x	x	x	Atp6v1a Vacuolar ATP synthase catalytic subunit A, ubiquitous isoform	IPI00119112	68	100,0%	14	14	16	29,0%
x	x	x	Atp6v1b2 Bone marrow macrophage cDNA, RIKEN full-length enriched library, clone:I830083B18 product:ATPase, H+ transporting, V1 subunit B, isoform 2	IPI00119113	58	100,0%	15	16	27	31,1%
x	x	x	Atp6v1c1 Vacuolar ATP synthase subunit C	IPI00130186	44	100,0%	4	4	5	14,1%
x	x	x	Atp6v1e1 Vacuolar ATP synthase subunit E	IPI00119115	27	100,0%	7	8	10	21,9%
x	x	x	Atp6v1h Vacuolar ATP synthase subunit H	IPI00311461	56	100,0%	6	7	8	20,1%
x	x	x	Calr Calreticulin precursor	IPI00123639	48	100,0%	3	3	4	8,2%
x	x	x	Cap1 Adenylyl cyclase-associated protein 1	IPI00137331	52	100,0%	7	9	12	17,9%
x	x	x	Capg Macrophage capping protein	IPI00136906	39	99,8%	2	3	3	8,0%
x	x	x	Capzb Isoform 2 of F-actin capping protein subunit beta	IPI00269481	31	99,8%	2	2	3	8,8%
x	x	x	Cct3 T-complex protein 1 subunit gamma	IPI00116283	61	100,0%	4	4	5	10,6%
x	x	x	Cct5 T-complex protein 1 subunit epsilon	IPI00116279	60	100,0%	3	3	3	8,0%
x	x	x	Cct6a T-complex protein 1 subunit zeta	IPI00116281	58	100,0%	3	3	4	6,6%

x	x	x	Cd14 Monocyte differentiation antigen CD14 precursor	IPI00308990	39	88,0%	1	1	1	5,2%
x	x	x	Cd180 CD180 antigen precursor	IPI00343568	74	100,0%	3	3	3	8,0%
x	x	x	Cd68 Macrosialin	IPI00117031	36	88,0%	1	1	3	2,7%
x	x	x	Cfl2 Cofilin-2	IPI00266188	19	88,0%	1	1	5	6,6%
x	x	x	Cltc Clathrin heavy chain	IPI00169916	192	100,0%	10	11	17	9,5%
x	x	x	Coro1a Coronin-1A	IPI00323600	51	100,0%	3	3	5	6,3%
x	x	x	Cst7 CMAP	IPI00134046	19	88,0%	1	1	2	6,6%
x	x	x	Ctsa Lysosomal protective protein precursor	IPI00137177	54	100,0%	6	8	12	10,1%
x	x	x	Ctsb Cathepsin B precursor	IPI00113517	37	99,9%	2	2	3	8,9%
x	x	x	Ctsc Dipeptidyl-peptidase 1 precursor	IPI00130015	52	100,0%	3	3	3	10,6%
x	x	x	Ctsd Cathepsin D precursor	IPI00111013	45	100,0%	4	7	10	17,1%
x	x	x	Ctsz Cathepsin Z	IPI00125220	34	100,0%	7	7	14	28,3%
x	x	x	Cybb Cytochrome b-245 heavy chain	IPI00117117	65	100,0%	3	3	5	5,6%
x	x	x	D8Ertd354e Heparan-alpha-glucosaminide N-acetyltransferase	IPI00317488	73	88,0%	1	1	1	1,7%
x	x	x	Eef1a1 Elongation factor 1-alpha 1	IPI00307837	51	99,8%	2	2	2	11,1%
x	x	x	Eef1a2 Elongation factor 1-alpha 2	IPI00119667	50	99,9%	2	3	4	5,0%
x	x	x	Eef2 Elongation factor 2	IPI00466069	95	100,0%	8	9	19	11,4%
x	x	x	EG214738;LOC675985 similar to 40S ribosomal protein S6	IPI00108454	29	99,8%	2	2	4	9,6%
x	x	x	EG432919;LOC630967 similar to Glyceraldehyde-3-phosphate dehydrogenase	IPI00135284	36	100,0%	3	4	7	10,8%
x	x	x	EG619883 similar to ribosomal protein L30	IPI00118775	13	88,0%	1	2	3	13,9%
x	x	x	EG620772 similar to Cofilin-1 (Cofilin, non-muscle isoform) isoform 1	IPI00409405	18	88,0%	1	1	3	8,4%
x	x	x	EG622339 similar to Glyceraldehyde-3-phosphate dehydrogenase	IPI00123176	37	100,0%	4	5	10	19,8%
x	x	x	Eif4a1 Eukaryotic initiation factor 4A-I	IPI00118676	46	100,0%	5	5	6	16,3%
x	x	x	Eif5a Eukaryotic translation initiation factor 5A-1	IPI00108125	17	88,0%	1	2	3	7,8%
x	x	x	Eno1;LOC433182 Alpha-enolase	IPI00462072	47	100,0%	4	4	5	10,1%
x	x	x	Eno2 Eno2 protein	IPI00122684	35	88,0%	1	2	2	5,7%
x	x	x	Erp29 Endoplasmic reticulum protein ERp29 precursor	IPI00118832	29	88,0%	1	1	1	3,4%
x	x	x	Fbxw14 In vitro fertilized eggs cDNA, RIKEN full-length enriched library, clone:7420414F09 product:F-box only protein 12	IPI00224904	54	88,0%	1	1	1	3,4%
x	x	x	Fcer1g High affinity immunoglobulin epsilon receptor gamma-subunit precursor	IPI00119293	10	100,0%	3	4	5	25,6%
x	x	x	Fcgr2b 34 kDa protein	IPI00117140	34	98,2%	1	1	1	5,3%
x	x	x	Flna Isoform 1 of Filamin-A	IPI00131138	281	99,5%	1	1	1	0,5%
x	x	x	Ftl2 Ferritin light chain 2	IPI00228379	21	99,8%	2	2	3	17,5%
x	x	x	Fv4 Retrovirus-related Env polyprotein from Fv-4 locus	IPI00114007	74	99,8%	2	3	6	3,1%
x	x	x	Gaa Lysosomal alpha-glucosidase precursor	IPI00111960	106	88,0%	1	1	1	2,8%
x	x	x	Ganab Isoform 2 of Neutral alpha-glucosidase AB precursor	IPI00115679	109	88,0%	1	1	1	1,6%
x	x	x	Gapdhs glyceraldehyde-3-phosphate dehydrogenase, spermatogenic	IPI00108939	47	88,0%	1	2	4	3,2%
x	x	x	Gba Glucosylceramidase precursor	IPI00108811	58	100,0%	5	5	6	15,5%
x	x	x	Glb1 Beta-galactosidase precursor	IPI00135915	73	88,0%	1	2	2	2,3%
x	x	x	Gnai2 Guanine nucleotide-binding protein G(i), alpha-2 subunit	IPI00228617	40	100,0%	3	4	9	10,4%
x	x	x	Gnai3 Guanine nucleotide-binding protein G	IPI00338854	41	88,0%	1	1	1	2,8%
x	x	x	Gnao1 Guanine nucleotide-binding protein G(o) subunit alpha 2	IPI00115546	40	98,8%	1	1	2	3,1%
x	x	x	Gnb1 Guanine nucleotide-binding protein G(I)/G(S)/G(T) subunit beta 1	IPI00120716	37	100,0%	5	5	6	19,4%
x	x	x	Gnb2 Guanine nucleotide-binding protein G(I)/G(S)/G(T) subunit beta 2	IPI00162780	37	100,0%	4	4	4	14,7%
x	x	x	Gnb2l1 Guanine nucleotide-binding protein subunit beta 2-like 1	IPI00317740	35	100,0%	6	6	7	22,1%
x	x	x	Gnb3 Guanine nucleotide-binding protein G(I)/G(S)/G(T) subunit beta 3	IPI00116938	37	99,8%	1	1	1	2,1%
x	x	x	Gns N-acetylglucosamine-6-sulfatase precursor	IPI00221426	61	100,0%	5	5	9	10,3%
x	x	x	Gpr84 Probable G-protein coupled receptor 84	IPI00118169	44	88,0%	1	1	1	6,3%

x	x	x	H2afj;LOC632401 H2afj protein	IPI00153400	14	100,0%	2	3	6	21,7%
x	x	x	H2-D1 H-2 class I histocompatibility antigen, D-D alpha chain precursor	IPI00110805	41	100,0%	3	3	3	12,1%
x	x	x	Hexa Beta-hexosaminidase alpha chain precursor	IPI00125522	61	100,0%	5	6	8	12,5%
x	x	x	Hexb Beta-hexosaminidase beta chain precursor	IPI00115530	61	100,0%	10	11	12	19,6%
x	x	x	Hist1h2bj;Hist1h2bf;Hist1h2bn;Hist1h2bl Histone H2B type 1-F/J/L	IPI00114642	14	99,8%	2	4	8	19,8%
x	x	x	Hist1h4i;Hist1h4b;Hist4h4;Hist1h4h;Hist1h4d;Hist1h4k;Hist1h4m;Hist1h4c;Hist2h4;Hist1h4j;Hist1h4a;Hist1h4f;4930558J22Rik 10 days embryo whole body cDNA, RIKEN full-length enriched library, clone:2610027B07 product:histone 4 protein, full insert	IPI00329998	11	88,0%	1	1	2	9,7%
x	x	x	Hsp90ab1 Heat shock protein 84b	IPI00229080	83	100,0%	17	20	38	30,9%
x	x	x	Hsp90b1 Endoplasmin precursor	IPI00129526	92	100,0%	6	6	9	10,8%
x	x	x	Hspa1l Heat shock 70 kDa protein 1L	IPI00133208	71	100,0%	3	4	11	6,2%
x	x	x	Hspa5 78 kDa glucose-regulated protein precursor	IPI00319992	72	100,0%	16	18	29	32,8%
x	x	x	Hspa8 Heat shock cognate 71 kDa protein	IPI00323357	71	100,0%	15	21	28	28,0%
x	x	x	Hspd1 60 kDa heat shock protein, mitochondrial precursor	IPI00308885	61	100,0%	9	10	14	25,7%
x	x	x	Hyou1 Activated spleen cDNA, RIKEN full-length enriched library, clone:F830010A06 product:hypoxia up-regulated 1	IPI00123342	111	88,0%	1	1	1	1,6%
x	x	x	Ifitm2 Ifitm2 protein	IPI00114948	16	88,0%	1	1	2	5,6%
x	x	x	Ifitm3 10 day old male pancreas cDNA, RIKEN full-length enriched library, clone:1810061A10 product:INTERFERON-INDUCIBLE PROTEIN homolog	IPI00133243	15	100,0%	3	7	14	27,0%
x	x	x	Krt1 Keratin, type II cytoskeletal 1	IPI00625729	66	99,8%	2	2	3	1,9%
x	x	x	Krt2 keratin complex 2, basic, gene 17	IPI00622240	71	88,0%	1	1	1	2,0%
x	x	x	Krt28 similar to Keratin, type I cytoskeletal 10	IPI00750213	107	100,0%	3	3	5	3,4%
x	x	x	Krt73 Keratin 73	IPI00347110	59	88,0%	1	1	1	2,2%
x	x	x	Lamp1 Adult male lung cDNA, RIKEN full-length enriched library, clone:1200007I01 product:lysosomal membrane glycoprotein 1	IPI00469218	44	99,9%	2	3	5	5,7%
x	x	x	Lamp2 Isoform LAMP-2A of Lysosome-associated membrane glycoprotein 2 precursor	IPI00134549	46	88,0%	1	1	1	1,9%
x	x	x	Laptm4a lysosomal-associated protein transmembrane 4A	IPI00122648	35	88,0%	1	1	2	4,2%
x	x	x	Lcp1 Plastin-2	IPI00118892	70	100,0%	14	16	21	33,2%
x	x	x	Ldha L-lactate dehydrogenase A chain	IPI00319994	36	100,0%	8	8	11	20,5%
x	x	x	Lgals3 Galectin-3	IPI00131259	27	88,0%	1	1	1	4,2%
x	x	x	Lgals3bp Mama protein	IPI00119809	64	88,0%	1	1	1	2,3%
x	x	x	Lgmn Legumain precursor	IPI00130627	49	100,0%	3	5	7	8,5%
x	x	x	Lipa Lysosomal acid lipase/cholesteryl ester hydrolase precursor	IPI00129265	46	99,8%	2	2	5	5,3%
x	x	x	LOC432548 similar to 40S ribosomal protein SA	IPI00111272	33	99,8%	2	2	3	10,5%
x	x	x	LOC629750;LOC639383 similar to ubiquitin A-52 residue ribosomal protein fusion product 1	IPI00108590	15	100,0%	3	5	10	28,4%
x	x	x	LOC633858;LOC626683 similar to 60S ribosomal protein L7a	IPI00122931	30	100,0%	3	3	4	12,4%
x	x	x	LOC672854;LOC668706 similar to 60S ribosomal protein L12	IPI00338838	18	100,0%	3	4	5	24,9%
x	x	x	LOC672898 similar to 60S ribosomal protein L18	IPI00465823	34	100,0%	3	3	3	11,7%
x	x	x	Lyzs Osteoclast-like cell cDNA, RIKEN full-length enriched library, clone:I420013M05 product:lysozyme, full insert sequence	IPI00107952	18	100,0%	3	5	8	28,8%
x	x	x	Man2b1 Lysosomal alpha-mannosidase precursor	IPI00381303	115	88,0%	1	1	2	1,1%
x	x	x	Mapbpip Mitogen-activated protein-binding protein-interacting protein	IPI00119807	13	88,0%	1	1	1	8,0%
x	x	x	Mela Envelope protein	IPI00406960	74	88,0%	1	1	1	2,7%
x	x	x	Mon2 MKIAA1040 protein (Fragment)	IPI00330176	189	88,0%	1	1	2	0,9%
x	x	x	Mpeg1 Mpeg1 protein	IPI00126418	78	100,0%	9	11	17	17,8%

x	x	x	Msn Moesin	IPI00110588	68	99,9%	2	2	2	7,5%
x	x	x	Myh9 Myosin-9	IPI00123181	226	100,0%	3	3	3	2,5%
x	x	x	Naga Alpha-N-acetylgalactosaminidase precursor	IPI00315593	47	100,0%	4	5	8	11,8%
x	x	x	Naglu Naglu	IPI00314726	83	88,0%	1	1	2	2,3%
x	x	x	Napa Alpha-soluble NSF attachment protein	IPI00118930	33	100,0%	3	3	3	13,2%
x	x	x	Ncl Nucleolin	IPI00317794	77	100,0%	10	10	21	16,4%
x	x	x	Nkx2-9 Homeobox protein Nkx-2.8	IPI00119496	26	88,0%	1	1	1	7,2%
x	x	x	Nme2 Nucleoside diphosphate kinase B	IPI00127417	17	100,0%	3	4	5	25,0%
x	x	x	Npc1 Niemann-Pick C1 protein precursor	IPI00132600	143	88,0%	1	1	1	0,9%
x	x	x	Npm1 Nucleophosmin	IPI00127415	33	100,0%	3	6	7	14,7%
x	x	x	Nsf 13 days embryo lung cDNA, RIKEN full-length enriched library, clone:D430035B05 product:N-ethylmaleimide sensitive fusion protein, full insert sequence	IPI00311934	83	100,0%	7	7	11	11,6%
x	x	x	Osbpl1a RCB-0545 OHTA cDNA, RIKEN full-length enriched library, clone:G430090F17 product:similar to OSBP-RELATED PROTEIN 1	IPI00404881	44	88,0%	1	1	1	3,8%
x	x	x	P4hb 17 days embryo kidney cDNA, RIKEN full-length enriched library, clone:I920160L24 product:prolyl 4-hydroxylase, beta polypeptide	IPI00122815	57	100,0%	4	4	4	8,6%
x	x	x	Pabpc1 Polyadenylate-binding protein 1	IPI00124287	71	99,8%	2	2	2	3,6%
x	x	x	Pcbp2 Isoform 1 of Poly(rC)-binding protein 2	IPI00127707	38	99,9%	2	2	2	6,9%
x	x	x	Pdia3 protein disulfide isomerase associated 3	IPI00230108	57	100,0%	4	4	4	8,7%
x	x	x	Pdia6 CRL-1722 L5178Y-R cDNA, RIKEN full-length enriched library, clone:I730077L17 product:thioredoxin domain containing 7	IPI00222496	49	100,0%	3	3	3	10,3%
x	x	x	Pfn1 Profilin-1	IPI00224740	15	100,0%	5	7	13	38,6%
x	x	x	Pgk1;EG433594;EG668435 phosphoglycerate kinase 1	IPI00230002	45	100,0%	4	4	6	13,4%
x	x	x	Pkm2 Pyruvate kinase isozyme M2	IPI00407130	58	100,0%	24	27	43	55,5%
x	x	x	Pld3 Phospholipase D3	IPI00130624	54	88,0%	1	1	2	2,5%
x	x	x	Pld4 Isoform 1 of Phospholipase D4	IPI00221418	56	100,0%	4	4	5	9,5%
x	x	x	Pls3 13 days embryo liver cDNA, RIKEN full-length enriched library, clone:I920006B08 product:plastin 3 (T-isoform)	IPI00115528	71	100,0%	3	4	6	6,5%
x	x	x	Ppt1 Palmitoyl-protein thioesterase	IPI00331318	35	100,0%	4	5	8	20,9%
x	x	x	Prcp Lysosomal Pro-X carboxypeptidase precursor	IPI00132020	55	88,0%	1	1	1	2,9%
x	x	x	Prdx1 Peroxiredoxin-1	IPI00121788	22	100,0%	4	4	6	22,6%
x	x	x	Prss1 Trypsinogen 16	IPI00130391	26	88,0%	1	1	1	8,1%
x	x	x	Psmb6 Proteasome subunit beta type 6 precursor	IPI00119239	25	99,5%	1	1	1	4,6%
x	x	x	Rab1 Ras-related protein Rab-1A	IPI00114560	23	99,8%	2	2	4	13,2%
x	x	x	Rab10 Ras-related protein Rab-10	IPI00130118	23	88,0%	1	1	3	5,5%
x	x	x	Rab14 Ras-related protein Rab-14	IPI00126042	24	88,0%	1	1	2	7,0%
x	x	x	Rab2 Ras-related protein Rab-2A	IPI00137227	24	99,8%	2	2	2	11,3%
x	x	x	Rab21 Ras-related protein Rab-21	IPI00337980	24	88,0%	1	1	1	5,0%
x	x	x	Rab22a Ras-related protein Rab-22A	IPI00116729	22	88,0%	1	1	2	5,7%
x	x	x	Rab33b 16 days embryo head cDNA, RIKEN full-length enriched library, clone:C130023M09 product:RAB33B, member of RAS oncogene family, full insert sequence	IPI00136271	30	99,8%	2	2	3	4,9%
x	x	x	Rab5b;LOC640369;LOC433464 Rab5B	IPI00116563	25	99,8%	2	2	4	9,6%
x	x	x	Rab5c Ras-related protein Rab-5C	IPI00224518	23	100,0%	3	4	7	18,5%
x	x	x	Rab7 Ras-related protein Rab-7	IPI00408892	23	100,0%	7	9	11	44,9%
x	x	x	Rac1 Mammary gland RCB-0527 Jyg-MC(B) cDNA, RIKEN full-length enriched library, clone:G930005L08 product:RAS-related C3 botulinum substrate 1, full insert sequence	IPI00127408	23	100,0%	4	4	5	18,5%
x	x	x	Rac2 Ras-related C3 botulinum toxin substrate 2 precursor	IPI00137618	21	100,0%	3	4	4	12,5%
x	x	x	Ralb Ras-related protein Ral-B precursor	IPI00121110	23	88,0%	1	1	1	5,3%
x	x	x	Rap1a Ras-related protein Rap-1A precursor	IPI00138406	21	99,9%	2	2	2	14,1%
x	x	x	Rhoa Transforming protein RhoA precursor	IPI00315100	22	88,0%	1	1	1	6,2%

x	x	x	Rpl13 60S ribosomal protein L13	IPI00224505	24	88,0%	1	1	1	6,2%
x	x	x	Rpl18 60S ribosomal protein L18	IPI00555113	22	88,0%	1	1	2	5,9%
x	x	x	Rpl22 60S ribosomal protein L22	IPI00222546	15	99,8%	2	2	4	18,8%
x	x	x	Rpl23 60S ribosomal protein L23	IPI00139780	15	98,3%	1	2	2	14,3%
x	x	x	Rpl24;LOC675789;EG668829 similar to ribosomal protein L24	IPI00134202	12	88,0%	1	1	1	12,5%
x	x	x	Rpl35 11 days embryo whole body cDNA, RIKEN full-length enriched library, clone:2700038I05 product:ribosomal protein L35, full insert sequence	IPI00263879	15	88,0%	1	1	1	10,6%
x	x	x	Rpl4 60S ribosomal protein L4	IPI00111412	47	100,0%	8	10	12	22,7%
x	x	x	Rpl6 60S ribosomal protein L6	IPI00313222	33	99,8%	2	3	6	9,5%
x	x	x	Rpl8 60S ribosomal protein L8	IPI00137787	28	97,6%	1	1	1	4,3%
x	x	x	Rps24 Isoform 2 of 40S ribosomal protein S24	IPI00402981	15	99,8%	2	2	2	20,8%
x	x	x	Rps28 40S ribosomal protein S28	IPI00137736	8	99,8%	2	2	4	30,4%
x	x	x	Rps3a 40S ribosomal protein S3a	IPI00331345	30	100,0%	5	6	7	22,7%
x	x	x	Rps9 40S ribosomal protein S9	IPI00420726	23	99,8%	2	2	2	8,8%
x	x	x	Scamp3 12 days embryo male wolffian duct includes surrounding region cDNA, RIKEN full-length enriched library, clone:6720482P16 product:secretory carrier membrane protein 3	IPI00132604	39	99,8%	2	2	2	10,9%
x	x	x	Scpep1 Serine carboxypeptidase 1	IPI00108371	51	100,0%	3	3	4	6,4%
x	x	x	Sdcbp Syntenin-1	IPI00117375	32	99,8%	2	2	3	7,0%
x	x	x	Serinc3 Serine incorporator 3	IPI00319078	53	99,3%	1	1	1	2,5%
x	x	x	Shprh SNF2 histone linker PHD RING helicase isoform a	IPI00380430	192	99,0%	1	1	1	1,4%
x	x	x	Slc12a9 CIP1	IPI00117986	96	88,0%	1	2	3	1,8%
x	x	x	Slc2a6 Mammary gland RCB-0526 Jyg-MC(A) cDNA, RIKEN full-length enriched library, clone:G830035N13 product:solute carrier family 2 (facilitated glucose transporter), member 6	IPI00225113	55	100,0%	3	4	5	9,6%
x	x	x	Slc37a2 10 days neonate skin cDNA, RIKEN full-length enriched library, clone:4732478E01 product:solute carrier family 37 (glycerol-3-phosphate transporter), member 1	IPI00404341	55	99,8%	2	3	5	7,7%
x	x	x	Slc3a2 CD98 heavy chain	IPI00114641	59	88,0%	1	1	1	3,8%
x	x	x	Snd1 Staphylococcal nuclease domain-containing protein 1	IPI00123129	102	99,8%	2	2	2	4,1%
x	x	x	Snx22;Ppib peptidylprolyl isomerase B	IPI00135686	24	100,0%	3	3	4	15,3%
x	x	x	Stard3 StAR-related lipid transfer protein 3	IPI00122397	50	99,8%	2	2	3	6,3%
x	x	x	Stard3nl MLN64 N-terminal domain homolog	IPI00317163	27	88,0%	1	1	1	4,3%
x	x	x	Stom Erythrocyte band 7 integral membrane protein	IPI00323748	31	100,0%	5	5	9	25,7%
x	x	x	Stx12 Syntaxin-12	IPI00111416	31	88,0%	1	1	1	6,2%
x	x	x	Stx7 Syntaxin-7	IPI00118217	30	100,0%	3	4	8	14,6%
x	x	x	Sybl1 Synaptobrevin-like protein	IPI00137647	25	88,0%	1	1	1	5,5%
x	x	x	Tcirg1 T-cell, immune regulator 1, ATPase, H+ transporting, lysosomal V0 protein A3	IPI00119320	93	100,0%	8	9	10	16,6%
x	x	x	Tkt Transketolase	IPI00137409	68	100,0%	4	5	6	9,6%
x	x	x	Tlr7 Toll-like receptor 7 precursor	IPI00122181	122	88,0%	1	1	1	1,1%
x	x	x	Tmem55b Transmembrane protein 55B	IPI00356633	30	88,0%	1	1	1	3,9%
x	x	x	Tmem63a Transmembrane protein 63A	IPI00130474	92	99,8%	2	2	3	2,9%
x	x	x	Tpi1 Triosephosphate isomerase	IPI00467833	27	100,0%	4	5	10	22,9%
x	x	x	Tpm1 Isoform 1 of Tropomyosin-1 alpha chain	IPI00123316	33	99,8%	2	2	3	3,9%
x	x	x	Try4;1810049H19Rik Pancreatic trypsin	IPI00128108	26	87,9%	1	1	4	8,1%
x	x	x	Tuba1a Tubulin alpha-1 chain	IPI00110753	50	100,0%	7	9	14	24,2%
x	x	x	Tuba1b Tubulin alpha-2 chain	IPI00117348	50	88,0%	1	1	1	2,9%
x	x	x	Tubb2b Tubulin beta-2B chain	IPI00109061	50	100,0%	11	12	21	32,6%
x	x	x	Tubb4 Tubulin beta-4 chain	IPI00109073	50	100,0%	3	4	6	11,9%
x	x	x	Tubb5 Tubulin beta-5 chain	IPI00117352	50	99,8%	2	3	7	6,1%
x	x	x	Unc93b1 Isoform 1 of UNC93 homolog B1	IPI00122625	67	100,0%	3	3	5	7,0%
x	x	x	Vamp8 Vesicle-associated membrane protein 8	IPI00453589	11	100,0%	3	4	5	32,7%
x	x	x	Vapa Vesicle-associated membrane protein-associated protein A	IPI00125267	28	99,8%	2	2	2	11,2%
x	x	x	Vcp Transitional endoplasmic reticulum ATPase	IPI00622235	89	100,0%	8	8	9	11,0%

x	x	x	Vdac1 Isoform PI-VDAC1 of Voltage-dependent anion-selective channel protein 1	IPI00122549	32	99,8%	2	2	2	8,5%
x	x	x	Vdac2 Voltage-dependent anion-selective channel protein 2	IPI00122547	32	100,0%	3	3	4	11,9%
x	x	x	Vim Vimentin	IPI00227299	54	100,0%	6	7	9	17,4%
x	x	x	Vti1b Vesicle transport through interaction with t-SNAREs homolog 1B	IPI00130115	27	88,0%	1	1	1	8,6%
x	x	x	Ywhaz 14-3-3 protein zeta/delta	IPI00116498	28	100,0%	4	4	4	20,0%
x	x		- Ig kappa chain V-V region HP 124E1	IPI00464385	12	88,0%	1	1	1	19,4%
x	x		4933429F08Rik Hypothetical protein	IPI00223868	77	88,0%	1	1	1	3,3%
x	x		Abca2 ATP-binding cassette sub-family A member 2	IPI00112616	270	88,0%	1	1	1	0,5%
x	x		Acot7 Isoform B of Cytosolic acyl coenzyme A thioester hydrolase	IPI00125939	43	88,0%	1	1	2	4,2%
x	x		Akr1c18 Isoform 1 of Aldo-keto reductase family 1 member C18	IPI00118068	37	88,0%	1	1	2	3,7%
x	x		Ank Progressive ankylosis protein	IPI00310247	54	98,7%	1	1	1	2,4%
x	x		Anxa1 Annexin A1	IPI00230395	39	100,0%	5	7	12	19,9%
x	x		Ap2m1 AP-2 complex subunit mu-1	IPI00116356	50	88,0%	1	1	2	3,7%
x	x		BC048644 Adult male testis cDNA, RIKEN full-length enriched library, clone:4930588P05 product:hypothetical Dictyostelium (slime mold) repeat/Cysteine-rich region profile/Insect antifreeze protein containing protein	IPI00652955	24	88,0%	1	1	1	8,3%
x	x		Capza1 F-actin capping protein subunit alpha-1	IPI00330063	33	88,0%	1	2	2	5,3%
x	x		Cct4 T-complex protein 1 subunit delta	IPI00116277	58	100,0%	3	4	4	7,4%
x	x		Cfl1 12 days embryo embryonic body between diaphragm region and neck cDNA, RIKEN full-length enriched library, clone:9430060J01 product:COFILIN 1, NON-MUSCLE homolog	IPI00407543	25	88,0%	1	1	3	4,8%
x	x		Dph4 Zinc finger, CSL-type containing 3	IPI00751149	13	88,0%	1	1	1	16,4%
x	x		EG243302 similar to 40S ribosomal protein S25	IPI00115992	14	88,0%	1	1	1	8,0%
x	x		EG243642 similar to 40S ribosomal protein S2	IPI00134607	34	100,0%	3	3	5	11,2%
x	x		EG432865 similar to ribosomal protein S12	IPI00116908	14	99,8%	2	2	2	12,9%
x	x		EG626175 similar to 40S ribosomal protein S26	IPI00261455	13	88,0%	1	1	2	13,0%
x	x		EG639162;LOC676847 similar to ribosomal protein S15a	IPI00113394	21	100,0%	3	3	3	16,5%
x	x		Ehd4 EH-domain containing 4-KJR (Fragment)	IPI00318671	62	88,0%	1	1	1	3,9%
x	x		Epb4.2 Erythrocyte membrane protein band 4.2	IPI00421166	77	88,0%	1	1	1	1,6%
x	x		Gars Glycyl-tRNA synthetase	IPI00112555	82	88,0%	1	1	1	1,8%
x	x		Gdi2 Isoform 1 of Rab GDP dissociation inhibitor beta	IPI00122565	51	100,0%	2	2	3	8,1%
x	x		Gpiap1 Cytoplasmic activation/proliferation-associated protein 1	IPI00757359	78	88,0%	1	1	1	1,7%
x	x		Gtdc1 2 days pregnant adult female ovary cDNA, RIKEN full-length enriched library, clone:E330008O22 product:solute carrier family 24 (sodium/potassium/calcium exchanger), member 2, full insert sequence	IPI00226094	53	88,0%	1	1	1	2,8%
x	x		Hnrpa2b1 heterogeneous nuclear ribonucleoprotein A2/B1 isoform 2	IPI00405058	32	100,0%	4	4	4	21,6%
x	x		Hnrph1 Heterogeneous nuclear ribonucleoprotein H	IPI00133916	49	88,0%	1	2	2	3,8%
x	x		Hspa4 Heat shock 70 kDa protein 4	IPI00331556	94	100,0%	8	8	9	12,7%
x	x		Iqgap1 Ras GTPase-activating-like protein IQGAP1	IPI00467447	189	88,0%	1	1	1	1,0%
x	x		Jmjd1c similar to jumonji domain containing 1C isoform 3	IPI00670418	287	88,0%	1	1	1	0,8%
x	x		Kars Kars protein	IPI00469103	71	88,0%	1	1	2	1,8%
x	x		Krt78 keratin Kb40	IPI00348328	90	88,0%	1	1	1	1,4%
x	x		Krt79 Keratin 79	IPI00124499	58	88,0%	1	1	2	2,3%
x	x		Lipa 2 days neonate thymus thymic cells cDNA, RIKEN full-length enriched library, clone:C920007B20 product:lysosomal acid lipase 1, full insert sequence	IPI00554860	45	88,0%	1	1	1	6,3%
x	x		LOC238943 similar to enolase 1, alpha non-neuron	IPI00342547	32	88,0%	1	1	1	3,7%

x	x		LOC631010 similar to MAP/microtubule affinity-regulating kinase 4	IPI00676232	83	97,7%	1	1	1	2,6%
x	x		LOC671641 similar to 40S ribosomal protein S12	IPI00120475	14	88,0%	1	1	1	7,9%
x	x		Lyst Isoform 1 of Lysosomal-trafficking regulator	IPI00399954	425	88,0%	1	1	1	0,6%
x	x		Map2k1ip1;EG545987 Mitogen-activated protein kinase kinase 1-interacting protein 1	IPI00133047	14	88,0%	1	1	3	8,9%
x	x		Mdn1 Midasin homolog	IPI00458039	630	88,0%	1	1	1	0,3%
x	x		Pdia4 protein disulfide isomerase associated 4	IPI00271951	72	98,8%	1	1	2	2,5%
x	x		Pgam1;EG667978;LOC669836;EG668045;LOC675179 Phosphoglycerate mutase 1	IPI00457898	29	100,0%	5	6	9	25,6%
x	x		Pgam2 Phosphoglycerate mutase 2	IPI00230706	29	88,0%	1	1	1	4,0%
x	x		Phf21a Isoform 1 of PHD finger protein 21A	IPI00453806	73	88,0%	1	1	1	4,1%
x	x		Pklr Pyruvate kinase isozymes R/L	IPI00133605	62	99,3%	1	1	3	1,9%
x	x		Prdx2 Peroxiredoxin-2	IPI00117910	22	88,0%	1	1	1	9,1%
x	x		Psma3 Proteasome subunit alpha type 3	IPI00331644	28	99,8%	2	2	3	8,2%
x	x		Rgs17 Adult male corpora quadrigemina cDNA, RIKEN full-length enriched library, clone:B230310H10 product:regulator of G-protein signaling 17, full insert sequence	IPI00137195	27	88,0%	1	1	1	7,8%
x	x		Rpl11 60S ribosomal protein L11	IPI00331461	20	88,0%	1	1	1	7,9%
x	x		Rpl13a 60S ribosomal protein L13a	IPI00223217	23	99,5%	1	1	1	3,9%
x	x		Rpl18a 60S ribosomal protein L18a	IPI00162790	21	88,0%	1	1	1	7,4%
x	x		Rpl3 60S ribosomal protein L3	IPI00321170	46	88,0%	1	1	2	4,0%
x	x		Rpl5 60S ribosomal protein L5	IPI00308706	34	100,0%	3	3	5	13,1%
x	x		Rpl9 60S ribosomal protein L9	IPI00122413	22	99,8%	2	2	2	7,8%
x	x		Rplp1 60S acidic ribosomal protein P1	IPI00113377	11	88,0%	1	2	3	14,0%
x	x		Rps10 40S ribosomal protein S10	IPI00112448	19	88,0%	1	1	1	5,5%
x	x		Rps13;EG625298;LOC633920 40S ribosomal protein S13	IPI00125901	17	88,0%	1	1	1	8,6%
x	x		Rps20 40S ribosomal protein S20	IPI00323819	13	88,0%	1	1	1	9,2%
x	x		Rps21 40S ribosomal protein S21	IPI00132950	9	88,0%	1	1	1	12,1%
x	x		Rps3 40S ribosomal protein S3	IPI00134599	27	100,0%	6	6	8	28,4%
x	x		Scamp2 Secretory carrier-associated membrane protein 2	IPI00319121	36	99,8%	2	2	2	9,7%
x	x		Serbp1 Isoform 1 of Plasminogen activator inhibitor 1 RNA-binding protein	IPI00471475	45	88,0%	1	2	2	3,9%
x	x		Slc38a1 12 days embryo whole body cDNA, RIKEN full-length enriched library, clone:E970021I18 product:solute carrier family 38, member 1, full insert sequence	IPI00459577	54	88,0%	1	1	1	4,3%
x	x		Slc44a2 Isoform 2 of Choline transporter-like protein 2	IPI00169896	80	99,8%	2	2	3	3,8%
x	x		Tcp1 T-complex protein 1 subunit alpha A	IPI00118678	60	100,0%	8	8	11	18,7%
x	x		Tmem79 Transmembrane protein 79	IPI00109411	43	88,0%	1	1	1	3,3%
x	x		Tpm3 15 days pregnant adult female placenta cDNA, RIKEN full-length enriched library, clone:I530023K22 product:tropomyosin 3, gamma, full insert sequence	IPI00230044	29	100,0%	2	3	3	6,1%
x	x		Wdr1 WD repeat protein 1	IPI00314748	66	88,0%	1	1	1	2,3%
x	x		Ybx1 Nuclease sensitive element-binding protein 1	IPI00120886	36	88,0%	1	1	1	4,7%
x	x		Ywhae 14-3-3 protein epsilon	IPI00118384	29	100,0%	3	3	4	16,5%
x	x		Zfp445 Zinc finger protein 445	IPI00336923	115	88,0%	1	1	1	1,4%
x		x	1700071K01Rik Adult male testis cDNA, RIKEN full-length enriched library, clone:1700071K01 product:Prohibitin (B-cell receptor associated protein 32) (BAP 32) homolog	IPI00126917	29	88,0%	1	1	1	3,7%
x		x	1810007P19Rik Organic solute carrier protein 1 isoform	IPI00222008	45	88,0%	1	1	1	3,3%
x		x	Ahcy Adenosylhomocysteinase	IPI00230440	48	88,0%	1	1	1	2,6%
x		x	Arhgdib Rho GDP-dissociation inhibitor 2	IPI00122568	23	100,0%	3	3	4	30,5%
x		x	Atp5b ATP synthase subunit beta, mitochondrial precursor	IPI00468481	56	100,0%	5	5	6	14,2%
x		x	Atp5o ATP synthase O subunit, mitochondrial precursor	IPI00118986	23	88,0%	1	1	1	5,2%

x	x	Atp6v1a Blastocyst blastocyst cDNA, RIKEN full-length enriched library, clone:I1C0017M12 product:ATPase, H+ transporting, V1 subunit A, isoform 1, full insert sequence	IPI00407692	68	88,0%	1	1	1	2,9%
x	x	Atp6v1d Vacuolar ATP synthase subunit D	IPI00118787	28	100,0%	3	3	3	19,8%
x	x	Atp6v1g1 Vacuolar ATP synthase subunit G 1	IPI00133163	14	99,8%	2	2	4	26,3%
x	x	AU022870 Uncharacterized protein C7orf28 homolog	IPI00224561	55	100,0%	2	2	2	5,2%
x	x	BC033915 Isoform 1 of Serine/threonine-protein kinase QSK	IPI00453673	146	88,0%	1	1	1	1,2%
x	x	Cct8 T-complex protein 1 subunit theta	IPI00469268	60	100,0%	4	4	5	8,4%
x	x	Cyb5r3 13 days embryo liver cDNA, RIKEN full-length enriched library, clone:2500002N19 product:NADH-CYTOCHROME B5 REDUCTASE (EC 1.6.2.2) homolog	IPI00110885	34	88,0%	1	1	1	4,0%
x	x	Ddx5 Probable ATP-dependent RNA helicase DDX5	IPI00420363	69	100,0%	4	4	4	7,3%
x	x	EG245391 similar to 60S ribosomal protein L17	IPI00108337	24	88,0%	1	1	2	4,8%
x	x	EG245516 similar to family with sequence similarity 48, member A isoform a	IPI00355970	57	88,0%	1	1	1	3,1%
x	x	EG382723 similar to ribosomal protein L10a	IPI00122598	24	88,0%	1	2	2	6,1%
x	x	Gfap Isoform 1 of Glial fibrillary acidic protein, astrocyte	IPI00117042	50	88,0%	1	1	3	2,6%
x	x	Hist1h1c Histone H1.2	IPI00223713	21	88,0%	1	1	1	5,2%
x	x	Hist1h4i;Hist1h4b;Hist4h4;Hist1h4h;Hist1h4d;Hist1h4k;Hist1h4m;Hist1h4c;Hist2h4;Hist1h4j;Hist1h4a;Hist1h4f;4930558J22Rik Hist2h4 protein (Fragment)	IPI00336741	12	88,0%	1	1	1	10,7%
x	x	Hnrpu Osteoclast-like cell cDNA, RIKEN full-length enriched library, clone:I420039N16 product:heterogeneous nuclear ribonucleoprotein U, full insert sequence	IPI00458583	88	100,0%	5	5	7	8,6%
x	x	Hsp90aa1 Heat shock protein HSP 90-alpha	IPI00330804	85	100,0%	6	6	7	11,9%
x	x	Hspa9 Stress-70 protein, mitochondrial precursor	IPI00133903	74	100,0%	3	3	5	6,0%
x	x	Igf2r Cation-independent mannose-6-phosphate receptor precursor	IPI00308971	274	88,0%	1	1	1	0,7%
x	x	Khdrbs2 Khdrbs2 protein (Fragment)	IPI00463153	28	88,0%	1	1	3	11,2%
x	x	Krt6b Keratin, type II cytoskeletal 6B	IPI00131366	60	88,0%	1	2	2	2,1%
x	x	Lipe lipase, hormone sensitive isoform 1	IPI00228826	88	88,0%	1	1	1	1,4%
x	x	Lmbrd1 Isoform 2 of LMBR1 domain-containing protein 1	IPI00352845	59	88,0%	1	1	1	3,5%
x	x	Lmln Adult male pituitary gland cDNA, RIKEN full-length enriched library, clone:5330415H22 product:LEISHMANOLYSIN-LIKE PEPTIDASE, VARIANT 2 (EC 3.4.24.36) homolog	IPI00223063	77	88,0%	1	1	1	2,5%
x	x	Lmod3 similar to leiomodin 3	IPI00672159	66	88,0%	1	1	2	4,0%
x	x	LOC675088;Rpl27;EG621100;LOC669376 60S ribosomal protein L27	IPI00122421	16	99,7%	1	1	1	6,6%
x	x	Mdh2 Malate dehydrogenase 2, NAD	IPI00331590	36	88,0%	1	1	1	3,6%
x	x	Mdh2 Malate dehydrogenase, mitochondrial precursor	IPI00323592	36	100,0%	5	5	7	19,2%
x	x	mt-Co2 Cytochrome c oxidase subunit 2	IPI00131176	26	88,0%	1	1	1	4,4%
x	x	Pa2g4 Proliferation-associated protein 2G4	IPI00119305	44	100,0%	4	4	4	13,5%
x	x	Pabpc2 poly A binding protein, cytoplasmic 2	IPI00120954	69	100,0%	3	3	3	5,6%
x	x	Pap 19 kDa protein	IPI00761692	19	88,0%	1	1	1	16,9%
x	x	Pgd 6-phosphogluconate dehydrogenase, decarboxylating	IPI00466919	53	100,0%	4	4	5	12,8%
x	x	Phb2;Grcc10 Prohibitin-2	IPI00321718	33	99,8%	2	2	2	10,4%
x	x	Ppp1ca Serine/threonine-protein phosphatase PP1-alpha catalytic subunit	IPI00130185	38	88,0%	1	1	1	3,0%
x	x	Ptprc Isoform 2 of Leukocyte common antigen precursor	IPI00126092	140	99,8%	2	2	2	1,7%
x	x	Rab8b Ras-related protein Rab-8B	IPI00411115	24	88,0%	1	1	1	6,8%
x	x	Rpl14 60S ribosomal protein L14	IPI00133185	24	100,0%	3	3	4	15,7%
x	x	Rpl30;LOC666899;LOC675333;LOC670014 60S ribosomal protein L30	IPI00222549	13	99,8%	2	2	2	27,0%

x		x	Rpl7 60S ribosomal protein L7	IPI00311236	31	100,0%	2	2	3	9,3%
x		x	Rps11 Adult male cerebellum cDNA, RIKEN full-length enriched library, clone:1500004H08 product:ribosomal protein S11	IPI00117569	19	100,0%	3	3	5	23,5%
x		x	Rps23 11 days embryo whole body cDNA, RIKEN full-length enriched library, clone:2700086E01 product:ribosomal protein S23, full insert sequence	IPI00131357	16	88,0%	1	1	1	7,6%
x		x	Rps4x 40S ribosomal protein S4, X isoform	IPI00331092	30	100,0%	5	6	9	18,3%
x		x	Sfrs3 Isoform Long of Splicing factor, arginine/serine-rich 3	IPI00129323	19	98,6%	1	1	2	8,5%
x		x	Slc25a3 Phosphate carrier protein, mitochondrial precursor	IPI00124771	40	99,7%	1	1	1	3,4%
x		x	Slc25a4 ADP/ATP translocase 1	IPI00115564	33	88,0%	1	1	1	3,4%
x		x	Slc2a1 Solute carrier family 2, facilitated glucose transporter member 1	IPI00308691	54	88,0%	1	1	2	2,0%
x		x	Slco2b1 Solute carrier organic anion transporter family member 2B1	IPI00465991	75	88,0%	1	1	2	2,2%
x		x	Snrpd1 Small nuclear ribonucleoprotein Sm D1	IPI00322749	13	88,0%	1	1	1	10,9%
x		x	Tln1 Talin-1	IPI00465786	270	100,0%	3	3	4	1,6%
x		x	Tmem55a Transmembrane protein 55A	IPI00113239	28	88,0%	1	1	1	4,3%
x		x	Tubb2c Tubulin beta-2C chain	IPI00169463	50	88,0%	1	1	2	2,7%
x		x	Ube2n Ubiquitin-conjugating enzyme E2 N	IPI00165854	17	98,4%	1	1	1	7,2%
	x	x	- 10 kDa protein	IPI00111076	10	87,9%	1	1	1	11,0%
	x	x	- 18 kDa protein	IPI00277450	18	99,7%	1	1	3	5,5%
	x	x	1300007C21Rik Gag protein	IPI00224370	60	99,8%	2	2	5	6,3%
	x	x	1300012G16Rik NOD-derived CD11c +ve dendritic cells cDNA, RIKEN full-length enriched library, clone:F630111F13 product:RDCR-0918-3 protein homolog	IPI00165730	66	100,0%	4	4	6	9,6%
	x	x	2010106G01Rik Signal peptide peptidase-like 2A	IPI00121776	58	99,8%	2	2	2	6,1%
	x	x	Acaca Acetyl-CoA carboxylase 1	IPI00474783	265	87,9%	1	1	1	0,7%
	x	x	Acp2 Lysosomal acid phosphatase precursor	IPI00154056	48	99,8%	2	2	2	4,3%
	x	x	Anxa7 Adult male medulla oblongata cDNA, RIKEN full-length enriched library, clone:6330545A10 product:annexin A7	IPI00461322	44	87,9%	1	1	2	2,4%
	x	x	Anxa7 Annexin A7	IPI00114017	50	100,0%	2	2	2	5,2%
	x	x	Ap2b1 Isoform 1 of AP-2 complex subunit beta-1	IPI00119689	105	97,9%	1	1	1	1,4%
	x	x	Arl8a ADP-ribosylation factor-like protein 8A	IPI00124610	21	100,0%	4	4	7	24,2%
	x	x	Arpc2 Actin-related protein 2/3 complex subunit 2	IPI00661414	34	99,5%	1	1	2	4,7%
	x	x	Arpc3 Actin-related protein 2/3 complex subunit 3	IPI00124829	21	87,9%	1	2	3	7,3%
	x	x	Arpm1 Actin-related protein M1 homolog	IPI00226663	40	87,9%	1	1	2	6,0%
	x	x	Arsb Isoform 1 of Arylsulfatase B precursor	IPI00652358	60	100,0%	3	4	6	8,4%
	x	x	Atp2a1 Sarcoplasmic/endoplasmic reticulum calcium ATPase 1	IPI00311654	109	99,8%	2	2	2	2,8%
	x	x	Atp2a3 ATPase, Ca++ transporting, ubiquitous	IPI00311200	114	87,9%	1	1	1	1,4%
	x	x	Bard1 BRCA1-associated RING domain protein 1	IPI00118250	84	87,9%	1	1	2	2,4%
	x	x	BC006779 MKIAA1769 protein	IPI00464131	182	87,9%	1	1	1	1,1%
	x	x	BC031853 BC031853 protein	IPI00395204	50	99,2%	1	1	1	1,9%
	x	x	Bcap31 B-cell receptor-associated protein 31	IPI00230422	28	87,9%	1	1	1	6,9%
	x	x	Calm2;Calm3;Calm1 12 days pregnant adult female placenta cDNA, RIKEN full-length enriched library, clone:I530005B05 product:calmodulin 1, full insert sequence	IPI00467841	22	99,8%	2	2	2	19,8%
	x	x	Canx Calnexin precursor	IPI00119618	67	100,0%	5	5	9	11,7%
	x	x	Cdc42 Isoform 2 of Cell division control protein 42 homolog precursor	IPI00113849	21	99,9%	2	2	2	15,7%
	x	x	Cpne1 Copine-1	IPI00224075	59	100,0%	5	5	7	10,5%
	x	x	Creg1 Protein CREG1 precursor	IPI00133103	24	100,0%	2	2	4	10,5%
	x	x	Csf1r Macrophage colony-stimulating factor 1 receptor precursor	IPI00108003	109	99,8%	2	2	2	2,3%

x	x	Ctbs Isoform 2 of Di-N-acetylchitobiase precursor	IPI00110868	35	87,9%	1	1	2	4,8%
x	x	Ctsl Cathepsin L precursor	IPI00128154	38	100,0%	7	9	9	38,9%
x	x	Cyb5 Cytochrome b5	IPI00230113	15	87,9%	1	1	1	9,0%
x	x	Cyb5b Cytochrome b5 type B precursor	IPI00315794	16	87,9%	1	1	1	8,9%
x	x	Dnajc11 Isoform 1 of DnaJ homolog subfamily C member 11	IPI00226466	63	87,9%	1	1	1	1,4%
x	x	Dpp7 Dipeptidyl-peptidase 2 precursor	IPI00331550	56	100,0%	3	3	6	5,7%
x	x	Dsc3 Isoform 3A of Desmocollin-3 precursor	IPI00113853	101	87,9%	1	1	1	2,5%
x	x	Eea1 Early endosome antigen 1	IPI00453776	161	100,0%	7	7	8	5,9%
x	x	EG667952;LOC671953 similar to Myosin light polypeptide 6	IPI00264053	22	99,4%	1	1	2	4,0%
x	x	Fcgr2b Fc receptor, IgG, low affinity IIb isoform 1	IPI00129485	38	99,8%	2	2	2	7,7%
x	x	Fth1 Ferritin heavy chain	IPI00230145	21	99,7%	1	1	1	8,2%
x	x	Ftl1 Ferritin light chain 1	IPI00315299	21	99,8%	2	2	2	11,5%
x	x	Gla Mammary gland RCB-0526 Jyg-MC	IPI00123814	48	99,8%	2	2	4	5,2%
x	x	Gng2 Guanine nucleotide-binding protein G(I)/G(S)/G(O) gamma-2 subunit precursor	IPI00230194	8	87,9%	1	1	1	22,5%
x	x	Gpsm3 Hypothetical protein NG1	IPI00130761	13	87,9%	1	1	1	16,1%
x	x	Gria4 Glutamate receptor 4 precursor	IPI00131471	101	87,9%	1	1	1	2,2%
x	x	Gusb Beta-glucuronidase precursor	IPI00309230	74	100,0%	3	4	5	5,4%
x	x	Hbxip hepatitis B virus x interacting protein	IPI00132747	15	87,9%	1	1	4	13,8%
x	x	Hsd17b12 Isoform 1 of Estradiol 17-beta-dehydrogenase 12	IPI00119219	35	99,8%	2	2	3	5,1%
x	x	Hspe1-rs1;EG628438;LOC636088 CPN10-like protein	IPI00120045	11	99,8%	2	2	2	25,5%
x	x	Ifi30 interferon gamma inducible protein 30	IPI00113659	28	100,0%	3	3	7	19,4%
x	x	Ift172 intraflagellar transport 172 protein	IPI00762129	198	87,9%	1	1	1	0,8%
x	x	Itga4 Integrin alpha-4 precursor	IPI00121334	116	99,8%	2	2	2	2,9%
x	x	Lamp2 lysosomal membrane glycoprotein 2 isoform 2	IPI00310109	46	87,9%	1	1	2	2,2%
x	x	Lgals1 Galectin-1	IPI00229517	15	87,9%	1	1	1	11,1%
x	x	Lgals3 Beta-galactoside-binding lectin (Fragment)	IPI00120051	16	99,9%	1	1	2	10,8%
x	x	Lgals3bp Lectin, galactoside-binding, soluble, 3 binding protein	IPI00648096	15	87,9%	1	1	2	10,8%
x	x	Lgals9 Isoform Long of Galectin-9	IPI00114396	40	99,8%	2	2	2	7,4%
x	x	Lnpep Leucyl-cystinyl aminopeptidase	IPI00223987	117	100,0%	2	2	3	2,3%
x	x	Lypla3 1-O-acylceramide synthase precursor	IPI00124428	47	100,0%	5	5	8	14,1%
x	x	Man2a2 N-glycan processing alpha-mannosidase IIx	IPI00224294	131	87,9%	1	1	1	1,7%
x	x	Man2b2 Epididymis-specific alpha-mannosidase precursor	IPI00117842	116	87,9%	1	1	1	1,1%
x	x	Manba Beta-mannosidase precursor	IPI00118011	101	87,9%	1	1	1	1,0%
x	x	Mbc2 Isoform 1 of Protein FAM62A	IPI00128450	122	100,0%	4	4	5	5,4%
x	x	Mela Gag-Pol polyprotein	IPI00108206	194	100,0%	4	4	6	1,9%
x	x	Msr1 Isoform II of Macrophage scavenger receptor types I and II	IPI00124283	39	99,3%	1	1	1	3,1%
x	x	Myadm Myeloid-associated differentiation marker	IPI00132938	35	87,9%	1	1	1	4,7%
x	x	Myl6b Myosin light polypeptide 6B	IPI00261638	23	87,9%	1	1	1	6,3%
x	x	Nbeal2 mKIAA0540 protein	IPI00421222	305	87,9%	1	1	1	0,9%
x	x	Npc2 Epididymal secretory protein E1 precursor	IPI00129186	16	99,8%	2	2	3	18,8%
x	x	Nptn Isoform 1 of Neuroplastin precursor	IPI00123831	31	87,9%	1	1	1	3,6%
x	x	Ppia Peptidyl-prolyl cis-trans isomerase A	IPI00554989	18	99,8%	2	2	3	13,4%
x	x	Psen1 Isoform 1 of Presenilin-1	IPI00117124	53	99,7%	1	1	1	4,3%
x	x	Psen2 Isoform 1 of Presenilin-2	IPI00357545	50	87,9%	1	1	1	4,5%
x	x	Ptgs1 Prostaglandin G/H synthase 1 precursor	IPI00128389	69	100,0%	3	3	3	7,3%
x	x	Rab11b Ras-related protein Rab-11B	IPI00135869	24	87,9%	1	1	1	5,1%
x	x	Rab27a Ras-related protein Rab-27A	IPI00112374	25	87,9%	1	1	1	5,0%
x	x	Rab31 Osteoclast-like cell cDNA, RIKEN full-length enriched library, clone:I420001G12 product:Similar to RAB31, member RAS oncogene family, full insert sequence	IPI00222632	21	100,0%	3	4	5	23,1%

	x	x	Rap1b Ras-related protein Rap-1b precursor	IPI00407954	21	99,8%	2	2	3	15,2%
	x	x	Rap2b Ras-related protein Rap-2b precursor	IPI00138716	20	99,7%	1	1	1	6,0%
	x	x	Rhog Rho-related GTP-binding protein RhoG precursor	IPI00116558	21	87,9%	1	1	1	6,8%
	x	x	Rpn1 Dolichyl-diphosphooligosaccharide--protein glycosyltransferase 67 kDa subunit precursor	IPI00309035	69	99,6%	1	1	1	2,8%
	x	x	Rpn2 Dolichyl-diphosphooligosaccharide--protein glycosyltransferase 63 kDa subunit precursor	IPI00475154	69	99,8%	2	2	2	6,3%
	x	x	Rtn4 Isoform 2 of Reticulon-4	IPI00270767	127	87,9%	1	1	3	1,1%
	x	x	Scarb2 Lysosome membrane protein 2	IPI00127447	54	100,0%	4	4	5	8,4%
	x	x	Sirpa Isoform 1 of Tyrosine-protein phosphatase non-receptor type substrate 1 precursor	IPI00129158	56	98,3%	1	1	1	3,3%
	x	x	Slc25a5 ADP/ATP translocase 2	IPI00127841	33	87,9%	1	1	1	3,7%
	x	x	Sqstm1 Isoform 1 of Sequestosome-1	IPI00133374	48	99,9%	2	2	2	8,1%
	x	x	Ssr4 10 day old male pancreas cDNA, RIKEN full-length enriched library, clone:1810061C01 product:signal sequence receptor, delta	IPI00122346	19	87,9%	1	1	1	7,5%
	x	x	Ssx2ip Afadin- and alpha-actinin-binding protein	IPI00121490	71	87,9%	1	1	1	3,4%
	x	x	Tagln2 MKIAA0120 protein (Fragment)	IPI00117007	24	99,9%	2	2	2	12,0%
	x	x	Tfrc Transferrin receptor protein 1	IPI00124700	86	100,0%	3	3	5	4,6%
	x	x	Tlr13 Toll-like receptor 13 precursor	IPI00342691	114	99,0%	1	1	1	1,0%
	x	x	Tm9sf2 Transmembrane 9 superfamily protein member 2 precursor	IPI00115787	75	87,9%	1	1	1	2,9%
	x	x	Tmed10 Isoform 1 of Transmembrane emp24 domain-containing protein 10 precursor	IPI00466570	25	87,9%	1	1	1	4,1%
	x	x	Tmem106a Transmembrane protein 106A	IPI00121229	29	87,9%	1	1	2	6,9%
	x	x	Tpp1 Tripeptidyl-peptidase 1 precursor	IPI00130661	61	100,0%	3	3	5	6,2%
	x	x	Uba52;LOC669193;LOC676687;LOC666586 Uba52 protein	IPI00138892	15	98,6%	1	1	3	7,0%
	x	x	Utrn utrophin	IPI00353420	393	87,9%	1	1	1	0,8%
	x	x	Vamp4 Vesicle-associated membrane protein 4	IPI00118372	16	87,9%	1	1	2	13,5%
	x	x	Vapb Vesicle-associated membrane protein-associated protein B	IPI00135655	27	99,7%	1	1	2	5,8%
	x	x	Vps11 Vacuolar protein sorting-associated protein 11 homolog	IPI00229777	108	99,8%	2	2	2	3,9%
	x	x	Vps13c vacuolar protein sorting 13C isoform 7	IPI00473340	415	87,9%	1	1	1	0,4%
	x	x	Vps35 Vacuolar protein sorting-associated protein 35	IPI00111181	92	87,9%	1	1	1	1,4%
x			- 10 kDa protein	IPI00272545	10	88,0%	1	1	1	9,8%
x			- 12 kDa protein	IPI00123164	12	88,0%	1	1	1	8,5%
x			- 12 kDa protein	IPI00761871	12	88,0%	1	1	1	20,4%
x			- 15 kDa protein	IPI00463248	15	88,0%	1	1	1	7,6%
x			- 18 kDa protein	IPI00116718	18	98,1%	1	1	1	9,7%
x			- 18 kDa protein	IPI00268802	18	99,8%	2	2	2	15,8%
x			- 2 cells egg cDNA, RIKEN full-length enriched library, clone:B020003N11 product:hypothetical protein, full insert sequence	IPI00652026	16	88,0%	1	1	1	19,9%
x			- 36 kDa protein	IPI00753274	36	88,0%	1	1	1	6,4%
x			- 37 kDa protein	IPI00137389	37	88,0%	1	1	1	5,5%
x			- 55 kDa protein	IPI00761249	55	88,0%	1	1	1	2,9%
x			- 70 kDa protein	IPI00381231	70	88,0%	1	1	1	5,2%
x			- Desmoglein4	IPI00828745	122	88,0%	1	1	1	1,0%
x			- Hypothetical protein (Fragment)	IPI00808130	46	88,0%	1	1	1	5,0%
x			- M.musculus endogenous provirus env (Frag.)	IPI00463556	35	99,8%	2	2	2	10,1%
x			- Novel protein	IPI00648985	49	88,0%	1	1	1	3,0%
x			- PKA phosphorylated calcium and CABYR-binding protein	IPI00828958	115	88,0%	1	1	1	2,2%
x			- Pol protein	IPI00380444	90	88,0%	1	1	1	2,2%
x			- Rims1 protein	IPI00755092	25	88,0%	1	1	1	10,6%
x			0910001A06Rik Protein FAM49B	IPI00122015	37	88,0%	1	1	1	5,6%
x			1700016K13Rik similar to septin 10 isoform 1	IPI00122828 IPI00331497	48	88,0%	1	1	1	2,2%

x	1700120B06Rik Adult male testis cDNA, RIKEN full-length enriched library, clone:1700120B06 product:hypothetical protein	IPI00463280	33	88,0%	1	1	3	5,5%
x	2210010A19Rik 2 days pregnant adult female ovary cDNA, RIKEN full-length enriched library, clone:E330016A09 product:hypothetical Pyridoxal-dependent decarboxylase family containing protein, full insert sequence	IPI00336503	87	88,0%	1	1	1	2,7%
x	2410017P07Rik Isoform 2 of Uncharacterized protein C6orf182 homolog	IPI00112580	41	88,0%	1	1	1	4,8%
x	2410104I19Rik 16 days embryo heart cDNA, RIKEN full-length enriched library, clone:I920055G02 product:RNA-binding protein SiahBP homolog	IPI00127174	59	88,0%	1	1	1	4,0%
x	2610019P18Rik 10 days embryo whole body cDNA, RIKEN full-length enriched library, clone:2610019P18 product:hypothetical protein	IPI00224957	29	88,0%	1	1	1	6,0%
x	2610301F02Rik Adult male aorta and vein cDNA, RIKEN full-length enriched library, clone:A530084A08 product:RIKEN cDNA 2610301F02	IPI00222928	84	88,0%	1	1	1	2,8%
x	2900073G15Rik myosin light chain, regulatory B-like	IPI00109044	20	99,8%	2	2	2	12,2%
x	4930471M23Rik Uncharacterized protein C2orf18 homolog precursor	IPI00165834	41	88,0%	1	1	1	3,2%
x	4930556P03Rik RIKEN cDNA 4930556P03 gene	IPI00137809	32	88,0%	1	1	1	3,5%
x	4930570C03Rik 0 day neonate thymus cDNA, RIKEN full-length enriched library, clone:A430032I09 product:hypothetical protein	IPI00111694	16	88,0%	1	1	2	8,2%
x	6030445D17Rik 13 days embryo male testis cDNA, RIKEN full-length enriched library, clone:6030445D17 product:hypothetical protein	IPI00228686	16	88,0%	1	1	1	11,5%
x	9030411M15Rik;LOC629416 similar to CG8486-PA, isoform A	IPI00670041	74	88,0%	1	1	1	1,7%
x	9130401M01Rik Uncharacterized protein C8orf76 homolog	IPI00135489	42	88,0%	1	1	1	5,1%
x	9230020A06Rik hypothetical protein LOC619299	IPI00652070	22	88,0%	1	1	1	11,9%
x	9530053A07Rik Adult male urinary bladder cDNA, RIKEN full-length enriched library, clone:9530053A07 product:hypothetical von Willebrand factor type D domain/EGF-like domain/Trypsin Inhibitor-like cysteine rich domain containing protein	IPI00227522	53	88,0%	1	1	1	4,4%
x	9930023K05Rik 9930023K05Rik protein	IPI00457712	11	88,0%	1	1	1	14,4%
x	A230046K03Rik hypothetical protein LOC319277	IPI00130714	146	88,0%	1	1	1	0,9%
x	Abcg3 ATP-binding cassette sub-family G member 3	IPI00120454	74	88,0%	1	1	1	1,2%
x	Aco2 Aconitate hydratase, mitochondrial precursor	IPI00116074	85	100,0%	3	3	3	5,4%
x	Acsl6 acyl-CoA synthetase long-chain family member 6 isoform 1	IPI00123390	81	88,0%	1	1	1	1,7%
x	Adss Adenylosuccinate synthetase isozyme 2	IPI00135969	50	88,0%	1	1	1	2,4%
x	AI481877 Novel protein	IPI00357650	168	88,0%	1	1	1	1,8%
x	Aldh2 Aldehyde dehydrogenase, mitochondrial precursor	IPI00111218	57	99,4%	1	1	1	3,3%
x	Aldoc Fructose-bisphosphate aldolase C	IPI00119458	39	88,0%	1	1	1	4,4%
x	Alox5ap Arachidonate 5-lipoxygenase-activating protein	IPI00129296	18	88,0%	1	1	1	8,1%
x	Amfr Isoform 1 of Autocrine motility factor receptor	IPI00319880	73	88,0%	1	1	1	2,3%
x	Ankrd10 Ankyrin repeat domain-containing protein 10	IPI00117242	44	88,0%	1	1	1	6,0%
x	Anln Actin-binding protein anillin	IPI00172197	123	88,0%	1	1	1	1,4%
x	Anxa11 Annexin A11	IPI00124264	54	100,0%	4	4	5	11,1%
x	Aof2 Lysine-specific histone demethylase 1	IPI00453837	93	88,0%	1	1	1	2,8%
x	Ap1s3 AP-1 complex subunit sigma-3	IPI00380276	18	88,0%	1	1	1	11,7%

x	Ap3b1 AP-3 complex subunit beta-1	IPI00130444	123	88,0%	1	1	1	1,5%
x	Ap4b1 Ap4b1 protein	IPI00468690	83	88,0%	1	1	1	4,2%
x	Apob Apolipoprotein	IPI00350772	418	88,0%	1	1	3	0,2%
x	Appbp2 Amyloid protein-binding protein 2	IPI00119142	67	88,0%	1	1	1	2,7%
x	Aprt Adenine phosphoribosyltransferase	IPI00128491	20	99,8%	2	2	2	15,6%
x	Asxl3 similar to Putative Polycomb group protein ASXL1	IPI00225360	233	88,0%	1	1	1	1,1%
x	Atic Bifunctional purine biosynthesis protein PURH	IPI00330303	64	99,2%	1	1	1	2,2%
x	Atp1b3 Sodium/potassium-transporting ATPase subunit beta-3	IPI00124221	32	99,8%	2	2	2	11,2%
x	Atp2c1 Calcium-transporting ATPase type 2C member 1	IPI00336323	100	88,0%	1	1	1	2,1%
x	Atp8b4 ATPase, class I, type 8B, member 4	IPI00662513	135	88,0%	1	1	1	1,9%
x	BC023829 similar to family with sequence similarity 11, member A isoform 6	IPI00755522	41	88,0%	1	1	1	2,5%
x	BC037393 CDNA sequence BC037393	IPI00131157	54	88,0%	1	1	1	5,3%
x	Bcl11b Isoform 1 of B-cell lymphoma/leukemia 11B	IPI00121608	95	99,2%	1	1	1	1,7%
x	C3 Isoform Long of Complement C3 precursor	IPI00323624	187	88,0%	1	1	1	0,7%
x	C330023M02Rik ES cells cDNA, RIKEN full-length enriched library, clone:C330023M02 product:WEAKLY SIMILAR TO DEC1 PROTEIN homolog	IPI00226576	112	88,0%	1	1	1	2,1%
x	C6 Complement component 6	IPI00314270	87	88,0%	1	1	1	3,4%
x	Cad carbamoyl-phosphate synthetase 2, aspartate transcarbamylase, and dihydroorotase	IPI00380280	243	99,8%	2	2	3	1,2%
x	Capn8 Calpain 8	IPI00126630	79	88,0%	1	1	1	2,4%
x	Capza2 F-actin capping protein subunit alpha-2	IPI00111265	33	99,8%	2	2	3	9,8%
x	Cbx3 Chromobox protein homolog 3	IPI00129468	21	99,8%	2	2	2	14,8%
x	Ccnf Isoform Short of G2/mitotic-specific cyclin-F	IPI00128673	86	88,0%	1	1	1	1,3%
x	Cct2 T-complex protein 1 subunit beta	IPI00320217	57	100,0%	3	3	4	12,0%
x	Cct7 T-complex protein 1 subunit eta	IPI00331174	60	99,9%	2	2	2	4,2%
x	Cdc37 Hsp90 co-chaperone Cdc37	IPI00117087	45	88,0%	1	1	1	5,5%
x	Cdca8 Isoform 2 of Borealin	IPI00221934	37	88,0%	1	1	1	4,9%
x	Cdh19 cadherin 19, type 2	IPI00660475	87	88,0%	1	2	2	2,6%
x	Cdk3 Isoform 1 of Cell division protein kinase 3	IPI00109650 IPI00109672	61	88,0%	1	1	1	1,5%
x	Cep350 centrosome-associated protein 350 isoform 1	IPI00118304	346	88,0%	1	1	1	0,4%
x	Cic CDNA, RIKEN full-length enriched library, clone:M5C1067E09 product:capicua homolog (Drosophila), full insert sequence	IPI00653910	258	88,0%	1	1	1	1,0%
x	Clic1 Chloride intracellular channel protein 1	IPI00130344	27	88,0%	1	1	1	7,1%
x	Copg 8 days embryo whole body cDNA, RIKEN full-length enriched library, clone:5730412D09 product:coatomer protein complex, subunit gamma 1, full insert sequence	IPI00223437	99	88,0%	1	1	1	1,9%
x	Cpne2 Copine-2	IPI00172189	61	88,0%	1	1	1	3,3%
x	Cpne3 Copine-3	IPI00266752	60	99,8%	2	2	2	7,1%
x	Cpne4 Copine-4	IPI00108980	62	88,0%	1	1	2	1,6%
x	Ctdp1 Isoform 1 of RNA polymerase II subunit A C-terminal domain phosphatase	IPI00338904	105	88,0%	1	1	1	1,5%
x	Ctsh Cathepsin H precursor	IPI00118987	37	99,8%	2	2	4	8,4%
x	Cyp4f15 Cytochrome P450 CYP4F15	IPI00117994	61	88,0%	1	1	1	3,9%
x	D8Ertd587e hypothetical protein LOC52335	IPI00605902	73	88,0%	1	1	1	5,2%
x	Dars Aspartyl-tRNA synthetase, cytoplasmic	IPI00122743	57	99,8%	2	2	3	6,0%
x	Dcps Scavenger mRNA decapping enzyme DcpS	IPI00459280	39	88,0%	1	1	1	3,3%
x	Ddb1 DNA damage-binding protein 1	IPI00316740	127	99,8%	2	2	2	1,8%
x	Ddx39 Isoform 1 of ATP-dependent RNA helicase DDX39	IPI00123878	49	99,4%	1	1	1	2,3%
x	Dhx15 Putative pre-mRNA-splicing factor ATP-dependent RNA helicase DHX15	IPI00128818	91	88,0%	1	1	3	1,5%

x	Dhx9 Isoform 1 of ATP-dependent RNA helicase A	IPI00339468	150	99,9%	2	2	2	2,0%
x	Dld TIB-55 BB88 cDNA, RIKEN full-length enriched library, clone:I730035F24 product:dihydrolipoamide dehydrogenase	IPI00331564	55	99,8%	2	2	4	6,3%
x	Dlst Dihydrolipoyllysine-residue succinyltransferase component of 2-oxoglutarate dehydrogenase complex, mitochondrial precursor	IPI00134809	49	88,0%	1	1	1	4,6%
x	Dmkn 18-day embryo whole body cDNA, RIKEN full-length enriched library, clone:1110014F24 product:hypothetical protein	IPI00271738	11	88,0%	1	1	1	16,4%
x	Dnahc8 Isoform 1 of Ciliary dynein heavy chain 8	IPI00172328	542	88,0%	1	1	1	0,6%
x	Dock7 Isoform 2 of Dedicator of cytokinesis protein 7	IPI00339428	241	88,0%	1	1	1	0,8%
x	Dpysl2 Dihydropyrimidinase-related protein 2	IPI00114375	62	99,8%	2	2	2	4,0%
x	Dscam Down syndrome cell adhesion molecule	IPI00112204	222	88,0%	1	1	1	1,3%
x	E030049G20Rik Nck-associated protein 5 isoform 2	IPI00463392	201	88,0%	1	1	1	0,8%
x	Eda Isoform TAA of Ectodysplasin-A	IPI00117049	42	88,0%	1	1	1	6,1%
x	Eef1d eukaryotic translation elongation factor 1 delta isoform a	IPI00118875	73	88,0%	1	1	1	3,6%
x	Eef1g Elongation factor 1-gamma	IPI00318841	50	99,8%	2	2	3	5,5%
x	Eftud2 116 kDa U5 small nuclear ribonucleoprotein component	IPI00469260	109	88,0%	1	1	1	1,2%
x	EG236622 similar to SMT3 suppressor of mif two 3 homolog 2 isoform 3	IPI00108762	11	88,0%	1	1	1	12,8%
x	EG330948 similar to ribosomal protein S8 isoform 1	IPI00274175	24	100,0%	4	4	6	19,2%
x	EG434077;LOC669183 similar to B0507.2	IPI00408556	46	88,0%	1	1	1	3,9%
x	EG546797 similar to 40S ribosomal protein S2	IPI00378671	31	88,0%	1	1	1	4,2%
x	EG619697 similar to putative pheromone receptor	IPI00409025	98	88,0%	1	1	2	1,8%
x	EG627889 similar to 60S ribosomal protein L6	IPI00282248	33	88,0%	1	1	2	3,1%
x	EG631797 similar to otoferlin isoform a	IPI00659709	211	88,0%	1	1	1	1,3%
x	EG632671 similar to putative pheromone receptor	IPI00465475	96	88,0%	1	1	1	2,3%
x	EG667965 similar to pleiomorphic adenoma gene-like 1	IPI00755396	21	88,0%	1	1	1	7,5%
x	EG668389 similar to Ig heavy chain V region PJ14 precursor	IPI00751105	30	88,0%	1	1	1	8,8%
x	Egfl9 EGF-like-domain, multiple 9	IPI00321725	45	88,0%	1	1	1	4,7%
x	Eif3s10 Eukaryotic translation initiation factor 3 subunit 10	IPI00129276	162	98,9%	1	1	2	0,8%
x	Eif3s4 Eukaryotic translation initiation factor 3 subunit 4	IPI00622371	36	88,0%	1	1	2	5,0%
x	Eif3s7 eukaryotic translation initiation factor 3, subunit 7	IPI00115751	64	99,8%	2	2	3	4,4%
x	Eif3s8 Eukaryotic translation initiation factor 3 subunit 8	IPI00321647	106	88,0%	1	1	1	1,1%
x	Eif3s9 Eif3s9 protein	IPI00229859	109	88,0%	1	1	2	1,3%
x	Eif4a3 Probable ATP-dependent RNA helicase DDX48	IPI00126716	47	88,0%	1	1	1	3,2%
x	Eif4b Eukaryotic translation initiation factor 4B	IPI00221581	69	88,0%	1	1	1	2,6%
x	Eif4g1 Isoform 1 of Eukaryotic translation initiation factor 4 gamma 1	IPI00421179	176	88,0%	1	1	1	1,2%
x	Eno3 Beta-enolase	IPI00228548	47	88,0%	1	1	1	6,9%
x	Epb4.1l5 CDNA, RIKEN full-length enriched library, clone:I530014H17 product:erythrocyte protein band 4.1-like 5, full insert sequence	IPI00116447	58	88,0%	1	1	1	3,2%
x	Eprs Bifunctional aminoacyl-tRNA synthetase	IPI00339916	170	99,3%	1	1	1	1,1%
x	Esr1 Estrogen receptor	IPI00117980	67	88,0%	1	1	1	3,3%
x	Fabp5 Fatty acid-binding protein, epidermal	IPI00114162	15	100,0%	3	3	4	23,7%
x	Fasn Fatty acid synthase	IPI00113223	272	100,0%	2	2	2	1,0%
x	Fbxo18 Isoform 1 of F-box only protein 18	IPI00322250	118	88,0%	1	1	1	2,2%
x	Fbxo2 F-box only protein 2	IPI00153176	34	88,0%	1	1	1	6,7%

x	Fdps Farnesyl pyrophosphate synthetase	IPI00120457	41	99,8%	2	2	2	8,2%
x	Fh1 Isoform Mitochondrial of Fumarate hydratase, mitochondrial precursor	IPI00129928	54	88,0%	1	1	1	2,8%
x	Fkbp4 FK506-binding protein 4	IPI00230139	52	99,9%	1	1	1	2,0%
x	Flot1 Flotillin-1	IPI00117181	47	88,0%	1	1	1	7,2%
x	Fn1 Fibronectin precursor	IPI00113539	272	98,9%	1	1	1	0,7%
x	Frap1;Angptl7 Isoform 1 of FKBP12-rapamycin complex-associated protein	IPI00268673	289	88,0%	1	1	1	0,5%
x	G430095P16Rik NOD-derived CD11c +ve dendritic cells cDNA, RIKEN full-length enriched library, clone:F630221H03 product:hypothetical protein, full insert sequence	IPI00653065	16	88,0%	1	1	1	12,8%
x	G6pc Glucose-6-phosphatase	IPI00119645	40	88,0%	1	1	1	5,0%
x	G6pdx Glucose-6-phosphate 1-dehydrogenase X	IPI00228385	59	88,0%	1	1	1	1,6%
x	Gadl1 glutamate decarboxylase-like 1	IPI00316617	63	88,0%	1	1	1	3,8%
x	Gck Isoform 1 of Glucokinase	IPI00130751	52	88,0%	1	1	1	2,6%
x	Gfpt2 Glucosamine--fructose-6-phosphate aminotransferase [isomerizing] 2	IPI00278312	77	88,0%	1	1	1	2,3%
x	Gm1323 similar to protein expressed in prostate, ovary, testis, and placenta 8 isoform 2	IPI00379098	33	88,0%	1	1	1	4,2%
x	Got1 Aspartate aminotransferase, cytoplasmic	IPI00230204	46	88,0%	1	1	1	2,7%
x	Gpi1 Glucose-6-phosphate isomerase	IPI00228633	63	88,0%	1	1	3	2,0%
x	Gpnmb Transmembrane glycoprotein NMB precursor	IPI00311808	64	100,0%	4	6	8	5,6%
x	Gramd1a GRAM domain containing 1A	IPI00124534	81	88,0%	1	1	1	2,4%
x	Gsn Isoform 1 of Gelsolin precursor	IPI00117167	86	100,0%	3	3	3	6,2%
x	H2-K1 H-2 class I histocompatibility antigen, K-D alpha chain precursor	IPI00110807	41	99,8%	2	2	2	6,3%
x	Hc Complement C5 precursor	IPI00330833	189	88,0%	1	1	1	0,8%
x	Hcls1 Hematopoietic lineage cell-specific protein	IPI00117011	54	99,5%	1	1	1	2,7%
x	Helz Helicase with zinc finger domain	IPI00453654	220	88,0%	1	1	1	0,8%
x	Hist1h1b Histone H1.5	IPI00230133	23	99,3%	1	1	1	4,9%
x	Hist1h1e Histone H1.4	IPI00223714	22	88,0%	1	1	1	5,5%
x	Hist1h2ba Histone H2B type 1-A	IPI00111957	14	99,3%	1	1	1	8,7%
x	Hnrpa0 12 days embryo head cDNA, RIKEN full-length enriched library, clone:3010025E17 product:Heterogeneous nuclear ribonucleoprotein A0 (hnRNP A0) homolog	IPI00109813	31	88,0%	1	1	1	6,6%
x	Hnrpa3 Isoform 1 of Heterogeneous nuclear ribonucleoprotein A3	IPI00269661	40	97,6%	1	1	3	2,6%
x	Hnrpab Heterogeneous nuclear ribonucleoprotein A/B	IPI00117288	31	100,0%	3	3	3	15,1%
x	Hnrpc Bone marrow macrophage cDNA, RIKEN full-length enriched library, clone:I830120C02 product:heterogeneous nuclear ribonucleoprotein C, full insert sequence	IPI00130343	37	88,0%	1	1	1	3,6%
x	Hnrpd Isoform 2 of Heterogeneous nuclear ribonucleoprotein D0	IPI00230086	36	88,0%	1	1	2	7,1%
x	Hnrpf Isoform 1 of Heterogeneous nuclear ribonucleoprotein F	IPI00226073	46	99,8%	2	2	3	8,0%
x	Hnrph2 Heterogeneous nuclear ribonucleoprotein H'	IPI00108143	49	99,8%	2	2	2	6,0%
x	Hnrpk Isoform 1 of Heterogeneous nuclear ribonucleoprotein K	IPI00223253	51	100,0%	4	4	4	13,0%
x	Hnrpl Heterogeneous nuclear ribonucleoprotein L	IPI00620362	64	100,0%	2	2	2	3,6%
x	Hnrpr Bone marrow macrophage cDNA, RIKEN full-length enriched library, clone:I830045N07 product:heterogeneous nuclear ribonucleoprotein R, full insert sequence	IPI00128441	71	88,0%	1	1	1	1,7%
x	Hsp110 Isoform HSP105-alpha of Heat-shock protein 105 kDa	IPI00123802	96	100,0%	3	3	6	4,8%
x	Hspbap1 Hspb associated protein 1	IPI00222501	54	88,0%	1	1	1	4,4%
x	Ibrdc1 similar to IBR domain containing 1	IPI00381171	75	88,0%	1	1	1	2,2%
x	Idh1 0 day neonate lung cDNA, RIKEN full-length enriched library, clone:E030024J03	IPI00135231	48	88,0%	1	1	1	3,1%

	product:isocitrate dehydrogenase 1 (NADP+), soluble, full insert sequence							
x	Ift74 Intraflagellar transport 74 homolog	IPI00222584	69	88,0%	1	1	1	3,5%
x	Igh-1a Igh-1a protein	IPI00556788	52	88,0%	1	1	1	4,0%
x	Impdh2 Inosine-5'-monophosphate dehydrogenase 2	IPI00323971	56	88,0%	1	1	1	2,1%
x	Irak3 Interleukin-1 receptor-associated kinase 3	IPI00420378	68	88,0%	1	1	1	2,6%
x	Itih4 Adult male liver cDNA, RIKEN full-length enriched library, clone:1300004A21 product:inter alpha-trypsin inhibitor, heavy chain 4, full insert sequence	IPI00119818	100	88,0%	1	1	1	2,3%
x	Itpr2 Isoform 2 of Inositol 1,4,5-trisphosphate receptor type 2	IPI00222043	182	99,8%	2	2	2	2,4%
x	Kin Antigenic determinant of rec-A protein	IPI00169984	45	88,0%	1	1	1	4,1%
x	Kpnb1 Importin beta-1 subunit	IPI00323881	97	100,0%	3	4	5	4,8%
x	Krt19 Keratin, type I cytoskeletal 19	IPI00112947	45	88,0%	1	1	1	1,7%
x	Krt42 Type I keratin KA22	IPI00468696	50	88,0%	1	1	1	4,2%
x	LOC382492 similar to 40S ribosomal protein S17	IPI00381546	29	88,0%	1	1	1	10,1%
x	LOC433460 similar to Glyceraldehyde-3-phosphate dehydrogenase	IPI00758061	37	88,0%	1	1	1	8,1%
x	LOC433546 similar to ribosomal protein L9	IPI00117610	22	88,0%	1	1	2	5,1%
x	LOC545588 similar to ribosomal protein L35a	IPI00115233	12	88,0%	1	1	2	8,2%
x	LOC546179 similar to Spindlin-like protein 2	IPI00474748	27	88,0%	1	1	1	6,8%
x	LOC632266;EG545091 similar to Heterogeneous nuclear ribonucleoprotein A1 (Helix-destabilizing protein) (Single-strand binding protein) (hnRNP core protein A1) (HDP-1) (Topoisomerase-inhibitor suppressed) isoform 1	IPI00129808	27	99,8%	2	2	2	12,3%
x	LOC633279 similar to palmitoyl-protein thioesterase-like protein	IPI00669306	17	88,0%	1	1	1	10,4%
x	LOC635561;EG665395;LOC675444 similar to 40S ribosomal protein S29	IPI00132856 IPI00625088	7	88,0%	1	1	1	14,3%
x	LOC638429 similar to olfactory receptor Olr121	IPI00674425	10	88,0%	1	1	1	22,3%
x	LOC654465 Beta-defensin 41	IPI00656305	9	88,0%	1	1	1	19,0%
x	LOC668899;LOC433476 similar to ribosomal protein L27a	IPI00137687	17	99,8%	2	2	3	16,2%
x	LOC670174;Ptges3 Prostaglandin E synthase 3	IPI00127989	19	99,9%	2	2	2	9,4%
x	LOC671726;EG666974 similar to Proteasome subunit alpha type 5 (Proteasome zeta chain) (Macropain zeta chain) (Multicatalytic endopeptidase complex zeta chain) isoform 1	IPI00122562	26	100,0%	2	2	2	9,1%
x	LOC671929;Rps2;EG667279;LOC665951 40S ribosomal protein S2	IPI00318492	32	88,0%	1	1	1	3,7%
x	LOC672818;EG545121 similar to ribosomal protein S14	IPI00112407	16	88,0%	1	1	1	7,3%
x	LOC675192;LOC672281;EG668182 similar to 60S ribosomal protein L13	IPI00134097	24	99,1%	1	1	1	5,3%
x	Lonrf2 LON peptidase N-terminal domain and ring finger 2	IPI00378496	58	88,0%	1	1	1	1,5%
x	Lrp8 Isoform 2 of Low-density lipoprotein receptor-related protein 8 precursor	IPI00121600	96	88,0%	1	1	1	2,0%
x	Lrpprc Leucine-rich PPR-motif containing	IPI00420706	147	88,0%	1	1	1	0,8%
x	Lrrc56 Leucine-rich repeat-containing protein 56	IPI00170019	60	88,0%	1	1	1	4,7%
x	Lrrn3 Leucine-rich repeat neuronal protein 3 precursor	IPI00314773	79	88,0%	1	1	1	3,0%
x	Ly6e 13 days embryo head cDNA, RIKEN full-length enriched library, clone:3110052M08 product:lymphocyte antigen 6 complex, locus E, full insert sequence	IPI00110520	14	88,0%	1	1	1	10,5%
x	Macf1 microtubule-actin crosslinking factor 1 isoform 2	IPI00663180	832	99,7%	1	1	1	0,2%
x	Mad2l1bp MAD2L1-binding protein	IPI00121481	31	88,0%	1	1	1	6,2%
x	Map3k7ip2 Mitogen-activated protein kinase kinase kinase 7-interacting protein 2	IPI00115639	76	88,0%	1	1	1	2,9%
x	March1 Isoform 3 of E3 ubiquitin-protein ligase MARCH1	IPI00421198	32	88,0%	1	1	1	4,9%

x	Mcm2 CRL-1722 L5178Y-R cDNA, RIKEN full-length enriched library, clone:I730064M13 product:minichromosome maintenance deficient 2 mitotin (S. cerevisiae), full insert sequence	IPI00323820	103	88,0%	1	1	1	1,2%
x	Mcm5 minichromosome maintenance deficient 5, cell division cycle 46	IPI00309398	82	88,0%	1	1	2	1,8%
x	Mdh1 Malate dehydrogenase, cytoplasmic	IPI00336324	36	100,0%	4	4	7	14,1%
x	Mfge8 Isoform 2 of Lactadherin precursor	IPI00322712	47	100,0%	3	3	3	8,7%
x	Mitf Isoform H of Microphthalmia-associated transcription factor	IPI00230197	57	88,0%	1	1	1	5,7%
x	Mon1b;4930481F22Rik MON1 homolog b	IPI00223080	60	88,0%	1	1	1	3,3%
x	Mphosph1 Isoform 1 of M-phase phosphoprotein 1	IPI00405665	203	88,0%	1	1	1	0,8%
x	Mug1 Murinoglobulin-1 precursor	IPI00123223	165	88,0%	1	1	1	0,5%
x	Mvp TIB-55 BB88 cDNA, RIKEN full-length enriched library, clone:I730057I21 product:major vault protein, full insert sequence	IPI00111258	97	88,0%	1	1	1	2,0%
x	Mybbp1a Myb-binding protein 1A	IPI00331361	152	88,0%	1	1	1	1,1%
x	Myef2 Isoform 2 of Myelin expression factor 2	IPI00154084	62	99,5%	1	1	1	7,0%
x	Myh11 Isoform 1 of Myosin-11	IPI00114894	227	98,2%	1	1	1	0,7%
x	Myl2 Myosin, light polypeptide 2, regulatory, cardiac, slow	IPI00230438	19	88,0%	1	1	1	7,8%
x	Naca Nascent polypeptide-associated complex subunit alpha, muscle-specific form	IPI00111831	221	99,8%	2	2	3	1,3%
x	Nap1l1 Nucleosome assembly protein 1-like 1	IPI00123199	45	88,0%	1	1	2	3,1%
x	Nap1l4 Bone marrow stroma cell CRL-2028 SR-4987 cDNA, RIKEN full-length enriched library, clone:G430136P17 product:nucleosome assembly protein 1-like 4, full insert sequence	IPI00133977	47	88,0%	1	1	1	4,0%
x	Nars Activated spleen cDNA, RIKEN full-length enriched library, clone:F830225J05 product:asparaginyl-tRNA synthetase, full insert sequence	IPI00223415	64	88,0%	1	1	1	2,0%
x	Nasp nuclear autoantigenic sperm protein isoform 1	IPI00115987	49	88,0%	1	1	1	2,2%
x	Nasp nuclear autoantigenic sperm protein isoform 2	IPI00830976	84	88,0%	1	1	1	1,6%
x	Neb similar to Nebulin	IPI00755239	747	88,0%	1	1	1	0,0%
x	Nolc1 Nolc1 protein	IPI00453865	41	88,0%	1	1	1	3,0%
x	Nudc Nuclear migration protein nudC	IPI00132942	38	88,0%	1	1	1	3,6%
x	Olfr1333 Olfactory receptor 1333	IPI00380564	36	88,0%	1	1	1	3,2%
x	Olfr615 Olfactory receptor MOR19-2	IPI00127910	35	88,0%	1	1	1	6,7%
x	Osbpl5 oxysterol-binding protein-like protein 5	IPI00624705	102	88,0%	1	1	1	3,0%
x	Palmd Palmdelphin	IPI00314152	63	88,0%	1	1	1	6,2%
x	Pcbp1 Poly(rC)-binding protein 1	IPI00128904	37	88,0%	1	1	1	3,1%
x	Pcna Proliferating cell nuclear antigen	IPI00113870	29	100,0%	2	2	3	12,3%
x	Pcnt pericentrin	IPI00457623	331	88,0%	1	1	1	0,3%
x	Pet112l Probable glutamyl-tRNA(Gln) amidotransferase subunit B, mitochondrial precursor	IPI00457976	62	88,0%	1	1	1	4,5%
x	Pfkl Phosphofructokinase, liver, B-type	IPI00387312	85	100,0%	3	3	3	6,3%
x	Phgdh;LOC673015 D-3-phosphoglycerate dehydrogenase	IPI00225961	57	100,0%	5	6	9	13,3%
x	Picalm Isoform 1 of Phosphatidylinositol-binding clathrin assembly protein	IPI00264501	72	88,0%	1	1	1	3,0%
x	Pik3r1 Phosphatidylinositol 3-kinase regulatory subunit alpha	IPI00263878	83	88,0%	1	1	1	2,8%
x	Pip5k1b Isoform 1 of Phosphatidylinositol-4-phosphate 5-kinase type-1 alpha	IPI00331736	60	88,0%	1	1	1	2,9%
x	Plk1 Serine/threonine-protein kinase PLK1	IPI00120767	68	88,0%	1	1	1	5,1%
x	Polr3a similar to polymerase (RNA) III (DNA directed) polypeptide A, 155kDa	IPI00753896	156	88,0%	1	1	1	0,9%
x	Ppfibp2 Ppfibp2 protein	IPI00400017	101	88,0%	1	1	1	1,8%
x	Ppp2cb Serine/threonine-protein phosphatase 2A catalytic subunit beta isoform	IPI00111556	36	88,0%	1	1	1	3,6%
x	Ppp2r1a Serine/threonine-protein phosphatase 2A 65 kDa regulatory subunit A alpha isoform	IPI00310091	65	88,0%	1	1	1	1,9%

x	Ppp4r1 13 days embryo head cDNA, RIKEN full-length enriched library, clone:3110001J10 product:protein phosphatase 4, regulatory subunit 1, full insert sequence	IPI00461455	39	88,0%	1	1	1	4,2%
x	Prdx4 Peroxiredoxin-4	IPI00116254	31	88,0%	1	1	1	2,9%
x	Prkcsh Isoform 1 of Glucosidase 2 subunit beta precursor	IPI00115680	59	88,0%	1	1	1	1,9%
x	Prkdc Isoform 1 of DNA-dependent protein kinase catalytic subunit	IPI00123886	471	97,7%	1	1	1	0,4%
x	Prmt1 Isoform 1 of Protein arginine N-methyltransferase 1	IPI00120495	42	88,0%	1	1	1	4,3%
x	Psat1 Phosphoserine aminotransferase	IPI00115620	40	100,0%	3	3	3	8,9%
x	Psma1 Proteasome subunit alpha type 1	IPI00283862	30	100,0%	2	2	2	10,3%
x	Psma6 Proteasome subunit alpha type 6	IPI00131845	27	100,0%	3	3	4	16,7%
x	Psma8 Proteasome subunit alpha type 7-like	IPI00109122	28	88,0%	1	1	1	5,6%
x	Psmb1 Proteasome subunit beta type 1 precursor	IPI00113845	26	98,5%	1	1	2	5,8%
x	Psmb4 Proteasome subunit beta type 4 precursor	IPI00129512	29	88,0%	1	1	1	5,7%
x	Psmb5 proteasome (prosome, macropain) subunit, beta type 5	IPI00317902	29	88,0%	1	1	1	5,3%
x	Psmc2 Adult male testis cDNA, RIKEN full-length enriched library, clone:4930525G09 product:PROTEASOME (PROSOME, MACROPAIN) 26S SUBUNIT, ATPASE 2	IPI00270326	53	88,0%	1	1	1	4,6%
x	Psmd11 26S proteasome non-ATPase regulatory subunit 11	IPI00222515	47	88,0%	1	1	1	3,1%
x	Ptprs Ptprs protein	IPI00230067	168	88,0%	1	1	1	0,9%
x	Ranbp1 Ran-specific GTPase-activating protein (Fragment)	IPI00321978	24	99,8%	2	2	2	10,8%
x	Rangap1 Ran GTPase-activating protein 1	IPI00467338	64	88,0%	1	1	1	2,0%
x	Rars Arginyl-tRNA synthetase, cytoplasmic	IPI00315488	76	100,0%	3	3	3	4,7%
x	Rbmx Heterogeneous nuclear ribonucleoprotein G	IPI00124979	42	88,0%	1	1	1	3,3%
x	Reln Isoform 1 of Reelin precursor	IPI00121421	387	88,0%	1	1	1	0,3%
x	Rnf123 Isoform 2 of E3 ubiquitin-protein ligase RNF123	IPI00471406	149	88,0%	1	1	1	1,2%
x	Rnf207 3 days neonate thymus cDNA, RIKEN full-length enriched library, clone:A630086J06 product:hypothetical Zn-finger, B-box/Zn-finger, RING containing protein, full insert sequence	IPI00136356	71	88,0%	1	1	1	2,1%
x	RP23-331I21.14 similar to poly(A) binding protein, cytoplasmic 4 isoform 1 isoform 1	IPI00461269	73	88,0%	1	1	1	3,2%
x	Rpl10 60S ribosomal protein L10	IPI00474637	25	88,0%	1	1	1	6,5%
x	Rpl15 60S ribosomal protein L15	IPI00273803	24	88,0%	1	1	2	6,9%
x	Rpl19 60S ribosomal protein L19	IPI00122426	23	88,0%	1	1	1	8,7%
x	Rpl28 60S ribosomal protein L28	IPI00222547	16	88,0%	1	1	1	5,1%
x	Rpl36 60S ribosomal protein L36	IPI00230679	12	97,8%	1	1	1	9,5%
x	Rps14 40S ribosomal protein S14	IPI00322562	16	99,8%	2	2	2	20,5%
x	Rps15a 40S ribosomal protein S15a	IPI00230660	15	99,8%	2	2	2	12,3%
x	Rps16 Rps16 protein	IPI00469918	19	100,0%	1	1	2	6,4%
x	Rps27l 40S ribosomal protein S27-like protein	IPI00124709	9	88,0%	1	1	2	15,5%
x	Rps7 40S ribosomal protein S7	IPI00136984	22	99,8%	2	2	3	10,3%
x	Rpsa Ribosomal protein SA	IPI00126010	33	88,0%	1	1	1	9,2%
x	Rrn3 RRN3 RNA polymerase I transcription factor homolog	IPI00127454	75	88,0%	1	1	2	1,8%
x	Ruvbl1 RuvB-like 1	IPI00133985	50	88,0%	1	1	1	2,4%
x	Ruvbl2 RuvB-like 2	IPI00123557	51	88,0%	1	1	1	2,4%
x	Sall2 Sal-like protein 2	IPI00134563	105	88,0%	1	1	1	3,0%
x	Sars ES cells cDNA, RIKEN full-length enriched library, clone:C330018O14 product:seryl-aminoacyl-tRNA synthetase 1	IPI00225307	61	99,8%	2	2	2	5,6%
x	Scye1 small inducible cytokine subfamily E, member 1	IPI00132194	35	88,0%	1	1	1	5,6%
x	Sdro Retinol dehydrogenase similar protein	IPI00170115	35	88,0%	1	1	1	8,0%
x	Sept2 Septin-2	IPI00114945	42	100,0%	2	2	3	7,8%

x	Sept6 Isoform V of Septin-6	IPI00226602	49	88,0%	1	1	1	2,6%
x	Sept7 cell division cycle 10 homolog	IPI00224626	51	99,8%	2	2	2	7,8%
x	Sept9 Isoform 1 of Septin-9	IPI00457611	66	88,0%	1	1	1	1,5%
x	Sesn2 Sestrin-2	IPI00115849	54	88,0%	1	1	1	5,0%
x	Set;LOC671392 Isoform 1 of Protein SET	IPI00111560	33	99,8%	2	3	6	8,3%
x	Sez6l2 Seizure related 6 homolog like 2	IPI00128454	99	88,0%	1	1	1	2,7%
x	Sf3b2 Bone marrow macrophage cDNA, RIKEN full-length enriched library, clone:I830028H02 product:splicing factor 3b, subunit 2	IPI00349401	98	88,0%	1	1	1	1,6%
x	Sf3b3 Isoform 1 of Splicing factor 3B subunit 3	IPI00122011	136	88,0%	1	1	1	0,9%
x	Sfpq Splicing factor, proline- and glutamine-rich	IPI00129430	75	99,8%	2	2	2	3,7%
x	Sfrs1 Isoform 1 of Splicing factor, arginine/serine-rich 1	IPI00420807	28	99,8%	2	2	3	8,9%
x	Sfrs2 Splicing factor, arginine/serine-rich 2	IPI00121135	25	88,0%	1	1	1	3,6%
x	Sfrs5 Splicing factor, arginine/serine-rich 5	IPI00314709	31	88,0%	1	1	1	8,5%
x	Sfrs7 Isoform 2 of Splicing factor, arginine/serine-rich 7	IPI00153743	27	99,9%	1	1	1	8,8%
x	Sfrs9 Splicing factor, arginine/serine-rich 9	IPI00132340	26	88,0%	1	1	1	3,2%
x	Slc22a1 LX1	IPI00331032	62	88,0%	1	1	1	4,3%
x	Slc24a6 Isoform 1 of Sodium/potassium/calcium exchanger 6 precursor	IPI00127134	64	88,0%	1	1	1	2,9%
x	Slc2a8 Solute carrier family 2, facilitated glucose transporter member 8	IPI00310367	52	88,0%	1	1	1	5,9%
x	Slc6a12 Solute carrier family 6 (Neurotransmitter transporter, betaine/GABA), member 12	IPI00466652	71	88,0%	1	1	1	2,1%
x	Slit3 Slit homolog 3 protein precursor	IPI00664551	168	88,0%	1	1	1	1,6%
x	Snrp70 Isoform 2 of U1 small nuclear ribonucleoprotein 70 kDa	IPI00230541	20	88,0%	1	1	1	9,6%
x	Snrpd3 Small nuclear ribonucleoprotein Sm D3	IPI00119224	14	99,8%	2	2	2	15,1%
x	Snrpf similar to Small nuclear ribonucleoprotein F	IPI00666526	26	88,0%	1	1	1	4,6%
x	Sorl1 Sortilin-related receptor precursor	IPI00129831	247	88,0%	1	1	2	0,7%
x	Spert Spermatid associated	IPI00112593	48	88,0%	1	1	1	3,4%
x	Spnb4 spectrin beta 4	IPI00270149	289	88,0%	1	1	1	0,5%
x	Srm Spermidine synthase	IPI00136912	34	99,8%	2	2	2	7,3%
x	Ssb Lupus La protein homolog	IPI00134300	48	88,0%	1	1	1	2,7%
x	Ssty1 spermiogenesis gene	IPI00756509	27	98,8%	1	1	1	3,8%
x	St13 Hsc70-interacting protein	IPI00116308	42	99,3%	1	1	1	2,7%
x	Stip1 Stress-induced-phosphoprotein 1	IPI00121514	63	100,0%	3	3	5	7,6%
x	Stk39 STE20/SPS1-related proline-alanine-rich protein kinase	IPI00622783	60	88,0%	1	1	1	5,6%
x	Strbp Isoform 1 of Spermatid perinuclear RNA-binding protein	IPI00128254	74	88,0%	1	1	1	2,4%
x	Stx8 Syntaxin-8	IPI00136653	27	99,0%	1	1	1	7,6%
x	Stxbp5l Isoform 3 of Syntaxin-binding protein 5-like	IPI00309953	129	88,0%	1	1	1	1,5%
x	Syngr1 Isoform 1A of Synaptogyrin-1	IPI00115763	26	88,0%	1	1	2	5,1%
x	Taldo1 Transaldolase	IPI00124692	37	100,0%	3	3	4	10,1%
x	Tardbp TAR DNA-binding protein 43	IPI00121758	45	88,0%	1	1	2	2,9%
x	Tcp1 T-complex protein 1 subunit alpha B	IPI00459493	60	99,8%	2	2	3	4,5%
x	Thoc1 THO complex subunit 1	IPI00153778	76	88,0%	1	1	1	3,8%
x	Tle4 Bce-1 protein	IPI00463249	12	88,0%	1	1	1	18,1%
x	Tmc4;Leng1 transmembrane channel-like gene family 4	IPI00387513	77	88,0%	1	1	1	1,2%
x	Tmc5 Transmembrane channel-like protein 5	IPI00468700	88	88,0%	1	1	1	1,7%
x	Tmem59 Transmembrane protein 59 precursor	IPI00135648	36	88,0%	1	1	1	3,1%
x	Tmem70 Transmembrane protein 70	IPI00467349	28	88,0%	1	1	1	6,7%
x	Tmie Transmembrane inner ear expressed protein precursor	IPI00170169	17	88,0%	1	1	1	20,3%
x	Tnxb Tenascin X	IPI00130794	435	88,0%	1	1	1	0,3%
x	Tpm3 Tropomyosin 3, gamma	IPI00169707	33	100,0%	2	2	2	8,1%
x	Tpm4 Tropomyosin alpha-4 chain	IPI00421223	28	88,0%	1	1	1	6,1%
x	Tpt1 Translationally-controlled tumor protein	IPI00129685	19	88,0%	1	1	1	8,1%

x		Tspan3 Tetraspanin-3	IPI00135517	28	88,0%	1	1	1	6,3%
x		Tspan32 Isoform 4 of Tetraspanin-32	IPI00263117	19	88,0%	1	1	1	16,2%
x		Ttll1 Isoform 1 of Probable tubulin polyglutamylase	IPI00126079	49	88,0%	1	1	1	3,8%
x		Ttyh3 Tweety homolog 3	IPI00226563	58	88,0%	1	1	1	2,7%
x		Tubb6 Tubulin beta-6 chain	IPI00122928	50	88,0%	1	1	1	3,8%
x		U2af2 Splicing factor U2AF 65 kDa subunit	IPI00113746	53	88,0%	1	1	1	3,8%
x		Ube1x;Ube1y1 Ubiquitin-activating enzyme E1 X	IPI00123313	118	100,0%	4	4	5	6,0%
x		Ush2a Isoform 1 of Usherin precursor	IPI00720231	570	88,0%	1	1	2	0,4%
x		Usp47 Isoform 2 of Ubiquitin carboxyl-terminal hydrolase 47	IPI00420143	155	88,0%	1	1	1	1,6%
x		Vat1 Synaptic vesicle membrane protein VAT-1 homolog	IPI00126072	43	88,0%	1	1	1	2,2%
x		Vcan Isoform V0 of Versican core protein precursor	IPI00121038	367	88,0%	1	1	1	0,7%
x		Vps13d similar to vacuolar protein sorting 13D isoform 2 isoform 5	IPI00649141	488	98,9%	1	1	1	0,3%
x		Vps26a Isoform 2 of Vacuolar protein sorting-associated protein 26A	IPI00329942	42	88,0%	1	1	1	4,7%
x		Xpnpep1 Bone marrow macrophage cDNA, RIKEN full-length enriched library, clone:G530009C13 product:X-prolyl aminopeptidase (aminopeptidase P) 1, soluble	IPI00420231	75	88,0%	1	1	2	2,4%
x		Ywhab Isoform Long of 14-3-3 protein beta/alpha	IPI00230682	28	99,9%	2	2	3	8,1%
x		Ywhag 14-3-3 protein gamma	IPI00230707	28	100,0%	2	2	2	13,4%
x		Zfp353 zinc finger protein 353	IPI00121571	62	88,0%	1	1	1	4,2%
x		Zfp385 zinc finger protein 385	IPI00135630	40	88,0%	1	1	1	5,2%
x		Zfp410 Isoform 1 of Zinc finger protein 410	IPI00123438	52	88,0%	1	1	1	4,4%
	x	- 13 days embryo heart cDNA, RIKEN full-length enriched library, clone:D330011K04 product:hypothetical EGF-like domain, subtype 2 containing protein, full insert sequence (Fragment)	IPI00652223	14	87,9%	1	1	1	11,5%
	x	- 195 kDa protein	IPI00788398	195	87,9%	1	1	1	1,3%
	x	- 25 kDa protein	IPI00755602	25	87,9%	1	1	2	5,6%
	x	- 39 kDa protein	IPI00753041	39	87,9%	1	1	1	4,7%
	x	- 9 kDa protein	IPI00138204	9	87,9%	1	1	1	20,5%
	x	- 95 kDa protein	IPI00762641	95	87,9%	1	1	1	2,8%
	x	- Gag protein	IPI00466581	65	87,9%	1	1	1	2,7%
	x	0610031J06Rik Bone marrow macrophage cDNA, RIKEN full-length enriched library, clone:I830015H17 product:Kidney predominant protein (RIKEN cDNA 0610031J06 gene)	IPI00459432	44	87,9%	1	1	1	5,0%
	x	1700016L21Rik hypothetical protein LOC72208	IPI00807926	12	87,9%	1	1	1	16,2%
	x	1700106N22Rik NOD-derived CD11c +ve dendritic cells cDNA, RIKEN full-length enriched library, clone:F630211G03 product:hypothetical protein, full insert sequence	IPI00378272	36	87,9%	1	1	1	9,9%
	x	2310047H23Rik RIKEN cDNA 2310047H23 gene	IPI00378224	38	99,6%	1	1	1	5,8%
	x	2410018C17Rik 6 days neonate head cDNA, RIKEN full-length enriched library, clone:5430419M09 product:hypothetical protein, full insert sequence	IPI00759959	37	87,9%	1	1	1	9,2%
	x	2700008B19Rik hypothetical protein LOC217026	IPI00420246	129	87,9%	1	1	1	2,7%
	x	3110043A19Rik 13 days embryo head cDNA, RIKEN full-length enriched library, clone:3110043A19 product:hypothetical protein, full insert sequence	IPI00110576	21	87,9%	1	1	1	9,0%
	x	4921505C17Rik Pianissimo	IPI00399440	192	87,9%	1	1	1	2,0%
	x	4930563M21Rik Adult male testis cDNA, RIKEN full-length enriched library, clone:4930563M21 product:hypothetical protein, full insert sequence	IPI00229144	22	87,9%	1	1	1	11,2%